PSDF

Power Systems Development Facility

Topical Report
Gasification Test Run TC13

September 30, 2003 -
November 2, 2003

DOE Cooperative Agreement Number
DE-FC21-90MC25140

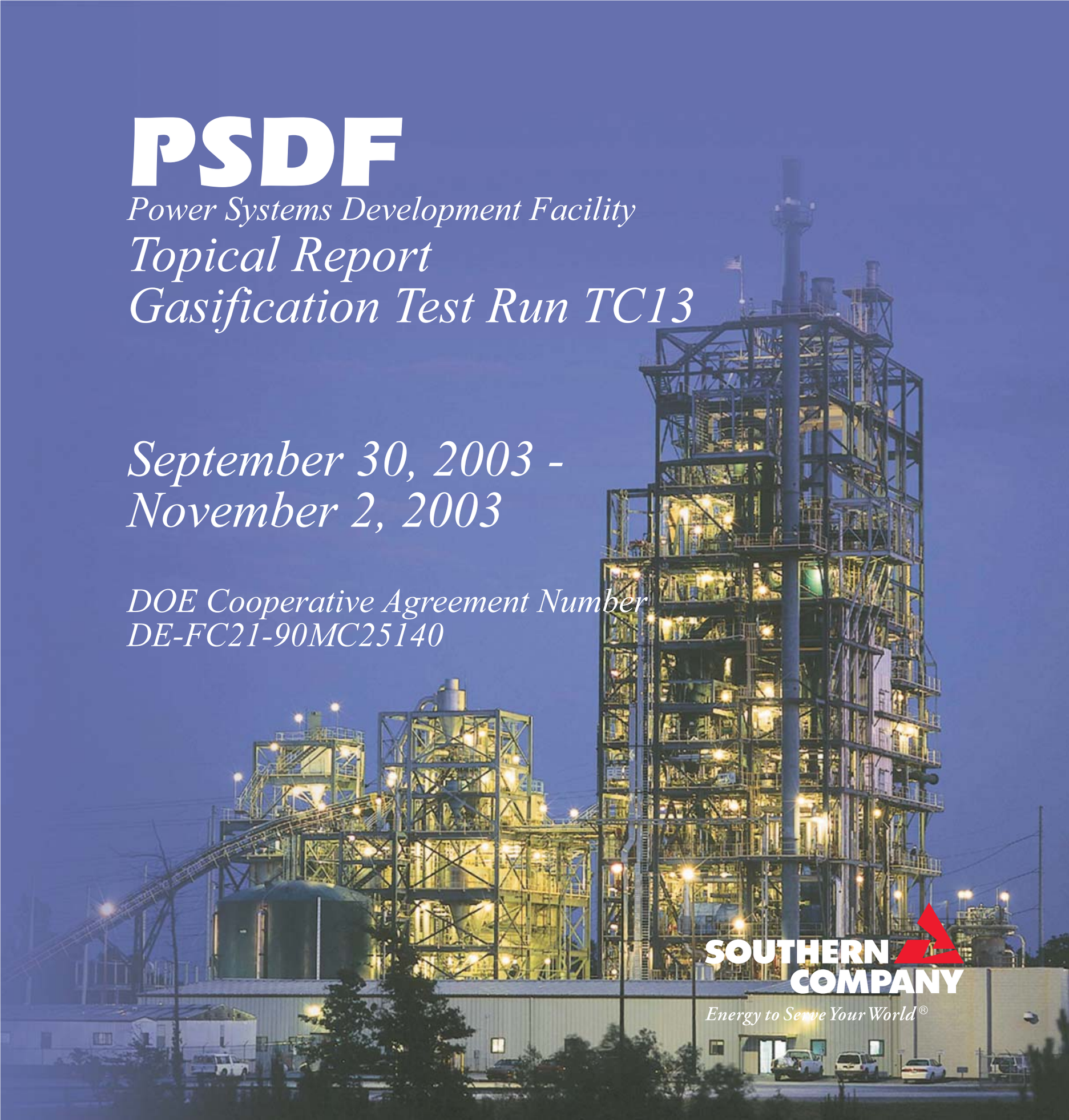

SOUTHERN COMPANY

Energy to Serve Your World®

POWER SYSTEMS DEVELOPMENT FACILITY
TOPICAL REPORT

GASIFICATION TEST RUN TC13

SEPTEMBER 30, 2003 – NOVEMBER 2, 2003

DOE Cooperative Agreement Number
DE-FC21-90MC25140

Prepared by:
Southern Company Services, Inc.
Power Systems Development Facility
P.O. Box 1069
Wilsonville, AL 35186
Tel: 205-670-5840
Fax: 205-670-5843
http://psdf.southernco.com

November 2006

POWER SYSTEMS DEVELOPMENT FACILITY

DISCLAIMER

Available to the public from the National Technical Information Service, U.S. Department of Commerce, 5285 Port Royal Road, Springfield, VA 22161. Phone orders accepted at (703) 487-4650.

ABSTRACT

This report discusses Test Campaign TC13 of the Kellogg Brown & Root, Inc. (KBR) Transport Gasifier train with a Siemens Westinghouse Power Corporation (Siemens Westinghouse) particulate collection device (PCD) at the Power Systems Development Facility (PSDF) located in Wilsonville, Alabama. The Transport Reactor is an advanced circulating fluidized-bed reactor designed to operate as either a combustor or a gasifier in air- or oxygen-blown mode of operation.

Test run TC13 began on September 30, 2003 with the startup of the main air compressor and the lighting of the gasifier startup burner. The Transport Gasifier operated until November 2, 2003, accumulating just over 500 hours of operation. Over the course of the entire test run, the gasifier tested three types of coal: high-sodium lignite from the Freedom Mine in North Dakota, low-sodium lignite from the same mine, and Powder River Basin (PRB) coal.

ACKNOWLEDGMENT

The authors wish to acknowledge the contributions and support provided by various project managers: Ron Breault (DOE), John Wheeldon (EPRI), Nicola Salazar (KBR), Ben Wiant (Siemens Westinghouse), and Vann Bush (SRI). Also, the enterprising solutions to problems and the untiring endeavors of many personnel at the site are greatly appreciated. The project was sponsored by the U.S. Department of Energy National Energy Technology Laboratory under contract DE-FC21-90MC25140.

CONTENTS

Section Page

Inside Cover
Disclaimer
Abstract
Acknowledgment

Listing of Tables and Figures v

1.0 EXECUTIVE SUMMARY 1.1-1

1.1 Summary 1.1-1
1.2 PSDF Accomplishments 1.2-1
1.2.1 Transport Gasifier Train 1.2-1
1.2.2 PCD 1.2-3

2.0 INTRODUCTION 2.1-1

2.1 The Power Systems Development Facility 2.1-1
2.2 Transport Gasifier System Description 2.2-1
2.3 Siemens Westinghouse Particulate Control Device 2.3-1
2.4 Operation History 2.4-1

3.0 TRANSPORT GASIFIER 3.1-1

3.1 Run Summary 3.1-1
3.2 Gas Analysis 3.2-1
3.2.1 Summary and Conclusions 3.2-1
3.2.1.1 Powder River Basin Coal 3.2-1
3.2.1.2 Freedom Mine Lignite Coal 3.2-1
3.2.1.3 Both Powder River Basin and Freedom Mine Lignite Coals 3.2-2
3.2.2 Introduction 3.2-2
3.2.3 Raw Gas Analyzer Data 3.2-3
3.2.4 Gas Analysis Results 3.2-7
3.2.5 Commercially Projected Syngas Lower Heating Values 3.2-11
3.2.6 Syngas Water Gas-Shift Equilibrium 3.2-14
3.2.7 Syngas Combustor Oxygen, Carbon, and Hydrogen Balance Calculations 3.2-15
3.2.8 Sulfur Emissions 3.2-16
3.2.9 Ammonia Equilibrium 3.2-18
3.3 Solids Analyses 3.3-1
3.3.1 Summary and Conclusions 3.3-1
3.3.1.1 Powder River Basin Coal 3.3-1
3.3.1.2 Low-Sodium Freedom Mine Lignite Coal 3.3-1
3.3.1.3 High-Sodium Freedom Mine Lignite Coal 3.3-1
3.3.1.4 Both Powder River Basin and Freedom Mine Lignite Coals 3.3-2

3.3.2 Introduction 3.3-2
3.3.3 Feeds Analysis 3.3-2
3.3.4 Gasifier Solids Analysis 3.3-3
3.3.5 Gasifier Products Solids Analysis 3.3-6
3.3.6 Solids Analysis Comparison 3.3-9
3.3.7 Reactive Sulfide Test Results 3.3-10
3.3.8 Feeds Particle Size 3.3-11
3.3.9 Gasifier Solids Particle Size 3.3-12
3.3.10 Particle Size Comparison 3.3-15
3.3.11 Standpipe and PCD Fines Bulk Densities 3.3-15
3.4 Mass and Energy Balances 3.4-1
3.4.1 Summary and Conclusions 3.4-1
3.4.1.1 Powder River Basin Coal 3.4-1
3.4.1.2 Low-Sodium Freedom Mine Lignite 3.4-1
3.4.1.3 High-Sodium Freedom Mine Lignite 3.4-1
3.4.1.4 Both Powder River Basin Coal and Freedom Mine Lignite 3.4-2
3.4.2 Introduction 3.4-2
3.4.3 Feed Rates 3.4-3
3.4.4 Product Rates 3.4-4
3.4.5 Overall Material Balance 3.4-6
3.4.6 Carbon Balances and Carbon Conversion 3.4-6
3.4.7 Nitrogen Balance 3.4-8
3.4.8 Sulfur Balance and Sulfur Removal 3.4-9
3.4.9 Hydrogen Balance 3.4-10
3.4.10 Oxygen Balance 3.4-11
3.4.11 Calcium Balance 3.4-11
3.4.12 Silica Balance 3.4-11
3.4.13 Energy Balance 3.4-12
3.4.14 Gasification Efficiencies 3.4-12
3.5 Atmospheric Fluidized-Bed Combustor Operations (AFBC) 3.5-1
3.6 Process Gas Coolers 3.6-1

4.0 PARTICLE FILTER SYSTEM 4.1-1

4.1 Run Overview 4.1-1
4.2 PCD Operation 4.2-1
4.2.1 Filter Elements and Failsafe Devices 4.2-1
4.2.2 General Operation and PCD Pressure Drop 4.2-2
4.2.3 Back-Pulse Optimization 4.2-3
4.2.4 PCD Solids Removal System Problems 4.2-4
4.3 PCD Hardware Inspection and Analysis 4.3-1
4.3.1 Filter Element and Seal Leaks 4.3-1
4.3.2 Filter Element Flow Resistance Evaluation 4.3-1
4.3.3 G-Ash Deposition 4.3-2
4.3.4 Failsafe Evaluation 4.3-3
4.3.5 Back-Pulse Pipe Inspection 4.3-3
4.3.6 PCD Screw Cooler Leak 4.3-3

4.3.7 PCD Solids Depressurization System 4.3-4
4.3.8 Filter Material Test Results 4.3-5
4.4 Gasification Ash Characteristics and PCD Performance 4.4-1
4.4.1 In situ Sampling 4.4-1
4.4.1.1 PCD Inlet Particle Mass Concentrations 4.4-2
4.4.1.2 PCD Outlet Particle Mass Concentrations 4.4-2
4.4.1.3 Syngas Moisture Content 4.4-3
4.4.1.4 Real-Time Particle Monitoring 4.4-3
4.4.2 Particle-Size Analysis of In situ Particulate Samples and PCD Hopper Samples 4.4-3
4.4.2.1 Particle Size of In situ Particulate Samples 4.4-4
4.4.2.2 Particle Size of PCD Hopper Samples 4.4-4
4.4.3 Measurement and Sampling of PCD Dustcakes 4.4-4
4.4.4 Characteristics of In situ Samples, Hopper Samples, and Residual Dustcake 4.4-5
4.4.4.1 Characteristics of In situ Particulate Samples 4.4-5
4.4.4.2 Characteristics of PCD Hopper Samples Used for Drag Measurements 4.4-8
4.4.4.3 Characteristics of Residual Dustcake Samples 4.4-10
4.4.5 Laboratory Measurements of Gasification Ash Drag 4.4-11
4.4.6 Analysis of PCD Pressure Drop 4.4-12
4.4.7 Conclusions 4.4-13

TERMS ..... PSDF Terms-1

TABLES

Table		Page
1.2-1	Operating Data Summary	1.2-5
2.2-1	Major Equipment in the Transport Reactor Train	2.2-3
2.2-2	Major Equipment in the Balance-of-Plant	2.2-4
3.1-1	Operating Conditions for Transport Gasifier	3.1-6
3.2-1	Operating Periods	3.2-20
3.2-2	Operating Conditions	3.2-21
3.2-3	Gas Analyzer Choices	3.2-22
3.2-4	H_2O Determination Methods	3.2-23
3.2-5	Gas Compositions, Molecular Weight, and Heating Value	3.2-24
3.2-6	Details of Projected LHV Changes	3.2-25
3.2-7	Commercially Projected Gas Compositions, Molecular Weight, and Heating Value	3.2-26
3.2-8	Water-Gas Shift Equilibrium Constant	3.2-27
3.2-9	Transport Gasifier Equilibrium Calculations	3.2-28
3.2-10	Syngas Combustor Calculations	3.2-29
3.2-11	Syngas Combustor Results	3.2-30
3.2-12	Ammonia Equilibrium Approach Temperatures	3.2-31
3.3-1	Coal Analyses	3.3-17
3.3-2	Limestone Analyses	3.3-18
3.3-3	Standpipe Solids Analyses	3.3-19
3.3-4	FD0510 Solids Sample Analyses	3.3-20
3.3-5	PCD Fines Solids From FD0520 Analyses	3.3-21
3.3-6	Reactive Sulfide Test Results	3.3-22
3.3-7	Historical as Fed Coal Average Particle Sizes, Percent Fines, and Percent Oversize	3.3-23
3.3-8	Historical Standpipe and PCD Fines Particle Sizes and Bulk Density	3.3-24
3.4-1	Feed Rates, Product Rates, and Mass Balances	3.4.-15
3.4-2	Carbon Balances	3.4-16
3.4-3	Test Campaign Carbon Balances and Coal Rate Methods	3.4-17
3.4-4	Nitrogen, Hydrogen, Oxygen, Calcium, and Silica Mass Balances	3.4-18
3.4-5	Typical Air-Blown Component Mass Balances	3.4-19
3.4-6	Typical Oxygen-Blown Component Mass Balances	3.4-20
3.4-7	Sulfur Balances	3.4-21
3.4-8	Energy Balances	3.4-22
4.2-1	PCD Operating Parameters	4.2-5
4.3-1	Test Matrix for Filter Element 39151	4.3-6
4.3-2	Axial Tensile Test Results for Pall PSS FEAL Element 39151	4.3-6

4.3-3 Room Temperature Hoop Tensile Test Results for Pall PSS FEAL Element 39151 ..... 4.3-7

4.4-1 PCD Inlet and Outlet Particulate Measurements for TC13 ..... 4.4-16
4.4-2 Residual Cake Measurements From TC13 and Previous Runs 4.4-17
4.4-3 Physical Properties of TC13 In situ Samples and Hopper Samples Used for RAPTOR 4.4-18
4.4-4 Chemical Composition of TC13 In situ Samples and Hopper Samples Used for RAPTOR 4.4-19
4.4-5 Physical Properties of TC13 Residual Dustcake 4.4-20
4.4-6 Chemical Composition of TC13 Residual Dustcake 4.4-20
4.4-7 Transient Drag Determined From PCD ΔP and From RAPTOR 4.4-21

FIGURES

Figure		Page
2.2-1	Flow Diagram of the Transport Gasifier Train	2.2-7
2.3-1	Siemens Westinghouse PCD (FL0301)	2.3-2
2.4-1	Operating Hours Summary for the Transport Reactor Train	2.4-4
3.2-1	Gas Sampling Locations	3.2-32
3.2-2	Carbon Monoxide Analyzer Data	3.2-32
3.2-3	Hydrogen Analyzer Data	3.2-33
3.2-4	Methane Analyzer Data	3.2-33
3.2-5	C_2^+ Analyzer Data	3.2-34
3.2-6	Carbon Dioxide Analyzer Data	3.2-34
3.2-7	Nitrogen Analyzer Data	3.2-35
3.2-8	Sums of GC Gas Compositions (Dry)	3.2-35
3.2-9	Hydrogen Sulfide Analyzer Data	3.2-36
3.2-10	Ammonia Data	3.2-36
3.2-11	Naphthalene Data	3.2-37
3.2-12	Sums of Dry Gas Compositions	3.2-37
3.2-13	H_2O Data	3.2-38
3.2-14	In situ H_2O and H_2O Analyzer Comparison	3.2-38
3.2-15	Wet Syngas Compositions	3.2-39
3.2-16	Syngas Molecular Weight and Nitrogen Concentration	3.2-39
3.2-17	Syngas Lower Heating Values	3.2-40
3.2-18	Raw Lower Heating Value and Overall Percent O_2	3.2-40
3.2-19	LHVs and Mixing Zone Temperature	3.2-41
3.2-20	PRB Projected LHVs and Overall Percent O_2	3.2-41
3.2-21	Freedom Lignite Projected LHVs and Overall Percent O_2	3.2-42
3.2-22	Water-Gas Shift Constants (In situ H_2O)	3.2-42
3.2-23	Water-Gas Shift Constant (AI475H H_2O)	3.2-43
3.2-24	Syngas Combustor Outlet Oxygen	3.2-43
3.2-25	Syngas Combustor Outlet Carbon Dioxide	3.2-44
3.2-26	Syngas Combustor Outlet Moisture	3.2-44
3.2-27	Syngas LHV	3.2-45
3.2-28	Sulfur Emissions	3.2-45
3.2-29	H_2S Analyzer AI419J and Total Reduced Sulfur	3.2-46
3.2-30	Minimum Equilibrium H_2S and Total Reduced Sulfur	3.2-46
3.2-31	NH_3 Analyzer AI475Q and Equilibrium	3.2-47
3.2-32	TC08 (PRB) NH_3 Analyzer AI475Q and Equilibrium NH_3	3.2-47
3.2-33	TC10 (PRB) NH_3 Analyzer AI475Q and Equilibrum NH_3	3.2-48
3.3-1	Solid Sample Locations	3.3-25
3.3-2	Coal Carbon and Moisture	3.3-25
3.3-3	Coal Sulfur and Ash	3.3-26
3.3-4	Coal Heating Value	3.3-26

3.3-5 Gasifier SiO_2, CaO, and Al_2O_3 ..... 3.3-27
3.3-6 Gasifier Organic Carbon and Sodium Oxide 3.3-27
3.3-7 Gasifier Circulating Solids Calcium and Calcium Sulfide 3.3-28
3.3-8 Gasifier PCD Fines Organic Carbon 3.3-28
3.3-9 PCD Fines Silica and Alumina 3.3-29
3.3-10 PCD Fines Calcium and Calcium Sulfide 3.3-29
3.3-11 PCD Fines Calcination and Sulfation 3.3-30
3.3-12 Standpipe and PCD Fines Solids Alumina 3.3-30
3.3-13 Gasifier Solids and PCD Fines Solids Calcium 3.3-31
3.3-14 Gasifier Solids and PCD Fines Solids Sodium in Ash 3.3-31
3.3-15 Coal Particle Size 3.3-32
3.3-16 Percent Coal Fines and Oversize 3.3-32
3.3-17 FD0220 Particle Sizes 3.3-33
3.3-18 Standpipe Solids Particle Size 3.3-33
3.3-19 Standpipe Solids Sodium Oxide and Particle Size 3.3-34
3.3-20 Standpipe Solids Fine and Coarse Particles 3.3-34
3.3-21 PCD Fines Particle Sizes 3.3-35
3.3-22 Particle Size Distribution 3.3-35
3.3-23 Gasifier Solids and PCD Fines Bulk Density 3.3-36

3.4-1 Coal Rates 3.4-23
3.4-2 Air, Nitrogen, Oxygen, and Steam Rates 3.4-23
3.4-3 Air and Syngas Rates 3.4-24
3.4-4 PCD Solids Rate 3.4-24
3.4-5 PCD Fines Rates 3.4-25
3.4-6 Mass Balance 3.4-25
3.4-7 Carbon Balance 3.4-26
3.4-8 Carbon Conversion 3.4-26
3.4-9 Carbon Conversion and Riser Temperature 3.4-27
3.4-10 Carbon Conversion of Four Coals 3.4-27
3.4-11 Nitrogen Balance 3.4-28
3.4-12 Coal Nitrogen Conversion to Ammonia 3.4-28
3.4-13 Coal Nitrogen Conversion to Ammonia and Percent Overall O_2 ..... 3.4-29
3.4-14 Sulfur Balance 3.4-29
3.4-15 Sulfur Removal 3.4-30
3.4-16 Sulfur Emissions 3.4-30
3.4-17 Hydrogen Balance 3.4-31
3.4-18 Steam Rates 3.4-31
3.4-19 Oxygen Balance 3.4-32
3.4-20 Calcium Balance 3.4-32
3.4-21 Silica Balance 3.4-33
3.4-22 Energy Balance 3.4-33
3.4-23 Cold Gasification Efficiency 3.4-34
3.4-24 Cold Gasification Efficiency and Steam-to-Coal Ratio 3.4-34
3.4-25 Hot Gasification Efficiency 3.4-35
3.4-26 Hot Gasification Efficiency and Steam-to-Coal Ratio 3.4-35
3.4-27 Commercially Projected Cold Gasification Efficiency 3.4-36

3.5-1 Sulfator Hotspot 3.5-2

3.6-1 HX0202 Heat Transfer Coefficient and Pressure Drop 3.6-3
3.6-2 HX0402 Heat Transfer Coefficient and Pressure Drop 3.6-3

4.2-1 PCD Filter Element Layout 4.2-6
4.2-2 Westinghouse PCD Failsafe Layout 4.2-7
4.2-3 PCD Normalized Pressure Drops 4.2-8
4.2-4 PCD Pressure Drop and Effect of Back-Pulse Timer 4.2-9

4.3-1 Primary Filter Gaskets on the Lower Plenum After TC13 ..... 4.3-8
4.3-2 Pressure Drop Versus Face Velocity for Pall FEAL Elements With a Fuse After TC13 ..... 4.3-9
4.3-3 Pressure Drop at 3 ft/min Face Velocity for Pall FEAL Elements With a Fuse 4.3-10
4.3-4 Pressure Drop at 3 ft/min Face Velocity for Pall FEAL Element With a Fuse 4.3-11
4.3-5 Pressure Drop Versus Face Velocity for Pall FEAL Elements With No Fuse After TC13 ..... 4.3-12
4.3-6 Pressure Drop at 3 fpm Face Velocity for Pall FEAL Elements Without a Fuse 4.3-13
4.3-7 Cross-Section of the Main Body of Element 39151 After TC13 ..... 4.3-14
4.3-8 Cross-Section of the Fuse of Element 39151 After TC13 ..... 4.3-15
4.3-9 Filter Internals After TC13 ..... 4.3-16
4.3-10 Ceramic Failsafe 4Ba Flow Test Results Before and After TC13 ..... 4.3-17
4.3-11 Ceramic Failsafe 5C Flow Test Results Before and After TC13 ..... 4.3-17
4.3-12 Ceramic Failsafe 5e Flow Test Results Before and After TC13 ..... 4.3-18
4.3-13 Back-Pulse Pipes After TC13 ..... 4.3-19
4.3-14 Cutting Plan for Pall PSS FEAL Filter Element 39151 ..... 4.3-20
4.3-15 Axial Tensile Specimen Configuration for Pall PSS FEAL 4.3-20
4.3-16 Hoop Tensile Specimen Configuration for Pall PSS FEAL 4.3-21
4.3-17 Axial Tensile Stress-Strain Responses Temperature for Pall PSS FEAL 4.3-21
4.3-18 Hoop Tensile Stress-Strain Reponses at RT for Pall PSS FEAL 4.3-22
4.3-19 Tensile Strength Versus Hours of Gasification Operation for Pall PSS FEAL 4.3-22
4.3-20 Tensile Strain-to-Failure Versus Hours of Gasification Operation for Pall PSS FEAL 4.3-23

4.4-1 PCD Inlet Particle Concentration as a Function of Coal-Feed Rate 4.4-22
4.4-2 PDC Outlet Emissions for Recent Gasification Runs 4.4-23
4.4-3 Relationship Between PCME Output and Actual Particle Concentration 4.4-24
4.4-4 Comparison of Average PCD Inlet Particle-Size Distributions on Mass Basis 4.4-25
4.4-5 Comparison of Average PCD Inlet Particle-Size Distributions on Percentage Basis 4.4-26
4.4-6 Comparison of In situ and Hopper Particle-Size Distributions 4.4-27
4.4-7 Laboratory Measurements of TC13 Dustcake Drag Versus Particle Size 4.4-28
4.4-8 Laboratory Measurements of TC11 Dustcake Drag Versus Particle Size 4.4-29

4.4-9 PCD Transient Drag Versus Carbon Content of G-Ash 4.4-30
4.4-10 Comparison of PCD Transient Drag With Laboratory Measurements 4.4-31

1.0 EXECUTIVE SUMMARY

1.1 SUMMARY

This report discusses Test Campaign TC13 of the Kellogg Brown & Root, Inc. (KBR) Transport Gasifier train with a Siemens Westinghouse Power Corporation (Siemens Westinghouse) particulate collection device (PCD) at the Power Systems Development Facility (PSDF) located in Wilsonville, Alabama. The Transport Reactor is an advanced circulating fluidized-bed reactor designed to operate as either a combustor or a gasifier in air- or oxygen-blown mode of operation. Test run TC13 began on September 30, 2003, with the startup of the main air compressor and the lighting of the gasifier startup burner. The Transport Gasifier operated until November 2, 2003, accumulating just over 500 hours of operation. Over the course of the entire test run, the gasifier tested three types of coal: high-sodium lignite from the Freedom Mine in North Dakota, low-sodium lignite from the same mine, and Powder River Basin (PRB) coal.

1.2 PSDF ACCOMPLISHMENTS

The PSDF has achieved over 4,985 hours of operation on coal feed and about 6,470 hours of solids circulation in combustion mode and 6,279 hours of solid circulation and 4,860 hours of coal feed in the gasification mode of operation. The major accomplishments in TC13 are summarized below. For previous combustion- and gasification-related accomplishments, see the technical progress reports located at the PSDF Web site (see title page).

1.2.1 Transport Gasifier Train

The major accomplishments and observations in TC13 included the following:

Process:

- The Transport Gasifier operated for 501 hours using Powder River Basin (PRB) coal and two different types of lignite from the Freedom Mine in North Dakota. The two types of lignite differed primarily in sodium content. The raw high-sodium lignite contained about 5.6-percent sodium (ash mineral analysis), whereas the raw low-sodium lignite possessed a sodium content of around 1.7 percent.
- The majority of the test run was air-blown (432 hours), with around 58 hours in oxygen-blown mode and 11 hours in transition between air- and oxygen-blown modes. All of the oxygen-blown testing occurred while feeding lignite.
- Although the low-sodium lignite portion of the test run was smooth, some deposits occurred while feeding high-sodium lignite at gasifier operating temperatures above 1,650°F. The test run was interrupted twice when deposits formed in the loop seal and once when deposits formed in the standpipe. The deposit in the standpipe was dislodged using aeration flows, however, each loop seal deposit required a complete system shutdown and depressurization to clear the material. The deposits were small, around 2 to 3 inches in diameter, and could be easily broken by hand. However, the deposits interlocked forming an obstruction that would not dislodge on its own. The exact cause of the deposits was not known. Lower temperatures (1,440 to 1,575°F) allowed for steady high-sodium lignite operations for long periods of time.
- Despite operating at lower temperatures with the high-sodium lignite, the gasifier produced a syngas free of oils and tar.
- Riser velocity data are listed in Table 1.2-1.
- Syngas heating value data are also listed in Table 1.2-1. PRB lower heating values were slightly higher than previous PRB lower heating values at similar operating conditions. The lower heating values of syngas generated from the Freedom Mine lignite were higher than those of syngas generated from Falkirk lignite at comparable operating conditions in both air- and oxygen-blown modes.
- Carbon conversion data are listed in Table 1.2-1. The lower carbon conversions using the high-sodium lignite were during periods of operating at lower temperatures in air-blown mode.

- The gasifier bed material changed rapidly during TC13, as process-derived materials replaced the sand present at startup. Standpipe solids samples taken during the test run had a mass mean diameter (D_{50}) of about 150 to 455 μm and carbon content typically below 1 percent. The process-derived solids created during the high-sodium lignite portion of the test run appeared to be agglomerates of fine ash particles. Most of the agglomerates were spherical, and seemed to either be hollow-centered or to have a glassy solidified silica core. The bulk density of the agglomerates was around 60 lb/ft^3.
- Solids obtained from the spent fines feeder had a mass mean particle diameter of around 16 μ during PRB, 20 μ during low sodium-lignite, and 20 μ during low temperature high-sodium operation, while solids obtained from the spent fines feeder had a mass mean particle diameter of around 30 μ during high-temperature, high-sodium lignite operation.
- The solids circulation rate remained high as the process-derived bed material replaced the start-up sand. The riser differential pressure was above 1 inch of water per foot of riser length.
- Sulfur emission data are also listed in Table 1.2-1. The wide range of coal-feed rates caused the high variation in air-blown sulfur emissions. For the lignite coals, only minimal sulfur capture occurred without limestone injection.
- Ammonia emission data are listed in Table 1.2-1. The ammonia emissions from the high-sodium lignite increased as the gasifier temperature decreased.
- The test run ended as scheduled on the afternoon of November 2, 2003. The shutdown was smooth. The post-run inspections showed there were no deposits in the loop seal.

Equipment:

- The coal grinding system showed promise in drying the lignite from a moisture content of 35 percent to a moisture content of 25 percent. The coal feeder experienced no difficulties in feeding the lignite to the gasifier.
- The primary gas cooler performed well, exhibiting no signs of oils or tar deposits.
- For the first time, the combustion turbine at the PSDF ran on syngas, using the PSB (piloted syngas burner). The syngas used in the PSB came from PRB coal.
- Establishing/increasing syngas flow to the PSB, changing syngas load, and terminating syngas flow was accomplished smoothly without any fluctuations in gasifier operations.
- To ensure safe operation of the PSB, several new interlocks were commissioned. All performed as expected during the interlock trials. When interlocks tripped the process gas to the PSB, valves diverted the flow to the flare to avoid causing gasifier pressure upsets. Once the syngas flowed to the flare, logic controls slowly restored the flow through the main pressure letdown valve to the atmospheric syngas burner (thermal oxidizer), which avoided swings in gasifier pressure. In practice, the gasifier pressure changed less than 2.0 psig during each trip.

- PSB operations were steady with the generator producing 1.2 MW. As the syngas flow to the PSB increased, the supplemental propane flow to the PSB decreased from 1,200 to 400 pph and could have decreased further had the PLC logic not prevented the controller from reducing flow below 400 pph.
- The PSB flame remained steady throughout testing. Process variances, such as the PCD back-pulse, did not affect PSB operations. PSB testing on syngas was completed after about 6 hours. When restarting the PSB on the following day, the hydraulics on the cranking motor failed preventing any further PSB testing in TC13.
- Most of the gas analyzers were online for the majority of the test run, presenting good gas composition data. The dry gas compositions added up to between 98 and 102 percent on a consistent basis.
- Extractive gas samples were taken to determine the amounts of trace metal hazardous air pollutants present in the syngas, but naphthalene and three-membered ring compounds formed deposits that hindered much of the planned extractive gas analysis.
- The atmospheric solids combustor ran smoothly during the test run, generating large quantities of high quality superheated steam for use in the gasifier. The bed level stayed fairly constant, and the system only occasionally required additional sand. Whenever solid fuel was unavailable, the fuel oil system worked well at maintaining the bed temperatures. During the test run, a high skin temperature developed near one of the steam coil bundles where some localized refractory erosion had occurred.
- A new FD0530 feeder for g-ash was operated at a rate much steadier than in previous test runs, although it still fed over a relatively narrow range of feed rates. The carryover rate and carbon content in the FD0530 solids was large during the low temperature testing, thus the combustor had difficulty burning the material at a rate sufficient to keep pace with the solids collected.

1.2.2 PCD

The highlights of PCD operation for TC13 are listed below.

- PCD operations were stable throughout TC13 including stable operation during the PSB testing. For most of the test run, the baseline pressure drop was about 50 to 75 inH_2O. During steady-state operations, the inlet temperature was about 600 to 800°F, and the face velocity remained around 3 to 4.5 ft/min.
- During the run, the back-pulse pressure was 320 psid on the top plenum and 400 psi on the bottom plenum. As in recent runs, the back-pulse timer varied from 5 to 20 minutes in an effort to further optimize the back-pulse parameters.
- Outlet loading samples indicated good sealing of the filter vessel. All the measurements showed outlet concentrations below the sampling system lower limit of detection of 0.1 ppmw except for two samples that indicated loadings of 0.25 and 0.11 ppmw.
- The fines removal system operated well during most of the run. One problem that occurred was the failure of the lock vessel Everlasting valve to close on several

occasions, presumably due to solids trapped in the valve. However, the lock vessel spheri valve operated successfully during the times when the Everlasting valve was not functioning. The drive-end seal on the spent fines screw cooler failed and caused a short delay in the run for repairs.

- Evaluation of new resistance probes for level detection in the fines lock hopper system continued. The testing included a new probe and transmitter, both exhibiting reliable results.
- The PCD was shut down "clean" and was back-pulsed continually for over half a day after the end of coal feed. The residual cake was thin and comparable to that seen from recent runs.
- A preliminary inspection of the PCD internals revealed no obvious problems. No g-ash bridging or filter failures were present. In addition, no plugging occurred in the Westinghouse inverted filter element assemblies.

Table 1.2-1

Operating Data Summary

		PRB	Low Sodium Freedom Lignite	Freedom Lignite	High Sodium Freedom Lignite
	Units	Air	Air	Oxygen	Air
Hours[1]	hrs	117	64	58	247
Temperature	°F	1,710-1,767	1,700-1,734	1,649-1,709	1,440-1,672
Pressure	psig	180-190	176-194	110-140	91-180
Riser Velocity	ft/s	34-50	40-56	51-55	36-49
Raw syngas lower heating value	Btu/scf	37-57	36-58	55-69	24-44
Projected syngas lower heating value for commercial operation	Btu/scf	96-107	76-91	132-148	70-90
Carbon conversion based on corresponding flow of PCD solids and synthesis gas	%	96-99	93-97	87-98	77-99
Sulfur content in syngas leaving the gasifier - total reduced sulfur (TRS)	ppm	222-449	1,377-1,732	1,451-2,209	844-1,318
Gasifier ammonia emissions	ppm	483-1,596	653-1,298	1,653-2,528	884-2,350

Note:
1. The hours do not include 4 hours of air-blown operation with a mixture of PRB and Freedom lignite and 11 hours in transition between air- and oxygen-blown modes.

2.0 INTRODUCTION

This report provides an account of the TC13 test campaign with the Kellogg Brown & Root, Inc. (KBR) Transport Gasifier and the Siemens Westinghouse Power Corporation (Siemens Westinghouse) filter vessel at the Power Systems Development Facility (PSDF) located in Wilsonville, Alabama, 40 miles southeast of Birmingham. The PSDF is sponsored by the U. S. Department of Energy (DOE) and is an engineering-scale demonstration of advanced coal-fired power systems. In addition to DOE, Southern Company Services, Inc., (SCS), Electric Power Research Institute (EPRI), and Peabody Energy are cofunders. Other cofunding participants supplying services or equipment currently include KBR, the Lignite Energy Council and Siemens Westinghouse. SCS is responsible for constructing, commissioning, and operating the PSDF.

2.1 THE POWER SYSTEMS DEVELOPMENT FACILITY

SCS entered into an agreement with DOE/National Energy Technology Laboratory (NETL) for the design, construction, and operation of a hot gas clean-up test facility for pressurized gasification and combustion. The purpose of the PSDF is to provide a flexible test facility that can be used to develop advanced power system components and assess the integration and control issues of these advanced power systems. The facility also supports Vision 21 programs to eliminate environmental concerns associated with using fossil fuels for producing electricity, chemicals and transportation fuels. The facility was designed as a resource for rigorous, long-term testing and performance assessment of hot stream clean-up devices and other components in an integrated environment.

The PSDF now consists of the following modules for systems and component testing:

- A Transport Reactor module.
- A hot gas clean-up module.
- A compressor/turbine module.
- A gas clean-up module.

The Transport Reactor module includes KBR Transport Reactor technology for pressurized combustion and gasification to provide either an oxidizing or reducing gas for parametric testing of hot particulate control devices. The Transport Gasifier can be operated in either air- or oxygen-blown modes. Oxygen-blown operations are primarily focused on testing and developing various Vision 21 programs to benefit gasification technologies in general. The hot gas clean-up filter system tested to date at the PSDF is the particulate control device (PCD) supplied by Siemens Westinghouse. The gas turbine is an Allison Model 501-KM gas turbine, which drives a synchronous generator through a speed reducing gearbox. The Model 501-KM engine was designed as a modification of the Allison Model 501-KB5 engine to provide operational flexibility. Design considerations include a large, close-coupled external combustor to burn a wide variety of fuels and a fuel delivery system that is much larger than the standard system. A small portion of the synthesis gas (taken from

downstream of the PCD) can also flow to a gas clean-up system to provide a synthesis gas suitable for use in testing additional downstream equipment, e.g., use in a fuel cell.

2.2 TRANSPORT GASIFIER SYSTEM DESCRIPTION

The Transport Gasifier is an advanced circulating fluidized-bed reactor operating in air- or oxygen-blown mode, using a hot gas clean-up filter technology (particulate control devices [PCDs]) at a component size readily scaleable to commercial systems. The Transport Gasifier train is shown schematically in Figure 2.2-1. A taglist of all major equipment in the process train and associated balance-of-plant is provided in Tables 2.2-1 and 2.2-2.

The Transport Gasifier consists of a mixing zone, a riser, a disengager, a cyclone, a standpipe, a loop seal, and a J-leg. Steam and air or oxygen are mixed together and introduced in the lower mixing zone (LMZ) while the fuel, sorbent, and additional air and steam (if needed) are added in the upper mixing zone (UMZ). The steam and air or oxygen along with the fuel, sorbent and solids from the standpipe are mixed together in the upper mixing zone. The mixing zone, located below the riser, has a slightly larger diameter than the riser. The gas and solids move up the riser together, make two turns and enter the disengager. The disengager removes larger particles by gravity separation. The gas and remaining solids then move to the cyclone, which removes most of the particles not collected by the disengager. The gas then exits the Transport Gasifier and goes to the primary gas cooler and the PCD for final particulate cleanup. The solids collected by the disengager and cyclone are recycled back to the gasifier mixing zone through the standpipe and a J-leg. The nominal Transport Gasifier operating temperature is 1,800°F. The gasifier system is designed to have a maximum operation pressure of 294 psig with a thermal capacity of about 41 MBtu/hr. Due to a lower oxygen supply pressure the maximum operation pressure is about 160 psi in oxygen-blown mode.

For start-up purposes, a burner (BR0201) is provided at the gasifier mixing zone. Liquefied propane gas (LPG) is used as start-up fuel. The fuel and sorbent are separately fed into the Transport Gasifier through lockhoppers. Coal is ground to a nominal average particle diameter between 250 and 400 μ. Sorbent is ground to a nominal average particle diameter of 10 to 30 μ. Limestone or dolomitic sorbents are fed into the gasifier for sulfur capture. The gas leaves the Transport Gasifier cyclone and goes to the primary gas cooler which cools the gas prior to entering the Siemens Westinghouse PCD barrier filter. The PCD uses ceramic or metal elements to filter out dust from the gasifier. The filters remove almost all the dust from the gas stream to prevent erosion of a downstream gas turbine in a commercial plant and to reduce the plant particulate emissions. The operating temperature of the PCD is controlled both by the gasifier temperature and by an upstream gas cooler. For test purposes, 0 to 100 percent of the gas from the Transport Gasifier can flow through the gas cooler. The PCD gas temperature can range from 700 to 1,600°F. The filter elements are back-pulsed by high-pressure nitrogen in a desired time interval or at a given maximum pressure difference across the elements. There is a secondary gas cooler after the filter vessel to cool the gas before discharging to the stack or atmospheric syngas combustor (thermal oxidizer). In a commercial process, the gas from the PCD would be sent to the gas turbine of a combined-cycle unit. At the PSDF, a small portion of the synthesis gas can also flow to a specialized gas clean-up system downstream of the PCD. The gas clean-up system removes sulfur, nitrogen, and chlorine compounds, providing a synthesis gas suitable for use in a fuel cell. The main flow of fuel gas continues down one of the following two alternative paths.

In one case, the fuel gas flows to the secondary gas cooler and is sampled for on-line analysis thereafter. After exiting the secondary gas cooler, the gas pressure is then lowered to about 2

psig through a pressure control valve. The fuel gas is then sent to the atmospheric syngas burner to burn the gas and oxidize all reduced sulfur compounds (H_2S, COS, and CS_2) and reduced nitrogen compounds (NH_3 and HCN). The atmospheric syngas burner uses propane as a supplemental fuel. The gas from the atmospheric syngas burner goes to the baghouse and then to the stack. In the alternative path, the fuel gas flows for combustion in the piloted syngas burner to supply the gas turbine/generator, and then the flue gas goes to the stack.

The Transport Gasifier produces both fine ash collected by the PCD and coarse ash extracted from the Transport Gasifier standpipe. Using screw coolers, the two solid streams are cooled, pressure reduced in lock hoppers, and then combined. Any fuel sulfur captured by sorbent should be present as calcium sulfide (CaS). Testing of the g-ash has shown that it does not contain hazardous levels of CaS and that the waste solids are suitable for commercial use or disposal. Therefore, the ash is sent directly to the ash silo for disposal, although, the capability to feed the ash to an atmospheric fluidized-bed combustor is retained.

Table 2.2-1

Major Equipment in the Transport Reactor Train

TAG NAME	DESCRIPTION
BR0201	Reactor Start-Up Burner
BR0401	Syngas Combustor (Thermal Oxidizer)
BR0602	AFBC (Sulfator) Start-Up/PCD Preheat Burner
CO0201	Main Air Compressor
CO0401	Recycle Gas Booster Compressor
CO0601	AFBC (Sulfator) Air Compressor
CY0201	Primary Cyclone in the Reactor Loop
CY0207	Disengager in the Reactor Loop
CY0601	AFBC (Sulfator) Cyclone
DR0402	Steam Drum
DY0201	Feeder System Air Dryer
FD0206	Spent Solids Screw Cooler
FD0200	Fluidized Bed Coal Feeder System
FD0210	Coal Feeder System
FD0220	Sorbent Feeder System
FD0502	Fines Screw Cooler
FD0510	Spent Solids Transporter System
FD0520	Fines Transporter System
FD0530	Spent Solids Feeder System
FD0602	AFBC (Sulfator) Solids Screw Cooler
FD0610	AFBC (Sulfator) Sorbent Feeder System
FL0301	PCD — Siemens Westinghouse
FL0302	PCD — Combustion Power
FL0401	Compressor Intake Filter
HX0202	Primary Gas Cooler
HX0203	Combustor Heat Exchanger
HX0204	Transport Air Cooler
HX0402	Secondary Gas Cooler
HX0405	Compressor Feed Cooler
HX0601	AFBC (Sulfator) Heat Recovery Exchanger
ME0540	Heat Transfer Fluid System
RX0201	Transport Reactor
SI0602	Spent Solids Silo
SU0601	Atmospheric Fluidized-Bed Combustor (AFBC)

Table 2.2-2 (Page 1 of 3)

Major Equipment in the Balance-of-Plant

TAG NAME	DESCRIPTION
BO2920	Auxiliary Boiler
BO2921	Auxiliary Boiler – Superheater
CL2100	Cooling Tower
CO2201A-D	Service Air Compressor A-D
CO2202	Air-Cooled Service Air Compressor
CO2203	High-Pressure Air Compressor
CO2601A-C	Reciprocating N_2 Compressor A-C
CR0104	Coal and Sorbent Crusher
CV0100	Crushed Feed Conveyor
CV0101	Crushed Material Conveyor
DP2301	Baghouse Bypass Damper
DP2303	Inlet Damper on Dilution Air Blower
DP2304	Outlet Damper on Dilution Air Blower
DY2201A-D	Service Air Dryer A-D
DY2202	Air-Cooled Service Air Compressor Air Dryer
DY2203	High-Pressure Air Compressor Air Dryer
FD0104	MWK Coal Transport System
FD0111	MWK Coal Mill Feeder
FD0113	Sorbent Mill Feeder
FD0140	Coke Breeze and Bed Material Transport System
FD0154	MWK Limestone Transport System
FD0810	Ash Unloading System
FD0820	Baghouse Ash Transport System
FL0700	Baghouse
FN0700	Dilution Air Blower
HO0100	Reclaim Hopper
HO0105	Crushed Material Surge Hopper
HO0252	Coal Surge Hopper
HO0253	Sorbent Surge Hopper
HT2101	MWK Equipment Cooling Water Head Tank
HT2103	SCS Equipment Cooling Water Head Tank
HT0399	60-Ton Bridge Crane
HX2002	MWK Steam Condenser
HX2003	MWK Feed Water Heater

Table 2.2-2 (Page 2 of 3)

Major Equipment in the Balance-of-Plant

TAG NAME	DESCRIPTION
HX2004	MWK Subcooler
HX2103A	SCS Cooling Water Heat Exchanger
HX2103C	MWK Cooling Water Heat Exchanger
LF0300	Propane Vaporizer
MC3001-3017	MCCs for Various Equipment
ME0700	MWK Stack
ME0701	Flare
ME0814	Dry Ash Unloader for MWK Train
ML0111	Coal Mill for MWK Train
ML0113	Sorbent Mill for Both Trains
PG0011	Oxygen Plant
PG2600	Nitrogen Plant
PU2000A-B	MWK Feed Water Pump A-B
PU2100A-B	Raw Water Pump A-B
PU2101A-B	Service Water Pump A-B
PU2102A-B	Cooling Tower Make-Up Pump A-B
PU2103A-D	Circulating Water Pump A-D
PU2107	SCS Cooling Water Make-Up Pump
PU2109A-B	SCS Cooling Water Pump A-B
PU2111A-B	MWK Cooling Water Pump A-B
PU2300	Propane Pump
PU2301	Diesel Rolling Stock Pump
PU2302	Diesel Generator Transfer Pump
PU2303	Diesel Tank Sump Pump
PU2400	Fire Protection Jockey Pump
PU2401	Diesel Fire Water Pump #1
PU2402	Diesel Fire Water Pump #2
PU2504A-B	Waste Water Sump Pump A-B
PU2507	Coal and Limestone Storage Sump Pump
PU2700A-B	Demineralizer Forwarding Pump A-B

Table 2.2-2 (Page 3 of 3)

Major Equipment in the Balance-of-Plant

TAG NAME	DESCRIPTION
PU2920A-B	Auxiliary Boiler Feed Water Pump A-B
SB3001	125-V DC Station Battery
SB3002	UPS
SC0700	Baghouse Screw Conveyor
SG3000-3005	4160-V, 480-V Switchgear Buses
SI0101	MWK Crushed Coal Storage Silo
SI0103	Crushed Sorbent Storage Silo
SI0111	MWK Pulverized Coal Storage Silo
SI0113	MWK Limestone Silo
SI0114	FW Limestone Silo
SI0810	Ash Silo
ST2601	N_2 Storage Tube Bank
TK2000	MWK Condensate Storage Tank
TK2001	FW Condensate Tank
TK2100	Raw Water Storage Tank
TK2300A-D	Propane Storage Tank A-D
TK2301	Diesel Storage Tank
TK2401	Fire Water Tank
XF3000A	230/4.16-kV Main Power Transformer
XF3001B-5B	4160/480-V Station Service Transformer No. 1-5
XF3001G	480/120-V Miscellaneous Transformer
XF3010G	120/208 Distribution Transformer
XF3012G	UPS Isolation Transformer
VS2203	High-Pressure Air Receiver

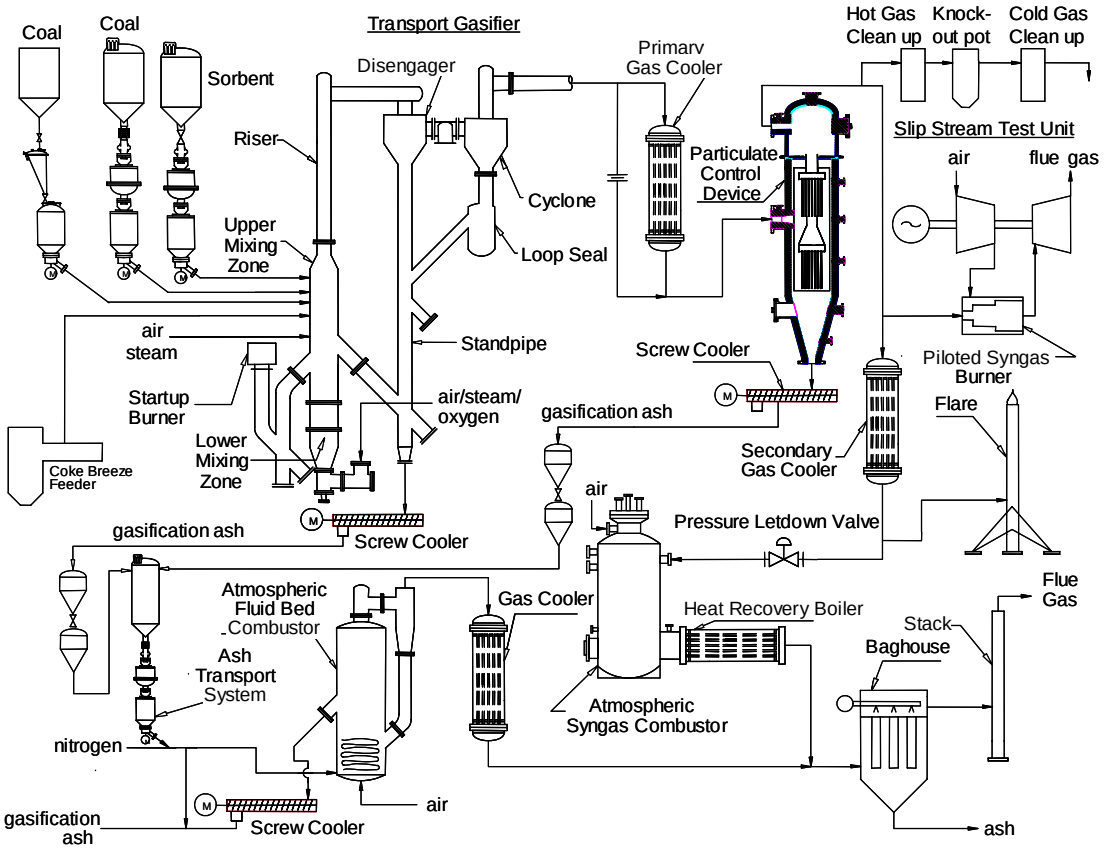

Figure 2.2-1 Flow Diagram of the Transport Gasifier Train

2.3 SIEMENS WESTINGHOUSE PARTICULATE CONTROL DEVICE

The PCD that has been used in all of the testing to date was designed by Siemens Westinghouse. The dirty gas enters the PCD below the tube sheet and flows through the filter elements, depositing the particulate on the filter element surface. The clean gas passes from the plenum/filter element assembly through the plenum pipe to the outlet pipe. As the particulate collects on the outside surface of the filter elements, the pressure drop across the filter system gradually increases. The filter cake is periodically dislodged by injecting a high-pressure gas pulse to the clean side of the filter elements. The cake then falls to the discharge hopper.

Until the first gasification run in late 1999, the Transport Reactor had been operated only in the combustion mode. Initially, high-pressure air was used as the pulse gas for the PCD, however, the pulse gas was changed to nitrogen early in 1997. The pulse gas was routed individually to the two plenum/filter element assemblies via injection tubes mounted on the top head of the PCD vessel. The pulse duration was typically 0.1 to 0.5 seconds.

A sketch of the Siemens Westinghouse PCD is shown in Figure 2.3-1.

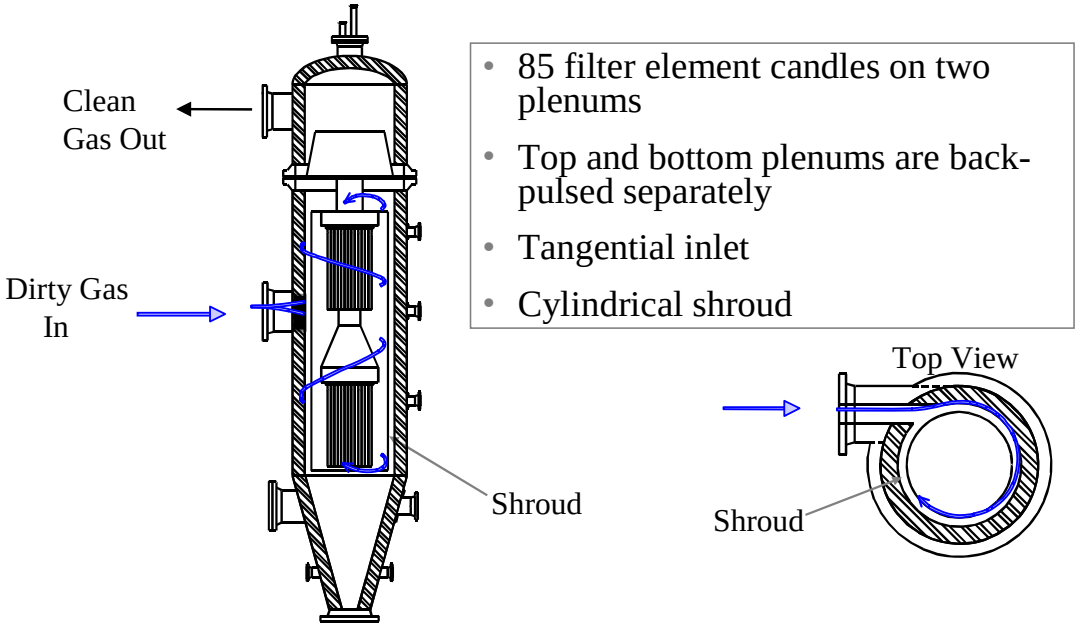

Figure 2.3-1 Siemens Westinghouse PCD (FL0301)

2.4 OPERATION HISTORY

Conversion of the Transport Reactor train to gasification mode of operation was performed from May to September 1999. The first gasification test run, GCT1, was planned as a 250-hour test run to commission the Transport Gasifier and to characterize the limits of operational parameter variations. GCT1 was started on September 9, 1999, with the first part completed on September 15 (GCT1A). The second part of GCT1 was started on December 7, 1999, and completed on December 15 (GCT1B-D). This test run provided the data necessary for preliminary analysis of gasifier operations and for identification of necessary modifications to improve equipment and process performance. Five different feed combinations of coal and sorbent were tested to gain a better understanding of the gasifier solids collection system efficiency.

GCT2, planned as a 250-hour characterization test run, was started on April 10, 2000, and completed on April 27. Additional data was taken to analyze the effect of different operating conditions on gasifier performance and operability. A blend of several Powder River Basin (PRB) coals was used with Longview limestone from Alabama. In the outage following GCT2, the Transport Gasifier underwent a major modification to improve the operation and performance of the gasifier solids collection system. The most fundamental change was the addition of the loop seal underneath the primary cyclone.

GCT3 was planned as a 250-hour characterization with the primary objective to commission the loop seal. A hot solids circulation test (GCT3A) was started on December 1, 2000, and completed December 15. After a 1-month outage to address maintenance issues with the main air compressor, GCT3 was continued. The second part of GCT3 (GCT3B) was started on January 20, 2001, and completed on February 1. During GCT3B, a blend of several PRB coals was used with Bucyrus limestone from Ohio. The loop seal performed well; needing little attention and promoting much higher solids circulation rates and higher coal feed rates that resulted in lower relative solids loading to the PCD and higher char retention in the gasifier.

GCT4, planned as a 250-hour characterization test run, was started on March 7, 2001, and completed on March 30. A blend of several PRB coals with Bucyrus limestone from Ohio was used. More experience was gained with the loop seal operations and additional data was collected to better understand gasifier performance.

TC06, a 1,025-hour test campaign, was started on July 4, 2001, and completed on September 24. A blend of several PRB coals with Bucyrus limestone from Ohio was used. Both gasifier and PCD operations were stable during the test run with a stable baseline pressure drop. Due to its length and stability, the TC06 test run provided valuable data necessary to analyze long-term gasifier operations and to identify necessary modifications to improve equipment and process performance.

TC07, a 442-hour test campaign, was started on December 11, 2001, and completed on April 5, 2002. A blend of several PRB coals and a bituminous coal from the Calumet mine in Alabama were tested with Bucyrus limestone from Ohio. Due to operational difficulties

with the gasifier (stemming from instrumentation problems), the unit was taken offline several times. PCD operations were relatively stable considering the numerous gasifier upsets.

TC08, a 365-hour test campaign (153 hours oxygen blown) to commission the gasifier in oxygen-blown mode of operation, was started on June 9, 2002, and completed on June 29. A blend of several PRB coals was tested in air-blown, enriched-air, and oxygen-blown modes of operation. The transition from different modes of operation was smooth and demonstrated that the full transition could be made within 15 minutes. Both gasifier and PCD operations were stable during the test run with a stable baseline pressure drop.

TC09 was a 309-hour test campaign (80 hours oxygen blown) to characterize the gasifier and PCD operations in air- and oxygen-blown mode of operations using a bituminous coal. TC09 was started on September 3, 2002, and completed on September 26. A bituminous coal from the Sufco Mine in Utah was successfully tested in air- and oxygen-blown modes of operation. Both gasifier and PCD operations were stable during the test run.

TC10 was a 416-hour test campaign (244 hours oxygen blown) to conduct long-term tests to evaluate the gasifier and PCD operations in oxygen-blown mode of operations using a blend of several PRB coals. TC10 was started on November 16, 2002, and completed on December 18. Despite problems with the coal mills, coal feeder, pressure tap nozzles, and the standpipe, the gasifier did experience short periods of stability during oxygen-blown operations. During these periods, the syngas quality was high. During TC10, over 609 tons of Powder River Basin subbituminous coal were gasified.

TC11 was a 192-hour test campaign (7 hours oxygen blown) to conduct short-term tests to evaluate the gasifier and PCD operations in air- and oxygen-blown mode of operations using lignite from North Dakota. TC11 was started on April 7, 2003, and completed on April 18. During TC11, the lignite proved difficult to feed due to difficulties in the mill operation as a result of the high moisture content in the fuel. However, the gasifier operated better using lignite than with any other feedstock used to date. The lignite allowed high circulation rates and riser densities. Consequently, the temperature distribution in both the mixing zone and the riser was more uniform than in any previous test run, varying less than 10°F throughout the gasifier.

TC12 was a 733-hour test campaign (603 hours oxygen-blown) to conduct short-term tests to evaluate the gasifier and PCD operations in air- and oxygen-blown mode of operations using a blend of several PRB coals. TC12 was started on May 16, 2003, and completed on July 14. A primary focus for TC12 was commissioning a new gas clean-up system and operating a fuel cell on syngas derived from the Transport Gasifier. The fuel cell system and gas clean-up system both performed well during the testing.

TC13, the subject of this report, was a 501-hour test campaign (58 hours oxygen-blown) to conduct short-term tests. Evaluations of the gasifier, the PSB, and PCD operations in air-blown mode of operations using a blend of several PRB coals were conducted, as well as, short-term tests to evaluate gasifier and PCD operations using two different types of lignite

coal from the Freedom Mine in North Dakota. One of the types of lignite had a high sodium content in the ash, while the other type had a low sodium content. TC13 was started on September 30, 2003, and completed on November 2. The PSB on syngas testing lasted for a total of about 6 hours. While successful, the hydraulic system on the turbine cranking motor failed and prevented further PSB testing. The low sodium lignite testing went well, but lowering the gasifier temperature to below 1,500°F was necessary to prevent deposits from forming with the high sodium lignite. As during the Falkirk lignite test run, gasifier temperatures appeared uniform with both of the lignite fuels.

Figure 2.4-1 gives a summary of operating test hours achieved with the Transport Reactor at the PSDF.

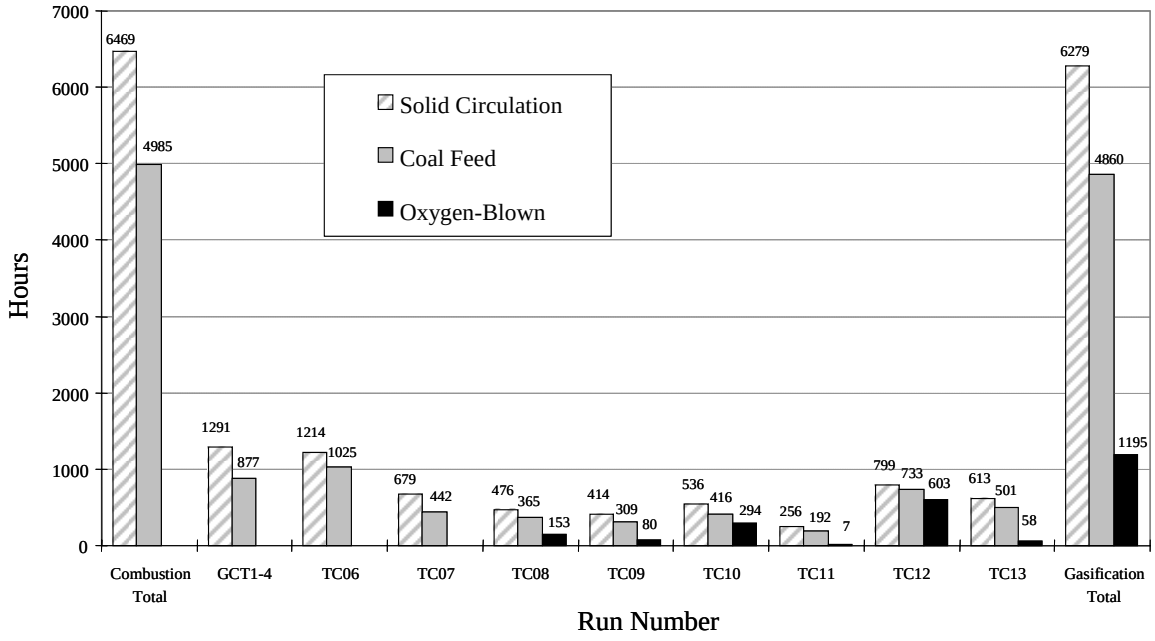

Figure 2.4-1 Operating Hours Summary for the Transport Reactor Train

3.0 TRANSPORT GASIFIER

3.1 RUN SUMMARY

Test run TC13 began on September 30, 2003, with the startup of the main air compressor and the lighting of the gasifier start-up burner. The Transport Gasifier operated until November 2, 2003, accumulating just over 500 hours of operation. Over the course of the entire test run, the gasifier tested three types of coal: high-sodium lignite from the Freedom Mine in North Dakota, low-sodium lignite from the same mine, and Powder River Basin (PRB) coal. The gasifier operating temperatures varied from 1,710 to 1,767°F while using PRB, from 1,649 to 1,734°F when using low-sodium lignite, and from 1,440 to 1,709°F when using high-sodium lignite.

The primary objectives of test run TC13 were as follows:

- Testing the operation of the Piloted Syngas Burner (PSB) on syngas – Evaluate the operation of the PSB and turbine on syngas derived from PRB coal in air-blown mode.
- The gasification of Freedom Mine lignite coals – Evaluate the operation of the Transport Gasifier using two different lignite coals from the Freedom Mine in North Dakota and study the effects of the lignite coals on process performance, operational stability, and temperature profiles.

Secondary objectives included the following:

- Evaluate the effects of the gasifier conditions on the process performance – Continue to evaluate the effects of different gasifier parameters such as the steam-to-coal ratio and the temperature on the CO/CO_2 ratio, the carbon conversion, the syngas composition, the sulfur and ammonia concentrations, the cold and hot gas efficiencies, and tar cracking effects.
- Test the new fluidized-bed coal-feed system – Test the new fluidized-bed coal-feed system and the integration of the gasifier logic with the feeder logic.
- Automation – Demonstrate and improve the automatic control of the gasifier including the single-parameter temperature controls in air-blown mode, the multiparameter temperature controls (MPTC) in oxygen-blown mode, and the steam drum level controls. Also, integrate the new fluidized-bed coal feeder into the MPTC logic; integrate the PSB logic with the gasifier controls and operation; and improve the temperature profile controls and coal-feed rate measurements.
- Evaluate instrumentation required for automation – Continue the evaluation of thermowells and pressure differential measurements in the Transport Gasifier including the use of various materials of construction, new designs, and new fabrication methods. Continue commissioning and evaluating the nuclear density instruments for solids flow rates and solids inventory measurements.
- Study the effect of moisture on the coal-feed system – Study the effect of the coal moisture content on the feed system operations. Improve the coal grinding process to reduce the amount of moisture in the coal.

The activities that occurred during the outage preceding test run TC13 included 22 equipment revisions. Those affecting the process the most were the modifications listed below:

- Provisions were made for sending syngas from the Transport Gasifier to the PSB and turbine. The new syngas-to-turbine line, and its associated valves and instruments, allows syngas to flow to the turbine originally integrated with the PSDF Foster Wheeler equipment.
- Several new types of thermowells for testing in the gasifier were installed.
- The oxygen-blown control loop was modified. The changes to the control loop were to help control the gasifier temperatures more accurately when in oxygen-blown mode.

Prior to startup, the PSB interlock trials took place. After several days of testing, the results proved satisfactory and the test run began. All gasifier start-up processes, including the PCD preheat, and gasifier preheat using the start-up burner, went smoothly. When the gasifier temperature reached 1,250°F on the evening of October 1, 2003, coke breeze feed began with coal feed beginning at 20:48. The gasifier operated for several hours at a maximum temperature of 1,775°F and at a coal-feed rate of around 2,000 pph. A plant power outage at 08:46 the next morning tripped the entire plant. The outage only lasted a few minutes, and coal feed resumed less than 1 hour later.

Once the gasifier was running normally again, PSB integration testing began. Due to an error in the PSB controls an excessive amount of propane entered the burner, resulting in a pressure excursion in the PSB. The unit was undamaged and testing resumed the following day.

During this time, the gasifier operated in a very stable manner at a coal-feed rate around 3,000 pph at 180 psig in air-blown mode, while generating a syngas with a raw lower heating value of around 50 Btu/scf. The PSB testing resumed on October 3. The tests succeeded in purging and warming the syngas-to-turbine line, as well as initiating syngas to the PSB without causing a significant pressure swing in the gasifier. Towards the end of the testing, the PSB achieved a syngas flow rate of up to 15,000 pph with only 460 pph of pilot and enrichment propane, while maintaining a generator output of 1.2 MW. The stack carbon monoxide level was around 60 ppm at the time. At the conclusion of the testing, the shutdown logic was able to divert the syngas first to the flare, then through the main pressure letdown valve to the atmospheric syngas combustor without disrupting the gasifier pressure. Upon the attempt to restart the turbine the next day, the hydraulic system on the crank motor failed, preventing further testing of the PSB.

Using PRB coal, the gasifier continued to run steadily at temperatures between 1,710 and 1,750°F and at a pressure of 180 psig. Early in the morning on October 5, the fluidized-bed coal feeder (FD0200) began to feed PRB coal along with the original coal-feed system (FD0210), bringing the total coal feed rate up to nearly 4,000 pph. Although the FD0200 feeder did experience a few plugging problems, for the most part it ran well and accumulated almost 138 hours during TC13. The FD0210 feeder experienced a small problem with debris that plugged a filter in the control nitrogen. The FD0200 feeder was able to provide coal to the gasifier for the brief periods of time that the FD0210 feeder was shut down for the repairs.

At 18:30 on October 6 the coal feed was transitioned from PRB to low-sodium lignite through FD0210. For a brief period of time the FD0200 feeder continued to feed PRB coal as the FD0210 feeder fed lignite. At 22:00 on October 6 the FD0200 began feeding the low-sodium lignite as well. As the transition occurred, the syngas sulfur content increased, but the lower heating value of the syngas remained roughly the same.

With the exception of the FD0200 feeder plugging occasionally, conditions generally remained steady. The total coal-feed rate was typically around 3,000 pph, and the steam flow rate to the gasifier was around 1,000 pph. The FD0220 feeder fed limestone periodically to control the sulfur content in the syngas.

On October 9 at 13:50 the transition to oxygen-blown operations took place. To avoid generating hot spots the transition occurred slowly, lasting almost 2 days in an oxygen-enriched-air mode before entering full oxygen-blown mode. The transition began while using the low-sodium lignite at 13:04 on October 11. At 23:55 on October 10, while still in the enriched-air period, the FD0200 feeder began feeding the high-sodium lignite to the gasifier as FD0210 continued feeding low-sodium lignite. The FD0210 feeder began to feed high-sodium lignite at 21:05 on October 11, concluding the low-sodium lignite tests. All testing with the low-sodium lignite went smoothly, generating syngas with a lower heating value, up to 58 Btu/scf at a coal-feed rate of around 5,000 pph in air-blown mode.

Testing with the high-sodium lignite proved to be a challenge. Initially the gasifier was operated at 1,700°F with the high-sodium lignite in oxygen-blown mode. On October 12, just 1 day into the testing, a solid restriction lodged in the loop seal, stopping circulation and forcing an outage to remove the material. The material in the loop seal was soft and crumbled when touched. In addition, a porous deposit had formed in the LMZ. Since the deposit allowed gas to pass through, it was not removed during the short outage.

Coal feed resumed on October 15 in air-blown mode with maximum gasifier temperatures around 1,700°F. The syngas generated from the lignite had a lower heating value of 37 to 42 Btu/scf at a coal-feed rate of around 2,900 pph. The test run was interrupted again, however, when more deposits formed in the gasifier and again restricted the loop seal, forcing another outage on October 20. Like the previous agglomeration, the material was soft and easy to break. The gasifier start-up procedure began the following day, but before coal feed began, additional material (presumably from the secondary crossover) fell into the loop seal causing yet another restriction and subsequent outage. After the loop seal was cleaned, the test run resumed.

The coal feeder began feeding coal again at 13:01 on October 23. Shortly after starting coal flow a restriction formed in the standpipe. Adjusting standpipe fluidization flows cleared the restriction and an outage was unnecessary. Once the standpipe was clear, and the gasifier was at sufficient temperatures, the test run resumed on October 25.

For the remainder of the test run, the maximum gasifier temperature was maintained at 1,500 to 1,575°F. These lower temperatures prevented any further restrictions from forming. The coal-feed rate was initially around 2,000 pph with a resulting syngas lower heating value of 25 Btu/scf. However, the same low temperatures that prevented deposits from forming kept the carbon

conversion low, at between 77 and 84-percent. Despite the lower temperatures, the water samples in the gas clean-up unit indicated that no tar or oil formed in the gasifier. The coal rate increased the LHV to 34 Btu/scf.

Another unscheduled outage occurred on October 28 when the packing in the spent fines screw cooler blew out. The incident required depressurizing the system for repairs. Once the repairs were complete, the test run resumed. The coal-feed rate after the outage ranged from 3,000 to 4,000 pph, generating syngas with a lower heating value of between 33 and 44 Btu/scf. Higher coal-feed rates were not possible due to the low carbon conversion and the size limitations on the spent solids systems and the atmospheric fluidized-bed combustor.

The gasifier remained stable at these conditions until the scheduled shutdown at 15:00 on November 2, 2003. The PCD shutdown was "clean," meaning that no transient cake was left on the PCD filter elements. During the test run the gasifier accumulated 501 hours of coal feed, 58 of which were in oxygen-blown mode. The Transport Gasifier has now gasified coal for over 4,860 hours.

The post-run inspections revealed that the gasifier refractory continued to show only minor wear since starting gasification. A moderate-sized deposit formed in the bottom of the secondary crossover, but it is unknown when this occurred.

The test run contained the following steady-state test periods:

Name	Comments
TC13-1	First steady-state period. PRB.
TC13-2	Increased temperature, circulation rate.
TC13-3	Increased steam flow rate. Increased temperatures.
TC13-4	Decreased steam.
TC13-5	Decreased temperatures.
TC13-6	Decreased circulation rate.
TC13-7	Increased coal-feed rate.
TC13-8	FD0200 on. Increased coal, temperatures, pressure.
TC13-9	FD0200 on. Increased mixing zone temperature.
TC13-10	First Low Na lignite test.
TC13-11	Increased temperatures.
TC13-12	FD0200 on. Increased pressure, coal.
TC13-13	FD0200 on. Began oxygen-blown testing.
TC13-14	FD0200 on. Decreased coal, pressure.
TC13-15	FD0200 on. 80/20. Hi/Lo Na lignite mixture test.
TC13-16	FD0200 on. High Na Lignite. Oxygen-blown test.
TC13-17	Air blown test. Increased pressure.
TC13-18	Decreased temperatures, circulation.
TC13-19	Decreased temperatures, circulation.
TC13-20	Decreased pressure, coal.
TC13-21	Increased temperature. Decreased pressure.
TC13-22	Decreased temperature and pressure.

TC13-23 Increased coal, pressure. Decreased temperatures.
TC13-24 Decreased temperatures. Increased coal.
TC13-25 Increased coal, temperatures.
TC13-26 Recovery after deviation from steady state.
TC13-27 Decreased temperatures.
TC13-28 Reduced circulation.
TC13-29 Reduced steam flow rate.

Table 3.1-1

Operating Conditions for Transport Gasifier

Start-Up Bed Material	Sand (~120 μm)
Start-Up Fuel	Coke Breeze
Fuel Type	Powder River Basin North Dakota Lignite (Freedom Mine) • Low Sodium • High Sodium
Fuel Particle Size (mmd)	PRB – 150 to 350 Lignite – 280 to 680
Coal-Feed Rate (pph)	1,900 to 5,000
Sorbent Type	Ohio Bucyrus Limestone
Sorbent Particle Size (mmd)	15 to 20 μm
Sorbent Feed Rate (pph)	0 to 180
Gasifier Temperature (°F)	1,440 to 1,767
Gasifier Pressure (psig)	91 to 194
Riser Gas Velocity (fps)	25 to 45
Riser Mass Flux ($lb/s \cdot ft^2$)	350 to 450 (average slip ratio = 2)
Standpipe Level, LI339 (inH_2O)	50 to 150
Primary Gas Cooler Bypass	0%
PCD Temperature (°F)	600 to 800
Total Gas Flow rate (pph)	13,000 to 26,000
Oxygen/coal mass ratio (lb/lb)	0.5 to 0.95
Steam/Coal Ratio	0.2 to 1.0
AFBC Temperature (°F)	1,400 to 1,550

3.2 GAS ANALYSIS

3.2.1 Summary and Conclusions

3.2.1.1 Powder River Basin Coal

- The raw syngas lower heating values (LHVs) were between 37 and 57 Btu/scf for air-blown operation.
- The LHVs were strong functions of the amount of nitrogen and steam dilution of the syngas.
- The commercially projected syngas LHVs were between 96 and 107 Btu/scf for air-blown operation.
- Total reduced sulfur (TRS), mostly H_2S emissions, were between 222 and 449 ppm.
- The NH_3 emissions agreed with equilibrium calculations at 60ºF plus the PCD inlet temperature.
- The CO/CO_2 ratio was between 0.7 and 1.0.
- The water-gas shift constants using the in situ H_2O measurements were between 0.76 and 0.8.
- The water-gas shift constants using the H_2O analyzer were between 0.65 and 0.76.
- The syngas molecular weight was between 26.4 and 27.3 lb/mole.

3.2.1.2 Freedom Mine Lignite Coal

- The raw syngas lower heating values (LHVs) were between 24 and 58 Btu/scf for air-blown operation and between 55 and 69 Btu/scf for oxygen-blown operation.
- The LHVs for both modes of operation were strong functions of nitrogen and steam dilution of the syngas.
- The commercially projected syngas LHVs were between 70 and 91 Btu/scf for air-blown operation and between 132 and 148 Btu/scf for oxygen-blown operation.
- For high-sulfur (low-sodium) lignite, TRS, mostly H_2S emissions, were between 1,377 and 1,732 ppm for air-blown mode and 2,136 and 2,209 ppm for oxygen-blown mode.
- For low-sulfur (high-sodium) lignite, TRS emissions were between 844 and 1,318 ppm for air-blown mode and 1,451 ppm for oxygen-blown mode.
- The TRS was three to five times higher than the minimum equilibrium H_2S concentration, indicating that the sulfur emissions are not controlled by H_2S equilibrium.
- For low-sodium lignite, the NH_3 emissions agreed with equilibrium calculations at 120ºF plus the PCD inlet temperature.
- For high-sodium lignite, the NH_3 emissions agreed with equilibrium calculations at 105ºF plus the PCD inlet temperature at mixing zone temperatures above 1,600ºF.
- For high-sodium lignite, the NH_3 emissions agreed with equilibrium calculations at 25ºF plus the PCD inlet temperature at mixing zone temperatures below 1,600ºF.
- The naphthalene analyzer measured off-scale high during the low mixing zone temperature lignite testing.

- The CO/CO_2 ratio was between 0.2 and 0.7 for air-blown mode and were about 0.4 for oxygen-blown mode.
- The water-gas shift constants using the in situ H_2O measurements were between 0.83 and 1.17.
- The water-gas shift constants using the H_2O analyzer were between 0.75 and 1.14.
- The syngas molecular weight was between 25.9 and 27.0 lb/mole for air-blown mode and between 23.6 and 24.0 lb/mole for oxygen-blown mode.

3.2.1.3 Both Powder River Basin and Freedom Mine Lignite Coals

- Syngas analyzer data for CO was excellent with all four of the six analyzers in agreement.
- Syngas analyzer data for H_2 was good with both gas chromatographic analyzers in agreement.
- Syngas analyzer data for CH_4 was good in that two of the four CH_4 analyzers were in agreement.
- Syngas analyzer data for CO_2 was good in that two of the four analyzers were in agreement.
- Syngas analyzer data for N_2 was good in that both GCs (AI464 & AI419) were in agreement.
- The syngas H_2O measured by AI475H agreed with the in situ H_2O measurements for concentrations of less than 25 percent.
- The sums of the dry gas analyzer concentrations were between 98 and 101 percent.
- The syngas H_2S analyzer gave good agreement when compared to the sulfur emissions by the syngas combustor SO_2 analyzer for the first half of TC13.
- The two NH_3 gas analyzers did not agree with each other during TC13.
- The syngas combustor oxygen balance was excellent for Powder River Basin and oxygen-blown lignite, but poor for air-blown lignite.
- The syngas combustor hydrogen balance was excellent.
- The syngas combustor carbon balance was excellent.

3.2.2 Introduction

PRB coal feed was first established with air on October 1, 2003. There was a brief coal trip on October 2, but the coal feed was resumed immediately. Syngas was successfully combusted in the PSB on October 4.

The unit was transitioned to Freedom Mine lignite on October 6, 2003. A mixture of PRB and lignite was fed to the Transport Gasifier for about 3 hours. Two types of Freedom Mine lignite were gasified during TC13; a high- and a low-sodium lignite. The low-sodium lignite was gasified from October 6 to 10 during both air- and oxygen-blown operation. The air-blown operation was from October 6 to 9 and the oxygen-blown operation was from October 9 to 10.

On October 11 the high-sodium lignite was fed to the reactor in coal feeder system FD0200 and the low-sodium lignite was fed to the reactor using coal feeder system FD0210 in oxygen-blown mode. Both lignite coals were fed to the reactor for about 21 hours. The gasifier was then run

on only the high-sodium lignite until the end of TC13 on November 2, 2003. There were four outages during the high-sodium lignite testing, two for loop seal blockage, one for standpipe blockage, and one for a FD0502 screw packing failure.

There were 29 steady periods of operation between October 1 and November 2. The steady periods are given in Table 3.2-1. Three of the operating periods (TC13-10, TC13-18, and TC13-22) were of sufficient length such that they were each subdivided into two operating periods making a total of 32. The operating periods had a cumulative time of about 216 hours which was about 43 percent of the total TC13 coal operation time.

The fuel, mode (air- or oxygen-blown), and mixing zone temperature divided the TC13 operating periods into seven different modes of operation:

1. Air-blown PRB - TC13-1 to TC13-9.
2. Air-blown, low-sodium lignite - TC13-10a to TC13-12.
3. Oxygen-blown, low-sodium lignite – TC13-13 to TC13-14
4. Oxygen-blown, mixture of low- and high-sodium lignite – TC13-15.
5. Oxygen-blown, high-sodium lignite – TC13-16.
6. Air-blown, high mixing zone temperature, high-sodium lignite – TC13-17 to TC13-21.
7. Air-blown, low mixing zone temperature, high-sodium lignite – TC13-22a to TC13-29.

Sorbent was injected into the Transport Gasifier during TC13-10a to TC13-21.

Table 3.2-2 lists some of the TC13 operating conditions, including mixing zone temperatures, system pressures, PCD inlet temperatures, air rate, oxygen rate, syngas rate, steam rate, and nitrogen rate. The system pressure was from 91 to 194 psig for the air-blown periods, and 110 to 140 psig for the oxygen-blown periods. The air-blown PRB and low-sodium lignite were gasified at pressures from 176 to 194 psig. The air blown high sodium lignite was gasified at lower pressures (91 to 180 psig) and lower mixing zone temperatures than was typical for other fuels. The lower temperature operation was used to prevent the high-sodium lignite ash from forming deposits. The steam rates were higher for oxygen-blown testing.

3.2.3 Raw Gas Analyzer Data

During TC13, Transport Gasifier and syngas combustor outlet gas analyzers were continuously monitored and recorded by the Plant Information system (PI). Twelve in situ grab samples of syngas were taken during PCD outlet loading sampling and measured for moisture content.

Syngas was analyzed by the gas analysis system for the following constituents during TC13:

CO	AI419C, AI425, AI434B, AI453G, AI464C, AI475C
CO_2	AI419D, AI434C, AI464D, AI475D
CH_4	AI419E, AI464E, AI475E
C_2^+	AI419F, AI464F
H_2	AI419G, AI464G
H_2O	AI419H, AI475H, AI479H, AI480H
N_2	AI419B, AI464B

H_2S	AI419J, AI480J
NH_3	AI475Q, AI480Q
HCl	AI479R
HCN	AI479S
COS	AI479T
CS_2	AI480W
$C_{10}H_8$	AI480X

The locations of the syngas analyzers are shown on Figure 3.2-1. The AI464 and AI419 analyzers use a gas chromatograph and typically have about a 6-minute delay. The other three CO analyzers (AI425, AI434B, and AI453B) and CO_2 analyzer (AI434C) are based on infrared technology and give measurements approaching "real time." All analyzers, except for the AI475, AI479, and AI480 bank of analyzers, require that the gas sample be conditioned to remove water vapor, therefore those analyzers report gas compositions on a dry basis.

The gas analyzers obtain syngas samples from three different locations:

- Between the PCD and the Secondary Gas Cooler (HX0402).
- Between the Secondary Gas Cooler and the pressure letdown valve (PCV-287).
- Between the pressure letdown valve and the atmospheric Syngas combustor (BR0401).

With six CO analyzers, there is a measure of self-consistency when all or several of the six analyzers read the same value. There is also the choice of which analyzer to use if all the analyzers do not agree. The TC13 hourly averages for the six CO analyzers are given on Figure 3.2-2. The CO analyzer AI475C data was corrected to a dry composition using the H_2O analyzer AI475H data to compare with the other CO analyzers that measured on a dry basis. For most of TC13, five of the six CO analyzers were in good agreement. The only analyzer that was not in agreement with the other analyzers was AI475C, although for the last 225 hours of TC13 AI475C agreed well with AI453G. The CO analyzer agreement was not as good as in past test campaigns. CO Analyzer AI425 usually read lower than the other analyzers and AI453G read higher. Note that AI464C was out of service for the last 25 hours of TC13. The periods of different types of coal being fed and whether the gasifier was operating in air- or oxygen-blown mode feed are shown on Figure 3.2-2 as well as four of the outages at hours 12, 255, 350, and 426. Two outages at hour 350 are shown as one because the run time between them was less than 2 hours.

The analyzer selection for each operating period is given in Table 3.2-3. Analyzer AI419C was used for all of the operating periods. The value from analyzer AI419C was typically an average of all of the other analyzers. Since the AI419 analyzer bank measured all the constituents of the dry gas, the consistency of the AI419 could be validated. The reasonable agreement between the CO analyzers gave confidence in the accuracy of the CO data. The low CO measurements are either periods when the gas analyzers were being calibrated or analyzer measurements were made during coal feeder trips.

TC13 hourly averages data for the H_2 analyzers are shown on Figure 3.2-3. There were several long periods where both AI464G and AI419G agreed with each other. When the two analyzers

did not agree, AI464G was typically higher than AI419G. The analyzer used for future data analysis is given in Table 3.2-3. When the two analyzers agreed, AI419G was used, and when they did not agree AI464G was used. The higher value of AI464G was used to improve the oxygen and hydrogen balance around the Syngas combustor.

The TC13 hourly average gas analyzer data for CH_4 are given on Figure 3.2-4. Analyzer AI419E and AI464E agreed with each other for nearly all of TC13, with analyzer AI419E usually slightly higher than analyzer AI464E. Analyzer AI475E (dry) was higher than AI419E and AI464E for most of TC13 and was often clearly in error. Analyzer AI419E was used for data analysis for all but one of the operating periods. The choice of which analyzer used is given in Table 3.2-3.

The TC13 hourly average gas analyzer data for C_2^+ are given on Figure 3.2-5. Neither analyzer read significantly above 0.0 percent during the PRB testing. Analyzer AI464F increased to about 0.1 percent during the air-blown, low-sodium lignite testing. The oxygen-blown testing increased AI464F to 0.35 percent for a while, and then it decreased to 0.15 percent. During the oxygen-blown testing, AI419F increased slightly to .025 percent. During the air-blown, high-sodium lignite testing, AI464F was about 0.05 percent and then increased to 0.18 percent by the end of TC13, while AI419F increased to 0.025 percent. The increase in C_2^+ during the end of TC13 was probably due to the decrease in operating temperatures. Analyzer AI464F was used for all of the TC13 operating periods.

The TC13 hourly average CO_2 analyzer data are given on Figure 3.2-6. Analyzers AI419D and AI464D agreed with each other for most of TC13. Analyzer AI464D (dry) was consistently higher than AI419D and AI434C for all of TC13 by about 5 to 7 percent. Analyzer AI434C was consistent with AI419D and AI464D for the first 115 hours of TC13 and then drifted higher than AI419D and AI464D by a slowly increasing amount (2 to 5 percent) for the rest of TC13. Analyzer AI419D was used for the operating periods. The analyzers used for each operating period are given in Table 3.2-3.

The nitrogen hourly average analyzer data is given on Figure 3.2-7. Analyzer AI464B and AI419B agreed for most of TC13 with only a few periods of disagreement. Analyzer AI464B nitrogen data was typically higher than analyzer AI419B nitrogen data for about 175 hours of TC13. Analyzer AI419B was used for all of the operating periods.

Since both GC analyzers (AI419 and AI464) were used for nearly the entire spectrum of expected gas components, a useful consistency check for each of the analyzers was developed. The sum of the gases measured by each bank of analyzers was plotted to see how close they were to 100 percent. The sums of both GC analyzer banks are given on Figure 3.2-8. Analyzer AI419 was fairly consistent during TC13, usually between 98 and 100 percent. The analyzer AI464 sums were erratic for most of TC13, varying between 95 and 105 percent. This poorer performance of the AI464 analyzer was the reason that AI419 was used for most analysis.

The H_2O analyzer AI419H is part of the AI419 GC. Since AI419 operates dry, and the syngas H_2O is removed prior to analysis, AI419H always read 0.0 percent, and will not be discussed further.

The raw H_2S analyzer AI419J data is shown on Figure 3.2-9. This data, like the other AI419 analyzer data, is reported on a dry basis. The AI419J H_2S data seems reasonable in that it was lower during PRB gasification, higher in the high-sodium, low-sulfur lignite gasification, and still higher during the low-sodium, high-sulfur lignite gasification. Oxygen-blown mode operation increased the H_2S concentration as expected due to the lower amount of nitrogen dilution. The AI480J data was not plotted since all of the reported concentrations were less than zero and clearly in error. The AI419J data is compared with syngas combustor SO_2 analyzer data in Section 3.2.8.

The raw ammonia analyzer AI475Q and AI480Q data are shown on Figure 3.2-10. Analyzer AI480Q was erratic for the first 50 hours, and then agreed with AI475Q from hour 55 to hour 182. After hour 183, analyzer AI480Q read either a constant value, was erratic, or was over the maximum analyzer range of 4,000 ppm. The results of AI475Q seem reasonable and produced the expected higher ammonia concentrations in oxygen-blown mode than in air-blown modes (due to less nitrogen dilution). The PRB ammonia concentrations were usually between 1,000 and 1,500 ppm. Air-blown, low-sodium lignite ammonia concentrations were between 500 and 1,500 ppm. For both lignites in oxygen-blown, ammonia concentrations were between 2,000 and 3,000 ppm. The air-blown, high-sodium lignite ammonia concentrations were between 500 and 2,500 ppm. The high-sodium lignite seemed to increase ammonia concentration as the reactor temperature was decreased toward the end of TC13. An increase of ammonia with a decrease in temperature is predicted by thermodynamic equilibrium as will be discussed in Section 3.2.9. The TC13 PRB ammonia data was consistent with previous air-blown testing. The TC13 Freedom Mine lignite ammonia data were higher than the TC11 Falkirk Mine ammonia emissions in both air- and enhanced-blown modes.

The hydrogen cyanide analyzer AI479S data are not plotted because of readings being either erratic or less than zero for most of TC13. The analyzer also did not respond to the expected changes in ammonia concentrations (hydrogen cyanide should rise and fall in tandem with the ammonia concentration).

The COS analyzer AI479T data are not plotted for TC13 since the data varied from 300 to 350 ppm and did not respond to changes in H_2S concentrations in different modes of operation. The poor response to mode changes and higher than expected values lead to the conclusion that the COS data from AI479T are not reliable and therefore should not be used for analysis.

The CS_2 analyzer AI480W data are not plotted for TC13 because the analyzer was either erratic or out of range (maximum analyzer value 100 ppm). The analyzer did not respond to changes in H_2S concentrations due to changes made switching from air- to oxygen-blown operation. The poor response to mode changes leads to the conclusion that the CS_2 data from AI480W were not reliable and therefore should not be used for analysis.

The HCl Analyzer AI479R data are not plotted for TC13. The data varied erratically or read less than zero for all of TC13. The values were not in the expected range of syngas HCl. The maximum HCl syngas concentration can be calculated from the chloride coal concentration, coal rate, and syngas rate. The maximum HCl syngas composition, assuming no HCl removal by the Transport Gasifier and PCD solids, is 14 ppm for PRB, 7 ppm for low-sodium lignite, and 8

ppm for high-sodium lignite. All three coals are very low chloride coals. The HCl data from AI479R are not reliable and therefore should not be used for analysis.

The raw naphthalene analyzer AI480X data are shown on Figure 3.2-11. The naphthalene analyzer was purchased to give guidance to how much hydrocarbons were being produced by the Transport Gasifier that were not measured by the C_2^+ component of the GCs. High amounts of naphthalene also might indicate periods of tar formation. Naphthalene analyzer AI480X results varied significantly during TC13. The most significant naphthalene data were taken during the end of TC13 when the Transport Gasifier was operating at a lower temperature. During this period the naphthalene analyzer was off the scale (reading above 400 ppm) indicating that there might have been more "heavier" hydrocarbons present in the syngas than indicated by the two GCs, AI419 and AI464. The reliability of the naphthalene measurement is not known at this time.

3.2.4 Gas Analysis Results

The dry, raw syngas analyzer data were adjusted to produce the best estimate of the actual gas composition in three steps:

1. Choice of CO, H_2, CH_4, N_2, and CO_2 analyzer data to use (see Table 3.2-3).
2. Normalization of dry gas compositions (force to 100-percent total).
3. Conversion of dry compositions to wet compositions.

The data analysis will be based only on the TC13 operating periods (Table 3.2-1). The operating period averages of the sums of the dry gas analyses selected are shown on Figure 3.2-12. All of the operating periods have the sums of dry gas compositions between 98.2 and 100.7 percent. Most of the data taken before hour 350 are biased low (the gas analyzers not measuring all of the syngas components), while all of the data after hour 413 are biased high. The average of all the operating sums of the dry gas composition is 99.2 percent.

During the TC13 testing there were two operating H_2O analyzers, AI475H and AI480H. The H_2O concentration was also measured 12 times using in situ "grab samples" at the PCD exit during PCD outlet particulate measurements. In previous gasification runs, the water-gas shift (WGS) reaction was used to determine H_2O measurements between in situ H_2O measurements and to check the consistency of the H_2O analyzer data. The water-gas shift equilibrium constant should be a function of a Transport Gasifier mixing zone or riser temperature.

The water-gas shift reaction and equilibrium constant are as follows, respectively:

$$CO + H_2O \leftrightarrow H_2 + CO_2 \quad (1)$$

$$Kp = \frac{(H_2)(CO_2)}{(H_2O)(CO)} \quad (2)$$

Plotted on Figure 3.2-13 are the AI475H, AI480H, in situ H_2O concentrations, and the H_2O concentrations calculated from the water-gas shift equilibrium constant. The water-gas shift H_2O concentrations are based on the mixing zone temperature TI344 using the measured H_2,

CO, and CO_2 concentrations. A -100ºF approach temperature gave the best fit of the in situ data.

Analyzer AI475H was close to the in situ data for all but 2 of the 12 in situ H_2O analyses. A direct comparison of analyzer AI475H and in situ H_2O concentrations is given on Figure 3.2-14. The agreement is very good (within 10 percent) except for the low-sodium lignite, oxygen-blown test, where the H_2O analyzer AI457H was operating near its maximum range of 30-percent H_2O. Table 3.2-3 lists whether the AI475H H_2O measurements or the WGS H_2O will be used for each operating period. Operating periods TC13-1 to TC13-12 (PRB and oxygen-blown, low-sodium lignite) had all three H_2O measurements in agreement, therefore, the H_2O analyzer AI475H H_2O data were used.

The H_2O increased up from 9.0 percent to around 11.0 percent after hour 40. During the rest of the PRB operation up to hour 104, the H_2O was constant at slightly over 11 percent. For the four air-blown, low-sodium lignite operating periods (hours 143 to 178) the H_2O was fairly constant at about 14 percent. This H_2O increase was caused by the higher moisture content of the low-sodium lignite, since the steam rate did not change. The water-gas shift equilibrium H_2O will be used for TC13-13 to TC13-16 (oxygen-blown testing for both low- and high-sodium lignite) since AI475H maximum range is 30 percent. The H_2O values were from 28 to 34 percent. From hours 268 to 391 (high-sodium lignite, air-blown operation) all three H_2O measurements agreed, so AI475H was used to determine the H_2O concentration. The H_2O concentration was fairly steady at about 13-percent H_2O. At hours 419, the AI475H data deviated from the in situ and WGS H_2O values, so the WGS values were used for hours 413 to 483, during high-sodium lignite, air-blown operation. The H_2O concentrations increased up to about 19 percent during this time. For the last operating period (TC13-29), the WGS and AI475H agreed with each other, so AI476H was used. The H_2O concentration had decreased to 16 percent.

For all operating periods, analyzer AI480H was 20 to 30-percent H_2O, much higher than the in situ H_2O measurements. Analyzer AI480H was giving erroneous results and will not be used for further analyses.

Table 3.2-4 lists the previous test campaign H_2O determination methods. Analyzer AI475H was used in TC12 for moistures less than 25 percent. The mixing zone approach to equilibrium temperature required to agree with the in situ H_2O data was either 0 or 100ºF, consistent with TC13. When using the riser temperature to fit the in situ moisture data, a higher approach temperature of +50ºF was required.

The H_2O concentrations used for the operating periods are given in Table 3.2-5. The best estimates of the wet gas compositions for the TC13 operating periods are given in Table 3.2-5 and shown on Figure 3.2-15. Also shown in Table 3.2-5 are the syngas molecular weights for each operating period.

The CO concentration increased from 6 to 8 percent and then leveled out at around 7 percent during the PRB coal operation. The CO concentration decreased to around 4 percent and then increased to 7 percent during the air-blown, low-sodium lignite operation. The CO concentration was 5.5 percent during the low-sodium lignite, oxygen-blown operation, 6 percent

during the oxygen-blown mixed lignite, and 4.6 percent during the oxygen-blown, high-sodium lignite. The air-blown, high-sodium lignite CO was at 5 percent at the beginning of the oxygen-blown, high-sodium lignite, and then decreased to about 2.5-percent CO at hours 380 to 442, then increased to nearly 4 percent by the end of TC13.

The H_2 concentration was 4 percent at the beginning of TC13 and then increased to 6 percent. For the remainder of the PRB testing, the H_2 slowly increased to 7 percent. The H_2 decreased to 5 percent at the start of the air-blown, low-sodium lignite and then increased to 7.5-percent H_2 by the end of the low-sodium lignite testing. The H_2 concentration was 11.5 percent for oxygen-blown, low-sodium lignite, 12 percent for the oxygen-blown mixed lignite, and 10.5 percent for the oxygen-blown, high-sodium lignite. The air-blown, high-sodium lignite H_2 was at 6 percent at the beginning of the air-blown, high-sodium lignite, and then decreased to about 4-percent H_2 at hour 380 before increasing back up to nearly 7 percent by the end of TC13.

Note that for PRB the CO was always higher than the H_2, while for all the Freedom Mine lignite the H_2 was higher than the CO. This is due to the higher moisture content of the Freedom Mine lignite compared to PRB. Feeding a higher moisture coal is equivalent to adding additional steam. The additional steam and the water-gas shift reaction produce more H_2 and CO_2 at the expense of CO and H_2O. The higher H_2 concentration at the expense of CO during the oxygen-blown testing was partially caused by the large increase of steam rate (the steam rate was approximately tripled). The gradual increase in the H_2 concentration during the last 100 hours of TC13 was also caused by an increase in steam rate during this time.

The CO_2 concentration gradually increased from 8 to 9 percent during the PRB TC13 testing. During the air-blown, low-sodium lignite testing, the CO_2 increased to about 10 percent. The CO_2 concentration was 13 percent for oxygen-blown, low-sodium lignite, 13 percent for the oxygen-blown mixed lignite, and 12 percent for the oxygen-blown, high-sodium lignite. The air-blown, high-sodium lignite CO_2 was at 10 percent at the beginning of the oxygen-blown, high-sodium lignite, and then decreased to about 8.5-percent H_2 at hour 380, then increased to 10 percent by the end of TC13.

For all three fuels in air-blown mode, the CH_4 concentration was between 0.5 and 1.4 percent. For both lignites in oxygen-blown mode, the CH_4 concentration increased up to about 1.5 percent.

The syngas molecular weight and nitrogen concentration are plotted on Figure 3.2-16. The air-blown molecular weights are all between 25.9 and 27 lb/lb mole. The oxygen-blown operating periods had molecular weights between 23.6 and 24 lb/lb mole. The molecular weights decrease in oxygen-blown mode because nitrogen is replaced by lower molecular compounds such as H_2 and H_2O.

The nitrogen trends follow the molecular weight trends, with the lower nitrogen concentrations in oxygen-blown mode and higher nitrogen concentrations in air-blown mode.

The CO/CO_2 ratios were calculated from the gas data for each operating period, and are listed in Table 3.2-5. The TC13 CO/CO_2 ratio varied from 0.2 to 1.0.

The lower heating value (LHV) for each gas composition was calculated and is given on Table 3.2-5 and plotted on Figure 3.2-17.

The LHV's value was calculated using the formula:

$$\text{LHV(Btu/scf)} = \left\{ \begin{matrix} 275\times(\text{H}_2\%)+322\times(\text{CO}\%)+ \\ 913\times(\text{CH}_4\%)+1641\times(\text{C}_2^+\%) \end{matrix} \right\}/100 \qquad (3)$$

While operating on PRB, TC13-1 had a LHV of 37 Btu/scf and then the LHV increased to 53 Btu/scf at hour 18. For the rest the PRB operation, the LHV slowly increased from 53 to 57 Btu/scf. This increase seemed to be the result of increasing coal-feed rate. For the air-blown, low-sodium lignite, the LHV increased from 36 up to 58 Btu/scf, again due to increasing coal rates. The LHV was about 66 Btu/scf for oxygen-blown, low-sodium lignite, 68 Btu/scf for the oxygen-blown mixed lignite, and 55 Btu/scf for the oxygen-blown, high-sodium lignite. The LHV for the air-blown, high-sodium lignite slowly increased up to 42 Btu/scf for the first four operating periods (hours 268 to 300) and then decreased to 24 Btu/scf at hour 391. At hour 318 (TC13-20), the pressure was decreased from 176 to 112 psig and the coal rate was also decreased. The coal rate decrease was mainly responsible for the decrease in syngas LHV. The pressure and coal rates decreased for the next two operating periods (hours 337 and 380) and the LHV continued to decrease to 24 Btu/scf. For the remainder of TC13 (hours 413 to 503) the pressure and coal-feed rates increased, causing the syngas LHV to increase to 44 Btu/scf.

Past test runs have indicated that LHV is most affected by coal rate and steam rate (see Figure 4.5-5 of TC06 Final Report.). As coal rate increases, the syngas production rate increases, but the aeration and instrument purge nitrogen flow rate remains constant. Therefore, the pure nitrogen constituent of the syngas decreases (less nitrogen dilution) and the syngas LHVs increases. When air is replaced by oxygen in oxygen-blown operation, the nitrogen content of the syngas is also decreased, increasing the LHVs. The increase in steam produces lower LHVs by the increased syngas dilution with H_2O. A way to combine the effects of changes in steam, mode of operation, and coal rates is to determine the overall percent of oxygen of all the gas that is fed to the Transport Gasifier. This compensates for the different amounts of nitrogen and steam that are added to the gasifier. The overall percent O_2 is calculated by the following formula:

$$\text{Overall }\%\text{O}_2 = \frac{.21*\text{air}+\text{oxygen}}{\text{air}+\text{oxygen}+(\text{pure nitrogen})+\text{steam}} \qquad (4)$$

The air, oxygen, nitrogen, and steam flows are in moles/hr. At the PSDF, a large amount of pure nitrogen is fed to the gasifier for instrument purges, coal and sorbent transport, and equipment purges. In PSDF air-blown operation, about 50 percent of the syngas nitrogen comes from air and 50 percent comes from the pure nitrogen flows. In PSDF oxygen-blown operation, the removal of air nitrogen removes about the same amount of nitrogen as if the pure nitrogen was replaced by syngas recycle in air-blown mode.

The TC13 Overall percent O_2 are listed in Table 3.2-5 and range from 10.7 to 12.3-percent O_2 in PRB air-blown mode, from 11.3- to 13.1-percent O_2 in low-sodium lignite air-blown mode,

14.1- and 15.2-percent O_2 in low-sodium, oxygen-blown mode, and from 9.3 to 11.5 percent in high-sodium lignite in air-blown mode. The oxygen-blown mixture overall percent O_2 was 15.4 and the oxygen-blown, high-sodium lignite was 14.5 percent. As the overall percent O_2 increases, the LHV also increases. Note that the oxygen-blown overall percent O_2s are higher than the air blown overall percent O_2s.

The TC13 raw LHV's data are plotted against overall percent O_2 on Figure 3.2-18. The smoothed curves of previous PRB data (TC6, TC7, TC8, TC10, and TC12), previous Hiawatha bituminous data (TC9) and Falkirk lignite (TC11) are also plotted.

The TC13 PRB data all fall in a straight line of LHV and overall percent O_2 and are consistent with previous PBR LHV data. All of the PRB data are lower than the equivalent Hiawatha bituminous data and higher than the equivalent Falkirk lignite data.

The TC13 Freedom lignite data all fall on a straight line of LHV with overall percent O_2 including both the air- and oxygen-blown data. This data are usually lower than the plot of previous PRB data and are always higher than the TC11 Falkirk lignite. All of the TC13 Freedom lignite LHVs are lower than the Hiawatha Bituminous LHVs at equivalent overall percent O_2. Many of the Freedom lignite LHV data are consistent with the previous PRB LHV data.

The raw LHV date are plotted against mixing zone temperature, TI344 on Figure 3.2-19. The PRB and air-blown Freedom Mine lignite data show no LHV dependence with temperature. The limited oxygen-blown data (shaded points on Figure 3.2-19 - low-sodium lignite, high-sodium lignite, and mixed lignite) show an increasing LHV with decreasing mixing zone temperature.

3.2.5 Commercially Projected Syngas Lower Heating Values

The PSDF Transport Gasifier produces syngas of a lower quality than a commercially sized gasifier due to the use of nitrogen at the PSDF rather than recycle gas in a commercial gasifier for aeration and PCD back-pulse cleaning. Also a commercially sized gasifier has a lower heat loss per pound coal gasified when compared to the PSDF Transport Gasifier due to the higher surface area/reactor volume ratio at the PSDF compared to a commercially sized gasifier. The following corrections are made to the measured, raw syngas composition to estimate the projected commercial synthesis LHVs.

1. All nonair nitrogen is subtracted from the syngas. This nitrogen is used for Transport Gasifier aeration and instrument purges. In a commercial plant there will be less instrumentation than at the PSDF. Because the instruments in a commercial plant will require the same purge flow rate as the instruments at the PSDF, the total instruments purge flow rate will be less. This projection assumes that recycled syngas or steam will be used in a commercial plant for aeration and steam will be used for instrument purges to replace the nonair nitrogen. The nonair nitrogen was determined by subtracting the air nitrogen from the syngas nitrogen. This projection increases all the nonnitrogen syngas compositions and decreases the nitrogen syngas composition. The syngas rate

will decrease. For oxygen-blown mode, this change removes all the nitrogen from the syngas, thus oxygen-blown syngas will have 0-percent nitrogen. The water-gas shift equilibrium constant and the CO/CO_2 ratios will not change.

2. The nonair nitrogen (that has been eliminated by not using nitrogen for aeration or instrument purges) no longer has to be heated to the maximum gasifier temperature. This eliminated heat is counteracted by the additional energy required to heat the gas used for aeration and instrument purges. A recent commercial design will be used to estimate the amount and temperature of the aeration and instrument gas required. Since the total amount of instrument and aeration gas required is reduced, the coal and air rates will decrease by the amount of energy no longer required. This results in decreased coal, air, and oxygen rates to the Transport Gasifier. It is assumed that this eliminated coal (to heat up the nonair nitrogen) is combusted to CO_2 and H_2O. Eliminating this additional coal reduces the syngas CO_2 and H_2O concentrations. The lower projected air rates for air-blown mode also decrease the nitrogen in the projected syngas and thus decreases the syngas flow rate. The water-gas shift constant and the CO/CO_2 ratio both change due to the reduction in CO_2 and H_2O.
3. The PSDF higher heat loss per pound of coal gasified due to its smaller size is also taken into account. Smaller scale pilot and demonstration units have higher surface area to volume ratios than their scaled up commercial counterparts, and hence the PSDF Transport Gasifier has a higher heat loss per pound of coal gasified than a commercial plant. Since the heat loss of a commercial plant is difficult to estimate, the projected heat loss is assumed to be zero (adiabatic). This change uses the same method to correct for the no longer required energy to heat up the decreased amounts of aeration and instrumentation gas. The coal, air, and oxygen rates are reduced; the syngas CO_2, H_2O, and N_2 concentrations are reduced; the water-gas shift equilibrium constant and the CO/CO_2 ratio change. This change is reasonable since the commercial plant heat loss per pound of coal gasified is much smaller than the PSDF Transport Gasifier heat loss per pound of coal gasified.
4. The steam rates are reduced for oxygen-blown operation, since in oxygen-blown operation steam is added to control the gasifier temperature. As the oxygen rate is decreased in a commercial plant, the steam rate will also be decreased. It was assumed that the steam-to-oxygen ratio will be the same for the PSDF and the commercial Transport Gasifier, and hence the corrected steam rate will be lower than the original steam rate. The effect of lowering the steam rate will decrease the amount of H_2O in the syngas by the amount the steam rate was reduced. This change reduces the steam rate and the H_2O content of the syngas and hence the LHVs and water-gas shift equilibrium constant also changes. The steam-to-oxygen ratio is a function of the detailed design of the Transport Gasifier. It is difficult to estimate what a commercial steam-to-oxygen ratio will be since typically in oxygen-blown mode steam is added to control local temperatures.
5. The water-gas shift is changed to reflect the gasifier mixing zone temperature. Changes No. 2, 3, and 4 all change the water gas shift equilibrium constant without changing the mixing zone temperature. The commercial plant will operate at the PSDF mixing zone temperature and hence have the same water-gas shift equilibrium constant as the commercial plant. The H_2O, CO_2, CO, and H_2 concentrations are then adjusted to return to the measured PSDF water-gas shift equilibrium for that particular operating period. With respect to LHV, it could go up if H_2 and CO_2 are converted to H_2O and

CO since the LHV for CO is higher than H_2. The LHV could decrease if H_2O and CO are converted to H_2 and CO_2. This change is usually small on a LHV basis, but is important if the syngas is used for fuel cell or chemical production where the H_2 concentration is a critical design parameter.

For change No. 2, it is assumed that the recycle gas is 2.4 percent of the syngas from the gasifier and is available at 234ºF. The recycle gas is taken from the exit of a "cold" syngas sulfur removal system which decreases the syngas temperature to 150ºF, prior to sulfur removal. Decreasing the syngas temperature to 150ºF will condense most of the syngas H_2O out as liquid water, which is then removed from the syngas. For the commercial design at 388 psia, the syngas water composition is 0.96 percent. In a commercial plant the cleaned syngas would be sent to a gas turbine, fuel cell, or for chemical production. For change No. 2, is it assumed that the aeration steam is 1.45 percent of the syngas from the gasifier and available at 660ºF. For change No. 3, is it assumed that the heat loss for the PSDF Transport-gasifier is 3.5 M Btu/hr. This heat loss will be discussed further in Section 3.4.

The sum of all five corrections is the commercially projected LHV. The LHV added to the raw LHV for each fuel and mode of operation is detailed in Table 3.2-6. Changes No. 1 and No. 2 both increase the oxygen-blown LHV more than for the air-blown LHV because 100 percent of the syngas nitrogen is removed in the oxygen-blown projection, while only about 50 percent of the syngas nitrogen is removed for the air-blown projection.

These calculations are an oversimplification of the gasification process. A more sophisticated model is required to correctly predict the effects of decreasing pure nitrogen and gasifier heat loss. It should be noted that the projected syngas compositions are based on a projected coal rate, projected air rate, projected oxygen rate, projected steam rate, and a projected syngas rate.

The projected LHVs for each operating period are given in Table 3.2-7. The PRB projected LHVs were between 96 and 107 Btu/scf for air-blown operation. The average corrections for TC13 LHVs for the different fuels and operating modes are shown in Table 3.2-6.

The Freedom Mine low-sodium lignite projected LHVs were between 76 and 91 Btu/scf for air-, and either 132 or 139 Btu/scf for oxygen-blown operation. The high-sodium projected LHVs were between 70 and 90 Btu/scf for air-blown and 138 Btu/scf for the oxygen-blown LHVs. The mixed lignite oxygen blown had a projected LHV of 148 Btu/scf. The correction is higher for oxygen-blown mode because there is less syngas in the oxygen-blown mode of operation, so taking about the same amount of pure nitrogen out the syngas has a larger effect.

For comparing the raw LHVs with the commercially projected LHVs, an equivalent to the overall percent O_2 is defined as:

$$\text{Projected Overall } \%O_2 = \frac{.21*(\text{projected air}) + (\text{projected oxygen})}{(\text{projected air}) + (\text{projected oxygen}) + (\text{projected steam})} \quad (5)$$

All flow rates are expressed as moles/hr. The projected air rate, projected oxygen rate, and projected steam rate are used in the determination of the projected LHVs.

The PRB projected LHVs are plotted against the projected overall percent O_2 on Figure 3.2-20. The linear fits of the projected Powder River Basin LHVs (from TC06, TC07, TC08, TC10, and TC12), the projected TC11 Falkirk lignite LHVs, and the projected TC09 Hiawatha bituminous LHVs are also shown on Figure 3.2-20. The TC13 PRB projected LHVs are consistent with the previous PRB projected data. The TC13 PRB data is lower than projected Hiawatha bituminous LHVs and higher than Falkirk lignite projected LHVs at comparable projected overall percent O_2.

The Freedom lignite adiabatic N_2-projected LHVs are plotted against the adiabatic overall percent O_2 on Figure 3.2-21. The linear fits of projected PRB LHVs (from TC06, TC07, TC08, TC10, and TC12), the projected TC11 Falkirk lignite LHVs, and the projected TC09 Hiawatha bituminous LHVs are also shown on Figure 3.2-21. All of the projected Freedom mine lignite LHVs form a straight line with the projected overall percent O_2. The Freedom lignite-projected LHV line is an extension of the projected PRB LHV line (same slope and intercept) and is higher and parallel to the Falkirk lignite projected LHV line.

Also given on Table 3.2-7 are the assumed recycle LHVs, which is the projected syngas that has been dried to 1-percent H_2O. In a commercial IGGC plant, this would be the gas actually fired in the gas turbine.

3.2.6 Syngas Water-Gas Shift Equilibrium

The water-gas shift (WGS) equilibrium constants (K_P) were calculated for 12 in situ moisture measurements and are given in Table 3.2-8. Only 2 of the 12 in situ moisture measurements were taken completely during an operating period (October 2 in situ H_2O in TC13-18 and October 17 in situ H_2O in TC13-20). Two other in situ samples took place during part of an operating period. The equilibrium constants calculated at the mixing zone temperatures for the WGS reaction varied from 0.74 to 1.29. Lower equilibrium (higher temperature) constants would tend to have less H_2 and CO_2 and higher H_2O and CO.

The thermodynamic equilibrium temperature for each equilibrium constant was calculated from thermodynamic data and is shown in Table 3.2-8. The thermodynamic equilibrium temperature varied from 1,404°F to 1,644°F. These temperatures are all within 150°F of the mixing zone temperatures, which are listed in Table 3.2-8 for the in situ sampling periods. The WGS equilibrium constants calculated from the mixing zone temperatures are compared with the measured WGS equilibrium constants on Figure 3.2-22 using the same approach temperature used to estimate the syngas H_2O concentration Figure 3.2-13 (-100°F). Both calculated and measured oxygen-blown K_P agree within ±10 percent of each other for all three fuels, both operating modes, and a range of mixing zone temperatures of 300°F. The WGS Kp was predictable despite the wide range of H_2O (8.1 to 32.6 percent), dry CO (3.5 to 8.9 percent), dry H_2 (6.0 to 18.0 percent), and dry CO_2 (9.3 to 19.9 percent) during TC13. This would indicate that the water-gas shift reaction is controlling the relative H_2, H_2O, CO, and CO_2 concentrations in the Transport Gasifier.

The measured water-gas shift equilibrium constants (K_P) were calculated for TC13 operating periods and are given in Table 3.2-9. The measured equilibrium constants varied from 0.65 to

1.14. The calculated thermodynamic equilibrium constants for each operating period are shown in Table 3.2-9. A measured K_p could not be determined for four oxygen-blown operating periods (TC13-13 to TC13-16), since the H_2O analyzer AI475H was out of range. The thermodynamic equilibrium constants were calculated from the mixing zone temperature TI344 and an approached 100ºF. The operating period WGS equilibrium constants calculated from the mixing zone temperatures are compared with the measured WGS equilibrium constants on Figure 3.2-23. There was good agreement between the measured equilibrium constants and the equilibrium constants based on the mixing zone temperature for the all of the air-blown lignite and PRB data except the low-temperature high-sodium data.

The ability to predict the water-gas shift constant is important in the process design of a commercial Transport Gasifier.

3.2.7 Syngas Combustor Oxygen, Carbon, and Hydrogen Balance Calculations

The syngas compositions and syngas flow rate can be checked by oxygen balances, hydrogen balances, and carbon balances around the syngas combustor since the syngas combustor flue gas composition is measured by the following syngas combustor flue gas analyzers (See Figure 3.2-1 for the analyzer location):

- AI8775 - O_2
- AI476H - H_2O
- AI476D - CO_2

The above analyzers all measure "wet" and do not have to be corrected for syngas combustor flue gas H_2O.

The syngas combustor gas composition was calculated for each operating period by using syngas composition syngas flow rate, FI463, and the following syngas combustor flow rate tags:

- Primary air flow, FI8773
- Secondary air flow, FI8772
- Quench air flow, FI8771
- Propane flow, FI8753

The O_2 concentrations measured by AI8775 and O_2 concentrations calculated by mass balance are shown on Figure 3.2-24 and Table 3.2-10. The measured and calculated syngas combustor O_2 concentrations agreed well for the PRB, oxygen-blown Freedom lignite, and the higher temperature air-blown, high-sodium Freedom lignite operating periods, with nearly all of the measured concentrations within 15 percent of the calculated oxygen concentrations. The air-blown, low-sodium lignite operated at typical mixing zone temperatures and the high-sodium lignite operated at lower mixing zone temperature did not have good syngas combustor oxygen balance with all but one having a higher calculated flue gas O_2 percent than measured. This could be an indication that the syngas LHV was higher than measured by the syngas gas analyzers.

For TC13-6, the pressurized syngas burner was operated for the last half of TC13-6. When the syngas burner is operated, syngas is quickly taken from the syngas combustor and replaced with propane. When this happens, the atmospheric syngas combustor oxygen, carbon dioxide, and moisture analyzers all change compositions rapidly and the atmospheric syngas combustor is not at steady state. For the syngas combustor calculations, TC13-6 was shortened to exclude the PSB operation.

The CO_2 concentration measured by AI476D and the CO_2 concentration calculated by syngas combustor mass balance are shown on Figure 3.2-25 and Table 3.2-10. The calculated CO_2 concentrations agreed well with the measured CO_2 concentrations. All of the measured carbon dioxide concentrations agreed within 10 percent of the calculated carbon dioxide concentrations, except for three air-blown operating periods, one PRB period, and two lignite periods. The syngas combustor CO_2 analyzer was not in operation for TC13-17.

Analyzer AI476H measured and mass balance calculated H_2O values are shown on Figure 3.2-26 and Table 3.2-10. The calculated H_2O concentration agreed well with the analyzer H_2O concentration with the measured and calculated H_2O concentrations within 10 percent for all operating periods except for the four air-blown, high-sodium lignite operating periods. The syngas combustor H_2O analyzer was not in operation for TC13-17.

The results of the SGC flue gas analyzers indicate that the syngas compositions and flow rates are consistent with the syngas combustor flow rates and flue gas compositions, with a few exceptions.

The syngas LHVs can be estimated by doing an energy balance around the syngas combustor. The syngas combustor energy balance is done by estimating the syngas combustor heat loss to make the syngas LHVs calculated by the syngas combustor energy balance agree with LHVs calculated from the syngas analyzer data. A comparison between the measured TC13 LHVs and the syngas combustor energy balance LHVs using a syngas combustor heat loss of 1.5-MBtu/hr is given on Figure 3.2-27. The syngas combustor energy balance LHVs and analyzer LHVs were within 10 percent of each other except for on PRB operating period and one air-blown Freedom lignite operating period.

Table 3.2-11 lists the previous gasification test campaign's syngas combustor heat loss. The average heat loss to fit the analyzer data was 1.5-MBtu/hr for TC13. Higher syngas combustor heat loss would imply that the gas analyzers are over predicting the actual gas LHV, while lower syngas combustor heat loss would imply that the gas analyzers are under predicting the gas LHV. The syngas combustor heat loss of 1.5-MBtu/hr is consistent with past test campaigns.

3.2.8 Sulfur Emissions

For the TC13 operating periods, the wet H_2S concentration measured by AI419J is plotted on Figure 3.2-28 and compared with the syngas combustor SO_2 analyzer AI476P, and the syngas total reduced sulfur (TRS). The wet H_2S concentration measured by AI419J and the syngas TRS are listed in Table 3.2-9. The AI419 analyzers measure the gas composition dry, so the values from AI419J were corrected to allow for the H_2O in the syngas. The syngas combustor SO_2 analyzer, AI476P, measures the total sulfur emissions from the Transport Gasifier. The higher

range of the two AI476 SO_2 analyzers was used since the low range SO_2 analyzer, AI476N, has a maximum of 500 ppm SO_2. The main sulfur species in coal gasification are considered to be H_2S and carbon oxysulfide (COS). There should also be a minor amount of carbon disulfide (CS_2).

The H_2S analyzer AI419J read less than the TRS during for the first two operating periods of TC13. From hour 29 to hour 249, (PRB coal, low-sodium lignite, and oxygen-blown, high-sodium lignite) the H_2S analyzer was close to the TRS value, indicating small amounts of COS. This is because the TRS consists of H_2S and COS. For the remainder of TC13 in air-blown, high-sodium lignite, the H_2S analyzer was below the TRS, indicating 140 to 460 ppm of COS. The lower amounts of COS are reasonable if it is assumed that the COS should be about 10 percent of the H_2S.

The measured TRS is plotted against the wet AI419J data on Figure 3.2-29. For the PRB, all but two of the AI41J data are within 10 percent of the TRS. All of the low-sodium lignite data are within 10 percent of the TRS. All of the high-sodium lignite AI41J data are less than the TRS data and appear to have less agreement as the AI419J H_2S concentration decreases. Since TC13 AI419J readings were not always consistent with AI476P, H_2S analyzer AI419J data will not be used for reporting sulfur flows and emissions. Figure 3.2-29 clearly show the different levels of the three fuels, with the PRB TRS lower than the high-sodium (low-sulfur) lignite, which is in turn lower than the low-sodium (high-sulfur) lignite. Operating in oxygen-blown mode also increase the TRS emissions due to less TRS dilution by the air nitrogen.

The TRS emissions began TC13 at 449 ppm and then decreased to 259 ppm at 29 hours. The TRS was then nearly constant at 222 to 281 ppm for the remainder of PRB air-blown testing. During the low-sodium (high-sulfur) lignite testing the TRS emissions steadily increased from 1,377 to 1,732 ppm. Limestone feed started at about the same time as the low-sodium lignite feed began, so the effect of limestone addition on the sulfur emissions of low-sodium lignite could not be determined. The oxygen-blown, low-sodium (high-sulfur) TRS increased further to about 2,200 ppm. When the high-sodium (low-sulfur) coal was fed the TRS decreased to about 1,200 ppm at hour 281. The TRS was between 1,000 and 1,300 ppm for the remainder of TC13 except for one TRS at 844 ppm (hour 300). At hour 349 the limestone feed was stopped and the sulfur emissions then decreased for two operating periods and then increased to a slightly higher value than with the limestone feed. Therefore, it can be concluded that the use of sorbent had little effect on the sulfur emissions. The limestone feed was stopped just before the temperature was decreased. Lower temperature should favor lower sulfur emissions because the minimum equilibrium H_2S concentration should decrease. For the last 150 hours of TC13, one change increased TRS emissions (no limestone) and one change decreased TRS emissions. It is possible that either both effects cancelled each other out or neither change made a significant difference.

The calculation of the minimum equilibrium synthesis H_2S concentration has been described in previous PSDF reports. In summary, the minimum equilibrium H_2S concentration is a function of the partial pressures of H_2O and CO_2 as long as there is calcium sulfide present in the solids. (The equilibrium H_2S concentration is a function of system temperature, while the minimum equilibrium H_2S concentration is not a function of temperature.) As the partial pressures of H_2O and CO_2 increase, the H_2S concentration should increase. Using Aspen simulations, the

minimum equilibrium H_2S concentrations were determined for all of the operating periods and the results are listed in Table 3.2-9.

Figure 3.2-30 plots the TRS and the minimum equilibrium H_2S directly against each other for TC13. The data are expected to all fall above the 45-degree line since the minimum equilibrium H_2S concentration should be the lowest H_2S concentration in a system with calcium sulfide present. All of the data indicate sulfur emissions greater than equilibrium, as expected. The PRB data are close to the equilibrium line which is typical because the sulfur emissions for PRB with no sulfur capture are close to the minimum equilibrium H_2S emissions. The measured TRS is greater than the equilibrium H_2S for all of the lignite testing, indicating that mass transfer or some other mechanism is limiting sulfur capture.

3.2.9 Ammonia Equilibrium

At the high temperature of the Transport Gasifier mixing zone, thermodynamic equilibrium predicts that there is minimal ammonia present. The presence of ammonia in the syngas is therefore a result of ammonia production while the syngas cools to the location where the ammonia is sampled. The ammonia formation reaction and equilibrium constant are as follows:

$$\left(\frac{1}{2}\right)N_2 + \left(\frac{3}{2}\right)H_2 \leftrightarrow NH_3 \tag{6}$$

$$Kp = \frac{P_{NH_3}}{\left(P_{N_2}\right)^{.5}\left(P_{H_2}\right)^{1.5}} \tag{7}$$

where P is the partial pressure of ammonia, hydrogen, or nitrogen.

The AI475Q measured ammonia concentrations and the equilibrium calculated ammonia concentrations are compared on Figure 3.2-31 and Table 3.2-9. The equilibrium ammonia concentration was estimated using the PCD inlet temperature TI458 and different approach temperatures for each fuel.

- Powder River Basin - All but one of the nine PRB operating period equilibrium calculation ammonia concentrations are within ±20 percent of the measured ammonia concentrations using an approach temperature of 60ºF. The outlier was at TC13-1 and had the lowest ammonia concentration. This approach temperature is consistent with past approach temperatures measured in previous PRB test campaigns as shown in Table 3.2-12. In previous test campaigns the air-blown PRB ammonia approach temperature varied from 30 to 80ºF.
- Low-Sodium Lignite - An approach temperature of 120ºF fit all but one of the six ammonia data points within ±20 percent, and included both air- and oxygen-blown blown. This is consistent with the Falkirk lignite approach temperature of 110ºF (TC11 Technical Progress Report Figure 3.2-30).
- High-Sodium Lignite at Mixing Zone Temperatures Above 1,620ºF (TC13-16 to TC13-21) - An approach temperature of 105ºF fit all of the seven ammonia data points within

±20 percent, and included both air- and oxygen-blown blown. This is consistent with the Falkirk lignite and low sodium lignite.

- Mixture of Low- and High-Sodium Lignite - An approach temperature of 90ºF fit the only ammonia data points in oxygen-blown mode at a mixing zone temperate above 1,620ºF. The approach temperature was not between the high- and low-sodium approach temperatures.
- High-Sodium Lignite at Mixing Zone Temperatures Below 1,600ºF (TC13-22a to TC13-29) - An approach temperature of 25ºF fit all of the nine ammonia data points within ±20 percent, and included both air- and oxygen-blown blown. This was not consistent with the other lignite data and highlights the risks in using equilibrium calculations to predict ammonia emissions. The equilibrium calculations do not seem to correctly account for the change in mixing zone temperature.

The TC08 Technical Progress Report did not include a figure of syngas ammonia concentration and equilibrium ammonia concentration, that figure is included as Figure 3.2-32 of this report. All of the air-blown TC08 ammonia data could be fit within±20 percent at an approach temperature of 80ºF. There was no oxygen-blown mode ammonia analyzer data because the ammonia analyzer was over its then maximum range of 2,000 ppm. The ammonia analyzer was sent back to the manufacturer to increase its range to 4,000 ppm during TC09. Hence there was no TC09 ammonia data.

The TC10 Technical Progress Report did not include a figure of syngas ammonia concentration and equilibrium ammonia concentration. That figure is included as Figure 3.2-33 of this report. There were only two air-blown TC10 operating periods. Both could not be fit within ±20 percent with a single approach temperature. The air-blown 1,382 ppm ammonia measured was the first operating period (TC10-1) and the ammonia analyzer was probably not in calibration yet. All of the oxygen-blown TC10 ammonia data could be fit with an approach temperature of 45ºF with 6 of the 19 oxygen-blown within ±20 percent of perfect agreement between the analyzer and equilibrium. The three AI475Q ammonia concentrations at about 4,000 ppm (the analyzer's maximum value) were taken during the early part of TC10 (TC10-2, TC10-3, and TC10-4a), when the ammonia analyzer was clearly not reporting the actual NH_3 concentration.

Table 3.2-1 Operating Periods

Operating Period	Start Time	End Time	Duration	Operating Period	
				Average Time	Relative hours
TC13-1	10/2/2003 01:15	10/2/2003 06:00	4:45	10/2/2003 03:37	7
TC13-2	10/2/2003 11:30	10/2/2003 18:00	6:30	10/2/2003 14:45	18
TC13-3	10/2/2003 19:30	10/3/2003 08:00	12:30	10/3/2003 1:45	29
TC13-4	10/3/2003 10:45	10/3/2003 17:00	6:15	10/3/2003 13:52	41
TC13-5	10/4/2003 00:30	10/4/2003 03:45	3:15	10/4/2003 02:07	53
TC13-6	10/4/2003 04:00	10/4/2003 16:30	12:30	10/4/2003 10:15	61
TC13-7	10/4/2003 17:45	10/5/2003 01:30	7:45	10/4/2003 21:37	73
TC13-8	10/5/2003 15:15	10/6/2003 01:15	10:00	10/5/2003 20:15	95
TC13-9	10/6/2003 01:45	10/6/2003 09:00	7:15	10/6/2003 05:22	104
TC13-10a	10/7/2003 16:00	10/8/2003 00:00	8:00	10/7/2003 20:00	143
TC13-10b	10/8/2003 00:00	10/8/2003 08:00	8:00	10/8/2003 04:00	151
TC13-11	10/8/2003 15:45	10/8/2003 19:30	3:45	10/8/2003 17:37	165
TC13-12	10/9/2003 05:15	10/9/2003 08:30	3:15	10/9/2003 06:52	178
TC13-13	10/10/2003 02:30	10/10/2003 05:15	2:45	10/10/2003 03:52	199
TC13-14	10/10/2003 18:45	10/10/2003 21:15	2:30	10/10/2003 20:00	215
TC13-15	10/11/2003 05:45	10/11/2003 08:00	2:15	10/11/2003 06:52	226
TC13-16	10/12/2003 04:15	10/12/2003 06:45	2:30	10/12/2003 05:30	249
TC13-17	10/15/2003 22:30	10/16/2003 07:45	9:15	10/16/2003 03:07	268
TC13-18a	10/16/2003 12:30	10/16/2003 20:15	7:45	10/16/2003 16:22	281
TC13-18b	10/16/2003 20:15	10/17/2003 04:00	7:45	10/17/2003 00:07	289
TC13-19	10/17/2003 10:00	10/17/2003 12:30	2:30	10/17/2003 11:15	300
TC13-20	10/18/2003 02:00	10/18/2003 07:00	5:00	10/18/2003 04:30	318
TC13-21	10/18/2003 22:00	10/19/2003 02:00	4:00	10/19/2003 00:00	337
TC13-22a	10/26/2003 09:30	10/26/2003 20:15	10:45	10/26/2003 14:52	380
TC13-22b	10/26/2003 20:15	10/27/2003 07:00	10:45	10/27/2003 01:37	391
TC13-23	10/27/2003 17:45	10/28/2003 06:45	13:00	10/28/2003 00:15	413
TC13-24	10/30/2003 20:00	10/31/2003 04:00	8:00	10/31/2003 00:00	442
TC13-25	10/31/2003 11:00	10/31/2003 17:45	6:45	10/31/2003 14:22	456
TC13-26	10/31/2003 18:00	11/1/2003 01:00	7:00	10/31/2003 21:30	463
TC13-27	11/1/2003 03:00	11/1/2003 07:00	4:00	11/1/2003 05:00	471
TC13-28	11/1/2003 11:00	11/1/2003 23:00	12:00	11/1/2003 17:00	483
TC13-29	11/2/2003 11:15	11/2/2003 15:00	3:45	11/2/2003 13:07	503

Notes:

1. TC13-1 to TC13-9 were air blown PRB.
2. TC13-10a to TC13-12 were air blown low sodium lignite.
3. TC13-13 to TFC13-14 were oxygen blown low sodium lignite.
4. TC13-15 was oxygen blown using a mixture of low and high sodium lignite.
5. TC13-16 was oxygen blown high sodium lignite.
6. TC13-17 to TC13-29 were air blown high sodium lignite.

Table 3.2-2

Operating Conditions

Operating Periods	Average Relative Hours	Mixing Zone Temperature TI350 °F	Pressure PI287 psig	PCD Inlet Temperature TI458 °F	Air Rate lb/hr	Oxygen Rate lb/hr	Synthesis Gas Rate lb/hr	Steam Rate lb/hr	Nitrogen Rate lb/hr
TC13-1	7	1,710	180	759	8,345	0	15,798	838	6,395
TC13-2	18	1,767	180	792	10,717	0	19,296	809	6,667
TC13-3	29	1,751	180	795	10,881	0	18,436	881	6,846
TC13-4	41	1,742	180	789	10,850	0	19,040	1,050	6,674
TC13-5	53	1,726	180	776	10,688	0	18,908	1,079	6,799
TC13-6	61	1,718	180	780	10,690	0	15,445	1,081	6,640
TC13-7	73	1,713	180	771	10,820	0	19,065	1,080	6,563
TC13-8	95	1,726	190	783	11,893	0	22,120	1,085	6,520
TC13-9	104	1,746	190	779	12,046	0	22,612	1,109	6,570
TC13-10a	143	1,712	176	724	9,507	0	18,177	1,071	6,250
TC13-10b	151	1,720	176	726	9,628	0	18,406	1,089	6,248
TC13-11	165	1,734	176	722	9,575	0	17,829	1,021	6,097
TC13-12	178	1,700	194	762	14,042	0	25,701	1,281	6,126
TC13-13	199	1,649	140	694	2,594	1,916	17,764	3,265	5,191
TC13-14	215	1,682	130	685	1,749	1,968	16,146	3,968	5,107
TC13-15	226	1,652	128	679	2,105	1,808	15,986	2,765	5,125
TC13-16	249	1,709	110	665	714	1,702	13,591	2,640	5,019
TC13-17	268	1,672	180	703	9,846	0	18,514	1,078	6,206
TC13-18a	281	1,653	176	693	9,287	0	17,937	1,249	6,172
TC13-18b	289	1,646	176	685	9,146	0	18,020	1,246	6,338
TC13-19	300	1,628	176	692	9,341	0	18,100	1,274	6,057
TC13-20	318	1,615	120	663	7,194	0	14,335	1,167	5,597
TC13-21	337	1,620	112	667	7,367	0	14,341	1,158	5,442
TC13-22a	380	1,511	91	614	6,286	0	11,929	975	6,074
TC13-22b	391	1,507	91	614	6,209	0	11,895	1,000	6,054
TC13-23	413	1,482	129	653	7,764	0	15,006	1,734	6,285
TC13-24	442	1,440	147	682	8,386	0	17,381	1,925	5,607
TC13-25	456	1,469	147	670	8,466	0	17,600	1,895	5,422
TC13-26	463	1,474	147	674	8,998	0	18,719	1,883	5,669
TC13-27	471	1,463	147	677	9,121	0	19,270	2,070	5,778
TC13-28	483	1,471	147	672	8,827	0	18,515	2,008	5,589
TC13-29	503	1,486	147	667	8,799	0	18,069	1,371	5,785

Notes:

1. TC13-1 to TC13-9 were air blown PRB.
2. TC13-10a to TC13-12 were air blown low sodium lignite.
3. TC13-13 to TC13-14 were oxygen blown low sodium lignite.
4. TC13-15 was oxygen blown using a mixture of low and high sodium lignite.
5. TC13-16 was oxygen blown high sodium lignite.
6. TC13-17 to TC13-29 were air blown high sodium lignite.

Table 3.2-3

Gas Analyzer Choices

Operating Periods	Average Relative Hours	Gas Compound						
		CO	H_2	CO_2	CH_4	C_2^+	N_2	H_2O[1]
TC13-1	7	419	419	419	419	464	419	475
TC13-2	18	419	419	419	419	464	419	475
TC13-3	29	419	419	419	419	464	419	475
TC13-4	41	419	419	419	419	464	419	475
TC13-5	53	419	419	419	419	464	419	475
TC13-6	61	419	464	419	419	464	419	475
TC13-7	73	419	419	419	419	464	419	475
TC13-8	95	419	419	419	419	464	419	475
TC13-9	104	419	419	419	419	464	419	475
TC13-10a	143	419	464	419	419	464	419	475
TC13-10b	151	419	464	419	419	464	419	475
TC13-11	165	419	464	419	419	464	419	475
TC13-12	178	419	464	419	419	464	419	475
TC13-13	199	419	464	419	419	464	419	WGS
TC13-14	215	419	419	419	419	464	419	WGS
TC13-15	226	419	419	419	419	464	419	WGS
TC13-16	249	419	464	419	419	464	419	WGS
TC13-17	268	419	419	419	464	464	419	475
TC13-18a	281	419	419	419	419	464	419	475
TC13-18b	289	419	419	419	419	464	419	475
TC13-19	300	419	419	419	419	464	419	475
TC13-20	318	419	464	419	419	464	419	475
TC13-21	337	419	464	419	419	464	419	475
TC13-22a	380	419	464	419	419	464	419	475
TC13-22b	391	419	464	419	419	464	419	475
TC13-23	413	419	464	419	419	464	419	WGS
TC13-24	442	419	464	419	419	464	419	WGS
TC13-25	456	419	464	419	419	464	419	WGS
TC13-26	463	419	464	419	419	464	419	WGS
TC13-27	471	419	464	419	419	464	419	WGS
TC13-28	483	419	464	419	419	464	419	WGS
TC13-29	503	419	464	419	419	464	419	475

Notes:

1. WGS means that H_2O calculated from water-gas shift equilibrium using T1344, and H_2, CO, and CO_2 data.

Table 3.2-4

H_2O Determination Methods

Test Campaign	Fuel	Mode	H_2O Determination Method	Temperature Indicator Used	Water Gas Shift Approach Temperature ^{O}F
TC06	Powder River Basin	Air	Ave In situ		
TC07	Powder River Basin	Air	WGS	TI350 - Mixing Zone	0
TC08	Powder River Basin	Air & Oxygen	WGS	TI350 - Mixing Zone	-100
TC09	Hiawatha Bituminous	Air & Oxygen	WGS	TI368 - Riser	50
TC10	PRB	Air & Oxygen	WGS	TI350 - Mixing Zone	-100
TC11	Falkirk Lignite	Air & Oxygen	WGS	TI350 - Mixing Zone	0
TC12	Powder River Basin	Air	AI475H		
TC12	Powder River Basin	Oxygen at < 25% H_2O	AI475H		
TC12	Powder River Basin	Oxygen at > 25% H_2O	WGS	TI367 - Transition	0
TC13	PRB	Air	AI475H		
TC13	Freedom Lignite	Air< 20% H_2O	AI475H		
TC13	Freedom Lignite	Air at > 20% H_2O & Oxygen	WGS	TI344 - Mixing Zone	-100

Table 3.2-5

Gas Compositions, Molecular Weight, and Heating Value

Operating Period[2]	Average Relative Hour	H_2O[1] Mole %	CO Mole %	H_2 Mole %	CO_2 Mole %	CH_4 Mole %	C_2H_6 Mole %	N_2 Mole %	Total Mole %	Syngas LHV Btu/SCF	Syngas MW lb./Mole	O_2 in Feed %	Syngas CO/CO_2 Ratio
TC13-1	7	9.0	6.2	4.3	8.3	0.5	0.0	71.7	100.0	37	27.3	10.7	0.7
TC13-2	18	9.3	8.3	5.9	8.5	1.0	0.0	66.9	100.0	53	26.8	11.9	1.0
TC13-3	29	10.5	7.4	6.1	8.7	0.9	0.0	66.4	100.0	49	26.6	11.8	0.9
TC13-4	41	11.4	7.2	6.4	9.0	1.0	0.0	64.9	100.0	50	26.5	11.7	0.8
TC13-5	53	11.1	7.1	6.5	8.9	1.0	0.0	65.3	100.0	50	26.5	11.5	0.8
TC13-6	61	11.1	7.0	6.5	9.0	0.9	0.0	65.6	100.0	48	26.5	11.6	0.8
TC13-7	73	11.3	7.3	6.8	8.9	1.0	0.0	64.6	100.0	51	26.4	11.7	0.8
TC13-8	95	11.4	7.6	7.0	9.0	1.0	0.0	64.0	100.0	53	26.4	12.2	0.8
TC13-9	104	11.2	7.6	7.0	9.3	1.4	0.0	63.5	100.0	57	26.4	12.3	0.8
TC13-10a	143	13.9	4.2	5.3	9.6	0.8	0.1	66.1	100.0	36	26.7	11.3	0.4
TC13-10b	151	14.0	4.2	5.3	9.7	0.8	0.1	65.8	100.0	37	26.7	11.3	0.4
TC13-11	165	12.2	5.3	5.6	9.4	0.9	0.1	66.5	100.0	42	26.7	11.5	0.6
TC13-12	178	14.3	6.9	7.5	10.4	1.4	0.1	59.3	100.0	58	26.1	13.1	0.7
TC13-13	199	32.0	5.5	11.9	13.1	1.7	0.2	35.6	100.0	69	23.6	15.2	0.4
TC13-14	215	32.8	5.4	11.4	13.2	1.4	0.1	35.6	100.0	64	23.7	14.1	0.4
TC13-15	226	28.4	6.1	11.7	13.1	1.5	0.1	39.0	100.0	68	24.0	15.4	0.5
TC13-16	249	34.1	4.6	10.5	12.1	1.1	0.1	37.5	100.0	55	23.7	14.5	0.4
TC13-17	268	13.0	5.4	5.3	9.8	0.6	0.0	65.9	100.0	37	26.8	11.5	0.5
TC13-18a	281	13.4	5.0	6.1	9.7	0.8	0.0	65.0	100.0	41	26.5	11.0	0.5
TC13-18b	289	12.9	5.0	6.0	9.7	0.9	0.1	65.3	100.0	42	26.6	10.8	0.5
TC13-19	300	13.4	5.1	6.2	10.0	0.9	0.0	64.5	100.0	42	26.5	11.1	0.5
TC13-20	318	12.9	3.6	4.8	9.3	0.6	0.0	68.8	100.0	30	26.9	10.2	0.4
TC13-21	337	12.5	3.9	4.9	9.4	0.5	0.0	68.7	100.0	32	26.9	10.4	0.4
TC13-22a	380	12.8	2.4	3.8	8.5	0.7	0.0	71.7	100.0	25	27.0	9.3	0.3
TC13-22b	391	13.2	2.4	3.7	8.5	0.6	0.0	71.5	100.0	24	27.0	9.3	0.3
TC13-23	413	16.4	2.6	5.6	9.5	0.9	0.1	64.8	100.0	34	26.3	9.6	0.3
TC13-24	442	19.7	2.3	5.9	10.2	0.9	0.1	61.0	100.0	33	26.0	10.2	0.2
TC13-25	456	18.5	2.8	6.3	10.3	1.0	0.1	60.9	100.0	38	26.0	10.4	0.3
TC13-26	463	18.3	3.2	6.9	10.4	1.1	0.1	59.9	100.0	42	25.9	10.6	0.3
TC13-27	471	18.9	2.8	6.4	10.4	1.1	0.1	60.3	100.0	39	26.0	10.4	0.3
TC13-28	483	18.9	2.9	6.6	10.4	1.1	0.1	60.0	100.0	40	25.9	10.4	0.3
TC13-29	503	15.8	3.8	6.9	10.0	1.2	0.1	62.2	100.0	44	26.1	10.9	0.4

Notes:

1. TC13-1 to TC13-12, TC13-17 to TC13-22b, and TC13-29 used AI475H for H_2O; TC13-13 to TC13-16 and TC13-23 to TC13-28 use WGS for H_2O.
2. TC13-1 to TC13-9 were air blown PRB; TC13-10a to TC13-12 were air blown low sodium lignite; TC13-13 to TC13-14 were oxygen blown low sodium lignite; TC13-15 was oxygen blown using a mixture of low and high sodium lignite; TC13-16 was oxygen blown high sodium lignite; TC13-17 to TC13-29 were air blown high sodium lignite.

Table 3.2-6

Details of Projected LHV Changes

	Fuel	PRB	Low Sodium Lignite		High Sodium Lignite	
Change	Mode	Air Blown	Air Blown	Oxygen Blown	Oxygen Blown	Air Blown
1	Non-air nitrogen deletion	18.7	14.4	25.0	28.5	15.1
2	Correct energy balance for nonair nitrogen deletion	9.4	6.7	13.9	12.2	8.0
3 + 4	Adiabatic gasifier, lower steam rate	22.0	18.5	30.1	41.5	22.9
5	Water Gas Shift	-0.6	-0.5	0.2	0.4	-0.6
Total		49.5	39.1	69.2	82.6	45.4

Table 3.2-7

Commercially Projected[1] Gas Compositions, Molecular Weight, and Heating Value

Operating Period[2]	Average Relative Hour	H_2O Mole %	CO Mole %	H_2 Mole %	CO_2 Mole %	CH_4 Mole %	C_2H_6 Mole %	N_2 Mole %	Total Mole %	Syngas LHV Btu/SCF	Syngas MW lb./Mole	O_2 in Feed %	Turbine LHV[3] Btu/SCF	Syngas CO/CO_2 Ratio
TC13-1	7	15.8	14.3	13.3	10.9	1.4	0.0	44.3	100.0	96	24.5	14.5	112	1.3
TC13-2	18	14.5	15.4	13.6	10.8	2.1	0.0	43.5	100.0	107	24.5	16.5	123	1.4
TC13-3	29	16.6	13.4	13.6	11.1	1.9	0.0	43.4	100.0	98	24.3	16.3	116	1.2
TC13-4	41	18.1	12.7	14.0	11.6	2.0	0.0	41.5	100.0	98	24.2	15.7	118	1.1
TC13-5	53	17.8	12.8	14.4	11.6	2.0	0.0	41.5	100.0	99	24.1	15.5	119	1.1
TC13-6	61	17.8	12.5	14.4	11.7	1.7	0.0	41.9	100.0	96	24.1	15.5	115	1.1
TC13-7	73	17.8	12.9	14.6	11.5	1.9	0.0	41.3	100.0	99	24.0	15.7	120	1.1
TC13-8	95	17.4	13.0	14.2	11.5	2.0	0.0	42.0	100.0	99	24.2	16.2	118	1.1
TC13-9	104	17.0	12.8	14.0	11.8	2.6	0.0	41.9	100.0	103	24.3	16.2	123	1.1
TC13-10a	143	23.2	7.7	12.3	12.7	1.7	0.2	42.2	100.0	76	24.3	14.9	98	0.6
TC13-10b	151	23.2	7.7	12.2	12.9	1.7	0.2	42.2	100.0	76	24.4	15.0	98	0.6
TC13-11	165	19.7	9.7	12.9	12.2	1.8	0.2	43.5	100.0	86	24.4	15.2	106	0.8
TC13-12	178	20.0	10.2	12.6	12.7	2.3	0.2	42.0	100.0	91	24.5	16.7	113	0.8
TC13-13	199	44.7	10.5	23.0	18.2	3.2	0.4	0.0	100.0	132	20.1	23.5	237	0.6
TC13-14	215	41.6	12.7	23.6	18.8	3.0	0.3	0.0	100.0	139	20.3	20.8	235	0.7
TC13-15	226	38.7	13.8	25.2	18.8	3.2	0.3	0.0	100.0	148	20.2	25.2	239	0.7
TC13-16	249	42.4	12.5	25.2	17.0	2.7	0.2	0.0	100.0	138	19.6	24.5	237	0.7
TC13-17	268	22.4	10.4	12.8	13.7	1.2	0.0	39.4	100.0	81	24.5	14.8	103	0.8
TC13-18a	281	22.9	9.5	14.3	13.3	1.7	0.1	38.2	100.0	87	23.9	14.0	112	0.7
TC13-18b	289	21.8	9.4	14.1	13.2	1.9	0.1	39.5	100.0	89	24.0	14.0	112	0.7
TC13-19	300	21.9	9.2	13.8	13.3	1.8	0.1	39.8	100.0	86	24.1	14.2	109	0.7
TC13-20	318	25.0	7.8	14.5	13.0	1.5	0.1	38.0	100.0	80	23.6	12.0	106	0.6
TC13-21	337	23.4	8.5	14.5	12.9	1.4	0.1	39.3	100.0	82	23.8	12.3	105	0.7
TC13-22a	380	30.1	6.1	15.5	12.5	2.3	0.2	33.3	100.0	86	22.7	10.5	122	0.5
TC13-22b	391	31.5	5.8	15.1	12.4	2.2	0.2	32.8	100.0	83	22.6	10.3	120	0.5
TC13-23	413	31.9	5.1	14.6	13.7	2.2	0.2	32.3	100.0	80	23.0	10.7	117	0.4
TC13-24	442	35.3	4.0	13.2	14.2	1.9	0.2	31.3	100.0	70	23.1	11.2	107	0.3
TC13-25	456	31.6	4.8	13.7	13.8	2.1	0.2	33.8	100.0	76	23.2	11.6	110	0.3
TC13-26	463	30.5	5.2	14.4	13.8	2.2	0.3	33.5	100.0	81	23.1	12.1	116	0.4
TC13-27	471	32.1	4.7	13.6	14.0	2.2	0.3	33.1	100.0	77	23.2	11.6	113	0.3
TC13-28	483	31.7	4.9	13.8	13.9	2.2	0.3	33.3	100.0	78	23.2	11.7	113	0.3
TC13-29	503	26.8	6.8	15.2	13.5	2.4	0.3	34.9	100.0	90	23.2	13.3	122	0.5

Notes:

1. Commercially projected syngas compositions assume that syngas and steam are used for aeration and instrument purges and that the reactor is adiabatic.
2. TC13-1 to TC13-9 were air blown PRB; TC13-10a to TC13-12 were air blown low sodium lignite; TC13-13 to TC13-14 were oxygen blown low sodium lignite; TC13-15 was oxygen blown using a mixture of low and high sodium lignite; TC13-16 was oxygen blown high sodium lignite; TC13-17 to TC13-29 were air blown high sodium lignite.
3. Turbine syngas LHV is the LHV after cold sulfur cleanup where the syngas H_2O is decreased to 1%.

Table 3.2-8

Water-Gas Shift Equilibrium Constant

In-situ Start[3]	In-situ End	Run Time Hours	Operating Period	Dry CO %	Dry H_2 %	Dry CO_2 %	In-situ H_2O %	Kp	WGS Eqm. Temp. F	Mixing Zone Temp. F	Mixing Zone Kp[2]
10/2/03 11:20	10/2/03 14:20	16	TC13-2	8.9	6.4	9.3	8.1	0.76	1,644	1,763	0.74
10/3/03 9:00	10/3/03 13:00	38	TC13-4 (Pt) [4]	8.3	7.1	10.0	10.0	0.78	1,632	1,750	0.75
10/6/03 9:30	10/6/03 13:30	111	None[1]	8.6	8.3	10.1	10.8	0.80	1,611	1,735	0.77
10/7/03 10:30	10/7/03 14:30	135	None[1]	5.4	6.4	11.1	13.6	0.83	1,592	1,734	0.77
10/8/03 10:00	10/8/03 14:00	159	None[1]	5.8	6.2	11.0	12.3	0.83	1,588	1,719	0.79
10/9/03 8:30	10/9/03 12:30	182	None[1]	8.1	9.4	12.2	13.9	0.88	1,559	1,705	0.81
10/10/03 9:45	10/10/03 13:45	207	None[1]	7.8	18.0	19.9	32.6	0.95	1,513	1,647	0.89
10/16/03 12:30	10/16/03 14:30	279	None[1]	5.7	6.9	11.2	13.1	0.90	1,542	1,649	0.89
10/17/03 9:00	10/17/03 12:42	300	TC13-20	5.8	6.9	11.3	13.4	0.87	1,561	1,632	0.92
10/27/03 10:00	10/27/03 12:00	400	None[1]	3.7	6.0	10.8	13.7	1.11	1,431	1,510	1.16
10/28/03 10:00	10/28/03 12:00	424	None[1]	3.8	7.0	11.7	15.8	1.16	1,406	1,494	1.19
10/31/03 10:00	10/31/03 14:00	430	TC13-26 (Pt) [4]	3.5	7.8	12.7	19.6	1.17	1,404	1,456	1.29

Notes:

1. Data not taken during operating period.
2. Equilibrium constant calculated at mixing zone temperature (TI344), with an -100ºF approach.
3. October 2 to 6 data taken during PRB air blown operation. October 7 to 9 data taken during low sodium Freedom mine lignite air blown operation.
   October 10 data taken during low sodium Freedom mine lignite oxygen blown operation.
   October 16 to 31 data taken during high sodium Freedom mine lignite air blown operation.
4. Insitu sample was taken during part of the indicated operating period.

Table 3.2-9

Transport Gasifier Equilibrium Calculations

Operating Period	Average Relative Hour	Measured Syngas Kp[1]	Mixing Zone Equilibrium Kp[2]	Wet AI419J H_2S ppm	Syngas Total Reduced Sulfur[3] ppm	Minimum Equilibrium H_2S[4] ppm	AI475Q Ammonia ppm	PCD Equilibrium Ammonia[5] ppm
TC13-1	7	0.65	0.80	272	449	188	483	752
TC13-2	18	0.65	0.73	203	308	197	1,092	968
TC13-3	29	0.67	0.75	232	259	224	1,073	984
TC13-4	41	0.71	0.76	256	258	246	1,151	1,096
TC13-5	53	0.73	0.78	250	222	239	1,199	1,202
TC13-6	61	0.76	0.79	257	224	240	1,043	1,185
TC13-7	73	0.73	0.80	277	253	245	1,291	1,323
TC13-8	95	0.72	0.78	281	252	250	1,270	1,336
TC13-9	104	0.76	0.76	294	281	249	1,596	1,384
TC13-10a	143	0.87	0.80	1,383	1,377	305	819	832
TC13-10b	151	0.88	0.79	1,431	1,430	308	759	833
TC13-11	165	0.82	0.77	1,611	1,664	266	653	923
TC13-12	178	0.79	0.82	1,578	1,732	335	1,298	1,163
TC13-13	199	(7)	0.89	2,266	2,136	735	2,316	2,013
TC13-14	215	(7)	0.84	2,129	2,209	737	2,075	1,859
TC13-15	226	(7)	0.89	1,688	1,608	633	2,528	2,532
TC13-16	249	(7)	0.81	1,509	1,451	703	1,653	1,826
TC13-17	268	0.75	0.86	696	(6)	285	1,164	1,066
TC13-18a	281	0.87	0.89	1,027	1,174	290	1,206	1,343
TC13-18b	289	0.91	0.90	1,022	1,190	279	1,384	1,410
TC13-19	300	0.90	0.92	637	844	291	1,420	1,376
TC13-20	318	0.96	0.95	880	1,120	243	884	831
TC13-21	337	0.94	0.94	881	1,134	231	890	796
TC13-22a	380	1.05	1.15	570	1,030	228	1,433	1,213
TC13-22b	391	1.02	1.16	605	1,007	229	1,377	1,156
TC13-23	413	(7)	1.22	872	1,089	325	1,873	2,040
TC13-24	442	(7)	1.33	994	1,242	406	1,763	1,945
TC13-25	456	(7)	1.26	1,042	1,268	390	2,111	2,385
TC13-26	463	(7)	1.24	1,177	1,318	388	2,326	2,612
TC13-27	471	(7)	1.27	1,132	1,284	399	2,264	2,289
TC13-28	483	(7)	1.25	1,058	1,246	399	2,250	2,467
TC13-29	503	1.14	1.21	785	1,188	332	2,350	2,777

Notes:

1. Syngas Kp determined by syngas hydrogen, water, carbon dioxide, and carbon monoxide concentrations.
2. Mixing zone Kp determined by equilibrium calculations using the mixing zone temperature (TI344).
3. Synthesis gas total reduced sulfur (TRS) estimated from Synthesis gas combustor SO_2 analyzer data.
4. Minimum equilibrium H_2S determined by equilibrium calculations and the carbon dioxide and water partial pressures.
5. Equilibrium ammonia concentrations determined by equilibrium calculations and the partial pressures of hydrogen and nitrogen.
6. Syngas Combustor SO_2 analyzer was out of service, so syngas total reduced sulfur could not be determined.
7. Moisture analyzer out of range so measured syngas Kp could not be determined.

Table 3.2-10

Syngas Combustor Calculations

Operating Period[3]	Average Relative Hour	Syngas Combustor Exit AI8775 O_2 M %	Syngas Combustor Exit Calculated O_2 M %	Syngas Combustor Exit AI476D CO_2 M %	Syngas Combustor Exit Calculated CO_2 M %	Syngas Combustor Exit AI476H H_2O M %	Syngas Combustor Exit Calculated H2O M %	Gas Analyzer LHV Btu/SCF	Energy Balance LHV[1] Btu/SCF	Combustor SO_2 AI476P ppm	Syngas Total Reduced Sulfur[2] ppm
TC13-1	7	3.4	3.2	8.8	10.1	11.0	11.2	37	32	248	449
TC13-2	18	2.9	3.2	10.1	10.9	11.5	11.7	53	49	179	308
TC13-3	29	3.4	3.6	9.4	10.3	12.1	12.3	49	46	144	259
TC13-4	41	3.7	3.9	10.3	10.2	12.7	12.8	50	48	140	258
TC13-5	53	3.6	3.8	10.3	10.1	12.9	12.8	50	47	120	222
TC13-6	61	3.3	3.4	10.4	10.4	13.3	13.1	48	44	125	224
TC13-7	73	3.3	3.6	10.9	10.4	13.3	13.1	51	49	144	253
TC13-8	95	3.1	3.3	11.4	10.7	13.6	13.3	53	51	148	252
TC13-9	104	2.8	3.1	11.5	10.9	13.7	13.5	57	55	164	281
TC13-10a	143	3.7	4.7	9.6	8.9	14.9	13.6	36	38	665	1377
TC13-10b	151	3.7	4.7	9.6	9.0	14.8	13.6	37	39	691	1430
TC13-11	165	3.8	4.8	10.3	9.2	13.7	12.7	42	43	814	1664
TC13-12	178	3.7	3.9	11.3	10.7	14.8	15.0	58	56	954	1732
TC13-13	199	5.1	5.3	10.5	10.0	22.7	24.0	69	67	1002	2136
TC13-14	215	5.4	5.3	9.8	10.0	22.0	23.6	64	60	988	2209
TC13-15	226	5.5	5.7	10.3	9.9	20.9	21.2	68	64	709	1608
TC13-16	249	6.1	6.9	9.3	8.3	20.1	21.1	55	57	550	1451
TC13-17	268	2.9	2.7	(5)	10.7	(5)	14.3	37	35	(4)	(4)
TC13-18a	281	3.8	4.0	10.0	9.6	14.0	14.1	41	40	594	1174
TC13-18b	289	3.8	4.1	9.8	9.5	13.8	13.7	42	40	588	1190
TC13-19	300	3.6	3.9	10.0	9.8	14.1	14.2	42	40	428	844
TC13-20	318	4.4	5.1	8.9	8.4	13.1	12.8	30	28	469	1120
TC13-21	337	4.4	5.1	9.0	8.5	12.9	12.6	32	30	479	1134
TC13-22a	380	6.3	7.0	7.3	6.9	11.9	11.4	25	26	332	1030
TC13-22b	391	6.3	7.0	7.2	6.9	11.8	11.5	24	25	325	1007
TC13-23	413	2.9	3.4	9.0	8.9	17.1	16.3	34	34	580	1089
TC13-24	442	3.0	4.1	9.0	8.7	21.2	17.3	33	34	596	1242
TC13-25	456	3.2	4.6	9.6	8.7	18.8	16.6	38	42	619	1268
TC13-26	463	3.0	3.6	9.8	9.3	19.1	17.6	42	42	691	1318
TC13-27	471	2.9	3.8	9.6	9.1	19.7	17.5	39	40	663	1284
TC13-28	483	3.0	4.2	10.0	8.9	19.5	17.3	40	43	633	1246
TC13-29	503	3.3	4.8	10.5	8.7	16.1	15.3	44	50	600	1188

Notes:

1. Energy LHV calculated assuming the syngas combustor heat loss was 1.5 million Btu/hr.
2. Syngas total reduced sulfur (TRS) estimated from syngas combustor SO_2 analyzer data.
3. TC13-1 to TC13-9 were air blown PRB; TC13-10a to TC13-12 were air blown low sodium lignite; TC13-13 to TC13-14 were oxygen blown low sodium lignite; TC13-15 was oxygen blown using a mixture of low and high sodium lignite; TC13-16 was oxygen blown high sodium lignite; TC13-17 to TC13-29 were air blown high sodium lignite.
4. Syngas Combustor SO_2 analyzer was out of service, so syngas total reduced sulfur could not be determined.
5. Syngas Combustor CO_2 and H_2O analyzers out of service

Table 3.2-11

Syngas Combustor Results

Test Campaign	Fuel	Mode	Heat Loss to Fit Gas Analyzer LHV Million Btu	Syngas Combustor Oxygen Balance Agreement ± Per Cent	Syngas Combustor Water Balance Agreement ± Per Cent	C_2^+ Determination
TC06	Powder River Basin	Air	2.25	15	(1)	0.00
TC07	Powder River Basin	Air	1.00	15	12	AI464F
TC08	Powder River Basin	Air & Oxygen	2.50	15	10	0.00
TC09	Hiawatha Bituminous	Air & Oxygen	1.50	25	12	AI464F or AI464F
TC10	Powder River Basin	Air & Oxygen	1.50	10	10	0.25
TC11	Falkirk Lignite	Air & Oxygen	2.00	15	10	AI419F
TC12	Powder River Basin	Air	2.50	15	15	0.00
TC13	PRB	Air	1.50	15	10	AI464F
TC13	Freedom Lignite	Air & Oxygen	1.50	15	10	AI464F

Notes

1. AI476H not in service.

Table 3.2-12

Ammonia Equilibrium Approach Temperatures

Test Campaign[1]	Fuel	Mode	NH_3 Equilibrium Approach to PCD Inlet Temperature °F
TC08[2]	PRB	Air	80
TC10[3]	PRB	Oxygen	45
TC11	Falkirk Lignite	Air & Oxygen	110
TC12	PRB	Air	30
TC12	PRB	Oxygen	70
TC13	PRB	Air	60
TC13[4]	Freedom Lignite - Low Sodium	Air & Oxygen	120
TC13[4]	Freedom Lignite - High Sodium, High Temperature[5]	Air & Oxygen	105
TC13[4]	Freedom Lignite - High Sodium, Low Temperature[6]	Air	25

Notes:

1. No ammonia data for TC06, TC07, and TC09 because the ammonia analyzer was not in service.
2. All TC08 oxygen-blown data was above 2,000 ppm, which is above the maximum range of the ammonia analyzer.
3. Two air-blown TC10 data points not included.
4. One TC13 mixture of low- and high-sodium lignite data not included.
5. High temperatue is mixing zone temperatures above 1,600°F.
6. Low temperatue is mixing zone temperatures below 1,600°F.

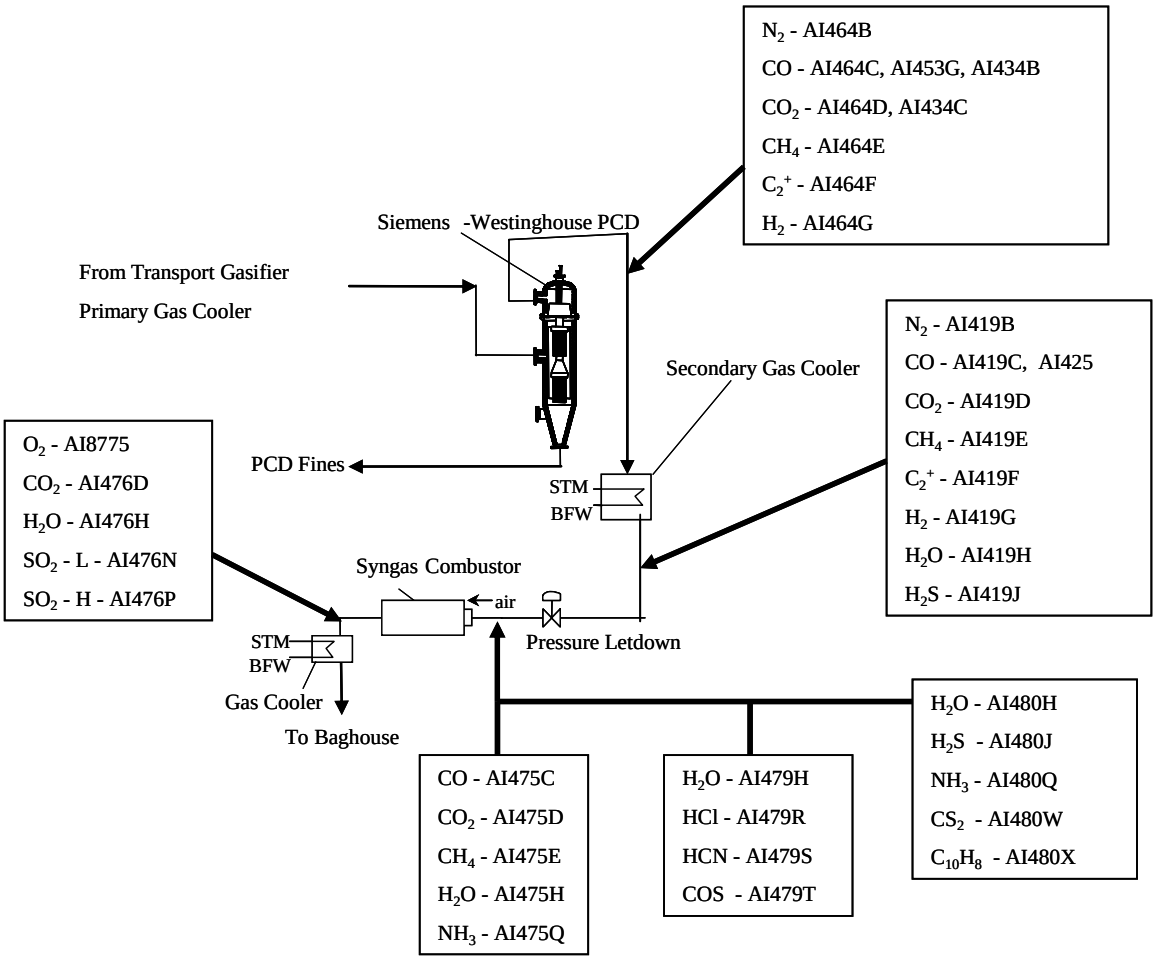

Figure 3.2-1 Gas Sampling Locations

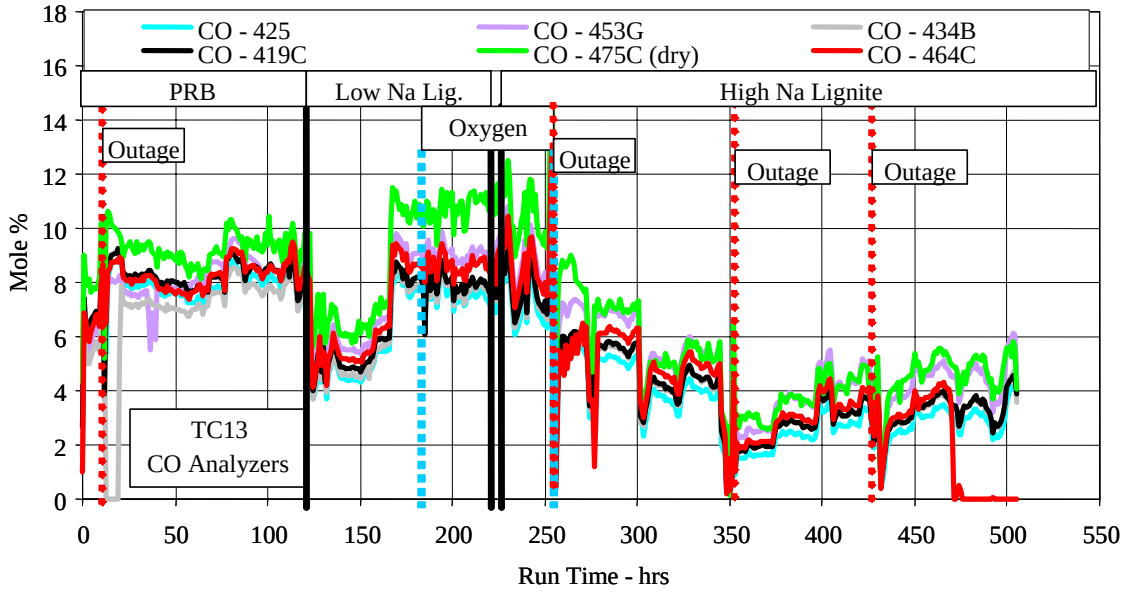

Figure 3.2-2 Carbon Monoxide Analyzer Data

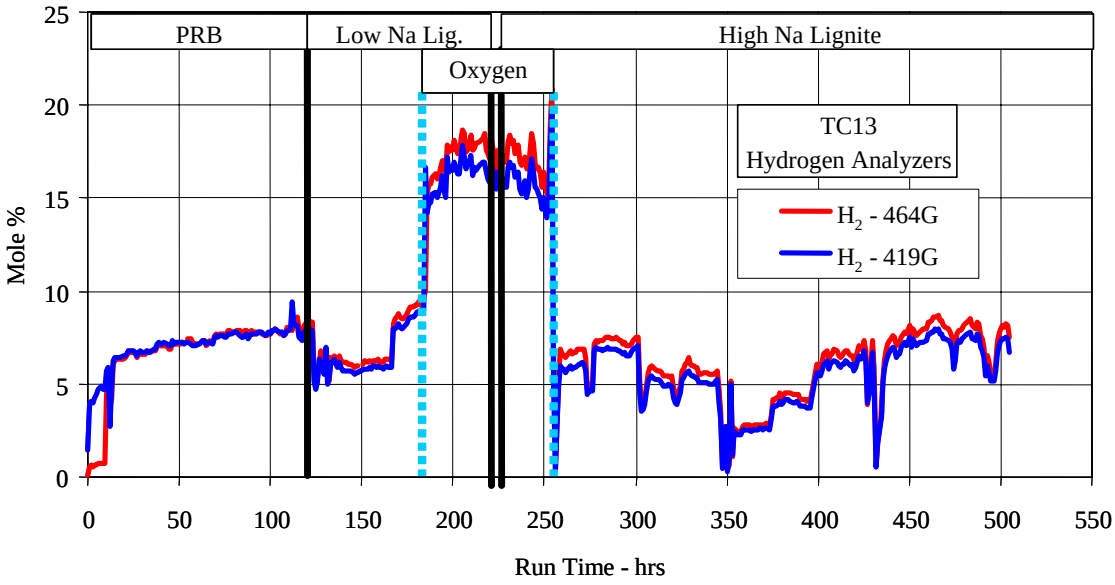

Figure 3.2-3 Hydrogen Analyzer Data

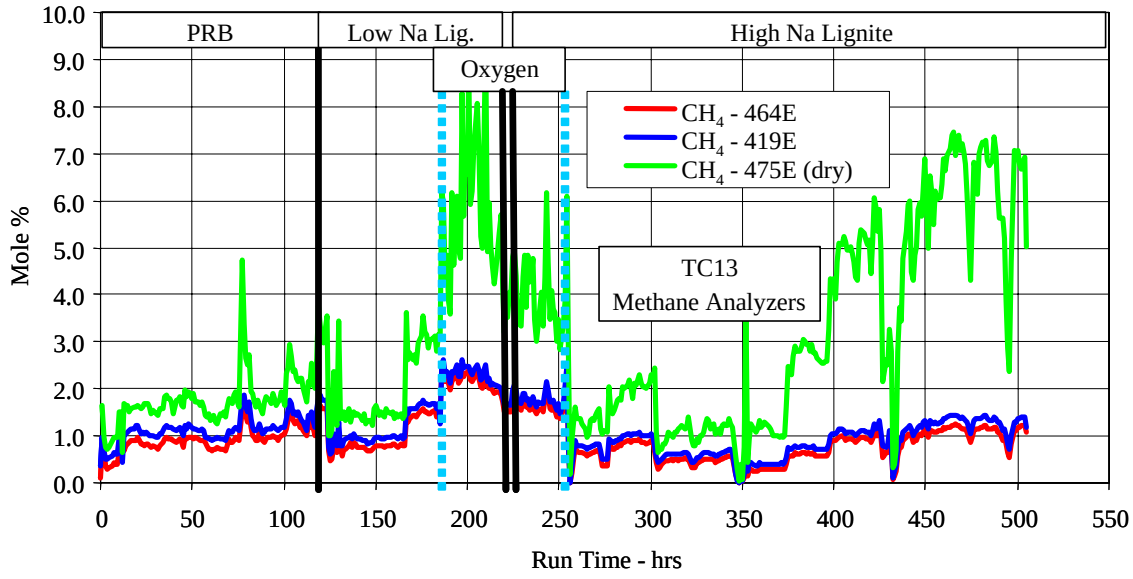

Figure 3.2-4 Methane Analyzer Data

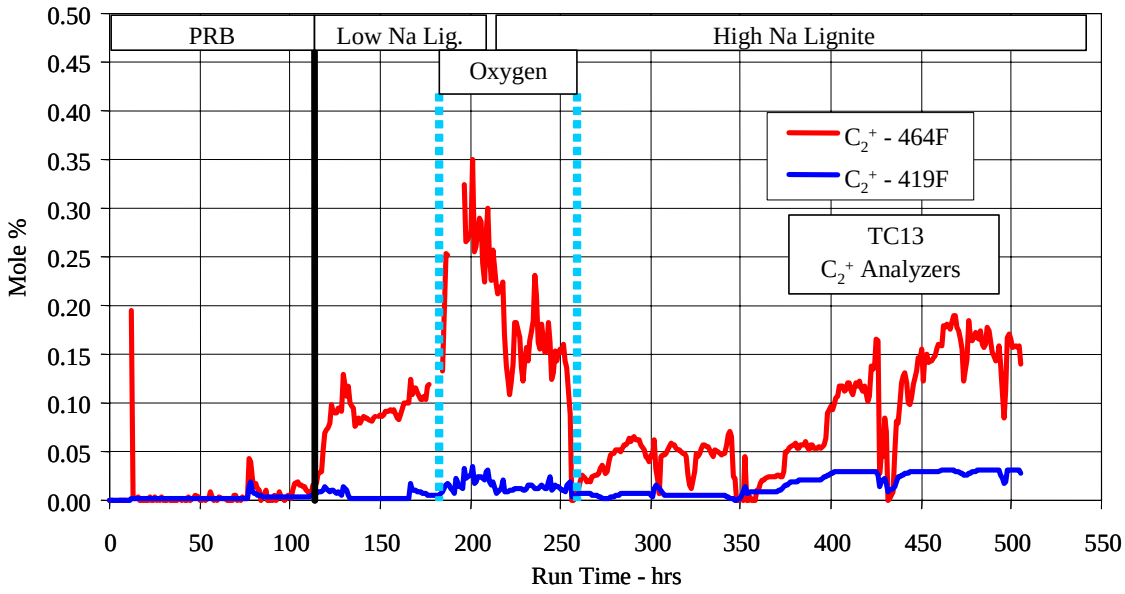

Figure 3.2-5 C_2^+Analyzer Data

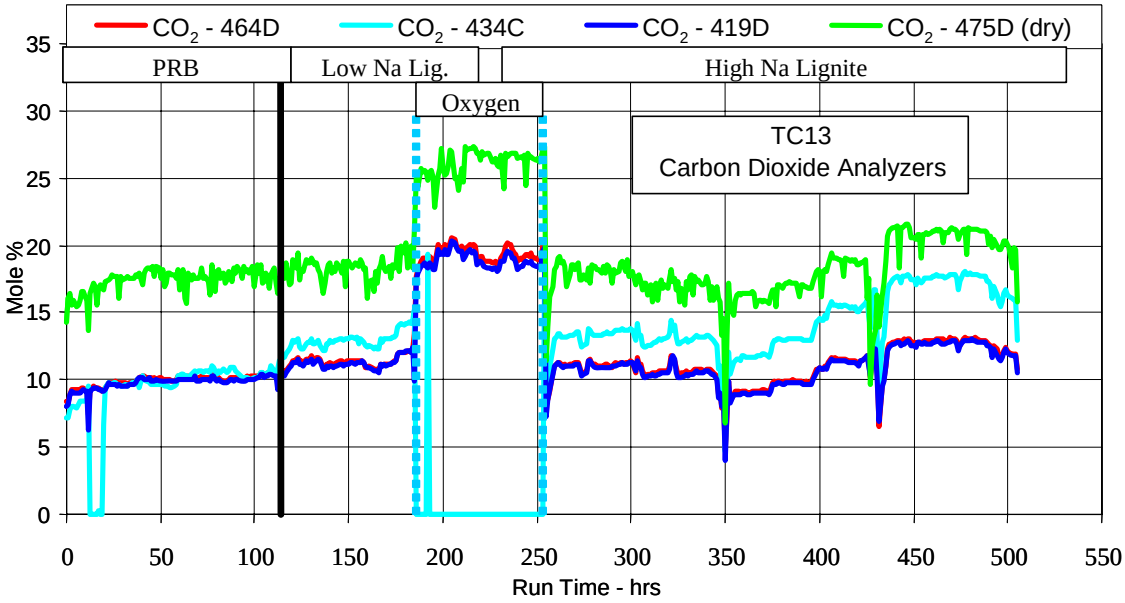

Figure 3.2-6 Carbon Dioxide Analyzer Data

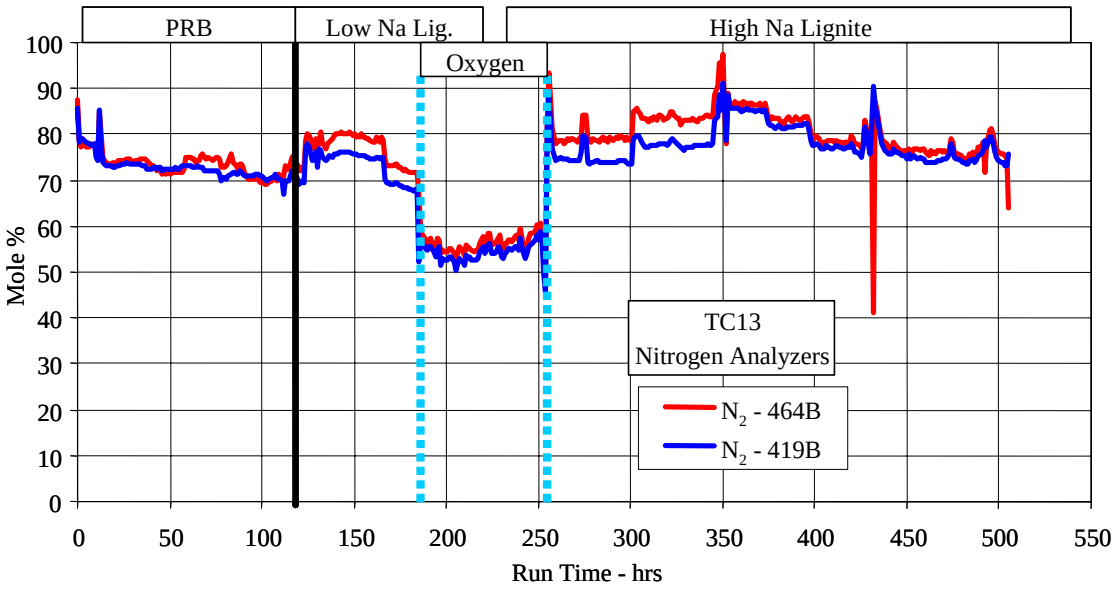

Figure 3.2-7 Nitrogen Analyzer Data

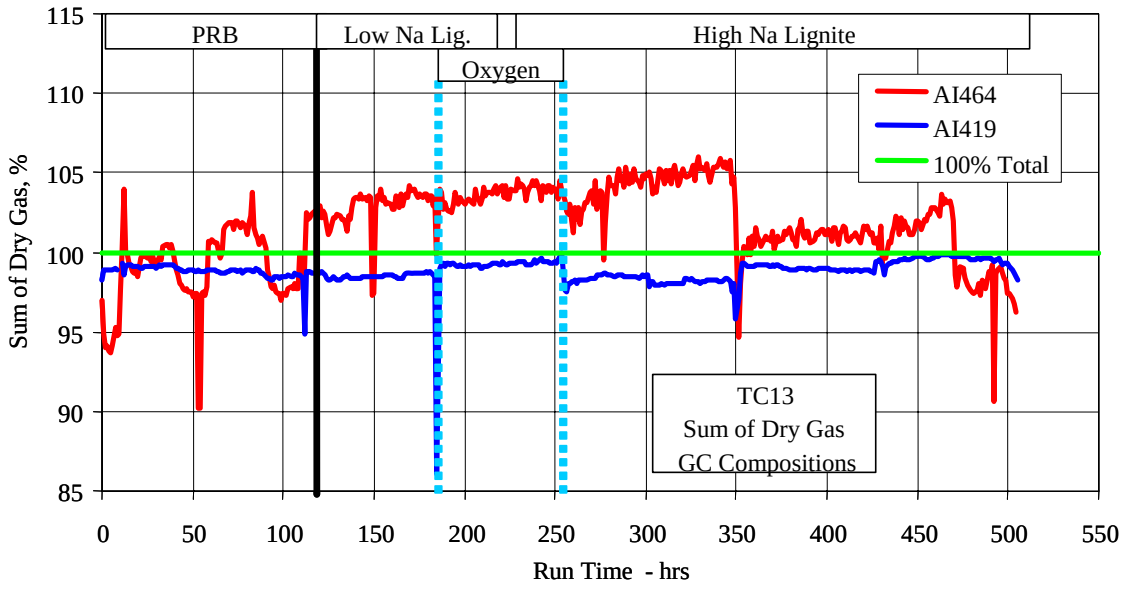

Figure 3.2-8 Sums of GC Gas Compositions (Dry)

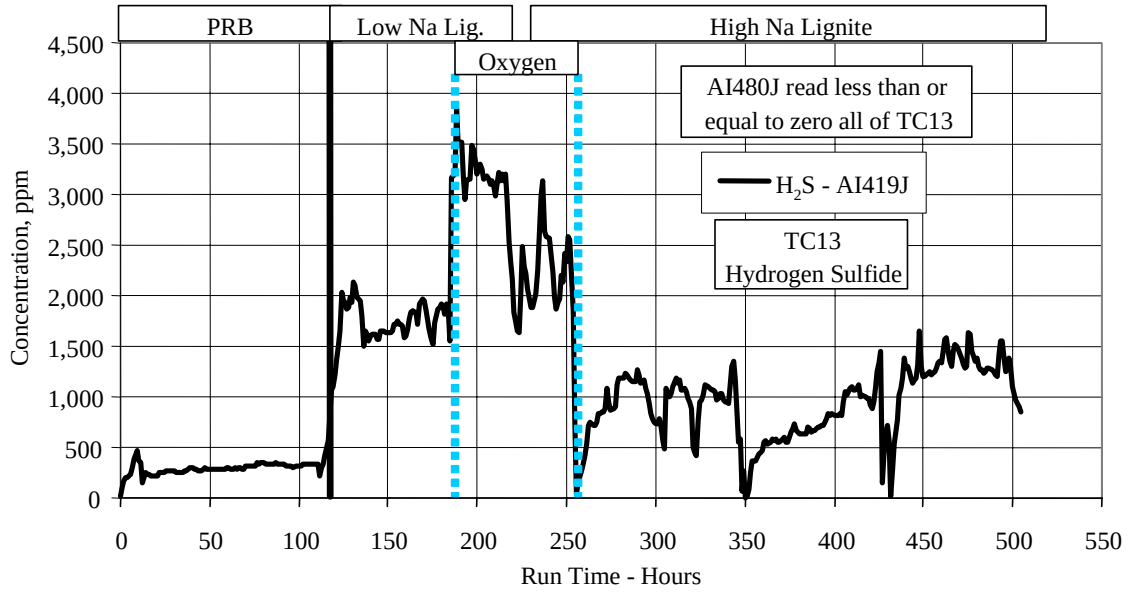

Figure 3.2-9 Hydrogen Sulfide Analyzer Data

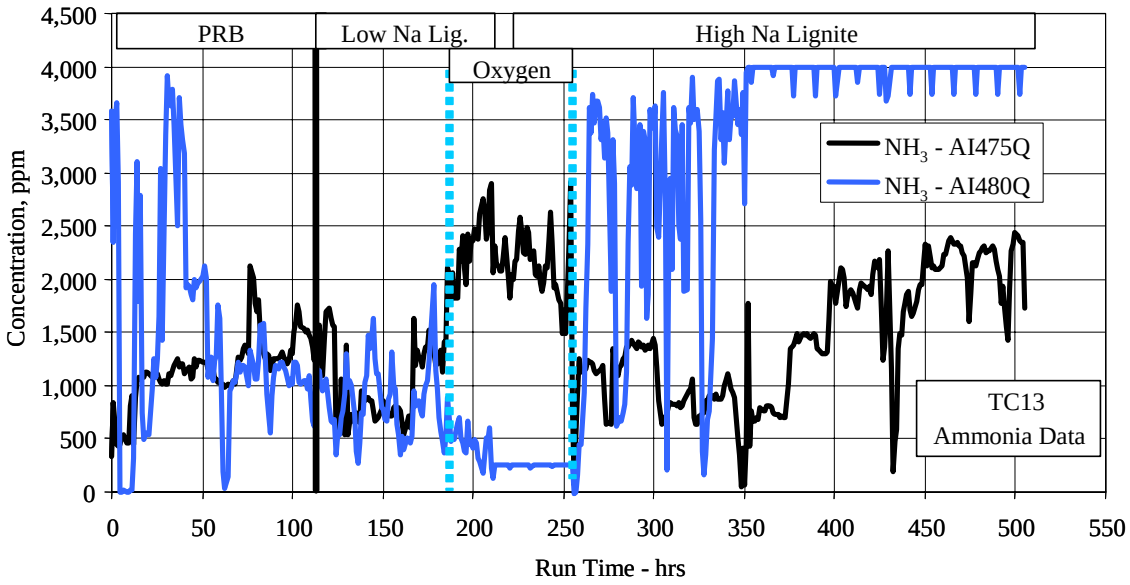

Figure 3.2-10 Ammonia Data

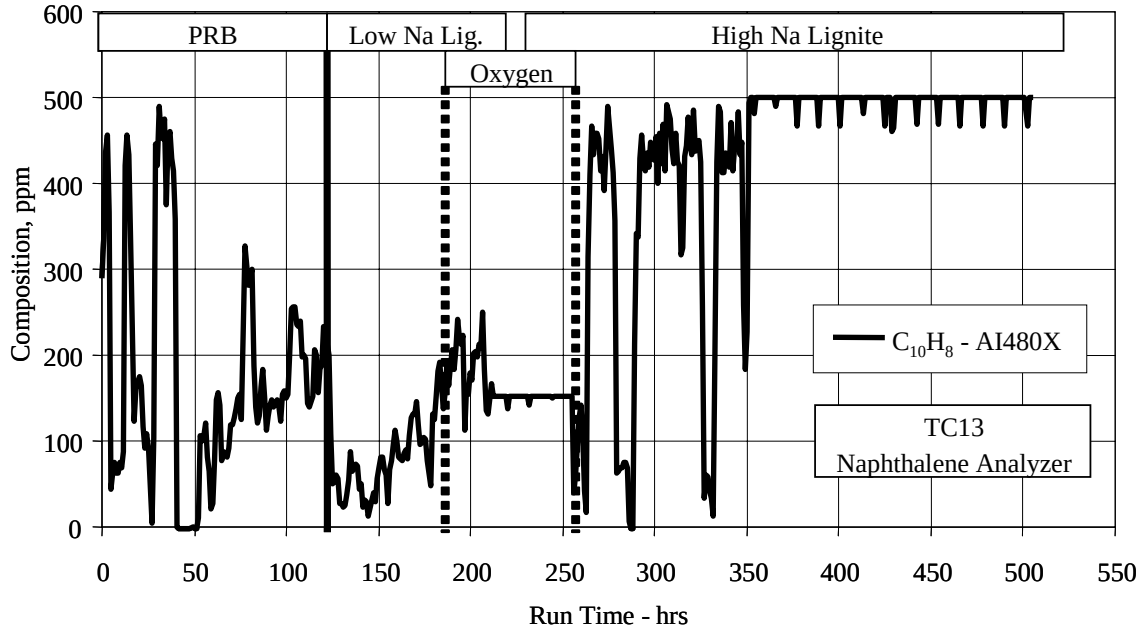

Figure 3.2-11 Naphthalene Data

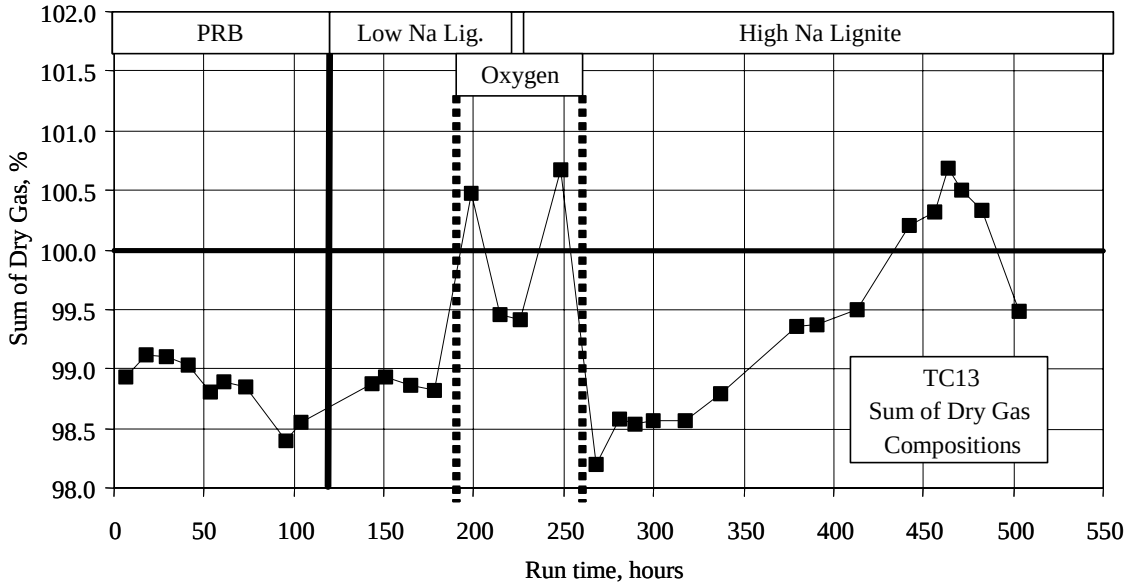

Figure 3.2-12 Sums of Dry Gas Compositions

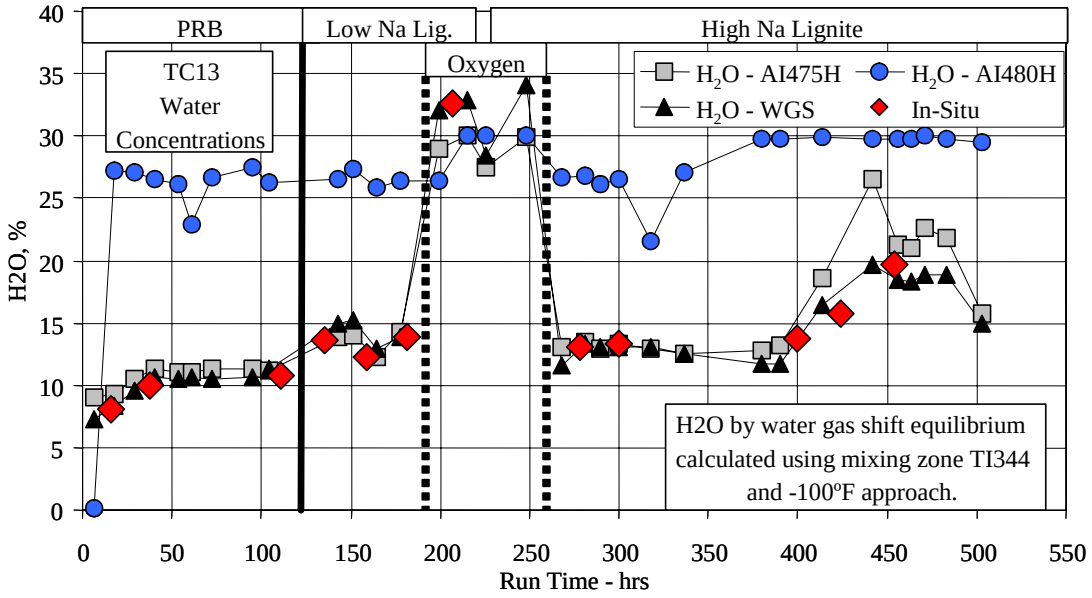

Figure 3.2-13 H_2O Data

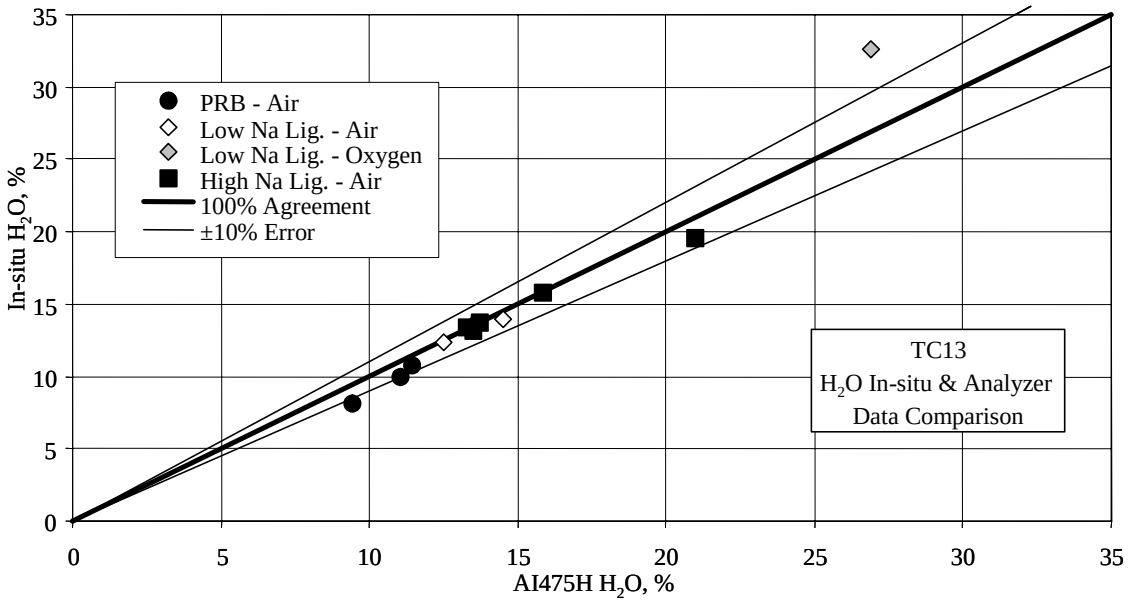

Figure 3.2-14 In situ H_2O and H_2O Analyzer Comparison

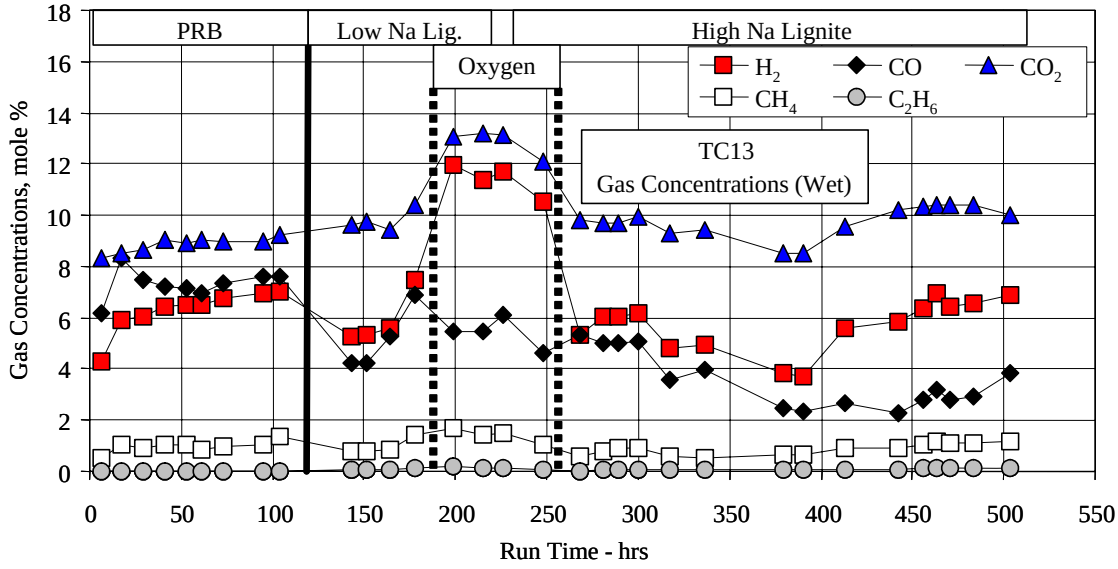

Figure 3.2-15 Wet Syngas Compositions

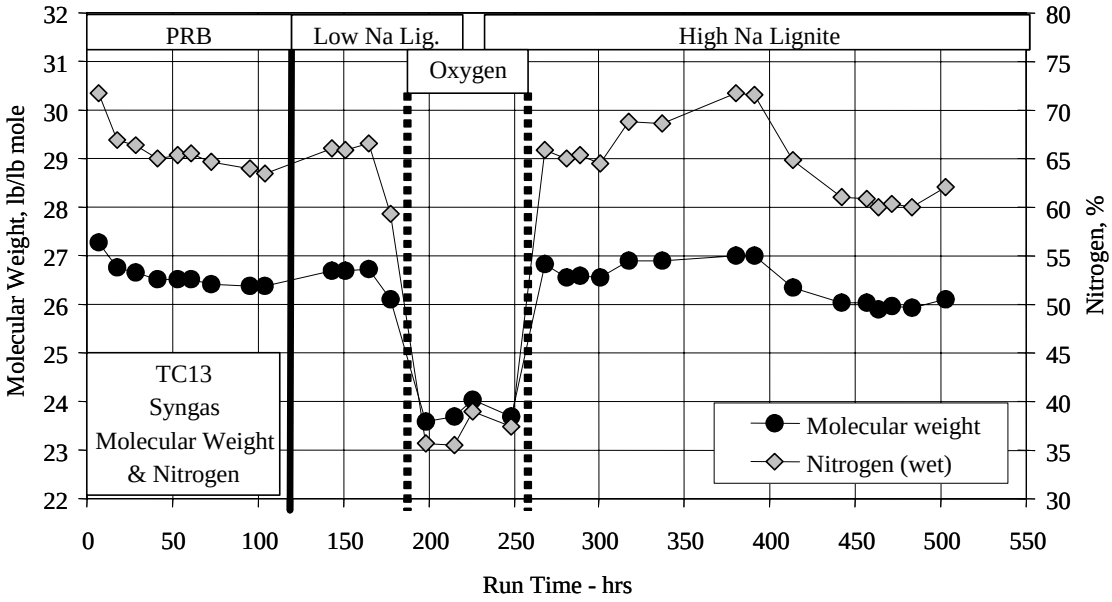

Figure 3.2-16 Syngas Molecular Weight and Nitrogen Concentration

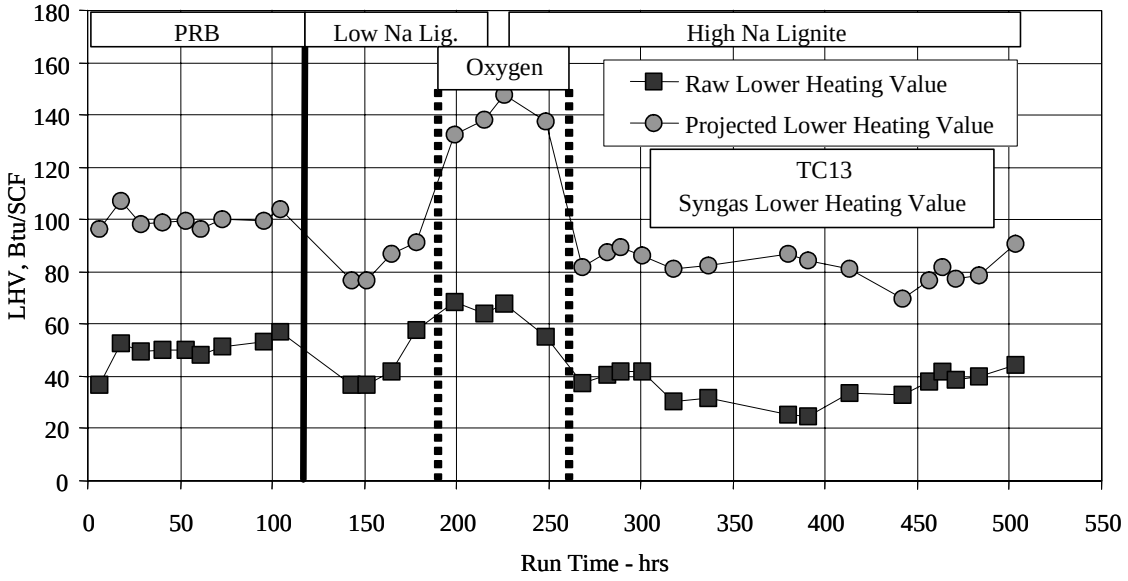

Figure 3.2-17 Syngas Lower Heating Values

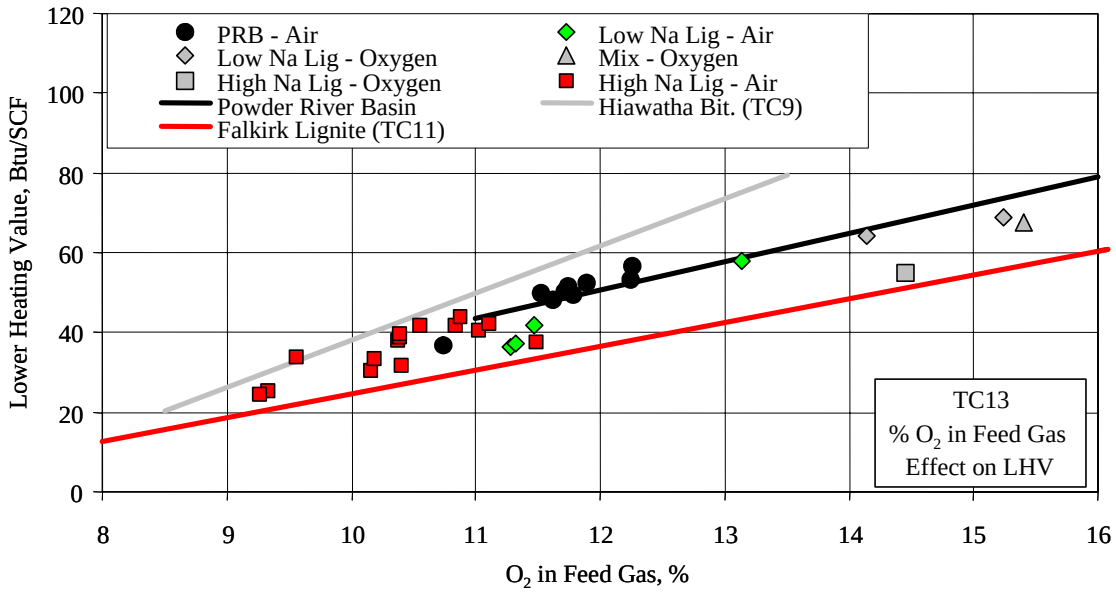

Figure 3.2-18 Raw Lower Heating Value and Overall Percent O_2

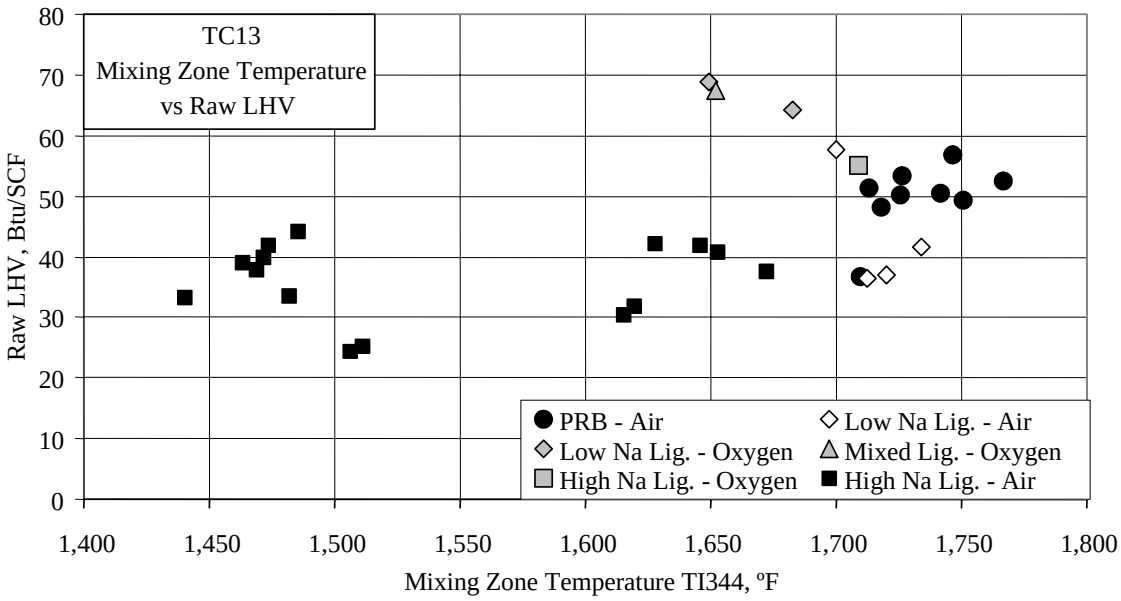

Figure 3.2-19 LHVs and Mixing Zone Temperature

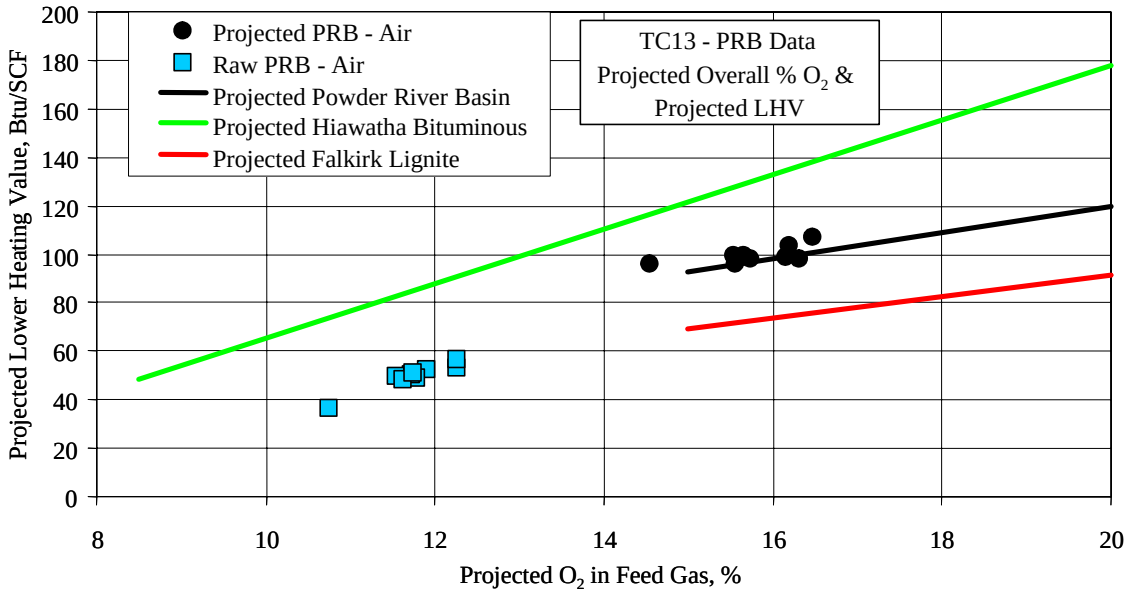

Figure 3.2-20 PRB Projected LHVs and Overall Percent O_2

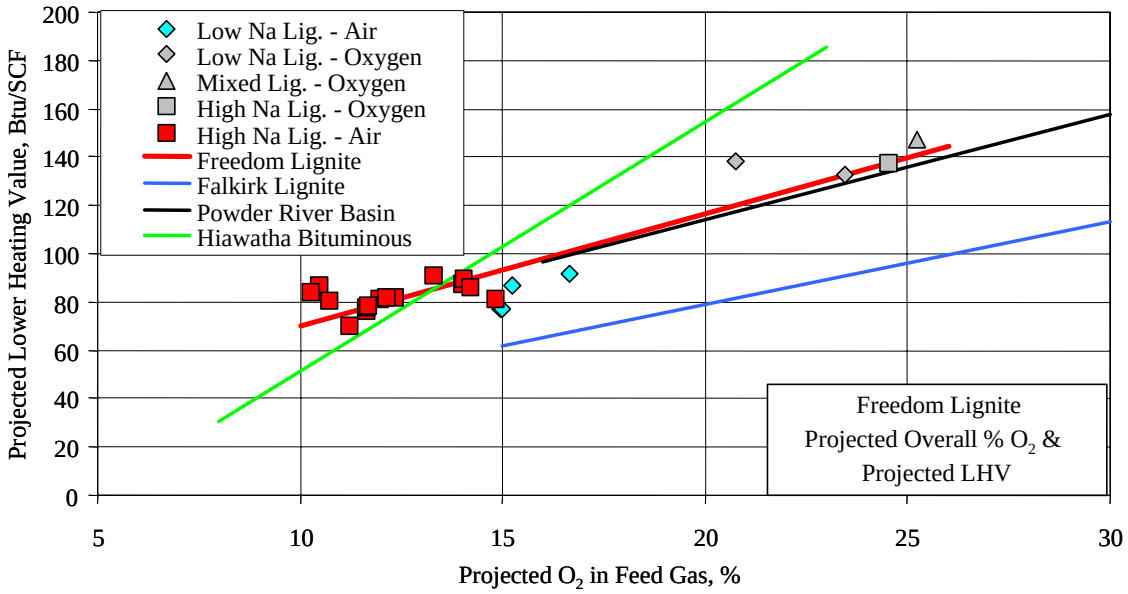

Figure 3.2-21 Freedom Lignite Projected LHVs and Overall Percent O_2

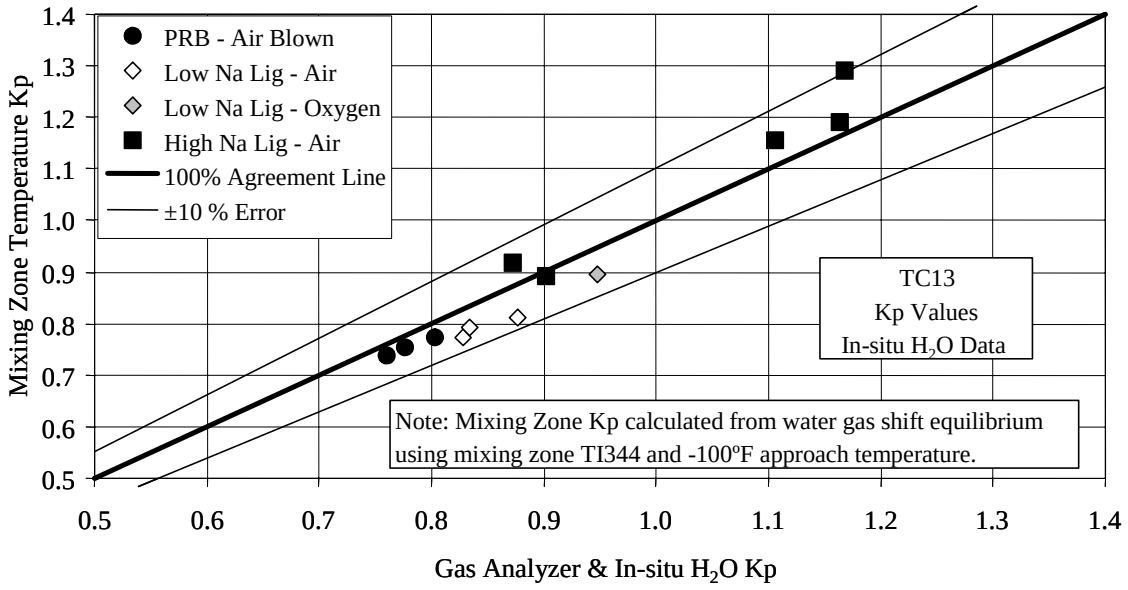

Figure 3.2-22 Water-Gas Shift Constants (In situ H_2O)

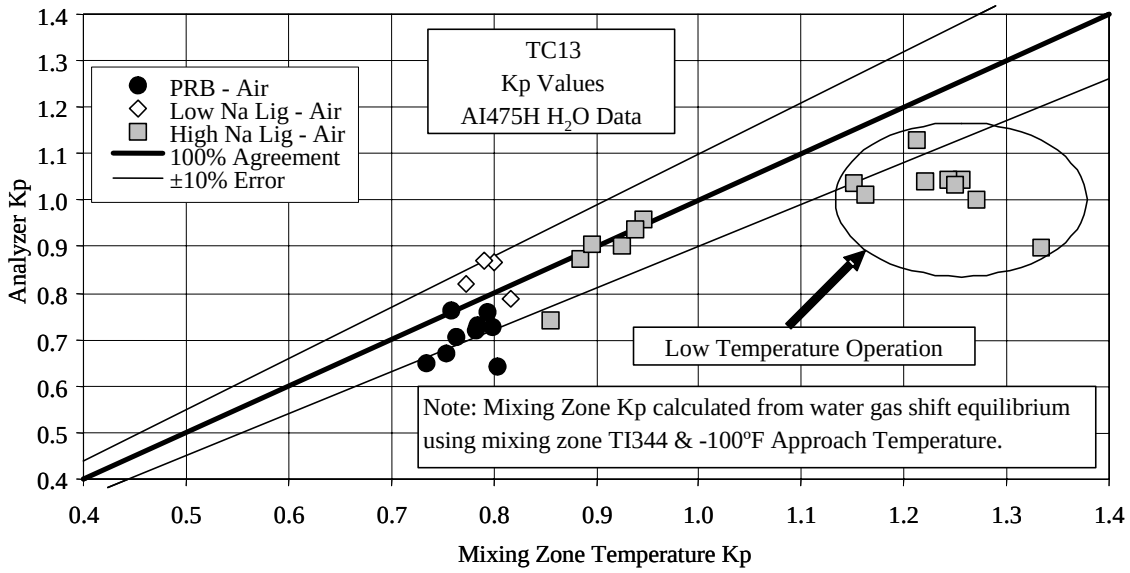

Figure 3.2-23 Water-Gas Shift Constant (AI475H H_2O)

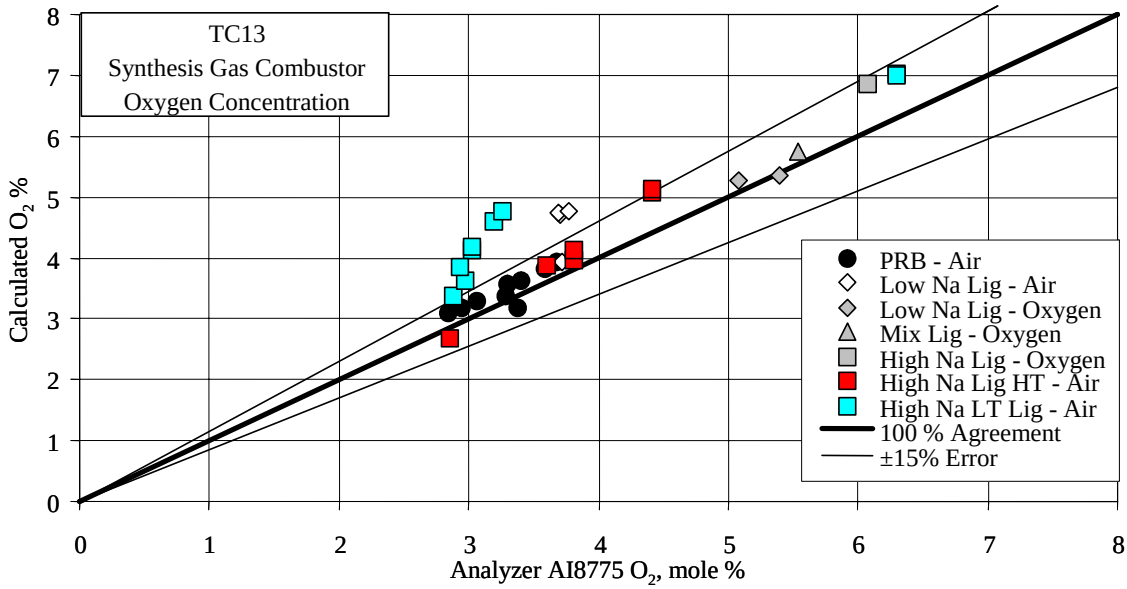

Figure 3.2-24 Syngas Combustor Outlet Oxygen

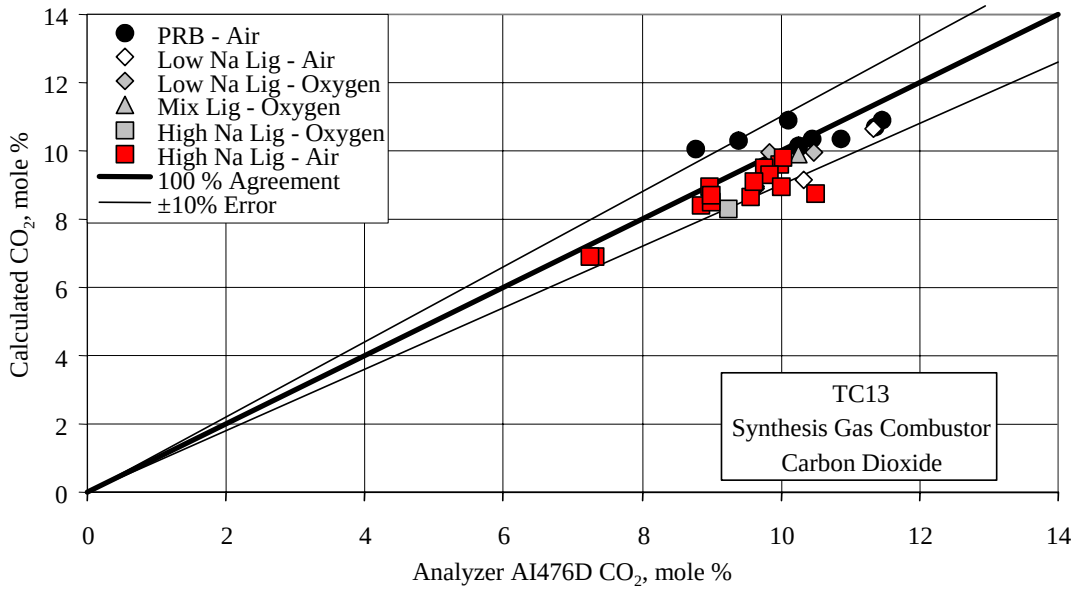

Figure 3.2-25 Syngas Combustor Outlet Carbon Dioxide

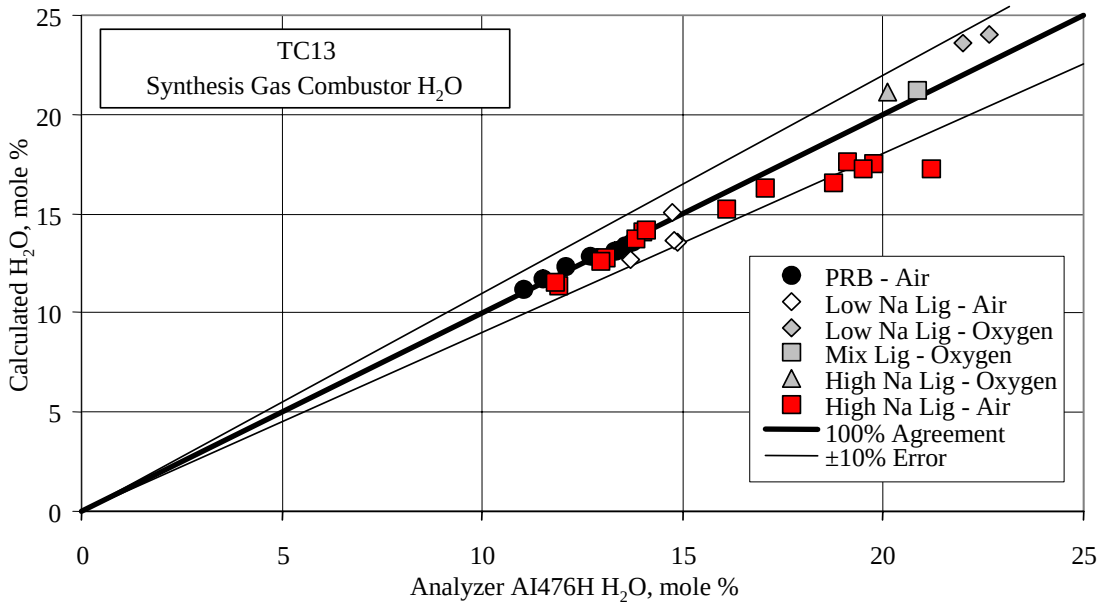

Figure 3.2-26 Syngas Combustor Outlet Moisture

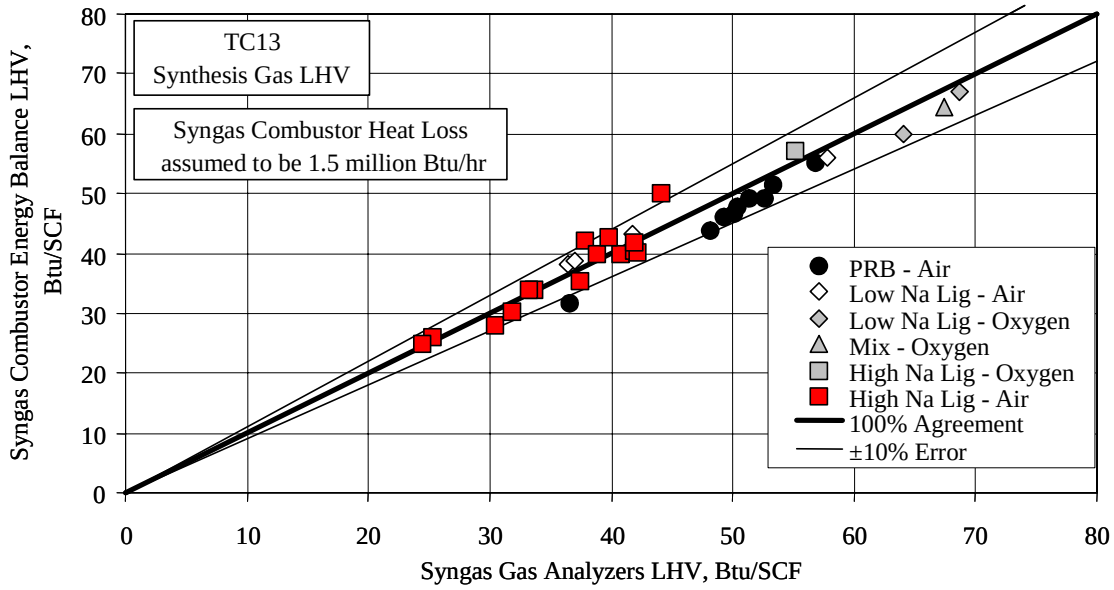

Figure 3.2-27 Syngas LHV

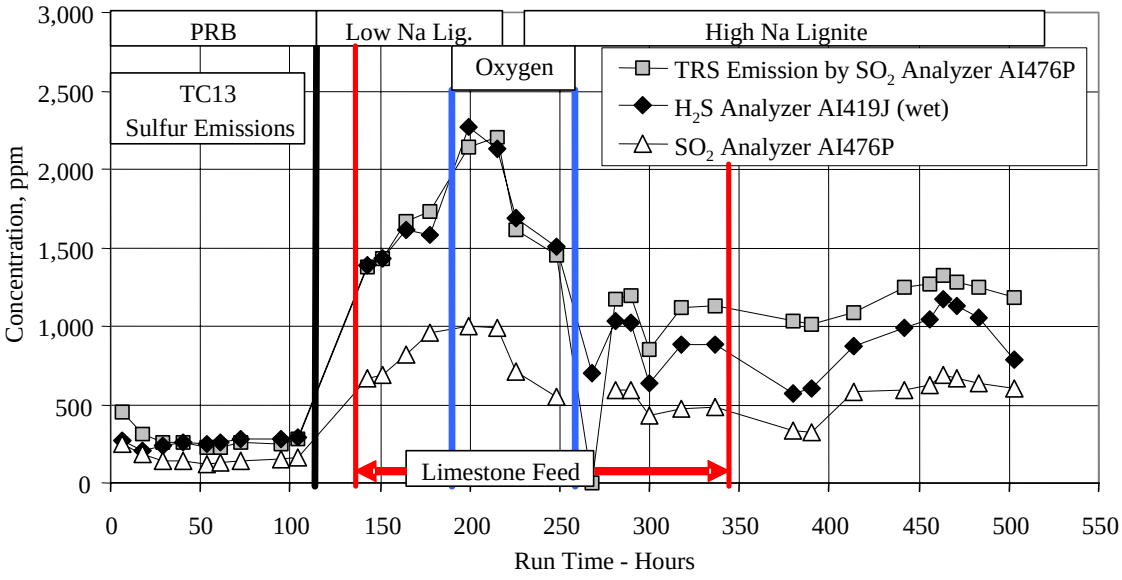

Figure 3.2-28 Sulfur Emissions

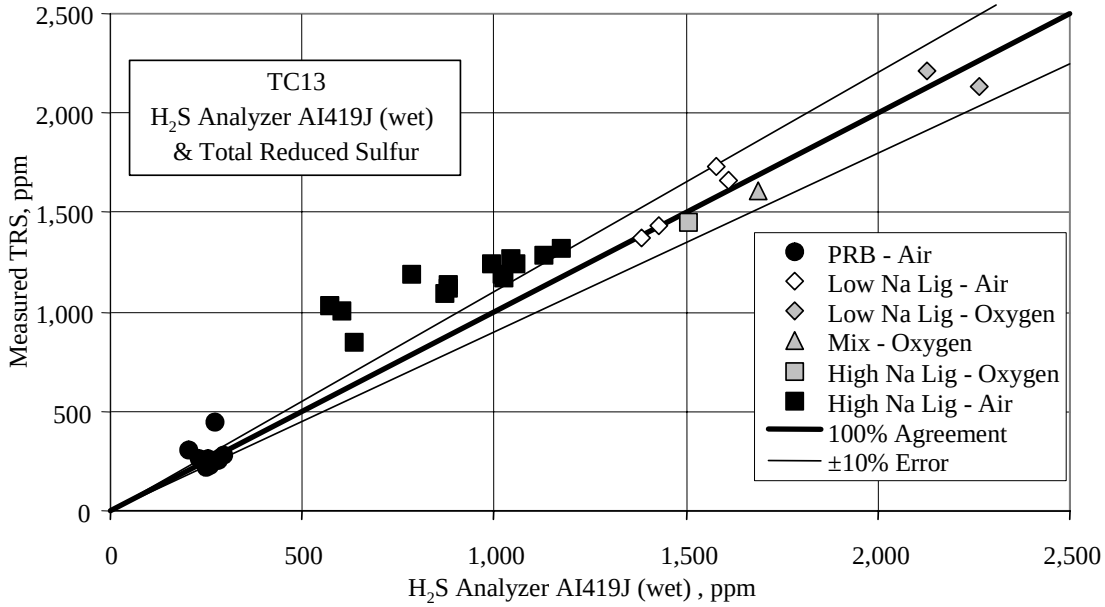

Figure 3.2-29 H_2S Analyzer AI419J and Total Reduced Sulfur

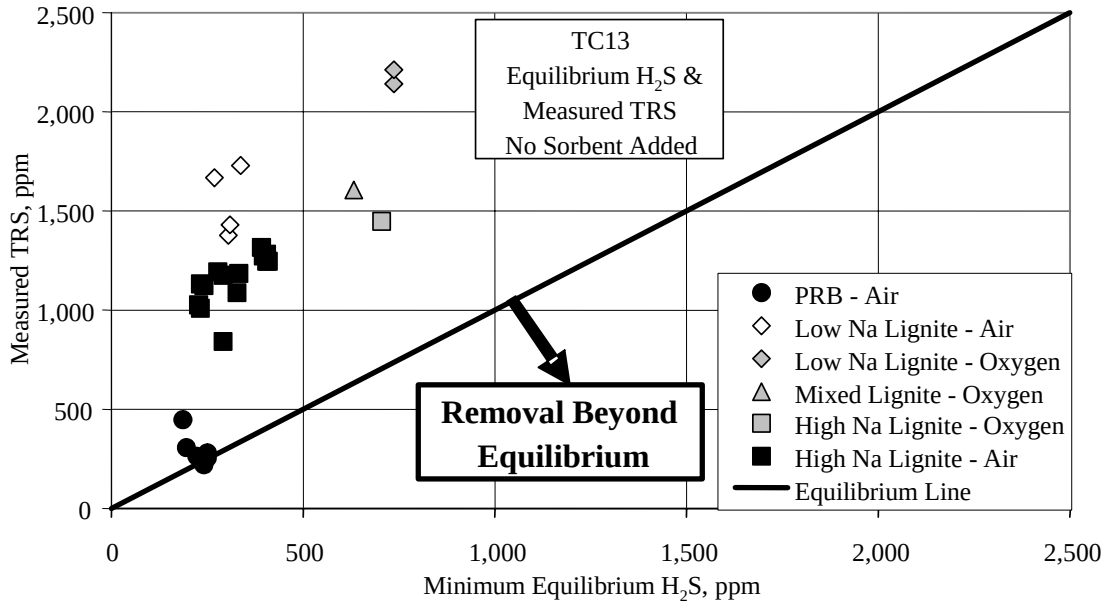

Figure 3.2-30 Minimum Equilibrium H_2S and Total Reduced Sulfur

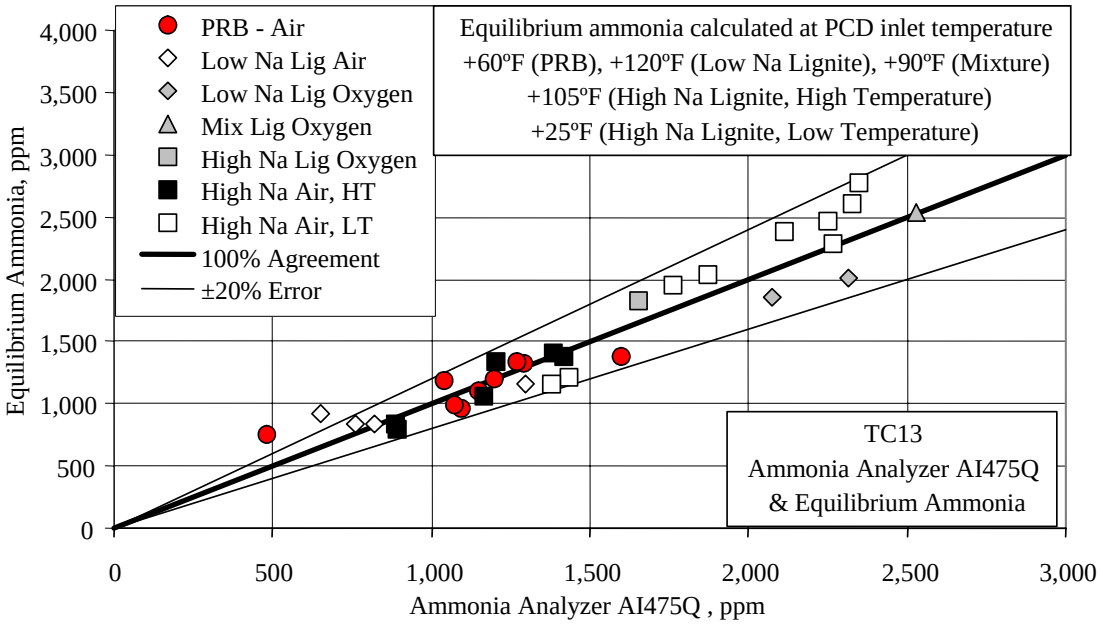

Figure 3.2-31 NH_3 Analyzer AI475Q and Equilibrium NH_3

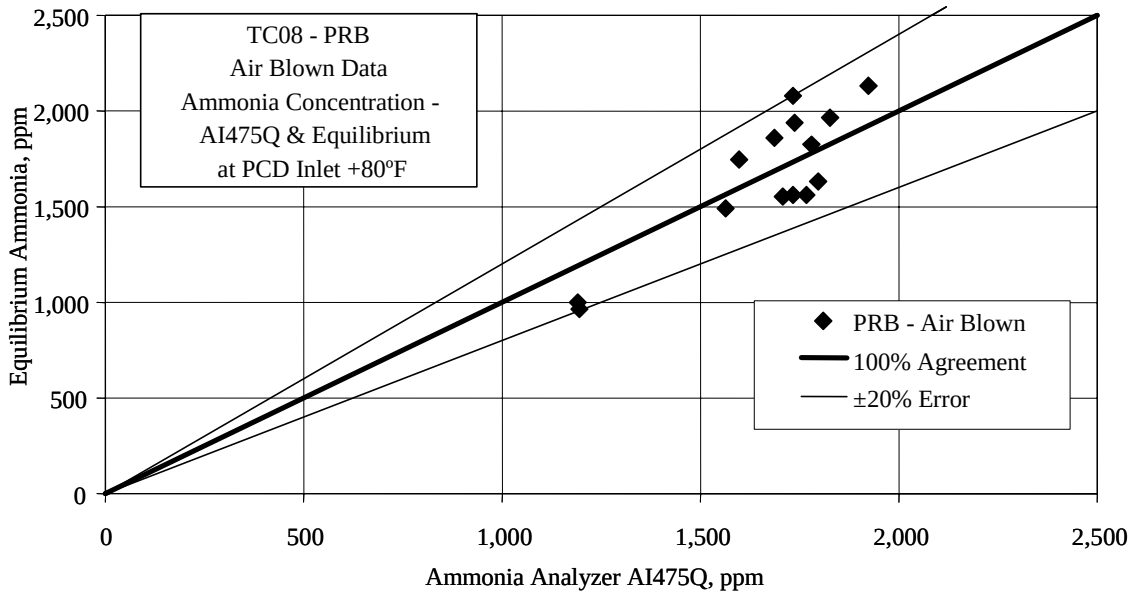

Figure 3.2-32 TC08 (PRB) NH_3 Analyzer AI475Q and Equilibrium NH_3

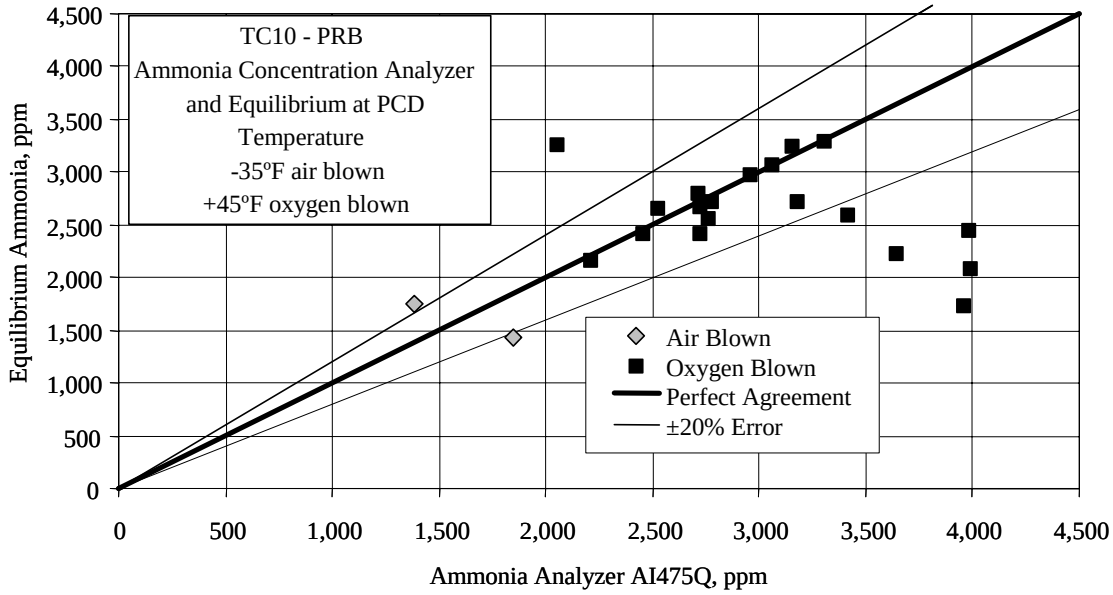

Figure 3.2-33 TC10 (PRB) NH_3 Analyzer AI475Q and Equilibrium NH_3

3.3 SOLIDS ANALYSES

3.3.1 Summary and Conclusions

3.3.1.1 Powder River Basin Coal

- PRB coal moisture, sulfur, and ash compositions were not constant. The PRB sulfur content decreased steadily during TC13.
- Standpipe solids contained negligible amounts of CaS.
- The PCD fines sulfur and standpipe solids sulfur content indicate minimal Transport Gasifier sulfur capture.
- The PCD fines calcium was 60- to 88-percent calcined.
- Coal-feed particle size varied between 125 to 280 μ Sauter Mean Diameter (SMD). The mass mean coal particle size varied between 150 to 350 μ.
- The PRB coal feed percent fines increased during TC13, while the percent coarse particles decreased.
- Standpipe solids particle size reached a steady-state value of 150 μ SMD.
- Standpipe solids bulk density decreased from 95 to 82 lb/ft^3.
- PCD solids particle size averaged 10 μ SMD, and was slightly increasing during TC13.
- PCD solids bulk density slowly decreased to 18 lb/ft^3.

3.3.1.2 Low-Sodium Freedom Mine Lignite Coal

- Low-sodium Freedom lignite coal moisture, sulfur, and ash compositions were constant during TC13 testing.
- Standpipe solids contained significant amounts of CaS.
- The PCD fines sulfur and standpipe solids sulfur content indicate significant Transport Gasifier sulfur capture.
- On average, the PCD fines calcium was 40- to 60-percent calcined.
- Coal-feed particle size varied between 200 to 280 μ SMD. The mass mean coal particle size varied between 300 to 680 μ, due to a large number of greater than 1,180 μ particles.
- The coal-feed percent fines and the percent coarse particles increased during TC13.
- Standpipe solids particle size varied between 150 and 230 μ SMD.
- Standpipe solids bulk density decreased from 80 to 55 lb/ft^3.
- PCD solids particle size varied between 10 and 23 μ SMD.
- PCD solids bulk density varied between 18 and 38 lb/ft^3.

3.3.1.3 High-Sodium Freedom Mine Lignite Coal

- High-sodium Freedom lignite coal moisture, sulfur, and ash compositions were constant during TC13 testing.
- Standpipe solids contained significant amounts of CaS.
- The PCD fines sulfur and standpipe solids sulfur content indicate significant Transport Gasifier sulfur capture.
- The PCD fines calcium was 40- to 70-percent calcined during high temperature operation and 0 percent during low temperature operation.

- Coal-feed particle size varied between 180 to 300 μ SMD. The mass mean coal particle size varied between 280 to 550 μ, due to a large number of particles greater than 1,180 μ.
- The coal-feed percent fine and percent coarse particles had significant variations during TC13.
- Standpipe solids particle size reached as high as 455 μ. Particle size increased slower during low temperature operation.
- Standpipe solids particle sizes were much larger than in previous testing.
- Standpipe solids bulk densities were variable during the high temperature operation and decreased from 105 to 68 lb/ft^3 during low temperature operation.
- PCD solids particle size varied between 15 and 30 μ SMD for high temperature operation and averaged 12 to 15 μ SMD during low temperature operation.
- PCD solids bulk density varied between 18 and 68 lb/ft^3 during high temperature operation and was constant at 25 lb/ft^3 during low temperature operations.

3.3.1.4 Both Powder River Basin and Freedom Mine Lignite Coals

- Standpipe carbon was less than 1 percent for most of the samples, with a few between 1- and 2-percent carbon.
- PCD inlet in situ samples carbon, $CaCO_3$, CaO, CaS, and SiO_2 concentrations were consistent with FD0520 samples concentrations.
- Standpipe solids particles size increased with particle sodium oxide concentration.
- In situ PCD fines particle sizes were consistent with the FD0520 samples particle sizes.
- In situ PCD fines bulk densities were consistent with the FD0520 bulk densities.

3.3.2 Introduction

During TC13, solid samples were collected from the original star fuel feed system (FD0210), new fluidized-bed fuel feed system (FD0200), the sorbent feed system (FD0220), the Transport Gasifier standpipe, the Transport Gasifier loop seal downcomer, and the PCD fine solids transport system (FD0520). In situ solids samples were also collected from the PCD inlet. All sample locations except for the FD0200 coal sampling system are shown in Figure 3.3-1. These solids were analyzed for chemical composition and particle size. During TC13 sorbent and sand were added through FD0220.

3.3.3 Feeds Analysis

Table 3.3-1 gives the average coal composition for the samples analyzed as sampled from FD0210 during TC13. The average analysis and standard deviation are also listed on Table 3.3-1 for the three fuels tested:

- Powder River Basin.
- High-sodium (low-sulfur) Freedom lignite.
- Low-sodium (high-sulfur) Freedom lignite.

One sample was excluded from the low-sodium lignite averages because it appears that a mixture of PBB and low-sodium lignite was sampled well after the PRB coal feed had stopped. This sample will not be used to estimate the hourly feed coal compositions and will not be plotted on

the figures. Note that the high- and low-sodium Freedom lignites only vary significantly in the sulfur and Na_2O compositions. Coal was also fed to the gasifier from FD0200, but only one sample was taken and it was not analyzed.

The fuel carbon and moisture contents are shown in Figure 3.3-2. The moisture of the PRB increased during TC13 with the exception of the two samples at hours 33 and 41 which had some of the lowest feed moisture for PRB coal that have been measured. Both the low- and high-sodium lignites had about the same carbon and moisture contents. The moisture of the Freedom lignite varied slightly during TC13 and was about 1 percent less that the Falkirk lignite moisture.

Figure 3.3-3 shows the fuel sulfur and ash as sampled from FD0210 during TC13. The average values are given on Table 3.3-1 for the three fuels, with two sulfur analyses excluded. The PRB sulfur level decreased steadily from 0.66- to 0.27-weight percent during the first 105 hours of TC13. Based on the sulfur content, the first sample of the low-sodium lignite at hour 121 appears to be a mixture of PRB and low-sulfur lignite. Excluding the sample at hour 121, the low-sodium lignite samples were fairly constant. The second sample taken at hour 250 (during the high-sodium lignite) may have been residual low-sodium lignite since the sulfur content was high. The high-sodium lignite sulfur analyses with the exclusion of the hour 250 sample were fairly constant, therefore the hour 250 sulfur analysis was excluded when calculating the sulfur content of the high-sodium lignite.

The fuel higher heating value (HHV) and lower heating value (LHV) are given on Figure 3.3-4 with the TC13 average values for each fuel given in Table 3.3-1. Coal HHV is determined by a bomb calorimeter which condenses all the coal combustion moisture (from coal elemental hydrogen) as liquid water. The heat of vaporization of the syngas or flue gas moisture is then counted as part of the coal HHV. The LHV subtracts the heat vaporization of the coal moisture from the HHV. Since heat recovery steam generators do not recover the coal syngas moisture heat of vaporization, the LHV is a more realistic measure of coal heating value. The heating values for both fuels were fairly constant and there was not much difference between the low- and high- sodium lignite heating values.

Average values for TC13 fuel moisture, carbon, hydrogen, nitrogen, oxygen, sulfur, ash, volatiles, fixed carbon, higher heating value, lower heating value, CaO, SiO_2, Al_2O_3, MgO, Na_2O, and Fe_2O_3 are given in Table 3.3-1. Also given in Table 3.3-1 are the molar ratios for coal calcium to sulfur (Ca/S). PRB has sufficient alkalinity in the ash to remove all of the coal sulfur. The low-sodium (high-sulfur) lignite does not have enough alkalinity to remove all of the coal sulfur, while the high-sodium (low-sulfur) lignite barely has enough alkalinity to remove all of the coal sulfur.

FD0220 was used during TC13 to feed limestone or sand into the Transport Gasifier. Seven FD0220 solids samples were taken, but only three of them contained limestone. The average analyses of the three limestone samples are given in Table 3.3-2.

3.3.4 Gasifier Solids Analysis

The chemical compositions of the solid compounds produced by the Transport Gasifier were determined based on the chemical analysis and the following assumptions:

1. All carbon dioxide measured came from $CaCO_3$, hence moles CO_2 measured = moles $CaCO_3$.
2. All sulfide sulfur measured came from CaS.
3. All calcium not taken by CaS and $CaCO_3$ came from CaO.
4. All magnesium came from MgO.
5. Total carbon is measured, which is the sum of organic and inorganic (CO_2) carbon. The organic carbon is the total carbon minus the inorganic carbon (CO_2).
6. All iron reported as Fe_2O_3 is assumed to be present in the gasifier and PCD solids as FeO.
7. Inerts are the sum of the P_2O_5, K_2O, and TiO_2 concentrations.

For the TC13 solids samples, both elemental sulfur (ultimate analysis) and ash inerts sulfur was measured. Typically the elemental sulfur was less than the ash inerts sulfur. The sulfur balances were much better when the ash inerts sulfur was used, so for TC13, the ash inerts sulfur was used to determine the standpipe solids, FD0510 coarse solids, and the PCD fines sulfur content.

It will be assumed that all iron in both the standpipe and PCD solids is in the form of FeO and not in the form of Fe_3O_4 or Fe_2O_3. Thermodynamically, the mild reducing conditions in the Transport Gasifier should reduce all Fe_2O_3 to FeO.

It will also be assumed that no FeS is formed in the Transport Gasifier and that all the sulfur in the standpipe and PCD fines solids is present as CaS. It is thermodynamically possible that some FeS is formed. However, most of the captured sulfur should be in the form of CaS due to the larger amount of calcium than iron in the system.

Table 3.3-3 gives the results from the standpipe solids analyses. The standpipe solids are solids that recirculate through the mixing zone, riser, and standpipe and change slowly with time, since a small amount of solids are taken out of the standpipe via the coarse standpipe spent solids transporter system (FD0510). At hour 249, two analyses were made of the same sample; both are shown on Table 3.3-3 to demonstrate the repeatability of the solids analyses. After hour 379, the standpipe sampler plugged and standpipe solids could not be taken from the standpipe. Samples were then taken from the coarse solids transport system FD0510. Table 3.3-4 gives the results from the solids removed from the bottom of the standpipe. FD0510 was operated intermittently during TC13 to control the standpipe level. The flow rates for FD0510 and FD0520 solids during the stable operating periods are given in Section 3.4.

On startup, the standpipe solids mainly contained sand at 96.7-percent SiO_2. The standpipe did not contain pure sand at zero "run time" hours since there were several periods of coal and coke breeze operation prior to the starting of the clock for the test, which diluted the standpipe sand. Limestone was added to the gasifier through FD0220 from hours 141 to 347, which should result in higher sulfur capture (higher CaS in the coarse standpipe and PCD fine solids) and increased concentrations of calcium in the coarse standpipe and PCD fine solids. During the periods of limestone addition, the limestone feed was not constant, and typically had periods of 10 to 30 hours without sorbent injection. Section 3.4 will detail which of the operating periods had limestone addition.

Between sand additions, the start-up sand was slowly replaced by CaO, Al_2O_3, Fe_2O_3, and other inerts. This is shown in Figure 3.3-5 which plots standpipe and FD0510 SiO_2, CaO, and Al_2O_3 versus run time. During the PRB and low-sodium lignite the SiO_2 content slowly decreased as the Al_2O_3 and the CaO were slowly increasing to replace the SiO_2. The increase in SiO_2 content at hour 217 was probably due to the purging of sand in FD0220 for the preparation of limestone feed. Sand was added prior to the restart on air-blown, high-sodium lignite at hours 256 and 352, which significantly increased the SiO_2 content and decreased the Al_2O_3 and the CaO. For PRB and low-sodium lignite, the gasifier did not reach steady-state solids conditions as the standpipe - solids SiO_2, Al_2O_3, and CaO were steadily decreasing. For high-sodium lignite, the gasifier appeared to reach constant solids conditions as the standpipe solids SiO_2, Al_2O_3, and CaO quickly leveled out at about 49-percent SiO_2, 22-percent Al_2O_3, and 8-percent CaO at hour 271. Note that the CaO concentration, as expected, increased after starting of limestone feed at hour 141. The CaO concentration decreased at hour 347 when limestone feed stopped and sand was added. The value of CaO for high-sodium lignite was higher (22 percent) during limestone injection and lower after limestone injection ceased (10 to 15 percent). Note that there does not seem to be any difference between the solids data from the standpipe samples and the FD0510 samples. The last standpipe solids sample, AB14118, was taken after the end of coal feed, and is not plotted on any of the figures.

The gasifier solids organic carbon content is plotted on Figure 3.3-6. The organic carbon is the total carbon minus the separately measured inorganic carbon (CO_2). For the TC13 standpipe solids, only 4 of the 30 solids samples were analyzed for CO_2, so for the other 26 solids, the solids CO_2 content was interpolated from the analyzed samples' CO_2. The standpipe organic carbon content was a very inaccurate measurement because the value comes from the difference of two small values that are nearly equal. The standpipe organic carbon content during PRB seemed to increase during TC13, and a few samples which measured above 1percent carbon were higher than typical standpipe carbon contents during PRB operation. The air-blown sodium lignite carbon contents were very low with all values 0.0-percent carbon. During oxygen-blown, low-sodium lignite operation the carbon content increased to about 1 percent. During the air-blown, high-sodium lignite testing, the standpipe carbon content varied between 0- and 0.6-percent carbon, with an average value of 0.24 percent, excluding the two outliers. The outliers were one sample taken at hour 347 during a loop seal plug where circulation was being lost in the gasifier and another sample taken at hour 287 with a carbon content of 1.5 percent. There did not appear to be any change in standpipe carbon content as the mixing zone temperature was lowered after hour 380. The last FD0510 solids analysis on Table 3.3-4 was taken the day after coal feed was stopped and is not plotted on Figure 3.3-6.

The gasifier solids sodium oxide content (Na_2O) is plotted on Figure 3.3-6. As expected, the use of fuels with progressively higher sodium contents increases the sodium concentration of the gasifier solids during TC13. The gasifier solids sodium oxide concentration slowly increased during PRB operation from 0.2 to 1.7 percent as the start-up sand was replaced by PRB ash. The gasifier solids sodium oxide continued to slowly increase during low-sodium lignite operation from 2.2 to 2.8 percent until hour 201. At hour 217, the sodium oxide suddenly increased to 4.7 percent and then decreased to 2.3 percent for the sample taken during the mixed lignite testing. The transition to high-sodium lignite resulted in gasifier solids sodium oxide levels of 8.6 to 10.2 percent from hours 245 to 249. At hour 249 the unit was shut down to clean out the loop seal, which had plugged ending the oxygen-blown operation. After the shutdown at hour 249, sand

was added to the gasifier thus diluting all the nonsilica compounds. The gasifier solids sodium oxide then increased from 1.6 percent at hour 263 to 10.2 percent at hour 303. The sodium oxide concentration then leveled out at about 8 percent from hour 303 to 343. The loop seal plugged again at hour 350, but did not require a shutdown to clear. Large amounts of sand were added to the gasifier which diluted the sodium oxide content down to 0.7 percent. The sodium oxide then increased to 11.7 percent at hour 488 near the end of TC13. There was no more loop seal plugging after the gasifier temperature was lowered by about 200°F after hour 350 despite the high-sodium oxide concentrations.

The standpipe solids CaS and total calcium concentrations are plotted on Figure 3.3-7. The period of limestone feed is also shown. The PRB without limestone feed had minimal sulfur capture, which is consistent with previous PRB test data without limestone feed. The calcium slowly increased as the calcium in the PRB ash replaced the start-up sand silica. The CaS and calcium increased as limestone was added during low-sodium (high-sulfur) lignite. During the limestone feed portion of high-sodium (low-sulfur) operation the CaS decreased to about 0.2 percent and the calcium lined out at about 16 percent. The sand addition after hour 249 quickly decreased the standpipe solids calcium to 5 percent, but the calcium content quickly increased back to about 15 percent. After the limestone feed was stopped at hour 347 and sand added, the CaS and calcium slowly increased to 10-percent calcium and 1-percent sulfur. This was also during the mixing zone low temperature operation. Note that high CaS in the standpipe solids does not indicate high sulfur capture, since most of the gasifier solids leave through FD0520 rather than FD0510.

The standpipe $CaCO_3$ was between 0.7 and 3.5 percent for TC13. The standpipe calcium was about 83-percent calcined to CaO for PRB, increased from 86 to 96 percent or low-sodium lignite, was 98-percent calcined for high-sodium lignite with limestone at higher temperature, and 92-percent calcined without limestone addition and at lower temperature.

The MgO, Fe_2O_3, and other inerts contents are not plotted, but they follow the same trends as the Al_2O_3, that is, they are accumulating in the gasifier as the start-up sand is replaced by feed solids. The standpipe analyses consistency was quite good with a low bias as the total sum of the compounds in Table 3.3-3 and Table 3.3-4 together averaged 99.6 percent with a standard deviation of 1.17 percent.

Only two loop seal downcomer samples were taken. Both were taken when the gasifier was down. Neither sample was analyzed.

3.3.5 Gasifier Products Solids Analysis

Figure 3.3-8 plots the organic carbon (total carbon minus CO_2 carbon) for the PCD solids sampled from FD0520. The organic carbon content for every PCD fines sample analyzed is also provided on Table 3.3-5. Since FD0520 ran continuously during TC13, solid samples were taken often, with a goal of one sample every 4 hours. Approximately 38 percent of these samples were analyzed. In situ PCD inlet particulate solid samples taken by Southern Research Institute (SRI) were also analyzed.

The in situ carbon contents are compared with the FD0520 solids on Figure 3.3-9. The in situ solids organic carbon analyses were in agreement with the FD0520 solids for all of the 10 in situ solid samples.

The PCD fines organic carbon began TC13 at 29 percent, then quickly dropped to 6 percent, and then rose to 30 percent at the end of the PRB testing. For low-sodium lignite, the organic carbon was between 1.5 and 20 percent from hours 141 to 161 and then rose to 50 percent at hour 181 then dropped again to 17 percent at the end of low-sodium lignite testing. The high-sodium lignite testing varied a lot between hours 249 and 343 with values ranging from nearly zero to 50 percent. After the mixing zone temperature was lowered, the carbon content lined out at about 65 percent. Higher PCD fines organic carbon concentrations are a result of lower carbon conversions in the Transport Gasifier.

Figure 3.3-9 and Table 3.3-4 gives the amounts of SiO_2 and Al_2O_3 in the PCD solids as sampled from FD0520. Also plotted on Figure 3.3-9 are the in situ solids concentrations for SiO_2 and Al_2O_3. The last eight TC13 SiO_2 in situ solids analyses compared well with the FD0520 SiO_2 samples, while the first two showed slight differences. All 10 Al_2O_3 in situ concentrations showed good agreement with the FD0520 solids.

The SiO_2 PCD fines concentrations are a function of both the efficiency of the disengager and cyclone as well as the circulating solids SiO_2 concentration since the SiO_2 in the PCD fines is made of fresh coal ash SiO_2, start-up sand SiO_2 that is slowly being purged from the gasifier, and additional sand that is added to the gasifier to increase standpipe level. The SiO_2 PCD fines concentrations decreased for the PRB testing from 42 percent at the start of TC13 to about 30 percent at the end of the PRB testing. For the low-sodium lignite, the SiO_2 PCD fines concentrations were constant for the first 50 hours, and then decreased to 9 percent at hour 181. The SiO_2 PCD fines concentrations then increased to 29 percent during the oxygen-blown testing with both low- and high-sodium lignite testing. During air-blown, high-sodium lignite testing, the SiO_2 PCD fines concentration decreased due to the high organic carbon concentrations caused by low carbon conversion in the gasifier. The peak of organic carbon at hours 279 to 291 was matched by a decrease in SiO_2 concentrations. The same was true for the last 50 hours of TC13.

The PCD fines Al_2O_3 comes from the coal ash, since there is minimal Al_2O_3 in either the start-up sand or the limestone. The PCD fines Al_2O_3 concentrations were constant at around 10 percent for the 110 hours of PRB operation. The PCD fines Al_2O_3 concentrations decreased to 5 percent during the air-blown, low-sodium lignite testing and then increased to 7 percent by the end of the oxygen-blown, low-sodium lignite testing. This decrease was probably due to a decrease in coal-feed rates from hours 143 to hours 165. The PCD fines Al_2O_3 concentration was at 10 percent for the mixture of low- and high-sodium lignite sample and remained below 10 percent for the oxygen-blown, high-sodium lignite testing. The air-blown, high-sodium lignite PCD fines Al_2O_3 concentrations decreased from 10 to 5 percent between hours 249 to 291 before increasing to 9 percent by hour 300. From hour 300 to 387, the PCD fines Al_2O_3 concentrations again slowly decreased from 9 to 5 percent. For the remainder of TC13, the PCD fines Al_2O_3 concentrations were fairly constant at about 4 percent.

Figure 3.3-10 provides the "as analyzed" total calcium concentrations as well as the concentration of CaS in the PCD solids as sampled from FD0520. Table 3.3-5 lists the concentrations of CaO,

CaS, and $CaCO_3$. Also plotted on Figure 3.3-10 are the in situ solids concentrations for calcium and CaS. All of the in situ samples calcium and CaS concentrations agreed well with FD0520 solids calcium and CaS concentrations.

The PCD fines calcium concentration fluctuated from 12 to 8 percent during the PRB testing. There was no limestone feed during the PRB so all of the PCD fines calcium came from the PRB coal ash. The calcium increased to 14 percent when the low-sodium lignite was started, due to the higher calcium content of the low-sodium lignite. During the period of limestone feed, the calcium concentration varied from 7 to 22 percent. This was possibly due to the intermittent nature of the limestone feed, since the feed was turned off or on every 10 to 30 hours. After the limestone feed was stopped, the calcium content decreased to about 5 percent and remained at that concentration for the remainder of the run.

The PCD fines CaS concentration for PRB was about 1.0 percent, indicating very low sulfur capture due to the low sulfur level in PRB and the lack of limestone feed. The low-sodium (high-sulfur) lignite operation without limestone feed increased the CaS to 5 percent. When limestone injection was started, the CaS increased to 10 percent. The CaS decreased to 5 percent at about 200 hours, during the low-sodium lignite testing, and then continued to decrease to 3-percent CaS. When limestone feed stopped, the CaS slowly decreased to 2 percent at hour 442 where it remained constant for the remainder of TC13.

The PCD fines calcination is defined as:

$$\%\ \text{Calcination} = \frac{\text{M}\%\ \text{CaO}}{\text{M}\%\ \text{CaO} + \text{M}\%\ \text{CaCO}_3} \quad (1)$$

The PCD fines calcinations are plotted on Figure 3.3-11. Since there were several samples in which the available calcium could be satisfied by the sulfur and carbon dioxide (as $CaCO_3$), the CaO was zero and the percent calcination was zero. For the PRB testing without limestone injection, the PCD fines calcination was from 60 to 89 percent. All previous PRB runs were consistent with these results. The low-sodium lignite calcinations were quite variable, with values for 0 to 75 percent. Most of the low-sodium calcinations were between 40 to 60 percent, so the calcinations were lower for low-sodium lignite than PRB. The high-sodium lignite with limestone was consistent with the low-sodium lignite in that the calcinations varied between 0 and 75 percent with most of the values between 40 and 60 percent. Likely causes of these low calcinations would be the lower temperature operations higher temperatures increase calcination.

The calcium sulfation is defined as:

$$\%\text{Sulfation} = \frac{\text{M}\%\text{CaS}}{\text{M}\%\text{CaO} + \text{M}\%\text{CaCO}_3 + \text{M}\%\text{CaS}} \quad (2)$$

The PCD fines sulfation is plotted on Figure 3.3-11 with the PCD fines calcination. The PCD fines sulfation started TC13 at about 5 percent and held steady until the end of PRB testing. Previous PRB testing were consistent with these results. The low-sodium (high-sulfur) lignite increased the sulfation from 20 to 57 percent and then during oxygen-blown mode decreased to 10 percent. The high-sodium (low-sulfur) lignite had variable sulfations during limestone feed at from 10 to 20 percent. Whenever the limestone feed was stopped, the sulfation was fairly steady

at 20 to 30 percent. This would indicate that the lignite ash calcium was able to capture sulfur to some extent. This will be discussed further in Section 3.4.

Table 3.3-5 gives the PCD fines compositions for the samples collected in FD0520. The consistency is not as good as the standpipe solids in that the totals were between 94 and 110 percent. The average of the totals was 99.5 percent with a standard deviation of 3.5. Additional components on Table 3.3-5, other than those plotted on Figures 3.3-6, 3.3-7, and 3.3-8, are MgO, FeO, CaO, and $CaCO_2$. The MgO concentrations were between 2.3 and 4.2 percent. The $CaCO_3$ concentrations were between 3.6 and 23.2 percent and were a function of the whether limestone was fed to the gasifier. Some of the CaO concentrations were zero which reflected that there was more moles of sulfur and CO_2 in the PCD fines than there were moles of total calcium. Also given in Table 3.3-5 are the higher heating value (HHV), lower heating value (LHV), and organic carbon for the PCD fines. As expected, the trend of heating values follows the carbon content of the PCD fines. Note the very low heating values of the samples taken at hours 17 and 307.

3.3.6 Solids Analysis Comparison

With the addition of the loop seal downcomer solids sampling system, it is now possible to sample solids at three different points in the Transport Gasifier. Unfortunately the loop seal sampler was plugged and samples could not be taken. The coarse standpipe and PCD fines solid samples will be compared for various compounds.

Figure 3.3-12 compares the alumina concentration between the standpipe and PCD fines solids samples. Alumina is not a constituent of either sand or limestone but is a constituent of coal ash, so following the alumina concentration should give a good indication of where the coal ash is distributed in the Transport Gasifier. During the PRB operation, the standpipe PCD fine alumina concentration was larger than the standpipe alumina, with the standpipe alumina steadily increasing and the PCD fines nearly constant. During the low-sodium lignite, the standpipe alumina continued to increase and the PCD fines alumina decreased with the two alumina concentrations being equal at 7-percent alumina at hour 155. During this period, the coal ash was accumulating in the standpipe, displacing the sand. Near the end of the low sodium lignite testing, the PCD fines alumina reached a valley at about 5 percent from hours 177 to 201 and then began increasing. At the beginning of the high-sodium lignite the standpipe and PCD fines alumina concentrations both peaked at 10 to 11 percent. The sand addition at hour 255 diluted the alumina concentration in the standpipe and from hour 263 to 283 the standpipe alumina increased (as coal ash accumulated in the standpipe) and the PCD fines alumina decreased as coal ash was preferentially removed by the disengager and cyclone. From hour 299 to 343, both the standpipe and PCD fines alumina concentrations were constant at from 6 to 8.5 percent, indicating that the coal ash was at steady state in the standpipe. The sand addition at hour 350 again diluted the standpipe alumina down to 2 percent. The standpipe then slowly accumulated alumina until the end of TC13. Based on the last two FD0510 samples, the standpipe may have been at constant conditions with respect to alumina after hour 488. After the sand addition at hour 350, the PCD fines alumina slowly decreased to 4 percent at hour 411 and then was constant at 4 percent until the end of TC13.

Figure 3.3-13 compares the calcium concentration between the standpipe and PCD fines solids samples. Note that the calcium is distributed between the compounds CaO, $CaCO_3$, and CaS. The standpipe and PCD fines solids calcium content is similar to the alumina comparison, despite the added complication of a period of limestone injection between hours 141 and 347. During the first 225 hours of operation (PRB and low-sodium lignite), the standpipe calcium steadily increased from 5 to 25 percent. The rate increased after limestone feed started at hour 141. The standpipe PCD fines calcium concentration was larger than the standpipe calcium for the first 155 hours with the PCD fines decreasing for the first 109 hours. The PCD fines then increased and both the standpipe and PCD fine calcium increased until hour 161 when the two calcium concentrations were nearly the same at 15-percent calcium. During the end of the low-sodium lignite, the standpipe and the PCD fines calcium both increased as a result of the limestone feed. At the beginning of the high-sodium lignite the standpipe calcium concentration peaked at 25 percent. The sand addition at hour 255 diluted the calcium concentration in the standpipe down to 5 percent, but it quickly recovered. From hour 271 to 343, both the standpipe calcium concentrations were constant at 14 to 18 percent, indicating that standpipe calcium was at steady state. The PCD fines calcium was steady but very variable at from 6 to 23 percent. The sand addition at hour 350 again diluted the standpipe calcium down to 2 percent. The standpipe then slowly accumulated calcium until the end of TC13. After the sand addition at hour 350 the PCD fines calcium decreased to 5 percent at hour 411 and then were constant at 4 percent until the end of TC13.

Figure 3.3-14 compares the percent sodium in ash between the coal, loop seal, standpipe, and PCD fines solids samples. Loop seal solids were only available up to hour 193 when the loop seal sample system plugged. During the first 225 hours of operation (PRB and low-sodium lignite), the standpipe and PCD sodium steadily increased from 0.5 to 2 percent. The loop seal sodium increased from 1 to 3 percent. When the high-sodium coal was initiated standpipe and PCD fine sodium increased to between 5.5 and 7.5 percent. The sand addition at hour 255 diluted the sodium concentration in the standpipe down to 1 percent, but it quickly recovered. From hour 271 to 343, the standpipe sodium concentrations were constant at about 6 percent and the PCD fines sodium concentrations were constant at about 4.5 percent. The sand addition at hour 350 diluted the standpipe sodium down to 0.5 percent. The standpipe then slowly accumulated sodium until the end of TC13, reaching a final value of 8 percent. After the sand addition at hour 350 the PCD fines sodium increased to 6.5 percent at hour 395 and then was constant until the end of TC13.

3.3.7 Reactive Sulfide Test Results

The results of the reactive sulfide test on 21 TC16 solid samples are given in Table 3.3-6. The solids samples were from silo SI0814, standpipe solids, and PCD fines from FD0520. The reactive sulfide test measures the H_2S released after some acid is added. The concern with waste gasification solids is that CaS in the solids will release H_2S causing and odor and health problems. The limit for H_2S releasable is 500 mg/kg. Solids testing higher than 500 mg/kg classify the solid as a hazardous waste.

All samples analyzed passed the reactive sulfide test and produced H_2S releasable less than 500 mg/kg. The highest H_2S releasable was 255 mg/kg for a PCD fines sample during low-sodium (high-sulfur) Freedom lignite testing. As expected, the solids resulting from the gasification of

coals with the highest sulfur level, the low-sodium Freedom lignite (1.39-percent sulfur) have higher H_2S releasable than the high-sodium Freedom lignite (0.88-percent sulfur), which in turn had higher H_2S releasable than PRB (0.41-percent sulfur).

3.3.8 Feeds Particle Size

The TC13 Sauter mean diameter (SMD) and mass mean diameter (MMD) particle sizes of the coal sampled from FD0210 are plotted on Figure 3.3-15. The PRB coal SMD particle size was steady at 200 to 250 μ during the first 60 hours of TC13. After hour 60, the SMD increased to 250 μ, and then decreased to about 150 μ prior to the start of Freedom Mine lignite. The average SMD for the PRB was 195 μ with a standard deviation of 50 μ. The standard deviation of the coal-feed size is a measure of the consistency of the coal-feed size, the higher the standard deviation, the more the individual coal particle sizes differed from the average.

Past test campaign average and standard deviation SMD, MMD, percent particles above 1,180 μ , and percent particles below 45 μ are give in Table 3.3-7. The TC13 PRB SMD was consistent with the SMD for all previous PRB testing with the exception of the first 467 hours of TC12, during which the PRB as-received coal had very high moisture content. The standard deviation for the TC13 PRB testing was higher than the previous test campaigns.

The Freedom Mine lignite coal SMD was fairly constant during TC13 with values between 170 and 290 μ. The Freedom lignite average SMD was 227 μ with a standard deviation of 28 μ, which was higher than the TC11 Falkirk SMD and consistent with most of the previous PRB SMD. The lignite average SMD was slightly larger and more consistent (lower standard deviation) than the TC13 PRB feed coal SMD.

The average PRB MMD was 262 μ with a standard deviation of 71 μ. As is typical, the coal MMD is larger than the SMD. The PRB MMD had more variation than the PRB SMD. The PRB MMD increased from 272 at the start of TC13 to 353 μ at hour 33, and then decreased to 168 μ at hour 73. The PRB MMD generally followed the same trends as the TC13 SMD, but had a different size differential from the SMD as TC13 progressed. The differential between the two diameters decreased during the PRB TC13 testing. The MMD had a sudden peak of 350 μ at hours 81 and 89 and then decreased to below 200 μ for the rest of TC13 testing.

The Freedom lignite had an average MMD of 435 μ with a standard deviation of 81. The Freedom lignite MMD was much higher than the Freedom lignite SMD, the Falkirk lignite, and the PRB MMD. The low-sodium Freedom lignite increased from 423 to 673 μ with a decrease to 299 μ at hour 153. During the high-sodium lignite the MMD varied a lot from 280 to 575 μ between hour 233 and 350. After hour 350, the MMD had less variation.

Figure 3.3-16 plots both the coal feed percent above 1,180 μ (coarse particles) and percent below 45 μ (fines). The percent above 1,180 μ is a function of whether the mill 1,180 μ screen is in place. As shown in Table 3.3-7 for TC06 to TC10, the 1,000 μ screen in place scalped nearly all of the greater than 1,180 μ particles. The presence of large amount of 1,180 μ particles also increases the difference between the SMD and the MMD. This is because the SMD is a surface area average, and so the larger particles with less surface area per pound have less effect on the

SMD than the MMD, where the larger particles skew the MMD due to their higher weight per particle.

The average percent above 1,180 μ for the PRB was 4.3 percent with a standard deviation of 1.9 percent. This was below the typical average percent above 1,180 μ for PRB test campaigns with either the 1,000 μ screen removed or the 2,800 μ screen installed. Higher amount of coarse particles might lower the carbon conversion or lead to increased carbon in the recirculating solids. The PRB percent above 1,180 was constant for the first 57 hours at about 5 percent, then was below 5 percent for the rest of the PRB testing.

The average percent above 1,180 μ for the Freedom lignite was 11.6 percent with a standard deviation of 4.8. For the low-sodium Freedom lignite, the average percent above 1,180 μ increased from 12 to 25 percent (with one dip to 4 percent). This was the cause for the increase in differential between the low-sodium lignite MMD and SMD. The high-sodium lignite percent above 1,180 μ went from 5 to 18 percent and then back down to 5 percent from hours 225 to 337. After hour 353, the percent above 1,180 μ slowly increased from 7 to 12 percent, with much variation. Once the percent above 1,180 μ became a bit more stable the difference between the SMD and MMD also stabilized.

The feed coal average percent below 45 μ are plotted on Figure 3.3-16. In past testing, a high fines content in the feed coal resulted in an increased number of coal feeder outages due the packing of coal fines in the coal-feed system lock vessel. The PRB average percent below 45 μ was 9.4 percent with a standard deviation of 5 percent. This was higher than typical for PRB operation, but there did not appear to be any coal feed problems during TC13 PRB operations. During the first 57 hours of TC13 the PRB coal has about 6-percent average below 45 μ. After hour 65, the PRB average percent below 45 μ had a wide variation between 5 and 18 percent.

The Freedom lignite average percent below 45 μ was 8.6 percent with a standard deviation of 2.4 percent, which was about the same as the TC13 PRB, but more consistent. The TC13 Freedom lignite had fewer fines than the TC11 Falkirk lignite. The low-sodium lignite coal fines increased from 6 to 12 percent from hours 129 to 217. The high-sodium lignite fines decreased from 11 to 5 percent between hours 233 and 327. After hour 363, the high-sodium lignite fines were variable, varying from 5 to 15 percent.

Figure 3.3-17 plots the limited SMD and MMD of the solids samples from FD0220. The solids were either limestone or sand or a mixture of the two. The limestone has a SMD of about 10 μ and a MMD of about 18 μ The sand had a SMD and MMD of 140 μ which is close to the vendor specifications of 150 μ.

3.3.9 Gasifier Solids Particle Size

The TC13 standpipe solids particle sizes are given in Figure 3.3-18. The PRB standpipe solids particle sizes were constant as the run progressed, which is unusual, since the particle size of the solids usually increase as the start-up sand is replaced by coal ash. The PRB standpipe solids particle sizes did not increase and remained the same size as the start-up sand at 140 μ SMD and 150 μ MMD. For the low sodium testing the standpipe solids SMD particle sizes increased slowly from 153 to 170 μ between hour 125 and hour 153. At hour 157, the SMD particle sizes

increased rapidly to 227 μ and remained constant until hour 197. At around hour 177, when the standpipe particle size was above 200 μ SMD, the standpipe became unstable but was brought back under control. The higher standpipe solids particle size might have been due to particle agglomeration as the gasifier solids sodium oxide concentration increased. Between hour 197 and hour 205, the standpipe solids SMD decreased from 230 to 154 μ and the standpipe then became more stable. This sudden decrease in particle size was not caused by sand addition or a sudden increase in limestone addition (limestone addition rate was constant). The most likely cause was the operation of the coarse ash removal system between the hours 155 and hour 201. The operation of the coarse ash system would decrease the standpipe particle size by removing larger particles from the system that would be collected by the disengager and cyclone. The coal rate was also decreased to reduce the rate of standpipe level increase. It is still puzzling why the decrease in standpipe solids particle size was so sudden. A possible explanation would be that 150 μ sand being fed to the gasifier through the sorbent feeder was replaced by 20 μ limestone at hour 200. However, around hour 200, neither the standpipe silica nor the total calcium concentration changed, so this is unlikely. From hour 201 to hour 221, the standpipe solids SMD was stable at around 150 μ.

The period from hour 225 (start of high-sodium lignite) to the shutdown to clean the loop seal (which had plugged) had standpipe SMD from 172 to 424 μ, high sodium oxide concentrations of 8 to 19 percent, and was marked by no standpipe upsets. This period had two large sand additions, which probably mitigated any standpipe particle size increase. Prior to the restart at hour 256, sand was added to the standpipe. The standpipe solids particle size was then constant until hour 271, when the standpipe solids particle size increased to 425 μ at hour 291. During this period the sodium oxide concentration was continuously increasing. The sorbent feeder was turned off twice and was feeding either sand or limestone and the coarse ash system was operated nearly continuously. At hour 294 the loop seal flow stopped. The loop seal flow was regained after increased loop seal aeration. After the loop seal was cleared, the standpipe SMD then decreased to 207 μ, but the sodium oxide concentration did not decrease. A possible explanation for this would be that the loop seal contained fine particles that diluted the coarser standpipe particles down to a smaller size. During this wide change in standpipe particle size change, the calcium or silica chemical compositions did not change significantly. For a few hours (from hour 307 to 315), the gasifier solids particle size was constant at about 330 μ. A sand addition at hour 320 to 324 decreased the gasifier solids to about 200 μ, but after the sand addition, the particles sizes increased to 428 μ at hour 335. The loop seal was starting to developing flow problems and the limestone rate was increased, which decreased the particles size to around 270 μ. The unit was then shut down to clean the loop seal at hour 350. After the shut down additional sand was added and the particle size was decreased to 165 μ. The unit was started up and operated at a lower mixing zone temperature to prevent loop seal plugging. This seemed to work, there were no more loop seal plugs for the rest of TC13 despite the gasifier SMD increasing from 250 μ at hour 367 to 457 at hour 500. The sodium oxide also increased from 2.4 to 11.2 percent during this same period.

The increased sodium oxide in the gasifier solids should lead to solids agglomeration resulting in higher gasifier particle sizes. Figure 3.3-19 plots the gasifier solids sodium oxide and SMD. This figure shows that there is a general trend of increasing gasifier particle size with increasing gasifier solids sodium oxide. The lower temperature high sodium standpipe solids had higher particle sizes at equivalent sodium content when compared to the higher temperature high sodium

standpipe solids, indicting that the poor high temperatures operation of the high-sodium lignite was not caused by the particle size, but more likely the particle stickiness.

The TC13 mass mean diameter (MMD) was about 0 to 50 μ less than the TC13 SMD and followed the same trend as the SMD.

Flow problems in the standpipe or the loop seal might be caused by increasing amounts of large particles in the gasifier solids, so the percent of greater than 600 μ particles and the percent less than 45 μ gasifier solids are plotted on Figure 3.3-20. During PRB operation, the gasifier solids had about 1 percent coarse particles (greater than 600 μ) and about 0.5-percent fines (less than 45 μ). For the low-sodium lignite, the gasifier coarse particles were fairly constant at 1.8 percent from hours 125 to 153, and then increased from up to 3.7 percent at hour 161. The percent of coarse particles were then from 2 to 4 percent until the last low-sodium lignite sample taken at hour 221 which had 5.5 percent coarse particles. From hour 153 to 233 there were about the same amount of course and fine particles, which lasted through the end of the low-sodium lignite to the first few hours of the high-sodium lignite. For high-sodium lignite, the gasifier coarse particles increased to 4 percent just prior to the loop seal plugging at hour 254. After the loop seal plug was cleared and sand was added the gasifier fines remained at the low value except for a few excursions at hour 300 and 320. The gasifier coarse particles slowly grew from less than 1 to 10 percent at hour 350, just before the loop seal plugged. Again, the addition of sand reduced the amount of coarse particles in the gasifier. The amount of coarse particles was constant at about 1.75 percent after the reduction in gasifier temperature at hour 350. After hour 456, the gasifier coarse particles increased to 6.5 percent, and were variable to the end of the run. There were a few short coal trips at hour 492 and 495 which may have influenced the gasifier particle sizes.

For some of the previous test campaigns the gasifier recirculating solids achieved a steady particle size, which was larger than the 150 μ SMD start-up sand. For tests that reached steady-state the standpipe particle size slowly increased asymptotically to reach the steady-state value. The steady-state SMD particle sizes are listed in Table 3.3-8 along with the maximum SMD particle size. The PRB TC13 steady state and maximum standpipe particle sizes were consistent with the all of the previous PRB test campaigns. The TC13 low sodium Freedom Mine lignite had slightly higher maximum SMD particle size when compared to the TC11 Falkirk lignite, but in the same range as previous PRB testing. The TC13 high-sodium Freedom Mine lignite had much higher maximum standpipe particle sizes than had been measured in any previous test campaigns, and clearly hindered the operation of the Transport Gasifier.

Figure 3.3-21 plots the SMD and MMD for the PCD solids sampled from FD0520 and the 10 in situ solids recovered during the PCD inlet sampling. Eight of the 10 in situ solids particle size agreed with the particle size of the solids collected by FD0520. The in situ test at 400 hours was taken during a gasifier pressure increase, which might have compromised the in situ sample.

The PRB PCD fines SMD slowly increased from 9 to 11 μ with a 10 μ average, which was consistent with previous PRB testing. The low-sodium lignite PCD SMD increased from 11 to 23 μ from hours 121 to 157 and then decreased to 12 μ at hour 185. The SMD was then constant at 12 μ until hour 217 when the SMD increased just prior to the high-sodium lignite testing. For the first 25 hours of high-sodium lignite testing, the PCD fines SMD was between 20 and 30 μ. After the first loop seal upset and outage, the PCD fines SMD decreased to 15 μ

and remained there for 12 hours before increasing back to 20 to 25 μ from hours 273 to 343. There were several high spikes in SMD during the period from hour 273 to 343 above 30 μ with some values as high as 62 μ, which is off-scale on Figure 3.3-21 and is shown on Figure 3.3-22. During the second loop seal plug at hour 354, the PCD fines SMD were 199 μ, which was approximately equal to the standpipe SMD. This indicates that the cyclone and disengager were not separating the coarse particles from the solids to the PCD. After the second loop seal plug was cleared, the PCD fines SMD decreased to between 11 and 16 μ for the rest of TC13. This was during the low temperature mixing zone high-sodium lignite operation.

The MMD was about 5 μ larger than the SMD and followed the same trends as the SMD particle sizes, except during the high SMD spikes. The in situ PCD inlet MMD solids particle size also showed the same trend of slight disagreement with the FD0520 solids MMD particle size as the SMD particles sizes.

The TC13 PRB PCD fines particle sizes were consistent with previous PRB test campaign particle sizes. The TC13 low- and high-sodium low temperature Freedom lignite PCD fines particles sizes were higher than the previous PRB PCD fines particle sizes and consistent with the Alabama bituminous, Hiawatha bituminous and the Falkirk lignite PCD fines particle sizes. The average PCD fines particle sizes of the high-sodium Freedom lignite operated at high temperatures was higher than any previous testing.

3.3.10 Particle Size Comparison

Figure 3.3-22 plots all the solids SMD particle sizes, including the coal, standpipe, coarse reactor solids, and the PCD fines. The standpipe and coarse reactor solids from FD0510 are plotted together as standpipe solids. The Transport Gasifier is fed coal with an average of 200 μ SMD, which is approximately the same size as the standpipe solids. The plot highlights the variation in the standpipe solids when compared to the coal SMD. Note that the SMD of the standpipe solids was higher than the coal feed for the last 200 hours of TC13, during the low-temperature, high-sodium lignite testing. Figure 3.3-22 shows the magnitude of the PCD fines samples SMD that was off-scale on Figure 3.3-21. Note that the SMD of the PCD fines at hour 349 was about the same size as the standpipe solids.

3.3.11 Standpipe and PCD Fines Bulk Densities

The TC13 standpipe and PCD fines bulk densities are given in Figure 3.3-23. The PRB standpipe solids bulk density decreased as the start-up sand is replaced by ash. The standpipe solids bulk density decreased from 94 to 84 lb/ft^3 the first 50 hours after startup. The standpipe solids bulk density was constant at about 84 lb/ft^3 for the remainder of the PRB testing. During the low-sodium lignite testing, the standpipe solids density decreased to 62 lb/ft^3 at hour 161, and then leveled off at about 69 lb/ft^3 for a few hours before decreasing to 52 lb/ft^3 at the end of the low-sodium lignite testing. The standpipe density was constant at about 52 lb/ft^3 from the start of high-sodium lignite testing to the first loop seal plug at hour 254. After the loop seal plugged, sand was added to the gasifier, which increased the standpipe solids bulk density to 94 lb/ft^3. The standpipe solids density then decreased to 46 lb/ft^3 by hour 291. During the period from hours 300 to 350 the standpipe solids density was variable due to sand additions at hour 300 and hour 325. After the second loop seal plug occurred, sand was added, which increased the

standpipe solids density to 106 lb/ft^3. From hour 367 to hour 476, the standpipe solids density decreased from 106 to 70 lb/ft^3. For the last 25 hours of TC13 the standpipe solids density was constant at about 70 lb/ft^3.

The minimum standpipe solids densities for past PSDF gasification test campaigns are shown in Table 3.3-8. The minimum PRB standpipe solids density in TC13 was slightly higher than the last several PRB test campaigns but consistent with the first two PRB test campaigns. The TC13 minimum standpipe densities with lignite were significantly lower than the standpipe densities measured during TC11 when testing Falkirk lignite.

The bulk densities for the FD0520 PCD solids samples from both FD0520 and the in situ PCD inlet are plotted on Figure 3.3-23. The FD0520 and in situ solid samples bulk densities agreed very well with each other, even for the in situ samples whose particle sizes did not agree with the FD0520 samples. The PRB bulk densities of the FD0520 PCD fines decreased from 45 to 20 lb/ft^3 during the first 50 hours of testing. The bulk density then decreased slowly to 15 lb/ft^3 to the end of PRB testing. The low-sodium lignite PCD fines bulk density increased from 17 lb/ft^3 at hour 125 to 36 lb/ft^3 at hour 153 and then decreased back to 16 lb/ft^3 at hour 151. The low-sodium PCD fines bulk density then increased to 37 lb/ft^3 the end of the low-sodium lignite testing. The PCD fines bulk density was constant at 40 lb/ft^3 from the start of high-sodium lignite testing to the first loop seal plug. After the loop seal plug the bulk density decreased to 18 lb/ft^3 at hour 287 before increasing to 62 lb/ft^3 at hour 303. From hour 300 to the second loop seal plug at hour 354, the PCD fines solids density was higher than typical and often higher than the standpipe solids density, which could indicate poor disengager and cyclone performance. After the second standpipe plug and sand addition the PCD fines bulk density quickly decreased to 35 lb/ft^3 at hour 359. The PCD fines then slowly decreased from 40 to 20 lb/ft^3 from hours 363 to 400. From hour 400 to the end of TC13 the PCD fines bulk density was constant at about 22 lb/ft^3.

Table 3.3-1

Coal Analyses[1]

	PRB		Low Na Freedom Lignite[3,4]		High Na Freedom Lignite[5]	
	Mean[6]	Standard Deviation	Mean[7]	Standard Deviation	Mean[8]	Standard Deviation
Moisture, wt%	19.48	3.14	26.18	1.25	25.62	1.50
Carbon, wt%	54.99	1.19	47.60	1.64	48.50	1.23
Hydrogen[2], wt%	3.59	0.06	2.90	0.23	2.86	0.19
Nitrogen, wt%	0.69	0.02	0.57	0.03	0.68	0.04
Oxygen, wt%	14.30	0.91	12.54	0.43	12.67	0.72
Sulfur, wt%	0.41	0.15	1.39	0.25	0.88	0.09
Ash, wt%	6.55	1.11	8.89	0.69	8.77	0.76
Volatiles, wt%	34.44	1.22	33.53	0.44	33.13	2.03
Fixed Carbon, wt%	39.54	1.69	31.40	1.16	32.47	1.86
Higher Heating Value, Btu/lb	9,164	150	7,804	265	7,897	202
Lower Heating Value, Btu/lb	8,831	146	7,535	259	7,632	195
CaO, wt %	1.35	0.34	1.84	0.14	1.62	0.16
SiO_2, wt %	1.88	0.17	1.71	0.01	1.66	0.15
Al_2O_3, wt %	0.86	0.04	0.78	0.08	0.88	0.04
MgO, wt %	0.35	0.10	0.73	0.09	0.63	0.07
Na_2O, wt %	0.14	0.09	0.22	0.02	0.65	0.22
Ca/S, mole/mole	1.87	0.70	0.74	0.02	1.06	0.07

Notes:

1. All analyses are as sampled at FD0210.
2. Hydrogen in coal is reported separately from hydrogen in moisture.
3. FD0210 sample AB13801 excluded from averages due to low sample moisture.
4. FD0210 sample AB13767 (hour 121) excluded from average sulfur.
5. FD0210 sample AB13920 (hour 250) excluded from average sulfur.
6. Seven PRB samples analyzed for ultimate and proximate analysis, two samples analyzed for ash inerts.
7. Six low sodium lignite samples analyzed for ultimate and proximate analysis, three samples analyzed for ash inerts.
8. Eighteen high soldium lignite samples analyzed for ultimate and proximate analysis, four samples analyzed for ash inerts.

Table 3.3-2

Limestone Analyses[1,3]

Compound	Weight %	Standard Deviation
$CaCO_3$	74.80	2.05
$MgCO_3$	17.36	1.89
$CaSO_4$	0.61	0.05
SiO_2	6.46	3.02
Al_2O_3	0.44	0.09
Other Inerts[2]	0.24	0.09
H_2O	0.09	0.05
Total	99.99	

Notes:

1. All analyses are as sampled at FD0220.
2. Other inerts consist of Fe_2O_3, P_2O_5, Na_2O, K_2O, & TiO_2.
3. FD0220 samples AB13843, AB13922, and AB13972 used, since the other samples contained sand.

Table 3.3-3 Standpipe Solids Analyses

Sample Number	Sample Date & Time	Sample Run Time Hours[2]	SiO_2 Wt. %	Al_2O_3 Wt. %	FeO Wt. %	Other Inerts[1] Wt. %	$CaCO_3$[4] Wt. %	CaS Wt. %	CaO Wt. %	MgO Wt. %	Na_2O Wt. %	Organic Carbon Wt. %	Total Wt. %
AB13697	10/2/2003 2:00	5	86.5	2.7	1.0	1.7	2.2	0.1	5.0	1.2	0.2	0.0	100.6
AB13712	10/3/2003 10:00	37	80.4	5.4	2.2	1.6	2.2	0.1	6.0	1.5	0.8	0.3	100.6
AB13732	10/3/2003 18:00	45	80.1	4.9	2.6	1.8	2.2	0.0	6.3	1.6	0.9	0.0	100.3
AB13735	10/4/2003 18:00	69	80.0	5.8	2.2	1.7	**2.2**	0.0	5.7	1.6	0.9	0.0	100.1
AB13736	10/5/2003 2:00	77	77.9	6.1	2.6	1.8	2.3	0.1	6.5	1.6	0.9	0.8	100.6
AB13738	10/5/2003 18:00	93	77.8	6.4	2.6	1.7	2.5	0.0	6.7	1.7	1.1	0.0	100.5
AB13740	10/6/2003 10:00	109	73.5	6.9	3.0	2.0	2.8	0.1	8.4	2.1	1.7	1.4	101.8
AB13789	10/7/2003 10:00	133	63.6	7.3	6.9	1.7	3.1	0.3	10.7	3.2	2.2	0.0	99.1
AB13798	10/7/2003 22:00	145	60.6	6.9	7.2	1.6	3.3	1.5	11.3	3.6	2.5	0.0	98.5
AB13818	10/8/2003 14:00	161	51.2	6.7	7.8	1.5	**3.5**	2.5	16.8	4.7	2.4	0.0	97.2
AB13846	10/9/2003 10:00	181	46.7	7.9	8.4	1.1	3.1	2.5	19.3	5.4	2.6	0.0	96.9
AB13854	10/9/2003 22:00	193	41.6	8.3	8.3	1.0	2.8	0.6	26.4	6.1	2.8	0.0	97.9
AB13856	10/10/2003 6:00	201	33.4	7.8	10.7	1.0	2.6	1.1	30.0	7.9	2.8	1.0	98.3
AB13880	10/10/2003 22:00	217	40.3	9.3	6.4	1.0	2.3	0.5	28.3	6.1	4.7	0.3	99.1
AB13882	10/11/2003 6:00	225	34.4	9.1	8.4	0.7	2.1	0.8	32.4	6.8	2.3	0.8	97.8
AB13887	10/12/2003 2:00	245	37.7	10.1	7.8	1.0	1.6	1.3	20.2	7.4	10.2	0.0	97.3
AB13888	10/12/2003 6:00	249	38.5	11.1	8.5	1.1	1.5	1.7	20.3	6.3	8.8	0.0	97.8
AB13888R	10/12/2003 6:00	249	34.8	10.6	9.4	1.2	1.5	1.9	21.1	7.3	8.6	0.0	96.4
AB13918	10/15/2003 22:00	263	82.3	2.7	2.2	1.2	1.2	0.5	6.5	1.6	1.6	0.1	100.0
AB13929	10/16/2003 6:00	271	57.8	4.6	4.0	1.2	1.0	0.5	20.2	4.7	5.0	0.5	99.5
AB13936	10/16/2003 22:00	287	48.2	8.3	6.1	1.1	**0.7**	0.3	20.8	5.7	7.6	1.5	100.2
AB13979	10/17/2003 6:00	295	43.7	9.0	6.6	1.0	0.7	0.6	22.3	6.3	8.5	0.2	99.0
AB13981	10/17/2003 14:00	303	43.1	7.5	5.4	1.1	0.7	0.8	23.7	6.8	10.2	0.3	99.6
AB14015	10/17/2003 18:00	307	49.2	6.5	4.5	1.5	0.7	0.2	22.5	5.8	7.8	0.5	99.2
AB14017	10/18/2003 2:00	315	50.9	7.3	4.4	1.2	0.7	0.2	21.0	5.0	8.1	0.0	99.0
AB13985	10/18/2003 18:00	331	48.9	8.2	5.2	1.2	0.7	0.2	20.9	5.5	8.0	0.2	99.1
AB13988	10/19/2003 6:00	343	46.2	8.3	5.8	1.2	0.7	0.4	22.4	5.8	8.0	0.6	99.4
AB13989	10/19/2003 10:00	347	45.4	6.8	5.7	1.3	0.7	0.6	19.3	5.8	7.1	5.5	98.1
AB14038	10/25/2003 18:00	359	91.3	2.0	2.0	0.7	0.7	0.2	1.1	0.5	0.7	0.4	99.6
AB14043	10/26/2003 14:00	379	86.2	2.8	2.0	0.7	**0.7**	0.2	3.1	1.3	2.4	0.2	99.6

Notes:

1. Other inerts consist of P_2O_5, K_2O, & TiO_2
2. Hours 5 to 109 were PRB, Hours 133 to 217 were low sodium lignite, hour 225 was a mixture of low and high sodium lignite, hours 245 to 379 were high sodium lignite.
3. Limestone injected intermittently into the gasifier from hours 141 to 347.
4. CO_2 was analyzed for samples at hours 69, 161, 287, and 379. CO_2 values for the other samples were interpolated from the measured values.

Table 3.3-4

FD0510 Solids Sample Analyses

Sample Number	Sample Date & Time	Sample Run Time Hours[2]	SiO_2 Wt. %	Al_2O_3 Wt. %	FeO Wt. %	Other Inerts[1] Wt. %	$CaCO_3$[4] Wt. %	CaS Wt. %	CaO Wt. %	MgO Wt. %	Na_2O Wt. %	Organic Carbon Wt. %	Total Wt. %
AB14055	10/28/2003 2:00	415	78.3	3.1	3.2	0.6	**0.6**	0.5	4.7	1.9	5.4	0.6	98.7
AB14068	10/28/2003 10:00	423	78.6	3.1	3.2	0.6	0.6	0.4	5.1	1.9	5.6	0.3	99.3
AB14088	10/31/2003 14:00	456	72.2	3.9	5.3	0.6	0.8	0.9	5.4	2.3	6.4	0.5	98.4
AB14111	11/1/2003 6:00	472	63.6	5.7	6.3	0.8	**0.9**	0.6	8.5	3.3	8.0	0.1	97.8
AB14112	11/1/2003 10:00	476	54.6	6.6	8.9	0.9	**2.6**	1.1	9.9	4.3	10.0	0.0	99.0
AB14114	11/1/2003 22:00	488	48.2	7.6	10.5	1.1	2.6	1.2	10.9	4.6	11.7	0.3	98.7
AB14117	11/2/2003 14:00	504	48.3	7.6	9.9	0.9	2.6	0.9	12.2	5.3	11.2	0.0	99.0
AB14118[3,5]	11/3/2003 9:00		52.7	7.9	9.4	0.8	**5.1**	0.5	9.5	3.7	10.6	0.0	100.2

Notes:

1. Other inerts consist of P_2O_5, K_2O, & TiO_2.
2. Hours 415 to 504 were high sodium lignite.
3. Sample AB141118 taken from standpipe after TC13 was completed.
4. CO_2 was analyzed for samples at hours 415, 472, and 476 . CO_2 values for the other samples were interpolated from the measured values.
5. CO_2 was analyzed for sample AB14118.

Table 3.3-5

PCD Fines Solids From FD0520 Analyses

Sample Number	Sample Date & Time	Sample Run Time Hours[2]	SiO_2 Wt. %	Al_2O_3 Wt. %	FeO Wt. %	Other Inerts[1] Wt. %	$CaCO_3$ Wt. %	CaS Wt. %	CaO Wt. %	MgO Wt. %	Na_2O Wt. %	Organic C ($C\text{-}CO_2$) Wt. %	Total Wt. %	HHV Btu/lb.	LHV Btu/lb.
AB13698	10/2/2003 2:00	5	42.8	9.2	3.1	1.8	5.8	0.4	13.8	3.1	3.5	28.8	112.3	3,062	3,012
AB13703	10/2/2003 14:00	17	55.1	9.9	2.5	3.6	9.4	1.0	7.5	2.9	2.8	6.0	100.6	819	813
AB13704	10/3/2003 6:00	33	46.0	11.0	3.2	2.6	4.8	1.1	13.8	4.3	3.5	15.8	106.0	1,762	1,742
AB13741	10/3/2003 18:00	45	43.2	11.2	3.8	2.3	3.6	0.9	13.4	4.0	4.3	16.5	103.3	2,026	2,011
AB13743	10/4/2003 2:00	53	37.5	11.0	3.2	1.9	4.5	0.8	11.8	3.3	3.6	25.1	102.8	3,509	3,484
AB13746	10/4/2003 14:00	65	43.4	11.0	3.2	2.1	4.9	1.2	10.2	3.8	3.6	19.6	103.1	2,693	2,677
AB13747	10/4/2003 18:00	69	37.9	11.7	3.9	2.4	3.9	0.7	13.5	3.9	4.4	20.3	102.7	3,476	3,469
AB13749	10/5/2003 2:00	77	27.4	7.4	2.1	1.3	5.9	0.8	5.8	2.2	2.3	44.8	100.0	6,850	6,781
AB13753	10/5/2003 18:00	93	34.1	10.5	2.8	1.8	4.4	0.9	9.7	2.9	3.1	29.4	99.6	4,227	4,193
AB13757	10/6/2003 10:00	109	29.6	10.3	2.7	1.7	6.7	0.8	8.4	2.9	3.0	30.5	96.7	4,774	4,738
AB13776	10/7/2003 6:00	129	32.6	9.5	7.2	1.2	7.6	4.5	11.1	6.4	8.0	15.3	103.5	2,449	2,436
AB13802	10/7/2003 18:00	141	29.0	8.5	6.9	1.2	8.4	7.6	6.1	5.8	7.7	20.1	101.4	3,296	3,277
AB13803	10/7/2003 22:00	145	29.8	8.4	8.3	1.1	12.0	10.3	4.5	6.6	9.2	14.7	104.8	2,704	2,687
AB13812	10/8/2003 10:00	157	28.1	8.3	6.9	1.0	12.4	10.4	9.3	8.0	7.6	14.8	106.8	2,229	2,213
AB13812R	10/8/2003 10:00	157	28.3	8.4	6.9	1.0	12.4	10.4	9.4	8.0	7.7	13.2	105.8	1,919	1,896
AB13813	10/8/2003 14:00	161	20.8	7.8	5.9	0.9	12.3	11.0	6.8	7.8	6.6	24.1	104.0	3,958	3,934
AB13823	10/9/2003 6:00	177	11.5	4.9	3.7	0.7	15.8	12.6	0.0	6.0	4.1	49.0	108.3	7,378	7,313
AB13825	10/9/2003 10:00	181	9.0	4.8	3.6	0.6	12.2	11.5	0.0	5.1	4.0	49.9	100.8	7,925	7,870
AB13825R	10/9/2003 10:00	181	9.1	4.9	3.7	0.6	12.2	11.7	0.0	5.2	4.1	49.4	100.9	7,815	7,751
AB13852	10/10/2003 6:00	201	13.3	4.7	6.2	0.8	11.1	5.4	8.0	6.3	6.9	39.1	101.8	6,192	6,131
AB13869	10/10/2003 22:00	217	20.7	6.7	9.3	0.9	10.6	3.8	18.1	8.3	10.4	17.0	105.8	2,724	2,698
AB13871	10/11/2003 6:00	225	26.1	9.1	6.7	1.0	13.1	3.6	19.2	7.7	7.4	15.1	109.2	2,612	2,587
AB13877	10/12/2003 6:00	249	28.4	9.8	8.0	1.3	18.6	2.9	8.9	6.3	8.9	10.6	103.8	1,814	1,795
AB13925	10/15/2003 22:00	263	32.2	7.4	3.4	1.4	14.5	7.0	3.8	7.1	3.7	20.9	101.3	3,172	3,142
AB13926	10/16/2003 6:00	271	25.9	6.9	4.5	1.2	20.0	7.6	11.4	9.5	5.0	12.2	104.2	1,802	1,786
AB13933	10/16/2003 14:00	279	24.2	6.1	2.6	1.0	10.3	4.2	6.0	5.6	2.8	43.8	106.6	4,981	4,917
AB13943	10/16/2003 18:00	283	11.3	4.8	1.5	0.7	18.1	3.5	0.0	3.5	1.7	49.1	94.4	7,759	7,687
AB13945	10/17/2003 2:00	291	12.0	5.5	2.0	0.8	19.0	4.9	0.0	4.3	2.3	46.7	97.5	7,051	6,981
AB13956	10/17/2003 10:00	299	33.4	9.1	6.7	1.3	11.8	3.4	16.3	7.0	7.4	5.4	101.8	963	960
AB13958	10/17/2003 18:00	307	35.7	8.1	4.8	1.0	14.2	3.8	19.2	8.1	5.4	1.5	101.7	0	0
AB13960	10/18/2003 2:00	315	22.6	6.4	3.3	0.9	17.4	4.2	6.9	5.9	3.7	22.6	93.9	3,733	3,703
AB13960R	10/18/2003 2:00	315	25.0	7.1	3.7	1.0	17.4	4.6	8.6	6.5	4.1	22.5	100.5	3,513	3,481
AB13961	10/18/2003 6:00	319	25.8	7.5	5.0	1.1	8.6	6.0	15.1	8.5	5.6	19.2	102.5	2,265	2,227
AB13963	10/18/2003 14:00	327	24.1	6.6	3.4	0.9	17.3	4.3	10.3	6.5	3.7	17.6	94.6	2,838	2,816
AB13964	10/18/2003 18:00	331	18.9	5.8	3.0	1.0	13.1	5.7	8.7	7.4	3.3	35.4	102.4	2,186	2,119
AB13965	10/18/2003 22:00	335	25.9	6.6	4.1	0.7	23.2	4.5	0.0	3.4	4.5	29.5	102.4	5,382	5,339
AB13966	10/19/2003 2:00	339	32.5	8.6	5.6	1.1	20.0	4.5	13.4	7.4	6.2	4.2	103.3	1,270	1,265
AB13967	10/19/2003 6:00	343	23.8	7.0	4.1	1.0	18.3	5.4	8.1	6.3	4.6	20.3	98.9	3,258	3,230
AB14035	10/26/2003 22:00	387	21.7	4.7	2.9	0.5	13.7	3.0	0.0	2.5	3.2	46.0	98.2	7,393	7,321
AB14037	10/27/2003 6:00	395	12.4	6.0	3.0	0.6	11.5	3.0	0.4	3.3	3.3	54.3	97.9	7,975	7,884
AB14058	10/27/2003 22:00	411	8.3	4.3	2.4	0.5	12.1	2.3	0.0	2.9	2.6	63.6	99.0	9,893	9,787
AB14060	10/28/2003 6:00	419	7.2	4.0	2.1	0.4	9.3	2.2	0.0	2.8	2.4	64.5	94.9	10,082	9,970
AB14081	10/30/2003 22:00	440	8.7	4.5	3.4	0.5	10.2	1.7	0.0	2.9	3.7	61.1	96.8	9,398	9,287
AB14083	10/31/2003 6:00	448	8.5	4.4	3.3	0.5	9.9	1.9	0.2	2.9	3.6	62.4	97.5	9,636	9,520
AB14093	10/31/2003 22:00	464	6.6	4.0	2.4	0.4	10.0	2.7	0.0	2.8	2.7	65.3	96.8	10,151	10,041
AB14096	11/1/2003 14:00	480	6.5	3.9	2.6	0.5	12.6	2.4	0.0	2.8	2.9	64.1	98.4	10,153	10,044
AB14102	11/2/2003 14:00	504	5.7	3.6	2.3	0.5	9.2	2.6	0.6	2.6	2.5	66.0	95.6	10,350	10,241

Notes:

1. Other inerts consist of P_2O_5, K_2O, & TiO_2
2. Hours 5 to 109 were PRB, Hours 129 to 217 were low sodium lignite, hour 225 was a mixture of low and high sodium lignite, hours 249 to 504 were high sodium lignite.
3. Limestone injected intermittently into the gasifier from hours 141 to 343.

Table 3.3-6

Reactive Sulfide Test Results

Sample ID	Sample Point	Location ID	Collection Date & Time[4]	Sulfide, Total Releasable as H_2S, mg/kg[3]
AB13730[1]	KASHSILO	SI0814	10/4/03 18:00	20.1
AB13730[2]	KASHSILO	SI0814	10/4/03 18:00	48.4
AB13731[1]	KASHSILO	SI0814	10/5/03 18:00	52.0
AB13731[2]	KASHSILO	SI0814	10/5/03 18:00	38.1
AB13769[1]	KASHSILO	SI0814	10/6/03 18:00	30.1
AB13769[2]	KASHSILO	SI0814	10/6/03 18:00	42.1
AB13796[1]	KASHSILO	SI0814	10/7/03 18:00	Not Detected
AB13796[2]	KASHSILO	SI0814	10/7/03 18:00	32.1
AB13842[1]	KASHSILO	SI0814	10/9/03 18:00	Not Detected
AB13842[2]	KASHSILO	SI0814	10/9/03 18:00	62.3
AB13849[1]	KPCDSOL	FD0520	10/9/03 18:00	212
AB13849[2]	KPCDSOL	FD0520	10/9/03 18:00	255
AB13853[1]	KSPSOL	STANDPIPE	10/9/03 18:00	Not Detected
AB13853[2]	KSPSOL	STANDPIPE	10/9/03 18:00	10.0
AB13878	KPCDSOL	FD0520	10/12/03 10:00	110
AB13889	KSPSOL	STANDPIPE	10/12/03 10:00	80.1
AB13918	KSPSOL	STANDPIPE	10/15/03 22:00	114
AB13925	KPCDSOL	FD0520	10/15/03 22:00	16.1
AB13935	KSPSOL	STANDPIPE	10/16/03 18:00	Not Detected
AB13938	KASHSILO	SI0814	10/16/03 18:00	110
AB13943	KPCDSOL	FD0520	10/16/03 18:00	55.0

1. Acid concentration used per procedure.
2. Acid concentration used was 5 times that of routine procedure.
3. Passing the test requires less than 500 mg/kg
4. Samples taken from 10/4 to 10/5 were taken during PRB operation;
   Samples taken from 10/6 to 10/9 were taken during high sulfur lignite operation;
   Samples taken from 10/12 to 10/16 were taken during low sulfur lignite operation.

Table 3.3-7

Historical as Fed Coal Average Particle Sizes, Percent Fines, and Percent Oversize

Test Campaign	Fuel	Time Range Run Hours	Average Feed Coal SMD microns	Std. Dev. Feed Coal SMD microns	Average Feed Coal MMD microns	Std. Dev. Feed Coal MMD microns	Average Feed Coal % > 1180 microns	Std. Dev. Feed Coal % > 1180 microns	Average Feed Coal % < 45 microns	Std. Dev. Feed Coal % < 45 microns
TC06	Powder River Basin	all	188	43	277	52	0.1	0.1	11.8	7.1
TC07[1]	Powder River Basin	2 to 80	221	40	293	35	5.8	1.5	6.6	3.1
TC07	Alabama Bituminous	100 to 132	201	14	290	15	8.5	3.0	8.1	1.1
TC07[2]	Powder River Basin	162 to 142	197	17	289	21	0.1	0.3	8.8	1.9
TC08	Powder River Basin	all	195	15	282	18	0.1	0.1	8.7	1.7
TC09	Hiawatha Bituminous	all	232	13	297	36	0.3	0.1	4.6	1.3
TC10	Powder River Basin	0 to 90	231	10	299	15	0.2	0.2	4.4	0.4
TC10[3]	Powder River Basin	131 to 412	239	24	376	69	11.1	4.8	6.5	2.8
TC11[4]	Falkirk Lignite	all	165	28	283	40	10.0	3.1	14.2	3.8
TC12	Powder River Basin	0 to 467	313	44	479	135	14.6	7.6	3.5	1.9
TC12[5]	Powder River Basin	517 to 733	175	37	265	56	5.6	2.0	12.5	5.8
TC13	Powder River Basin	0 to 121	195	50	262	71	4.3	1.9	9.4	5.0
TC13	Freedom Lignite	129 to 504	227	28	435	81	11.6	4.8	8.6	2.4

Notes

1. 1000 micron screen was removed from mill prior to start of TC07.
2. 1000 micron screen was installed on mill between TC07 hours 132 and 162.
3. 1000 micron screen was removed from mill on 11/23/02 (TC10 hour 90).
4. 2800 micron screen was installed in mill prior to start of TC11.
5. As received PRB was very wet prior to hour 4/3/03 (TC12 hour 467). On 4/3/03 several loads of dry coal were received.

Table 3.3-8

Historical Standpipe and PCD Fines Particle Sizes and Bulk Density

Test Campaign	Fuel	Standpipe			PCD Fines			
		Maximum Particle Size SMD microns	Steady State Part. Size SMD microns	Minimum Bulk Density lb/ft^3	Average Particle Size SMD microns	Std. Dev. Particle Size SMD microns	Average Bulk Density lb/ft^3	Std. Dev. Bulk Density lb/ft^3
TC06	Powder River Basin	204	165	80	10.8	1.1	24	4
TC07	Powder River Basin	191	175	80	10.2	1.1	28	8
TC07	Alabama Bituminous	232	none	66	16.2	3.2	32	7
TC08	Powder River Basin	250	205	77	13.1	3.2	25	7
TC09	Hiawatha Bituminous	233	180	76	15.7	4.6	29	12
TC10	Powder River Basin	280	none	76	10.7	3.6	23	7
TC11	Falkirk Lignite	200	200	75	12.3	2.4	36	3
TC12	Powder River Basin	300	none	76	9.8	2.0	18	6
TC13	Powder River Basin	165	165	81	10.4	1.4	18	4
TC13	Freedom Lignite Low Sodium	230	none	56	15.3	3.9	26	6
TC13	Freedom Lignite High Sodium, High Temp.	425	none	46	30.0	32.3	39	14
TC13	Freedom Lignite High Sodium, Low Temp.	457	none	67	13.9	2.3	26	5

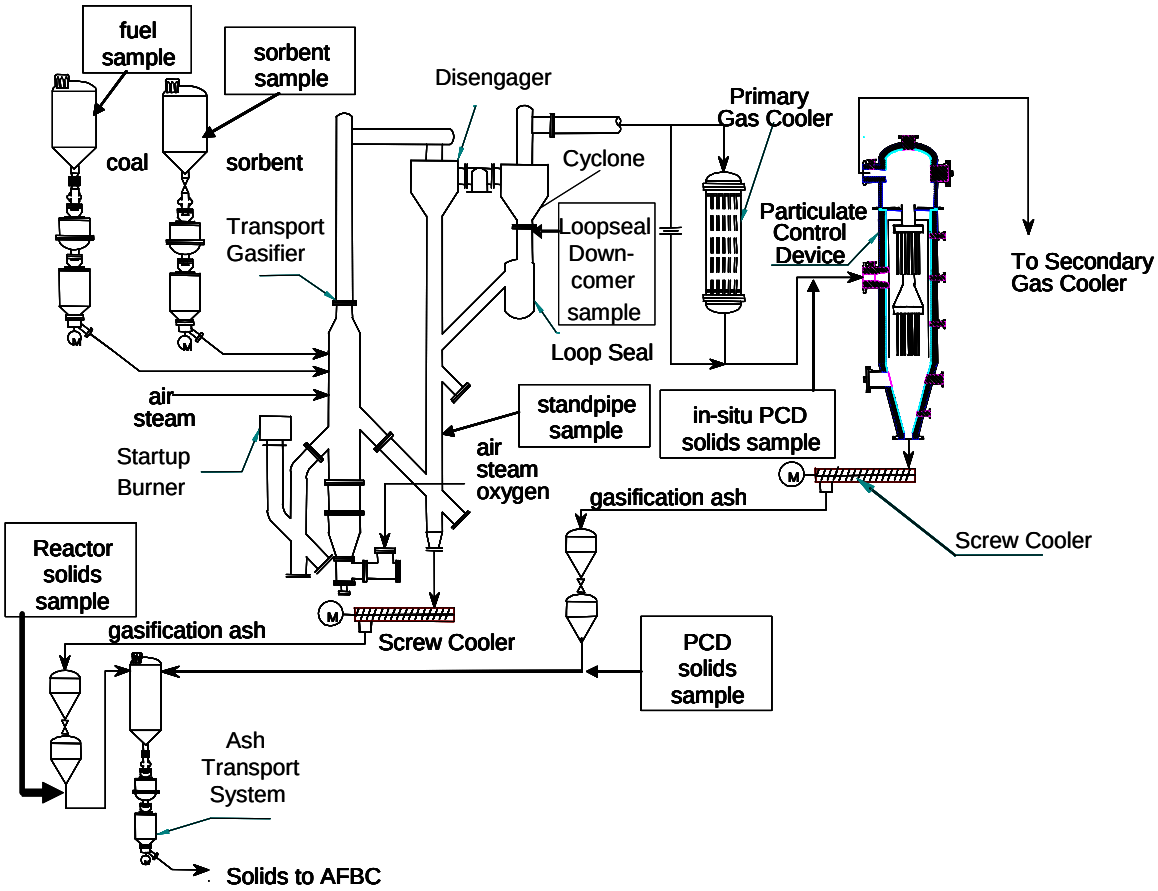

Figure 3.3-1 Solid Sample Locations

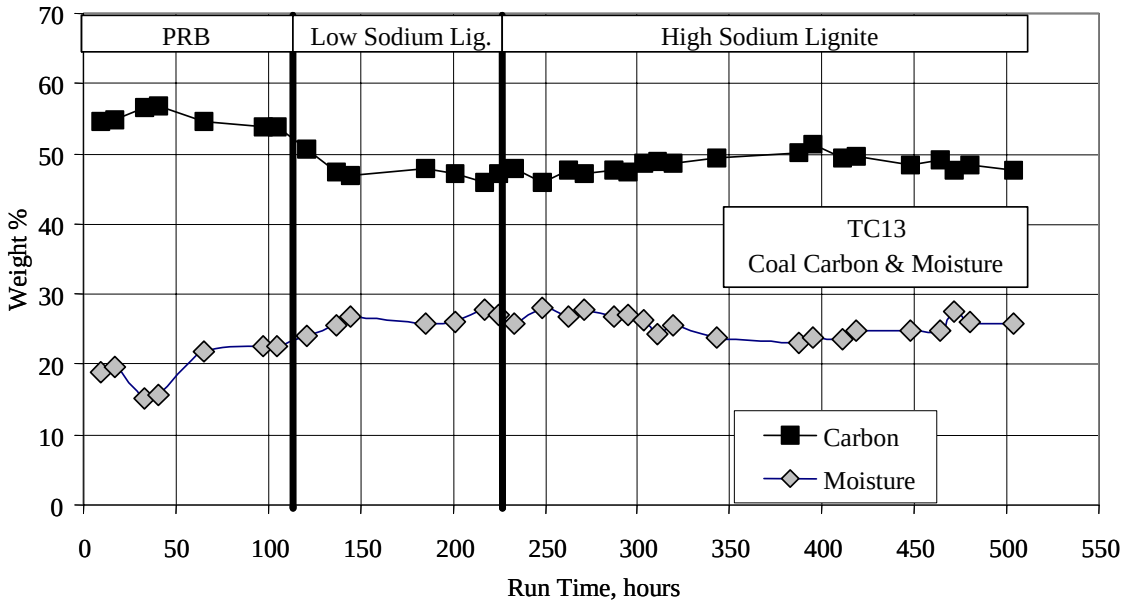

Figure 3.3-2 Coal Carbon and Moisture

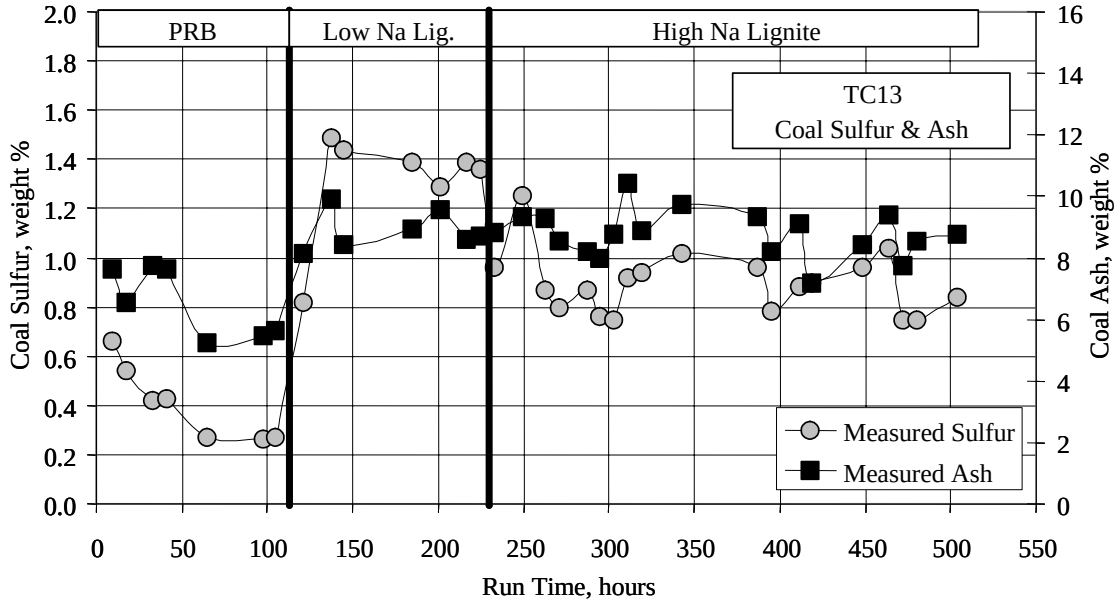

Figure 3.3-3 Coal Sulfur and Ash

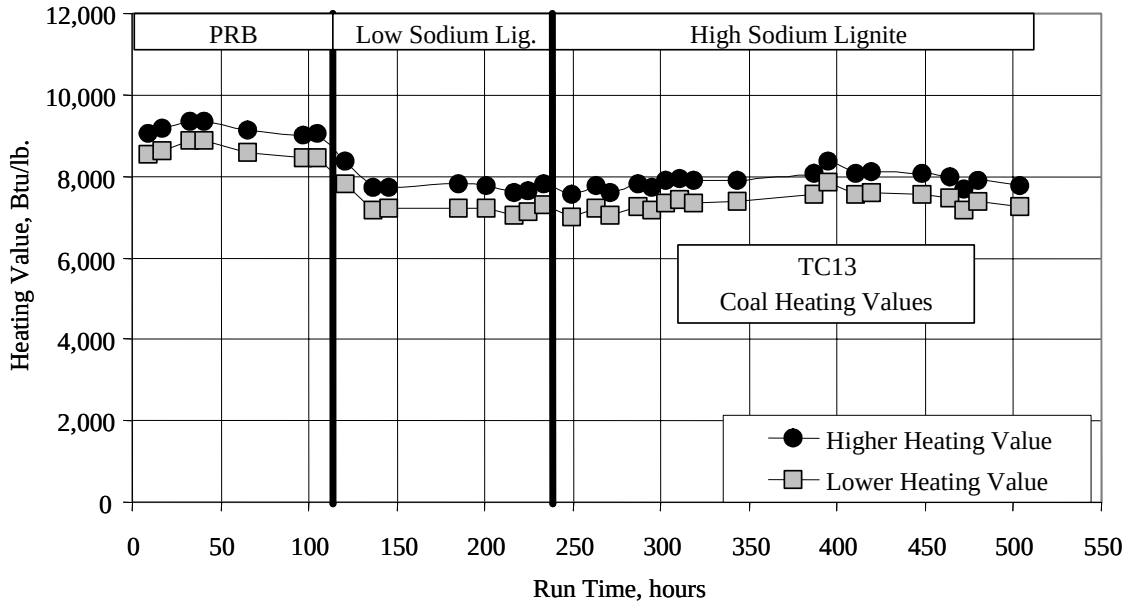

Figure 3.3-4 Coal Heating Value

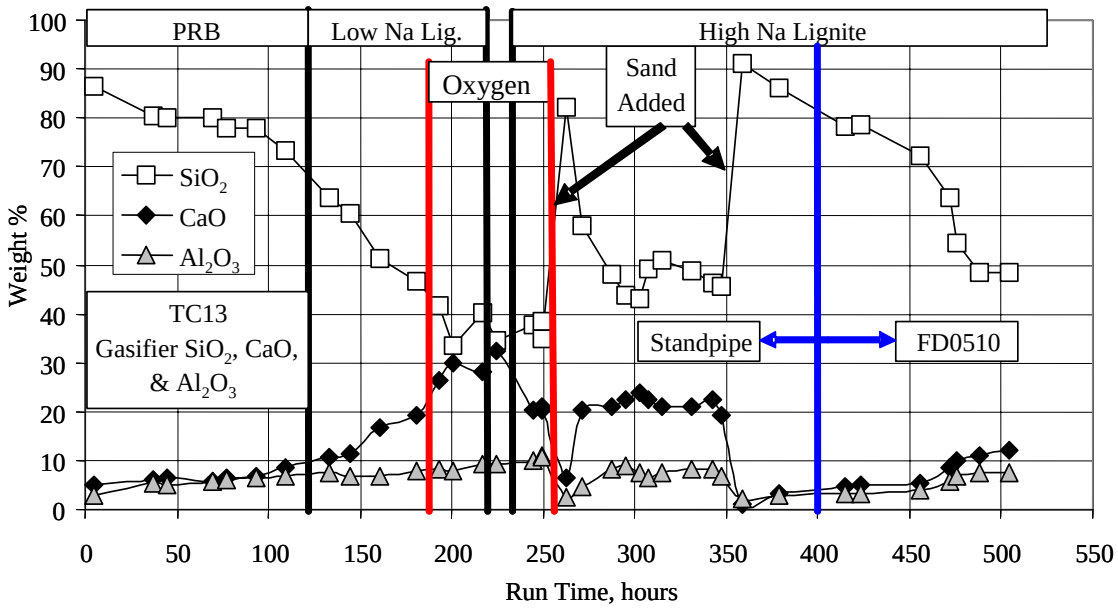

Figure 3.3-5 Gasifier SiO_2, CaO, and Al_2O_3

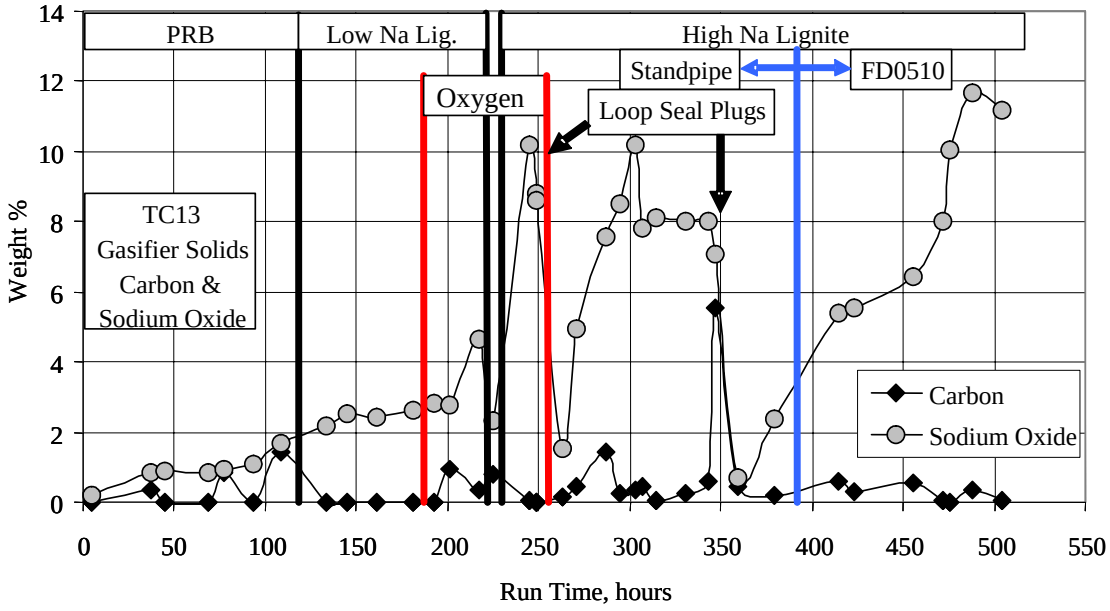

Figure 3.3-6 Gasifier Organic Carbon and Sodium Oxide

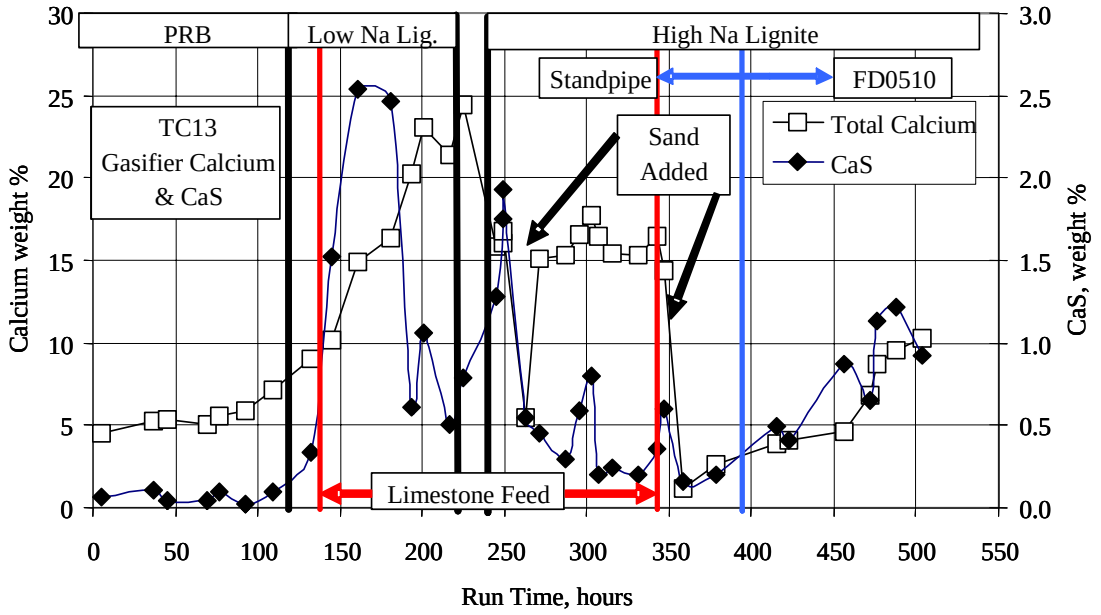

Figure 3.3-7 Gasifier Circulating Solids Calcium and Calcium Sulfide

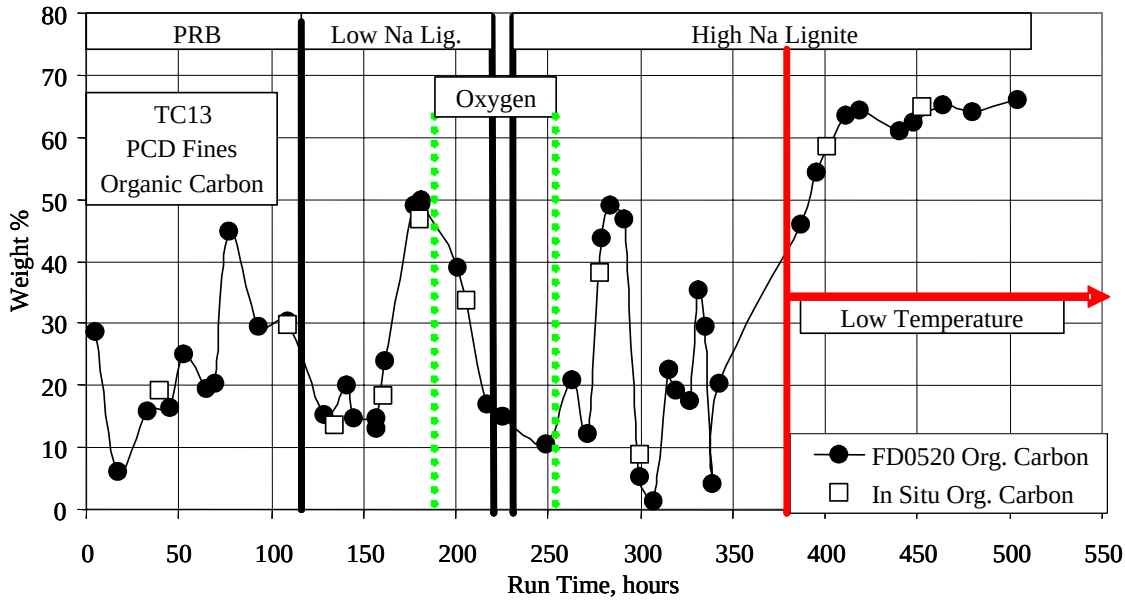

Figure 3.3-8 Gasifier PCD Fines Organic Carbon

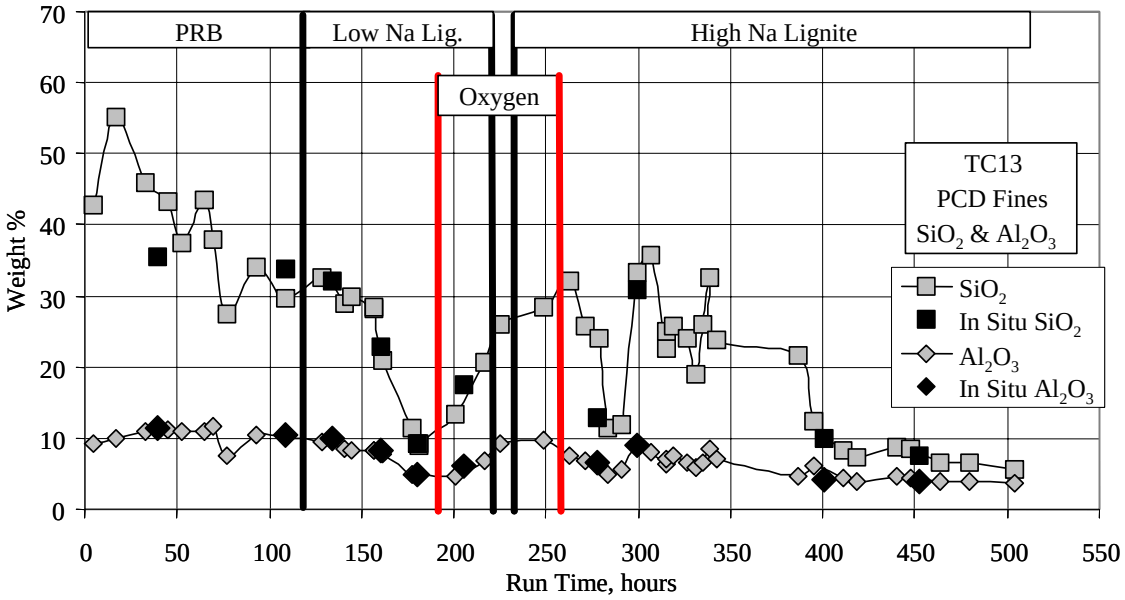

Figure 3.3-9 PCD Fines Silica and Alumina

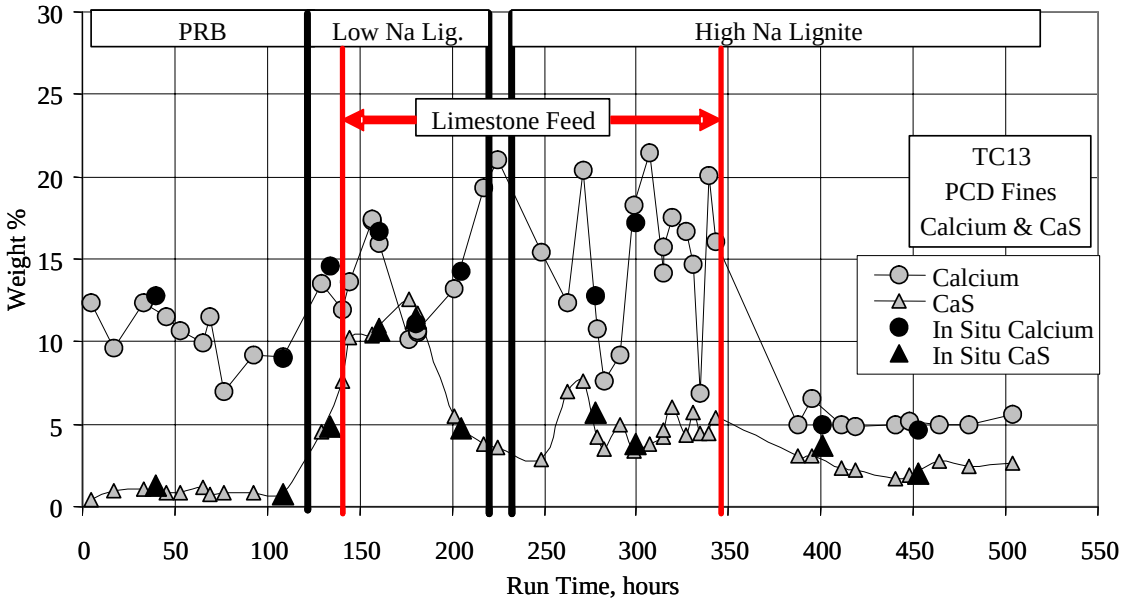

Figure 3.3-10 PCD Fines Calcium and Calcium Sulfide

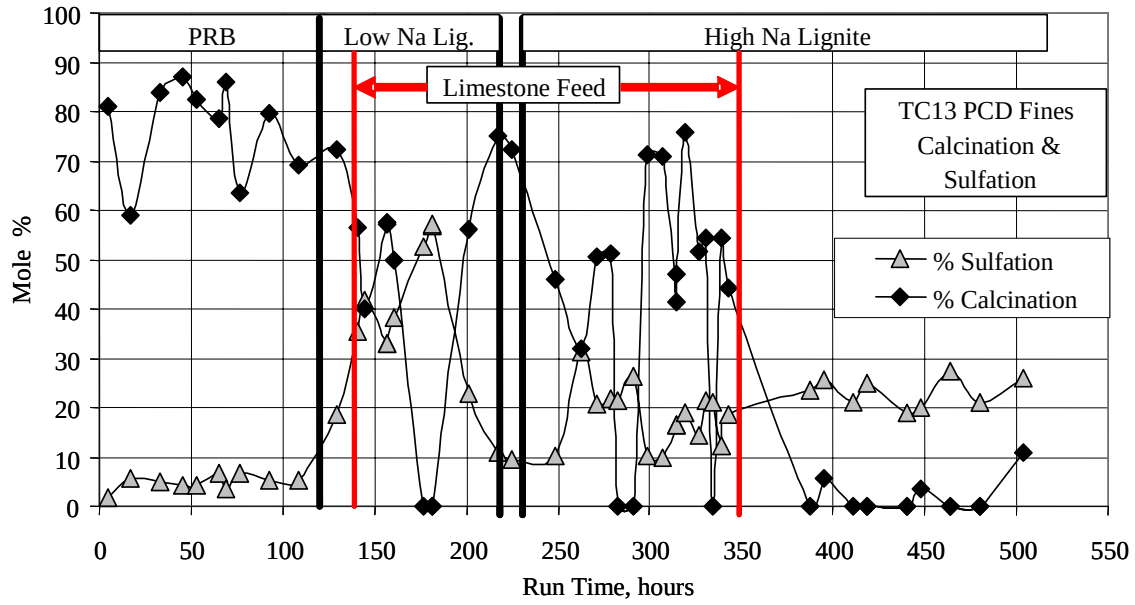

Figure 3.3-11 PCD Fines Calcination and Sulfation

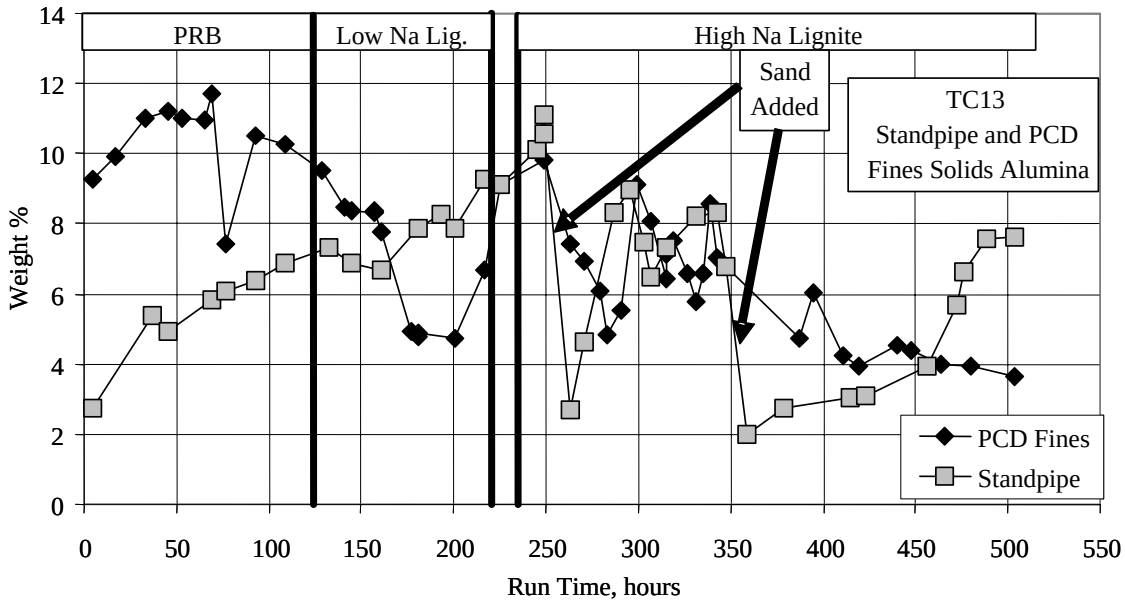

Figure 3.3-12 Standpipe and PCD Fines Solids Alumina

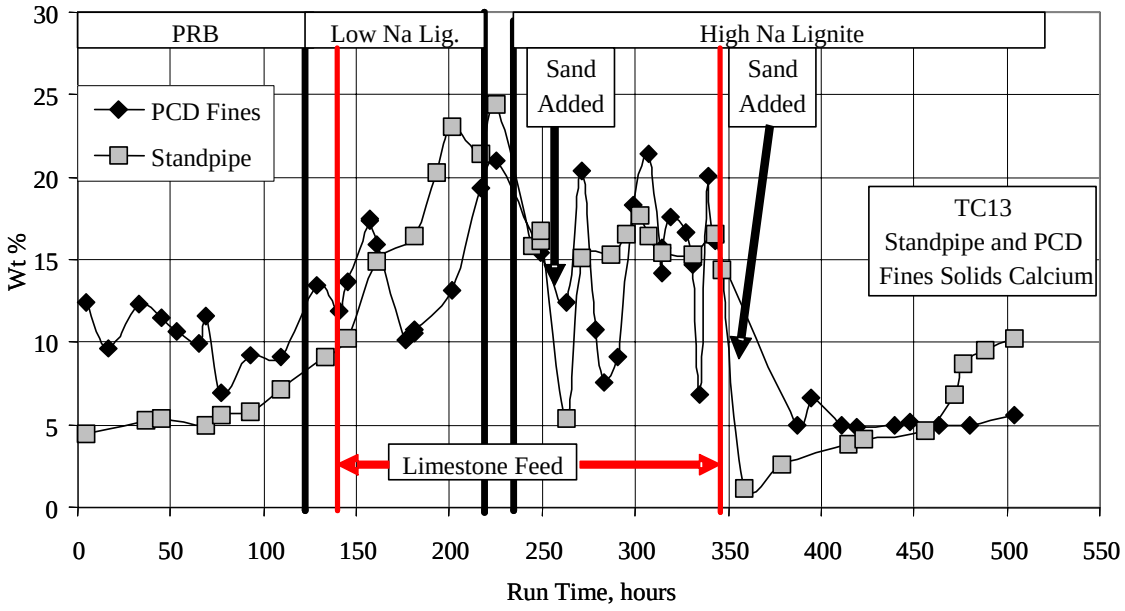

Figure 3.3-13 Gasifier Solids and PCD Fines Solids Calcium

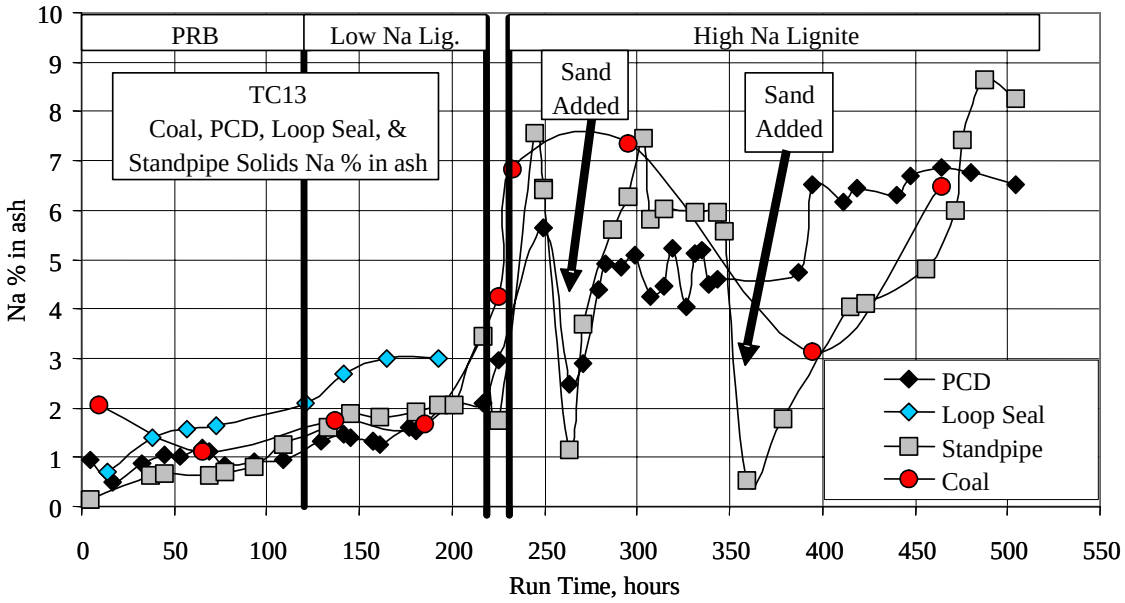

Figure 3.3-14 Gasifier Solids and PCD Fines Solids Sodium in Ash

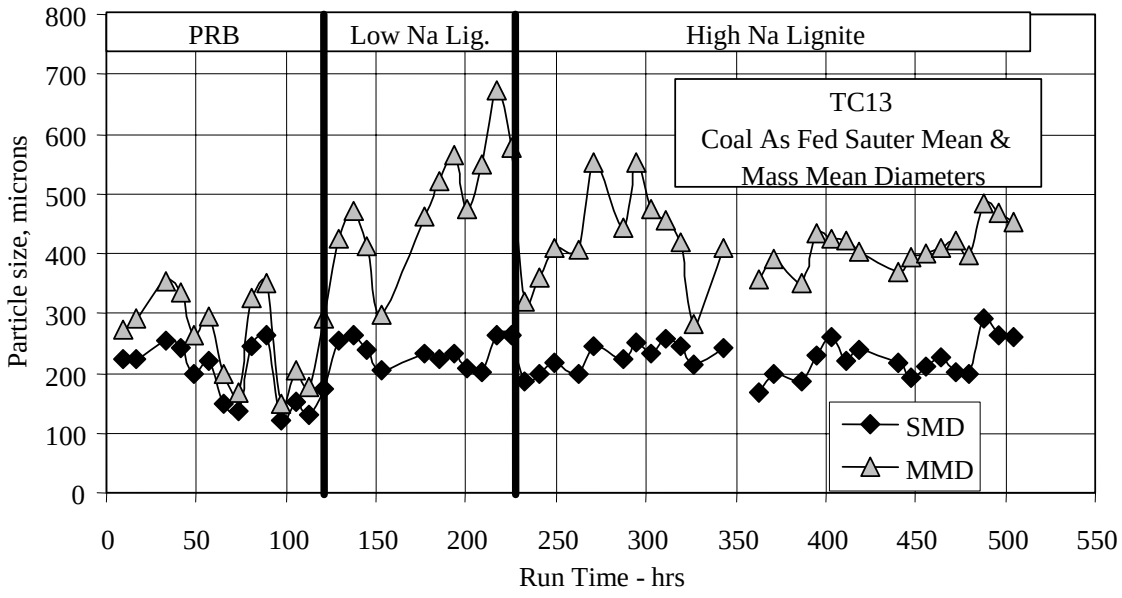

Figure 3.3-15 Coal Particle Size

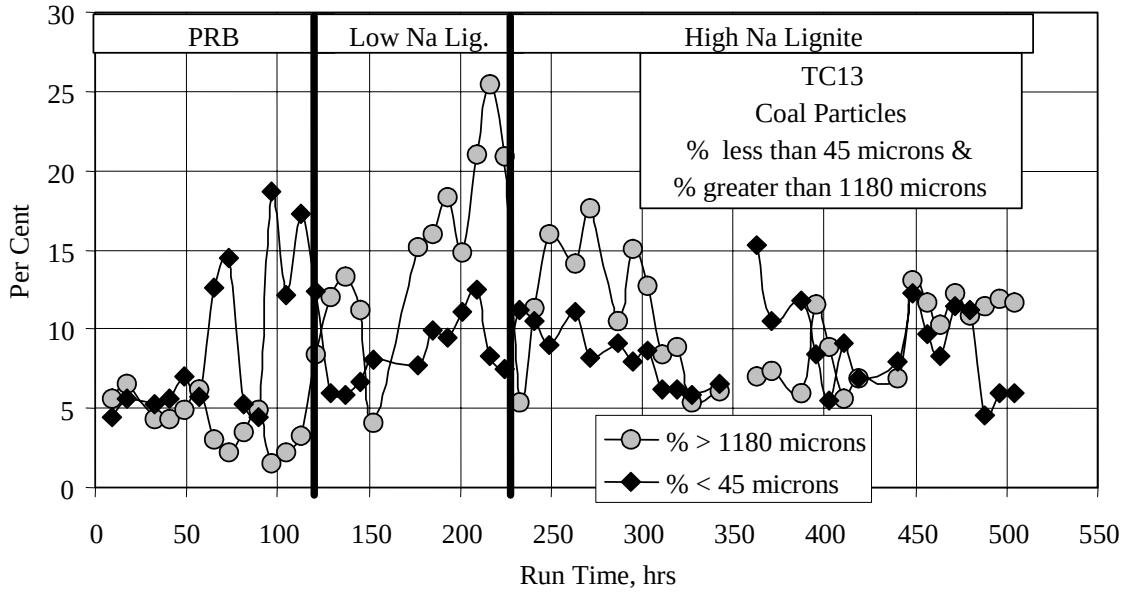

Figure 3.3-16 Percent Coal Fines and Oversize

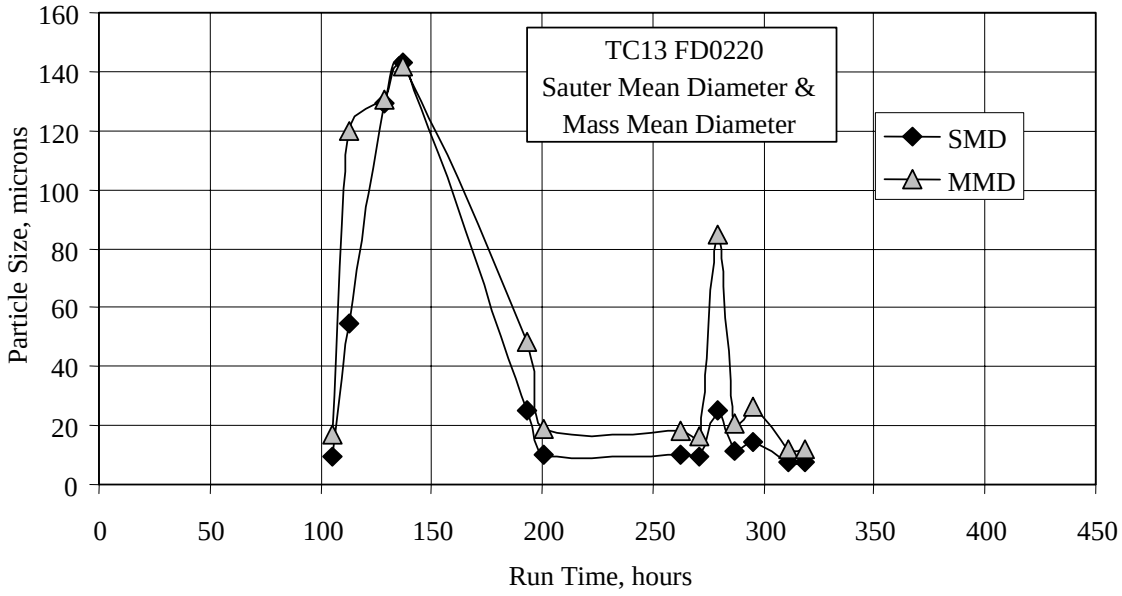

Figure 3.3-17 FD0220 Particle Sizes

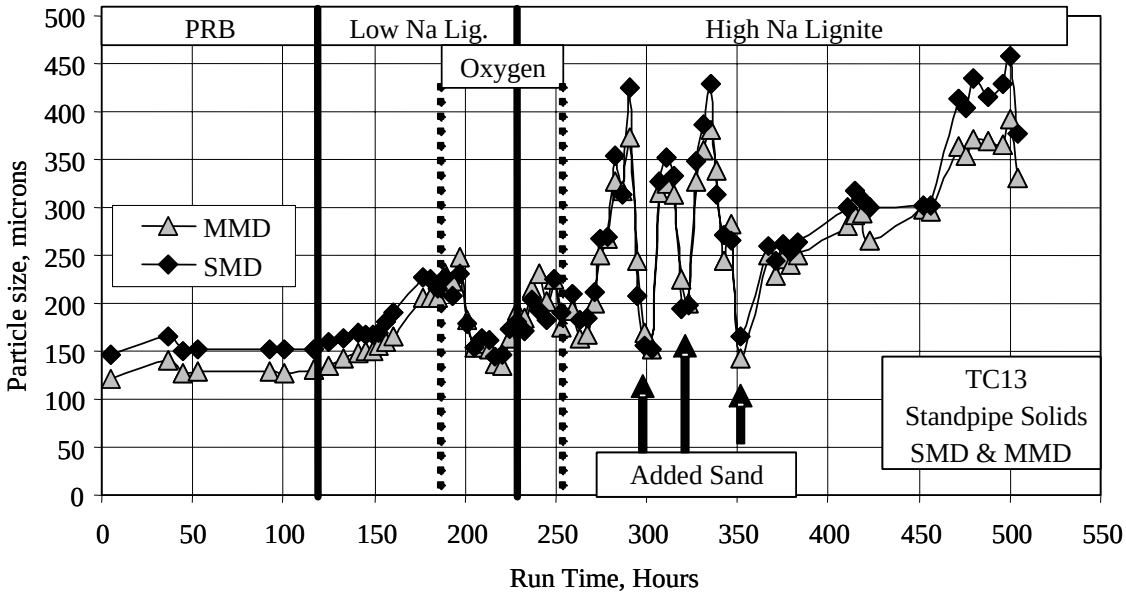

Figure 3.3-18 Standpipe Solids Particle Size

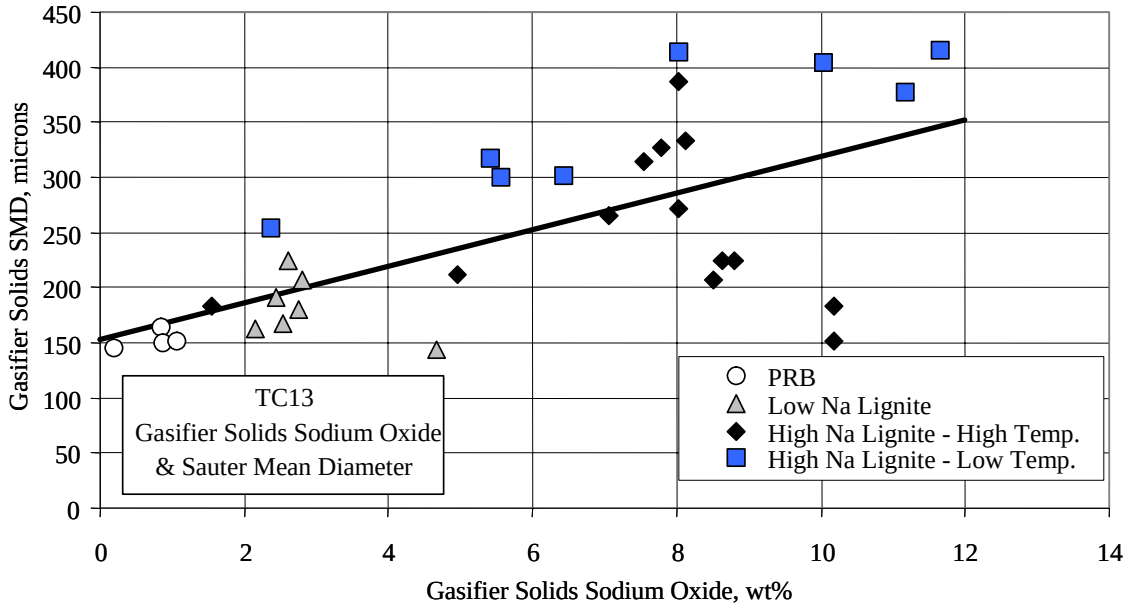

Figure 3.3-19 Standpipe Solids Sodium Oxide and Particle Size

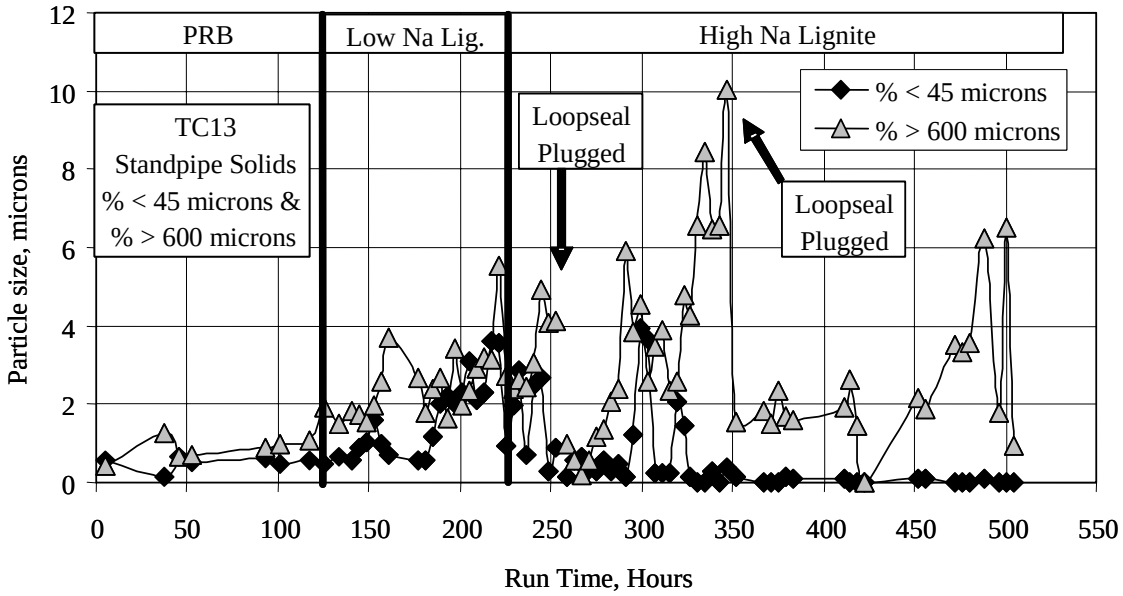

Figure 3.3-20 Standpipe Solids Fine and Coarse Particles

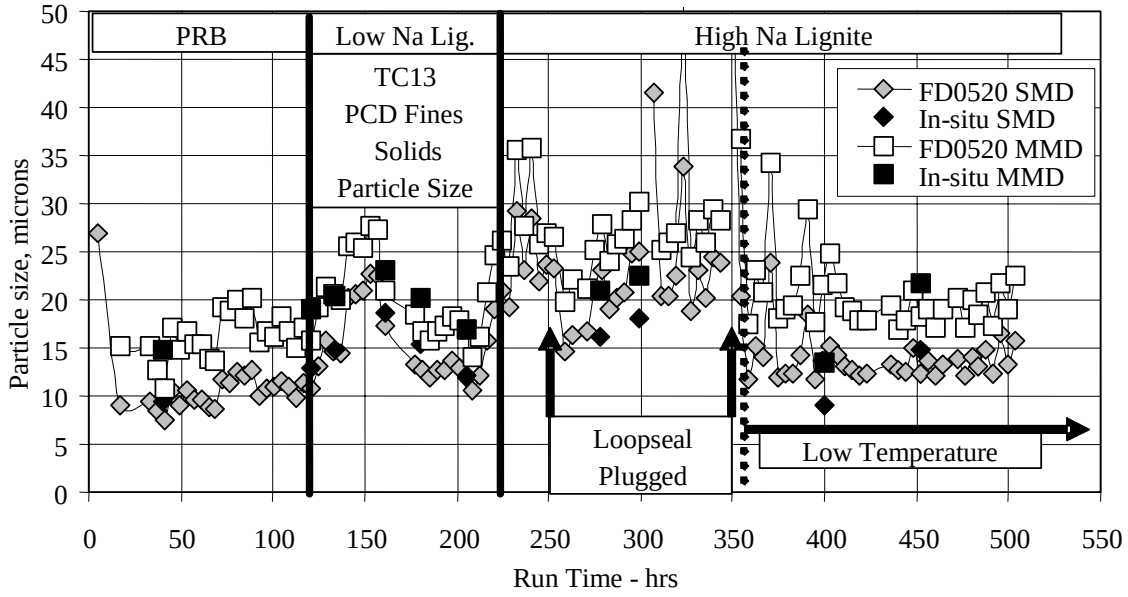

Figure 3.3-21 PCD Fines Particle Sizes

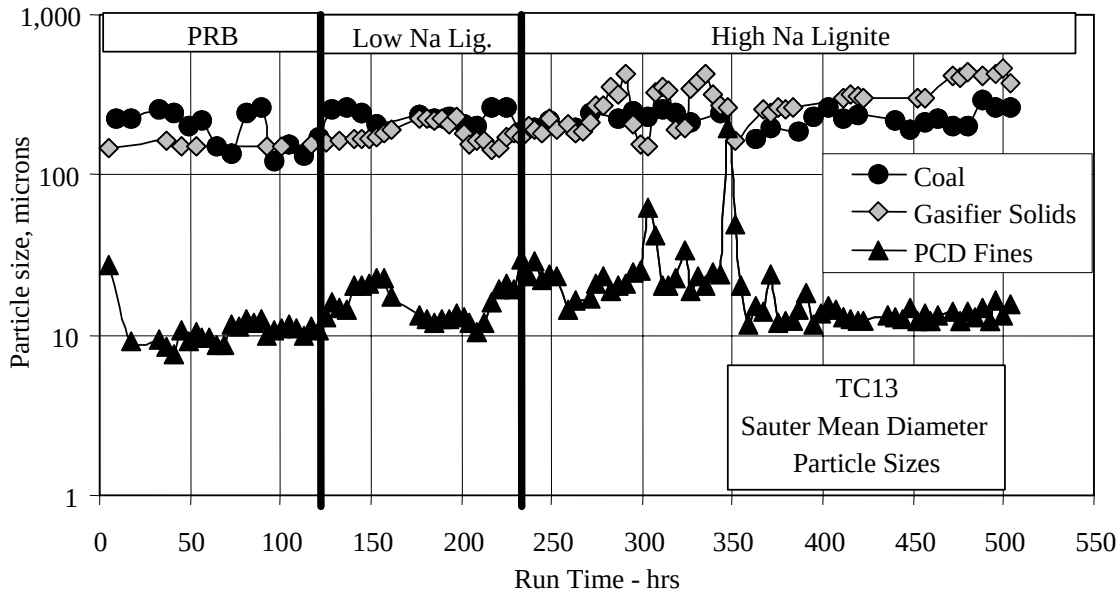

Figure 3.3-22 Particle Size Distribution

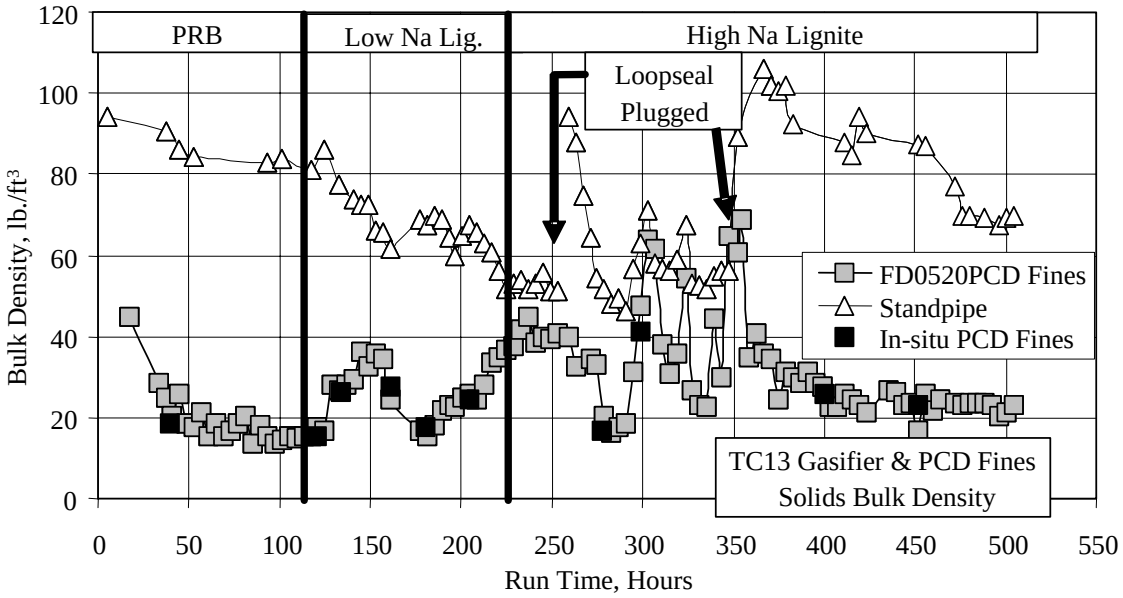

Figure 3.3-23 Gasifier Solids and PCD Fines Bulk Density

3.4 MASS AND ENERGY BALANCES

3.4.1 Summary and Conclusions

3.4.1.1 Powder River Basin Coal

- Carbon conversions were between 96 and 99 percent.
- Coal rates were varied from 2,000 to 3,900 lb/hr.
- The amount of fuel nitrogen converted to ammonia varied from 28 to 72 percent.
- Sulfur removal averaged 9 percent with no sorbent added.
- The raw cold gasification efficiency was 43 to 55 percent.
- The raw hot gasification efficiency was 79 to 87 percent.
- The commercially projected cold gas efficiency was 70 to 74 percent.

3.4.1.2 Low-Sodium Freedom Mine Lignite

- Carbon conversions were between 93 and 97 percent in air-blown mode and between 87 and 94 percent in oxygen-blown mode.
- Coal rates were varied from 2,800 to 5,100 lb/hr.
- The amount of fuel nitrogen converted to ammonia varied from 35 to 94 percent.
- Sulfur removal was about 24 percent, independent of whether sorbent was added.
- The raw cold gasification efficiency was 44 to 54 percent in air-blown mode and 53 to 55 percent in oxygen-blown mode.
- The raw hot gasification efficiency was 79 to 84 percent in air-blown mode and 78 to 82 percent in oxygen-blown mode.
- The commercially projected cold gas efficiency was 65 to 66 percent in air-blown mode and between 67 and 74 percent in oxygen-blown mode.

3.4.1.3 High-Sodium Freedom Mine Lignite

- Carbon conversions were between 90 and 99 percent during high temperature operation and were between 77 and 84 percent during low temperature operation.
- Coal rates were varied from 1,900 to 4,000 lb/hr.
- The amount of fuel nitrogen converted to ammonia varied from 51 to 90 percent.
- Sulfur removal was about 16 percent, independent of whether sorbent was added.
- The raw cold gasification efficiency was 28 to 48 percent in air-blown mode and 52 percent in oxygen-blown mode.
- The raw hot gasification efficiency was 59 to 83 percent in air-blown mode and 82 percent in oxygen-blown mode.
- The commercially projected cold gas efficiency was 50 to 71 percent in air-blown mode and 77 percent in oxygen-blown mode.

3.4.1.4 Both Powder River Basin Coal and Freedom Mine Lignite

- Overall mass balances were good at ±10 percent.
- Carbon balances were acceptable at ±19 percent.
- Oxygen-to-coal ratio (lb/lb) was 0.53 to 0.94.
- Nitrogen balances were good at ±10 percent.
- Sulfur balances were poor with many periods exhibiting greater than 25-percent error.
- Sulfur emissions were from 0.38 to 3.01 lb SO_2/MBtu coal.
- Hydrogen balances were acceptable at ±18 percent (one outlier).
- Oxygen balances were acceptable at ±15 percent.
- Calcium balances were poor with over half the periods having greater than 30-percent error.
- Silica balances were poor with only 10 periods having an error of less than 25-percent.
- Energy balances were good at ±10-percent error (one outlier), for all testing periods except the low-temperature, high-sodium lignite testing. The energy balances were poor for the low-temperature, high-sodium lignite testing at +8 to +18 percent.

3.4.2 Introduction

The process flows into the Transport Gasifier process were:

- Coal flow through FD0200.
- Coal flow through FD0210.
- Limestone/sand flow through FD0220.
- Coke breeze flow through FD0220.
- Air flow measured by FI205 during air-blown mode and measured by FI201 during oxygen-blown mode.
- Oxygen flow measured by FI726.
- Pure nitrogen flow measured by FI609.
- Steam flow measured by the sum of FI204, FI727b, FI734, and FI733.

Sand was added through FD0220 to increase the Transport Gasifier standpipe level. Limestone was also fed to the Transport Gasifier through FD0220 during TC13.

The process flows from the Transport Gasifier process were:

- Syngas flow rate from the PCD measured by FI465.
- PCD solids flow through FD0520.
- Gasifier solids flow through FD0510.

3.4.3 Feed Rates

The coal flow through FD0210 can be determined by three different methods:

- FD0210/FD0200 surge bin weigh cells.
- Transport Gasifier carbon balance.
- Syngas combustor carbon balance.

The FD0210/FD0200 surge bin weigh cells use the time between filling cycles and the weigh differential between dumps to determine the coal rate. The Transport Gasifier carbon balance method uses the syngas carbon rate from the syngas flow rate and composition plus the PCD carbon rate from the PCD fines carbon concentration and PCD solids flow rate. The syngas combustor carbon balance method uses the syngas combustor flue gas CO_2 analyzer and the syngas combustor flue gas rate to determine the carbon in the syngas. The carbon in the PCD fines is added to the carbon in the syngas to determine the coal rate.

The Transport Gasifier carbon balance coal rates, syngas combustor carbon balance coal rates, and FD0210 weigh cells coal-feed rates for the operating periods are compared on Figure 3.4-1. The values for the FD0210 weigh cell were averaged for each operating period. There is no value for the TC13-17 (hour 268) syngas combustor coal rate since the syngas combustor CO_2 analyzer was out of service during that operating period. Since the weigh cell values closely agreed to the carbon balance and syngas combustor balance values, the weigh cell values will be used as the coal-feed rate for the TC13 operating periods. The coal rates used are listed in Table 3.4-1 for each operating period. The three rates tracked each other well throughout TC13, with the small exception of the operating periods hours 463, 471, and 483, when the weigh cell feed rate was slightly higher than that of the other two methods.

The PRB coal rate at the beginning of TC13 at just over 2,000 lb/hr and then it increased to over 3,000 lb/hr at hour 17. The coal rate ran for 3,000 pph to 3,900 pph until the transition to low-sodium Freedom lignite. After hour 143, the lignite feed rate was decreased to 2,800 pph, then increased 45 hours later to as high as 5,000 pph. The transition to high-sodium lignite began at hour 219. The coal feed during TC13-15 at hour 226 was a mixture of high- and low-sodium lignites, and the feed rate was around 3,600 pph. The high-sodium lignite was gasified for the remainder of the test run (TC13-16 to TC13-29). The coal-feed rates started at around 2,800 pph, but went as high as 4,000 pph during TC13-27 at hour 471.

The limestone flow through the sorbent feeder, FD0220, was determined from a correlation between TC13 feeder speed and dumps from the FD0220 storage bin between fills. The correlation for the sorbent feeder is:

$$\text{FD0220 rate} = 65.687(\text{RPM}) + 39.655 \quad (1)$$

The limestone feed rates are shown on Table 3.4-1 for each operating period. The rates were from 0 to 180 lb/hr. Sorbent was fed to the Transport Gasifier during about half of the TC13 operating periods.

The operating period air, steam, oxygen, and nitrogen flow rates are shown in Figure 3.4-2 and on Table 3.4-1. The nitrogen rate for TC13-1 was 6,400 lb/hr and remained between 6,000 pph and 7,000 pph for the first 12 operating periods. During the first oxygen-blown operating period at hour 199, the nitrogen rate decreased to about 5,000 lb/hr and remained there for the remainder of the oxygen-blown portion of TC13. When air-blown operations resumed, the nitrogen flow rate increased to between 5,400 and 6,300 pph for the remainder of the test run.

The feed rate of the oxygen stream to the gasifier was zero for the air-blown operating periods TC13-1 through TC13-12 as well as TC13-17 through TC13-29. For the oxygen-blown operating periods, the oxygen rate was 1,700 to 2,000 lb/hr.

The total steam rate to the Transport Gasifier is calculated by the sum of FI204 (total steam flow to the upper mixing zone), FI727b (steam mixed with the air/oxygen fed to the lower mixing zone), FI734 (steam fed into the lower mixing zone), and FI733 (steam fed to a shroud into the lower mixing zone). The steam feed rates for each operating period are shown in Figure 3.4-2 and listed on Table 3.4-1. The steam rate started the test run at around 800 pph and remained there for the first three operating periods of TC13. The rate was about 1,100 lb/hr steam for the test periods TC13-4 through TC13-11. During the oxygen-blown periods (from hour 199 though hour 249), the steam flow rate increased to between 2,600 and 4,000 pph. The remainder of the test run (the high-sodium lignite test periods) saw a range of steam flows from 1,000 pph to 2,000 pph. Generally, higher steam flow rates resulted in decreased lower heating values due to dilution of the syngas. Little steam gasification appears to have taken place.

The operating period air feed rates are shown on Figure 3.4-3 and are listed in Table 3.4-1. Air rates for air-blown testing were taken from FI205, while air rates for oxygen-blown testing were taken from FI201. This is because FI205 has a higher maximum range than FI201 and FI201 and would be more accurate at lower air rates of oxygen-blown operation than FI205. The air rate during the first air-blown period was around 8,300 pph, but ran from 9,500 to 12,000 pph for the next 10 air-blown periods. The air flow rate in TC13-12 was much higher at 14,000 pph, due to the higher coal-feed rate. During the oxygen-blown test runs (TC13-13 through TC13-16), a very small amount of air—between 700 and 2,500 pph—still entered the gasifier as a nozzle purge for the upper mixing zone nozzles. When air-blown operations resumed in TC13-17, the air flow rate fluctuated between 6,200 and 9,800 pph for the remainder of the test run. Periods of high air flow corresponded to those of higher coal flow.

3.4.4 Product Rates

The syngas rates for each operating period are shown on Figure 3.4-3 and listed on Table 3.4-1. The syngas rates were taken from FI465.

The syngas rate was checked for all the operating periods using an oxygen, carbon, and hydrogen balance around the syngas combustor and found to be in good agreement with the syngas combustor data for most of the operating periods (see Section 3.2 Figures 3.2-24, 25, and 26). The syngas rate was 16,000 pph for the first operating period in TC13. The syngas rate ran from 20,000 to 23,000 for the next few air-blown operating periods (TC13-2 through TC13-9). When the low-sodium lignite operating periods was fed to the gasifier, the syngas flow rate was only around 18,000 pph due to the lower coal-feed rates. The low-sodium lignite operating

period with a high coal-feed rate (TC13-12), had a syngas flow rate of around 26,000 pph. During the oxygen-blown periods, TC13-13 through TC13-16, the syngas rate decreased to between 13,000 and 18,000 pph. Air-blown operations resumed with TC13-17 using high-sodium lignite, and the syngas flow rate increased to 20,000 pph. The syngas flow rate declined until TC13-22a/b, when low coal and air flow rates generated a syngas flow of only 13,000 pph. For the remainder of the test run the syngas flow rates fluctuated between 17,000 to 19,000 pph.

The solids flow from the PCD can be determined by two different methods:

- In situ particulate sampling data upstream of the PCD.
- Spent Solids Feeder System (FD0530) weigh cell data.

The best measurements of the PCD solids flow are the in situ PCD inlet particulate determinations. Using the syngas flow rate and the in situ PCD inlet particulate measurement, the instantaneous solids flow to the PCD can be determined. The PCD fines rate is a function of the coal rate, coal ash content, carbon conversion, and the sorbent feed rate.

The FD0530 weigh cell data can be used to determine the PCD solids flow only if both the FD0530 feeder and the FD0510 feeder (standpipe solids) are off. Both FD0520 and FD0510 feed into FD0530 and FD0530 feeds into the atmospheric fluidized bed combustor. This method assumes that the solids level in the PCD and fines screw cooler FD0502 are constant. A good check on the PCD fines flow rate is the calcium and silica balances since calcium and silica are only present in the feed coal and the PCD fines. Sand, which is mostly silica, is not added during operating periods. The two PCD fines rates methods are compared on Figure 3.4-4 where the 10 in situ rates are plotted against rates determined by the FD0530 weigh cells at about the same time.

The results for all of the FD0530 weigh cell data are compared with the in situ data over time in Figure 3.4-5. The FD0530 weigh cell measurements had a significant scatter. Since the in situ PCD fines rate are more reliable than the FD0530 weigh cell PCD fines rate, the in situ PCD fines solids rates were used for further analyses. Also plotted on Figure 3.4-5 are the interpolated PCD solids rates used for the mass balance during operating periods.

The operating periods PCD fines rates ranged from 150 to 660 lb/hr. Unfortunately no in situ PCD inlet measurements were taken for the first 40 hours and the last 48 hours of TC13, so the first 40 hours of PCD fines rate were based on the in situ fines rate taken at hour 40, and the last 48 hours of PCD fines rates were based on the in situ PCD fines rate taken at hour 452. The PCD fines flow rates would vary with the coal-feed rate during these times, but further analyses will assume that the PCD fines rate was constant (at 166 lb/hr at the beginning of TC13 and at 442 lb/hr during the end of TC13). The 442 lb/hr at the end of TC13 is probably a reasonable assumption, since the coal-feed rate did not vary by a large amount during that time. But, the coal-feed rate changed dramatically between TC13-1 and TC13-2. Thus, the PCD fines rate for TC13-1 is probably suspect. After the initial 40 hours of testing, the PCD fines rate gradually increased to between 200 and 300 pph during air-blown operation. The solids flow rate was even higher in oxygen-blown mode, reaching a value as high as 660 pph during TC13-13, mostly likely because limestone was fed to the gasifier at that time. The PCD fines discharge rate then

decreased to 190 pph during the next air-blown operating period, increased to 300 pph for a brief period of time, then decreased to 150 pph during a period of very low coal-feed rate. When the coal-feed rate increased again, the fines rate increased, reaching 442 pph at the end of the test run. The PCD fines rates for each operating period used in the mass balances are shown in Table 3.4-2.

FD0510 was operated during several of the operating periods. Estimating the amount of solids removed during those operating periods was difficult due to the fluctuating nature of LI339. The amount of solids removed from the gasifier were determined by differences in the standpipe level using LI339 before and after FD0206 and FD0510 operation. The amount of gasifier solids removed during each operating period is shown in Table 3.4-1. The FD0510 rates were zero for many of the operating periods.

3.4.5 Overall Material Balance

Material balances are useful in checking the accuracy and consistency of data as well as determining periods of operation where the data is suitable for model development or commercial plant design. Total material balances for each operating period are given on Figure 3.4-6, which compares the total mass in and the total mass out. The overall material balance was good, with all of the relative differences at ±10 percent. The relative difference (relative error) is defined as the Transport Gasifier feeds in minus products out divided by the feeds ({In-Out}/In). Note that most of the air-blown operating periods had higher overall mass flow rates than the oxygen-blown operating periods due to additional nitrogen fed to the Transport Gasifier.

The details of the overall mass balance are given in Table 3.4-1 with the relative differences and the absolute differences. The absolute difference (absolute error) is defined as the difference between the feeds and the products (In-Out).

The main contributors to the material balance are the syngas rate (13,400 to 25,400 lb/hr), air rate (700 to 14,000 lb/hr), oxygen rate (0 to 2,000 lb/hr), steam rate (800 to 4,000 lb/hr), nitrogen rate (5,000 to 6,800 lb/hr), and coal rate (1,900 to 5,100 lb/hr).

The oxygen-to-coal ratios are also listed on Table 3.4-1. The oxygen-to-coal ratio varied from 0.53 to 0.94 for air-blown operation and from 0.56 to 0.65 for oxygen-blown operation.

3.4.6 Carbon Balances and Carbon Conversion

The carbon balances are shown in Figure 3.4-7 and in Table 3.4-2. All but three of the carbon balances were between ±15-percent error. All of the oxygen-blown carbon balances had carbon balance errors between ±9 percent (two of the four within ±1 percent). The carbon balance is determined by the coal carbon rates and the syngas carbon rates.

Carbon conversion is defined as the percent of fuel carbon that is gasified to CO, CO_2, CH_4, C_2H_6, and higher hydrocarbons versus the amount of carbon that is rejected by the gasifier with the PCD and gasifier solids. In a typical IGCC flow sheet, the rejected carbon from the gasifier or PCD is burned in a less efficient combustor or sent for disposal.

The carbon conversion can be calculated at least three different ways due to inconsistencies in the carbon balance. Since the carbon balance is off by up to 19 percent (TC13-27), each result could be different. Three calculation methods used to determine carbon conversion were:

1. Gas Analyses – this method is based on the feed carbon (coal plus coke breeze) and the carbon in the syngas. This assumes that the feed carbon and the syngas carbon are correct.
2. Solids Analyses - this method is based on the feed carbon and the syngas carbon determined by a Transport Gasifier carbon balance, not the gas analyses. This assumes that the syngas carbon is incorrect.
3. Products Analyses - this method is based on the feed carbon determined by Transport Gasifier carbon balance and the syngas carbon. This assumes that the coal feed is in error.

The carbon conversions using all three methods are plotted on Figure 3.4-8. The products analysis method carbon conversions for each operating period are given in Table 3.4-2. The carbon conversions by the solids and products method are approximately the same for TC13. The carbon conversion by the gas method is typically greater than the carbon conversion by the products method when the carbon balance error is less than zero and is greater than the products method when the carbon balance error is greater than zero. The products method is the most reasonable since it is not based on the coal rate, but on the syngas and PCD solids rates.

The products method carbon conversion ranged from 96 to 99 percent during air-blown PRB testing. During the air-blown testing with low-sodium lignite, the carbon conversion was between 93 and 97 percent. The oxygen-blown testing with low-sodium lignite had carbon conversions of 87 and 94 percent. The test period with a mixture of high- and low-sodium lignites had a carbon conversion of 97 percent. The carbon conversions for the high-sodium lignite ranged from as low as 77 percent at low temperatures to as high as 98 percent at high temperatures. Note that the carbon conversions decreased after the gasifier temperature was decreased at hour 337.

The carbon conversion should increase as the gasifier temperature increases. The TC13 products method carbon conversions are plotted against riser exit temperature, TI360, in Figure 3.4-9. The air-blown data show a distinct increase in carbon conversion with temperature. The most significant trend was for the high-sodium lignite, since it operated at a wide range of temperatures. The data for the other fuels follows a similar trend, but the carbon conversion appears to be slightly lower for the other fuels at the same temperatures. In previous test runs (TC06 through TC12), the range of temperatures was often too small to notice the effects of temperature on carbon conversion.

The average carbon conversions of Powder River Basin, Hiawatha bituminous, Falkirk lignite coal, and Freedom lignite are compared on Figure 3.4-10 for both air and oxygen operation. The low- and high-sodium Freedom lignite are considered together since the Freedom lignite sodium concentration did not effect the carbon conversion. The low temperature Freedom lignite carbon conversion data is plotted separately from the high temperature Freedom lignite

carbon conversion data. Air-blown mode gives a slightly higher carbon conversion than oxygen-blown mode. The Falkirk lignite had the highest average carbon conversion of the four coals tested. PRB and the Freedom lignite had about the same average carbon conversion, while Hiawatha bituminous had the lowest average carbon conversion when the gasifier was operated at typical temperatures. The high-sodium lignite operated at low temperatures had the lowest average carbon conversion.

Table 3.4-3 lists the carbon conversions for each previous test campaign and the method to determine the coal rate. The small carbon conversion standard deviations within each test campaign demonstrate that unless the temperature is changed significantly, the carbon conversions are constant. As in the Figure 3.4-10, oxygen-blown carbon conversions are slightly less than air-blown carbon conversions for each fuel. The general trend in coal rate method is to use the weigh cell data. Carbon balances also are getting better with more recent test campaigns.

3.4.7 Nitrogen Balance

The nitrogen balances for the TC13 operating periods are plotted on Figure 3.4-11 and compare the nitrogen in and the nitrogen out and are listed in Table 3.4-4. Detailed nitrogen flows for a typical air-blown test (TC13-12) are shown in Table 3.4-5 and for a typical oxygen-blown test (TC13-16) are shown on Table 3.4-6. The air-blown mode nitrogen balances were good with errors less than 10 percent for all operating periods. For all but one of the air-blown operating periods the sum of the nitrogen fed was greater than the sum of the nitrogen exiting. For the oxygen-blown operating periods, the sum of the product nitrogen was always higher than that of the nitrogen fed. The nitrogen balances were very good for oxygen-blown mode, with around 3 to 6-percent error. Note that air-blown mode nitrogen rates were much higher than the oxygen-blown nitrogen rates.

The nitrogen flows as shown in Tables 3.4-5 and 3.4-6 are dominated by the air, nitrogen, and syngas flows. Previous gasification tests TC06 to TC10 and TC11 assumed that from 500 to 1,250 lb/hr nitrogen were lost due to seals and lock hoppers. In TC13 as in TC11, the nitrogen balances were good, and such a correction was unnecessary. A possible reason for not needing the correction was that system improvements have been made to eliminate nitrogen leaks. None of the solid streams contribute significantly to the nitrogen balance. The nitrogen balances in previous test campaigns had errors that were approximately 10 percent, which is consistent with the errors from TC13.

Using the ammonia analyzer data, the coal rates, and the coal nitrogen concentration, the amount of fuel nitrogen converted to NH_3 can be calculated. The amount of fuel nitrogen converted to NH_3 is shown on Figure 3.4-12. The amount of fuel nitrogen converted to ammonia varied from 28 to 72 percent, during air-blown PRB operations, from 37 to 61 percent during air-blown, low-sodium lignite operations, and from 51 to 90 percent in air-blown, high-sodium lignite operations. In the oxygen-blown operating periods using low-sodium lignite, the conversions were 83 and 94 percent. The single high-sodium lignite period in oxygen-blown mode had a conversion of 67 percent. The mixture of high- and low-sodium lignite had an erroneous conversion of 103 percent, according to the calculation. The reason for the error was most likely due to the fact that no exact nitrogen analysis was available for the mixture. The values for nitrogen conversion to ammonia were higher in TC13 than they were in previous test

runs. The data indicates that both oxygen-blown mode and lower temperature mode increase the coal nitrogen to ammonia.

The trends of several process parameters against percent fuel nitrogen conversion to ammonia were briefly investigated. The PCD inlet and Transport Gasifier temperatures did not seem to affect the ammonia conversion. The only parameters found that appear to influence ammonia conversion were the coal-feed rate and the overall percent O_2. The trend of the fuel nitrogen conversion with overall percent O_2 is shown in Figure 3.4-13. Although the high-sodium lignite data are scattered, the overall trend of the data indicate an increase in conversion with increasing overall percent oxygen. The trend with percent oxygen implies that the fuel nitrogen conversion to ammonia is a function of the amount of syngas dilution similar to the LHV. The low-temperature, high-sodium lignite coal ammonia conversions are noted on Figure 3.4-13, which indicate that low temperature gasifier operation results in higher ammonia conversions.

3.4.8 Sulfur Balance and Sulfur Removal

Sulfur balances for all the TC13 operating periods are given in Figure 3.4-14 and Table 3.4-7. The syngas sulfur compounds were not directly measured, but estimated from syngas combustor SO_2 analyzer data and flue gas flow. The coal sulfur and PCD fines sulfur values were interpolated between the solids sampling times. The TC13 sulfur balances were poor with a significant number of sulfur balances with relative errors of greater than ±25 percent. The sulfur balances for TC13-10a through TC13-15 (the six periods with the high-sulfur, low-sodium lignite and the period of mixed lignite feed were better (at less than 20-percent error) than those of the other balances due to the higher sulfur content of the coal. Part of the reason for the errors is the low-sulfur content of the coal; small mass imbalances create large percentage errors. High coal sulfur content improves the accuracy of the coal and syngas analyses.

With the errors in the sulfur balances, it is difficult to determine the correct sulfur removal. Similar to the coal conversions calculations, there are three different methods to determine Transport Gasifier sulfur removals:

1. Gas Analyses – this method is based on the syngas sulfur emissions (using the syngas combustor flue gas rate and syngas combustor flue gas SO_2 measurement) and the feed sulfur rate (using the feed coal rate and coal sulfur content).
2. Solids Analyses - this method is based on the PCD solids analysis (using PCD solids flow rate and PCD solids sulfur content) and the feed sulfur rate.
3. Product Analyses - this method is based on the gas analysis data and the PCD solids data.

The results from the three sulfur removal methods are plotted on Figure 3.4-15 and given on Table 3.4-7. There is no gas or products sulfur removal data for TC13-17 (hour 268) since the syngas combustor SO_2 analyzer was out of service. The sulfur in the fuel is an inaccurate measurement due to the multiplication of a very small number (coal sulfur) by a large number (coal-feed rate). The gaseous sulfur flow should be accurate, although it is also the product of a small number (syngas combustor SO_2) and a large number (syngas combustor flue gas rate). The syngas H_2S was measured by the H_2S analyzer AI419J and there seemed to be good agreement with the TRS by the syngas combustor AI476P from the beginning of the test run until hour

300, when it began to read about 200 to 300 ppm lower. The PCD fines sulfur rates have inaccuracies due to the low sulfur in the PCD solids. Apparently no sulfur-containing solids accumulated in the gasifier during TC13 since the standpipe and FD0510 gasifier samples contained negligible amounts of sulfur.

The TC13 results indicate that the gas method is less accurate than the product and the solids methods. The solids and products method methods usually agreed with each other and seemed to change slowly and consistently during the run. The gas method varied a lot during the run and five periods (TC13-10a, -18, -20, -21, -29) had negative sulfur removals. The products method is probably the most reliable sulfur removal.

The sulfur removal started TC13 at 3 percent and ran from 3 to 11 percent during the air-blown PRB portion of the run, from 23 to 26 percent during the air-blown, low-sodium (high-sulfur) lignite portion of the run, at 16 and 26 percent during the two oxygen-blown, low-sodium test period, at 12 percent during the mixed lignite run, and from 11 to 25 percent during the high-sodium lignite portion of the test run.

The syngas combustor SO_2 data was used to determine the sulfur emissions shown in Table 3.4-7. The sulfur emissions were from 0.38 to 3.01 lb SO_2/MBtu coal.

Figure 3.4-16 plots the measured sulfur emissions against the sulfur out of the reactor (sulfur emissions plus the PCD fines sulfur) expressed in terms of ppm of syngas. On Figure 3.4-16, the 45-degree line is the 0 percent sulfur removal line (PCD fines sulfur equals zero) and the X-axis is the 100 percent sulfur removal line (zero sulfur emissions). This plot is another way of displaying the products method sulfur removal calculation results since it is based on the PCD fines sulfur and the syngas sulfur. The average sulfur capture was 9 percent for Powder River Basin, 24 percent for low-sodium (high-sulfur) lignite and 16 percent for high-sodium (low-sulfur) lignite. The averages are plotted as lines on Figure 3.4-16, except for the Powder River Basin coal. The higher sulfur content resulted in higher sulfur capture. Sorbent addition did not appear to affect sulfur capture.

3.4.9 Hydrogen Balance

Operating period hydrogen balances are given in Figure 3.4-17 and Table 3.4-4. Typical hydrogen flows for an air-blown test (TC13-12) are shown in Table 3.4-5 and typical hydrogen flows for an oxygen-blown test (TC13-16) are shown in Table 3.4-6. The hydrogen balance is fair with all but five operating periods within ±15 percent of perfect agreement. The coal, steam, and syngas streams are the largest contributors to the hydrogen balance. The TC13 hydrogen balances show better agreement than previous test campaigns.

The steam rate for each operating period was calculated using a hydrogen balance, which is essentially the difference in hydrogen between the coal feed and syngas rate. The hydrogen balance steam rate is compared with the measured steam rate in Figure 3.4-18. About two-thirds of the measured steam rates are within 20 percent of the hydrogen balance steam rates.

3.4.10 Oxygen Balance

The operating period oxygen balances are given in Figure 3.4-19 and Table 3.4-4. Typical oxygen flows for an air-blown mode test (TC13-12) are shown in Table 3.4-5 and typical oxygen flows for an oxygen-blown mode test (TC13-16) are shown in Table 3.4-6. The oxygen balance determines if the steam and oxygen/air rates are consistent with the syngas rate and composition.

The TC13 operating periods oxygen balances for air-blown mode were acceptable with all but five operating periods with less than ±10-percent relative error (TC13-1, TC13-20, TC13-21, TC13-22a, and TC13-22b). All oxygen-blown operating period's oxygen balances had less than ±10-percent relative error. Acceptable oxygen balances indicate that the measured steam rates are consistent with the other oxygen flows (air, oxygen, steam, and syngas).

3.4.11 Calcium Balance

The operating period calcium balances are given in Figure 3.4-20 and Table 3.4-4. Typical calcium flows for an air-blown mode test (TC13-12) are shown in Table 3.4-5 and typical calcium flows for an oxygen-blown mode test (TC13-16) are shown on Table 3.4-6. The calcium balances are essentially a comparison between the coal and limestone calcium and the PCD fines calcium, since there was minimal flow through FD0510, and the gasifier accumulation term was assumed to be small.

The TC13 calcium balances were poor as over half of the operating periods had errors greater than 30 percent. The poor agreement is typical for the calcium balance because the comparison is between two solid streams that are difficult to measure. The periods with limestone feed (TC13-10a through TC13-21) were only marginally better than the other balances, even though the increased amount of calcium in the system should have improved measurement accuracy.

3.4.12 Silica Balance

Operating period silica balances are given in Figure 3.4-21 and Table 3.4-4. Typical silica flows for an air-blown mode test (TC13-12) are shown in Table 3.4-5 and typical silica flows for an oxygen-blown test (TC13-16) are shown on Table 3.4-6. The silica balances are essentially a comparison between the coal silica and the PCD fines silica, since those two streams are the only significant streams which contain silica. The gasifier typically starts up with sand that is mostly silica. The silica content of the gasifier solids decreases as the run progresses unless more sand is added (see Figure 3.3-5). Sand is only added when the unit is not operating.

The TC13 silica balances were poor as only 10 of the 32 balances had errors less than 25 percent. Silica balances are typically in error because the comparison is between two solid streams that are difficult to measure. Since the silica content of the gasifier solids changes drastically during operating, the poor silica balances could be due to inventory changes during the operating periods, which are not accounted for in the material balances. The TC13 silica balances were typical of previous silica balances.

3.4.13 Energy Balance

The TC13 Transport Gasifier energy balance is given in Figure 3.4-22 with standard conditions chosen to be 1.0 atmosphere pressure and 80°F temperature. Table 3.4-8 breaks down the individual components of the energy balance for each operating period. The "energy in" consists of the coal, air, and steam fed to the Transport Gasifier. The nitrogen, oxygen and sorbent fed to the gasifier were considered to be at standard conditions (80°F) and hence have zero enthalpy. The nitrogen and oxygen feeds actually enter the gasifier at a higher temperature than standard conditions, but compared to the other feed enthalpies, this neglected input energy is insignificant. The "energy out" consisted of the syngas and PCD solids. The lower heating value of the coal and PCD solids were used in order to be consistent with the lower heating value of the syngas. The energy of the syngas was determined at the Transport Gasifier cyclone exit. The nitrogen by FI607 fed to the PCD inlet and outlet particulate sampling trains was subtracted from the syngas rate to determine the actual syngas rate from the cyclone. The sensible enthalpy of the syngas was determined by the overall gas heat capacity from the syngas compositions and using gas heat capacities information. The syngas and PCD solids energy consists of both latent and sensible heat. The heat loss from the Transport Gasifier was estimated to be 3.5 MBtu/hr.

With the exception of seven periods, the TC13 energy balances were within 0 to 10-percent error. All but one of the six periods with greater than 10-percent energy balance error were during the low-temperature, high-sodium operating periods at the end of TC13. A gasifier heat loss of 5.45 MBtu/hr minimizes the TC13 operating period energy balance errors.

3.4.14 Gasification Efficiencies

Gasification efficiency is defined as the percent of the energy in (coal energy and steam energy) that is converted to potentially useful syngas energy. Two types of gasification efficiencies have been defined, which are the cold gas efficiency and the hot gas efficiency. The cold gas efficiency is the amount of energy fed that is available to a gas turbine as syngas latent heat. The hot gasification efficiency is the amount of feed energy that is available to a gas turbine plus a heat recovery steam generator.

The cold gas efficiency can be calculated at least three different ways, similar to sulfur removal and carbon conversion. Since the energy balance is off by up to 18.4 percent, each result could be different. Three calculation methods were performed for cold gasification efficiency consistent with the three methods of sulfur removal:

1. Gas Analyses– this method is based on the feed heat (coal latent heat plus steam heat) and the latent heat of the syngas. This assumes that the feed heat and the syngas latent heat are correct.
2. Solids Analyses - this method is based on the feed heat (coal latent heat plus steam heat) and the latent heat of the syngas determined by a Transport Gasifier energy balance, not the gas analyses. This assumes that the syngas latent heat is incorrect.
3. Products Analyses– this method is based on the feed heat determined by Transport Gasifier energy balance and the syngas sensible heat. This assumes that the coal feed or the steam rate is in error.

The cold gas gasification efficiencies for the three calculation methods are plotted in Figure 3.4-23. The results from the products method are listed in Table 3.4-8 since this method is usually considered the most accurate.

The products analyses cold gas gasification efficiency increased to as high as 55 percent during the PRB portion of the test run. During the air-blown, low-sodium lignite portion of the run, the cold gas efficiencies ranged from 44 to 54 percent. The oxygen-blown, low-sodium lignite testing had a cold gas efficiency of around 53 to 55 percent, while the operating period that used a mixture of lignite fuels had an efficiency of 58 percent. The only oxygen-blown, high-sodium lignite period had a cold gas efficiency of 52 percent. The remainder of the high-sodium lignite test periods had a wide range of cold gas efficiencies, from 28 to 48 percent.

Figure 3.4-24 shows the trend in cold gas efficiency with steam-to-coal ratio. As the steam-to-coal ratio increases, the cold gas efficiency decreases. The effect is more pronounced in air-blown mode than in oxygen-blown mode due to the higher number of data points. The oxygen-blown operating periods had higher cold gas efficiency than the air-blown modes at the same steam-to-coal ratio because the air-blown modes had to heat the air nitrogen, decreasing the cold gas efficiency. The steam rate effect on cold gas efficiency is not due to steam dilution but due to the increased loss in efficiency of heating steam to the Transport Gasifier temperature.

The hot gasification efficiency is the amount of feed energy that is available to a gas turbine plus a heat recovery steam generator. The hot gas efficiency counts both the latent and sensible heat of the syngas. Similar to the cold gasification efficiency and the sulfur removal, the hot gas efficiency can be calculated at least three different ways. The three calculation methods for hot gasification are identical to the three methods of cold gasification efficiency calculation except for the inclusion of the syngas sensible heat into the hot gasification efficiency.

The hot gasification efficiency assumes that the sensible heat of the syngas can be recovered in a heat recovery steam generator, so the hot gasification efficiency is always higher than the cold gasification efficiency. The three hot gasification calculation methods are plotted in Figure 3.4-25 and the products analysis hot gasification efficiencies are shown in Table 3.4-8.

As with the cold gasification efficiencies, the products method hot gasification efficiencies started TC13 low, at 79 percent due to a low coal-feed rate and generally increased with increasing coal rate. The air-blown hot gas efficiencies were between 79 and 86 percent for PRB, between 79 and 84 percent for low-sodium lignite, and between 59 and 83 percent for high-sodium lignite. The two oxygen-blown periods that used low-sodium lignite in TC13 had efficiencies of 78 and 82 percent. The single oxygen-blown period with high-sodium lignite had a hot gas efficiency of 82 percent. The period using a mixture of high- and low-sodium lignite had a hot gas efficiency of 85 percent.

Figure 3.4-26 plots the hot gas efficiency against the steam-to-coal ratio. The air-blown trend of decreasing gasification efficiency with increasing steam-to-coal ratio is clear. The oxygen-blown hot gasification efficiencies do not seem to be a function of steam-to-coal ratio, perhaps because of the low number of oxygen-blown data points in TC13. The oxygen-blown hot gas

efficiencies are similar to the air-blown hot gas efficiencies, even though they have much higher steam-to-coal ratios.

The two main sources in efficiency losses are the gasifier heat loss and the latent heat of the PCD solids. The gasifier heat loss of 3.5 MBtu/hr was about 13 percent of the feed energy, while the total energy of the PCD solids was about 3 percent of the feed energy. The heat loss percentage will decrease as the gasifier size is increased. While the Transport Gasifier does not recover the latent heat of the PCD solids, this latent heat could be recovered in a combustor. The total enthalpy of the PCD solids can be decreased by decreasing both the PCD solids carbon content (heating value) and the PCD solids rate.

Gasification efficiencies can be calculated from the commercially projected gas heating values and corrected flow rates that were determined in Section 3.2. The products projected cold gasification efficiencies are plotted on Figure 3.4-27 against the projected steam-to-coal ratio and are listed on Table 3.4-7 for all of the operating periods. Only the cold gasification efficiencies based on the products are given in Figure 3.4-27 and Table 3.4-7 because they are the most representative of the actual gasification efficiencies. Since the nitrogen and adiabatic syngas LHV corrections reduce the coal rate and the steam rate (for oxygen blown only), the projected coal rates, the projected steam rates were used in Figure 3.4-27. The projected efficiencies are calculated assuming an adiabatic gasifier, since zero heat loss was one of the assumptions in determining the projected LHV in Section 3.2. The projected cold gas efficiencies were from 70 to 74 percent for PRB in air-blown mode, from 65 to 66 percent for low-sodium lignite in air-blown mode, from 50 to 71 percent for high-sodium lignite in air-blown mode, from 67 to 74 percent for low-sodium lignite in oxygen-blown mode, 77 percent for high-sodium lignite in oxygen-blown mode, and over 77 percent for the high- and low-sodium lignite mixture. The trend shows a very slight decrease in efficiency as the steam-to-coal ratio increases. The projected cold gasification efficiencies increase due to the use of recycle gas rather than nitrogen for aeration and instrument purges by about:

- 20 percent for PRB in air-blown mode.
- 19 percent for low-sodium lignite in air-blown mode.
- 16 percent for low-sodium lignite in oxygen-blown mode.
- 19 percent for the high- and low-sodium lignite mixture in oxygen-blown mode.
- 25 percent for high-sodium lignite in oxygen-blown mode.
- 19 percent for high-sodium lignite in air-blown mode.

The commercial projection hot gasification efficiency does not increase when compared to the raw hot gasification efficiency because the deleted nitrogen lowers the syngas sensible heat and increases the syngas latent heat. Both changes effectively cancel each other.

Table 3.4-1

Feed Rates, Product Rates, and Mass Balances

		Feeds (In)							Products (Out)						
Operating Period	Average Relative Hours	Coal[1] lb/hr	Sorbent FD0220 lb/hr	Air[5] lb/hr	Oxygen FI726 lb/hr	Nitrogen[2] lb/hr	Steam lb/hr	Total lb/hr	Syngas lb/hr	PCD Solids FD0520 lb/hr	SP Solids FD0510 lb/hr	Total lb/hr	In - Out lb/hr	(In- Out)/In %	Oxygen to Coal Ratio lb/lb
TC13-1	7	2,050	0	8,345	0	6,395	838	17,628	15,798	166	0	15,964	1,664	9.4	0.94
TC13-2	18	3,016	0	10,717	0	6,667	809	21,209	20,065	166	0	20,231	978	4.6	0.82
TC13-3	29	3,032	0	10,881	0	6,846	881	21,640	20,249	166	0	20,415	1,224	5.7	0.83
TC13-4	41	3,083	0	10,850	0	6,674	1,050	21,657	20,539	168	0	20,708	949	4.4	0.82
TC13-5	53	3,115	0	10,688	0	6,799	1,079	21,682	20,318	189	0	20,506	1,176	5.4	0.80
TC13-6	61	3,005	0	10,690	0	6,640	1,081	21,417	20,196	203	0	20,398	1,019	4.8	0.82
TC13-7	73	3,274	0	10,820	0	6,563	1,080	21,736	20,504	223	0	20,727	1,009	4.6	0.77
TC13-8	95	3,338	0	11,893	0	6,520	1,085	22,836	22,340	263	5	22,608	228	1.0	0.83
TC13-9	104	3,868	0	12,046	0	6,570	1,109	23,593	22,607	278	0	22,885	708	3.0	0.72
TC13-10a	143	2,857	99	9,507	0	6,250	1,071	19,784	17,947	221	37	18,205	1,579	8.0	0.77
TC13-10b	151	2,942	95	9,628	0	6,248	1,089	20,003	18,169	220	34	18,423	1,580	7.9	0.76
TC13-11	165	2,983	0	9,575	0	6,097	1,021	19,677	17,648	257	8	17,913	1,764	9.0	0.74
TC13-12	178	5,070	110	14,042	0	6,126	1,281	26,629	25,427	374	37	25,838	791	3.0	0.64
TC13-13	199	4,524	111	2,594	1,916	5,191	3,265	17,600	17,594	662	0	18,256	-656	-3.7	0.56
TC13-14	215	4,135	111	1,749	1,968	5,107	3,968	17,037	15,969	508	0	16,477	560	3.3	0.57
TC13-15	226	3,596	132	2,105	1,808	5,125	2,765	15,531	15,786	301	6	16,094	-563	-3.6	0.64
TC13-16	249	2,852	70	714	1,702	5,019	2,640	12,997	13,398	233	27	13,658	-661	-5.1	0.65
TC13-17	268	2,912	180	9,846	0	6,206	1,078	20,222	19,872	194	50	20,117	105	0.5	0.78
TC13-18a	281	2,876	81	9,287	0	6,172	1,249	19,665	18,718	303	40	19,061	605	3.1	0.75
TC13-18b	289	2,893	97	9,146	0	6,338	1,246	19,721	18,015	303	4	18,322	1,399	7.1	0.73
TC13-19	300	2,892	95	9,341	0	6,057	1,274	19,659	18,103	252	0	18,355	1,305	6.6	0.75
TC13-20	318	1,901	96	7,194	0	5,597	1,167	15,955	14,321	150	22	14,493	1,463	9.2	0.88
TC13-21	337	1,895	124	7,367	0	5,442	1,158	15,986	14,330	150	20	14,501	1,485	9.3	0.90
TC13-22a	380	1,967	0	6,286	0	6,074	975	15,301	13,486	296	1	13,783	1,518	9.9	0.74
TC13-22b	391	2,008	0	6,209	0	6,054	1,000	15,271	13,419	402	2	13,823	1,448	9.5	0.72
TC13-23	413	2,956	0	7,764	0	6,285	1,734	18,740	17,062	489	23	17,574	1,166	6.2	0.61
TC13-24	442	3,269	0	8,386	0	5,607	1,925	19,186	18,653	442	26	19,120	66	0.3	0.59
TC13-25	456	3,496	0	8,466	0	5,422	1,895	19,279	17,578	442	64	18,083	1,196	6.2	0.56
TC13-26	463	3,934	0	8,998	0	5,669	1,883	20,485	18,723	442	62	19,227	1,258	6.1	0.53
TC13-27	471	3,980	0	9,121	0	5,778	2,070	20,949	19,256	442	51	19,749	1,200	5.7	0.53
TC13-28	483	3,822	0	8,827	0	5,589	2,008	20,246	18,515	442	34	18,990	1,256	6.2	0.54
TC13-29	503	3,739	0	8,799	0	5,785	1,371	19,694	18,074	442	22	18,538	1,156	5.9	0.55

Notes:

1. Coal Rate by FD0200 and FD0210 Weigh Cells
2. Nitrogen is measured by FI609
3. TC13-1 to TC13-12 and TC13-17 to TC13-29 were air blown; TC13-13 to TC13-16 were oxygen blown.
4. TC13-1 to TC13-9 were Powder River Basin, TC13-10a to TC13-14 were low sodium Freedom Mine Lignite, TC13-15 was a mixture of high and low sodium lignite, and TC13-16 to TC13-29 was high sodium Freedom Mine Lignite.
5. Air rate by FI205 for air blown testing and by FI201 for oxygen blown testing.

Table 3.4-2 Carbon Balances

Operating Period	Average Relative Hours	Carbon In (Feed)			Carbon Out (Products)				In - Out	(In- Out)/In	Carbon Conversion[1]
		Coal lb/hr	Coke B. lb/hr	Total lb/hr	Syngas lb/hr	Standpipe lb/hr	PCD Solids lb/hr	Total lb/hr	lb/hr	%	%
TC13-1	7	1,117	0	1,117	1,048	0.0	43	1,091	26	2	96.1
TC13-2	18	1,656	0	1,656	1,605	0.0	15	1,619	37	2	99.1
TC13-3	29	1,691	0	1,691	1,555	0.0	23	1,578	113	7	98.6
TC13-4	41	1,746	0	1,746	1,604	0.0	28	1,633	113	6	98.3
TC13-5	53	1,735	0	1,735	1,570	0.0	47	1,617	118	7	97.1
TC13-6	61	1,653	0	1,653	1,537	0.0	47	1,584	70	4	97.1
TC13-7	73	1,782	0	1,782	1,609	0.0	70	1,680	103	6	95.9
TC13-8	95	1,795	0	1,795	1,797	0.0	80	1,877	-82	-5	95.8
TC13-9	104	2,085	0	2,085	1,882	0.0	86	1,968	117	6	95.7
TC13-10a	143	1,345	9	1,354	1,192	0.0	41	1,233	121	9	96.7
TC13-10b	151	1,386	8	1,395	1,222	0.0	36	1,258	137	10	97.2
TC13-11	165	1,416	0	1,416	1,248	0.0	77	1,325	91	6	94.3
TC13-12	178	2,423	10	2,432	2,218	0.0	178	2,395	37	2	92.7
TC13-13	199	2,138	10	2,148	1,844	0.0	275	2,119	29	1	87.2
TC13-14	215	1,905	10	1,915	1,645	0.0	103	1,748	167	9	94.2
TC13-15	226	1,707	12	1,718	1,654	0.0	50	1,704	14	1	97.1
TC13-16	249	1,309	6	1,316	1,223	0.0	30	1,254	62	5	97.6
TC13-17	268	1,380	16	1,396	1,403	0.1	29	1,432	-36	-3	98.0
TC13-18a	281	1,366	7	1,373	1,318	0.0	139	1,458	-85	-6	90.6
TC13-18b	289	1,376	9	1,385	1,279	0.0	148	1,427	-42	-3	89.8
TC13-19	300	1,385	8	1,394	1,310	0.0	16	1,326	67	5	98.8
TC13-20	318	927	9	935	865	0.0	36	900	35	4	96.1
TC13-21	337	932	11	943	892	0.0	29	921	22	2	96.9
TC13-22a	380	987	0	987	703	0.0	141	844	142	14	83.5
TC13-22b	391	1,018	0	1,018	692	0.0	208	900	118	12	77.2
TC13-23	413	1,466	0	1,466	1,033	0.0	317	1,350	116	8	76.8
TC13-24	442	1,583	0	1,583	1,165	0.0	277	1,442	141	9	81.0
TC13-25	456	1,708	0	1,708	1,168	0.1	287	1,455	253	15	80.5
TC13-26	463	1,936	0	1,936	1,298	0.1	293	1,591	345	18	81.9
TC13-27	471	1,949	0	1,949	1,293	0.1	292	1,586	363	19	81.8
TC13-28	483	1,850	0	1,850	1,258	0.0	291	1,550	300	16	81.5
TC13-29	503	1,780	0	1,780	1,270	0.0	296	1,566	214	12	81.3

Notes:

1. Carbon Conversion based on products method.

3. TC13-1 to TC13-12 and TC13-17 to TC13-29 were air blown; TC13-13 to TC13-16 were oxygen blown.

4. TC13-1 to TC13-9 were Powder River Basin, TC13-10a to TC13-14 were low sodium Freedom Mine Lignite, TC13-15 was a mixture of high and low sodium lignite, and TC13-16 to TC13-29 was high sodium Freedom Mine Lignite.

Table 3.4-3

Test Campaign Carbon Balances and Coal Rate Methods

Test Campaign	Fuel	Mode	Carbon Conversion %	Standard Deviation %	Coal Rate Method	Carbon Balance
TC06	Powder River Basin	Air	95.7	1.4	Gasifier Carbon Balance	None
TC07	Powder River Basin	Air	94.6	2.1	Gasifier Carbon Balance	None
TC08	Powder River Basin	Air	95.6	1.3	Gasifier Carbon Balance	None
TC08	Powder River Basin	Oxygen	93.3	1.9	Gasifier Carbon Balance	None
TC09	Hiawatha Bituminous	Air	90.4	2.0	SGC Carbon Balance	-15% to 0%
TC09	Hiawatha Bituminous	Oxygen	87.3	1.6	SGC Carbon Balance	-21% to -8%
TC10	Powder River Basin	Air	94.8	1.9	Gasifier Carbon Balance	None
TC10	Powder River Basin	Oxygen	94.7	1.8	Gasifier Carbon Balance	None
TC11	Falkirk Lignite	Air	97.0	0.9	SGC Carbon Balance	-14% to +14%
TC11	Falkirk Lignite	Oxygen	96.3	1.7	SGC Carbon Balance	-8% to +4%
TC12	Powder River Basin	Air	96.9	0.9	Weight Cells	-6% to +6%
TC12	Powder River Basin	Oxygen	94.6	1.4	Weight Cells	-11% to +8%
TC13	Powder River Basin	Air	97.1	1.3	Weight Cells	-5% to +7%
TC13	Freedom Lignite, High Temperature	Air	95.1	3.1	Weight Cells	-6% to 10%
TC13	Freedom Lignite, Low Temperature	Air	80.6	2.2	Weight Cells	+9% to 19%
TC13	Freedom Lignite	Oxygen	94.0	4.8	Weight Cells	1% to 9%

Table 3.4-4

Nitrogen, Hydrogen, Oxygen, Calcium, and Silica Mass Balances

Operating Period	Average Relative Hours	Nitrogen		Hydrogen		Oxygen		Calcium		Silica	
		(In- Out) In %	In - Out lb/hr	(In- Out) In %	In - Out lb/hr	(In- Out) In %	In - Out lb/hr	(In- Out) In %	In - Out lb/hr	(In- Out) In %	In - Out lb/hr
TC13-1	7	9.0	1,145	22.2	47	11.4	382	0.1	0	-93.5	-36
TC13-2	18	5.5	812	2.9	8	0.6	25	43.1	13	-58.0	-33
TC13-3	29	6.9	1,043	-1.5	-4	-0.2	-10	34.3	10	-41.2	-23
TC13-4	41	5.9	883	-3.2	-10	-2.2	-98	33.5	10	-28.7	-17
TC13-5	53	6.3	949	0.9	3	0.3	15	32.9	10	-22.0	-13
TC13-6	61	5.7	843	0.8	2	0.3	12	22.6	7	-35.6	-20
TC13-7	73	5.4	796	0.1	0	-0.5	-21	32.9	10	-20.7	-13
TC13-8	95	2.8	430	-9.2	-29	-4.6	-223	24.9	8	-45.1	-28
TC13-9	104	3.4	540	-2.8	-10	-2.0	-100	32.1	12	-18.4	-13
TC13-10a	143	7.9	1,065	0.9	3	4.3	182	54.1	38	-53.7	-31
TC13-10b	151	7.8	1,060	1.2	4	3.9	166	45.7	32	-43.2	-25
TC13-11	165	8.3	1,120	8.7	25	7.9	332	6.4	3	1.3	1
TC13-12	178	4.1	693	-11.4	-50	-5.2	-325	53.8	56	40.2	39
TC13-13	199	-3.5	-249	-14.1	-88	-7.8	-553	12.3	12	2.3	2
TC13-14	215	-3.9	-251	6.0	41	5.7	423	-3.7	-3	-26.4	-21
TC13-15	226	-6.3	-425	-11.0	-57	-3.9	-240	24.3	21	-22.8	-15
TC13-16	249	-6.4	-359	-16.8	-77	-8.8	-462	23.1	12	-58.7	-28
TC13-17	268	0.4	60	-1.6	-5	-3.8	-167	50.3	44	-55.6	-31
TC13-18a	281	3.3	442	0.8	2	0.6	27	39.7	22	-26.9	-13
TC13-18b	289	7.0	932	6.0	18	5.2	225	55.2	34	23.4	12
TC13-19	300	6.7	884	4.4	13	3.8	165	22.7	14	-67.7	-34
TC13-20	318	7.5	837	15.0	36	12.2	416	49.4	25	-27.9	-10
TC13-21	337	7.5	835	16.0	38	13.0	452	59.9	35	-44.4	-16
TC13-22a	380	7.9	858	17.5	39	13.9	420	32.3	7	-116.2	-35
TC13-22b	391	7.8	846	18.3	41	13.9	424	-4.3	-1	-127.1	-39
TC13-23	413	3.8	467	12.9	47	9.0	396	23.4	8	-27.4	-12
TC13-24	442	-1.8	-216	0.5	2	-1.5	-71	35.8	13	-13.0	-7
TC13-25	456	3.3	391	9.8	40	6.5	319	35.0	14	-47.0	-25
TC13-26	463	3.4	426	6.3	27	4.5	230	41.8	18	-19.5	-12
TC13-27	471	1.9	243	9.1	42	5.6	298	42.8	19	-0.5	0
TC13-28	483	2.9	356	8.7	38	5.5	287	40.4	17	22.9	13
TC13-29	503	3.7	466	3.1	11	3.4	154	35.6	15	37.4	21

Notes:

1. Nitrogen is measured by FI609.
2. TC13-1 to TC13-12 and TC13-17 to TC13-29 were air blown; TC13-13 to TC13-16 were oxygen blown.
3. TC13-1 to TC13-9 were Powder River Basin, TC13-10a to TC13-14 were low sodium Freedom Mine Lignite, TC13-15 was a mixture of high and low sodium lignite, and TC13-16 to TC13-29 was high sodium Freedom Mine Lignite.

Table 3.4-5

Typical Air-Blown Component Mass Balances

	Nitrogen	Hydrogen	Oxygen	Calcium	Silica
Operating Period	TC13-12	TC13-12	TC13-12	TC13-12	TC13-12
Date Start	10/9/2003	10/9/2003	10/9/2003	10/9/2003	10/9/2003
Time Start	5:15	5:15	5:15	5:15	5:15
Time End	8:30	8:30	8:30	8:30	8:30
Fuel	Fre. Lig.	Fre. Lig.	Fre. Lig.	Fre. Lig.	Fre. Lig.
Riser Temperature, °F	1,700	1,700	1,700	1,700	1,700
Pressure, psig	194	194	194	194	194
In, Pounds/hr					
Fuel	29	296	1,810	72	90
Sorbent	0	0	50	33	7
Air	10,710	0	3,254	0	0
Nitrogen	6,126	0	0	0	0
Steam	0	142	1,139	0	0
Total	16,866	438	6,253	105	97
Out, pounds/hr					
Synthesis Gas	16,172	487	6,550	0	0
PCD Solids	1	1	25	42	40
Reactor	0	0	3	6	18
Total	16,173	488	6,578	48	58
(In-Out)/In, %	4.1%	-11.4%	-5.2%	53.8%	40.2%
(In-Out), pounds per hour	693	-50	-325	56	39

Table 3.4-6

Typical Oxygen-Blown Component Mass Balances

	Nitrogen	Hydrogen	Oxygen	Calcium	Silica
Operating Period	TC13-16	TC13-16	TC13-16	TC13-16	TC13-16
Date	10/12/2003	10/12/2003	10/12/2003	10/12/2003	10/12/2003
Time Start	4:15	4:15	4:15	4:15	4:15
Time End	6:45	6:45	6:45	6:45	0:00
Fuel	Fre. Lig.	Fre. Lig.	Fre. Lig.	Fre. Lig.	Fre. Lig.
Riser Temperature, ^{o}F	1,709	1,709	1,709	1,709	1,709
Pressure, psig	110	110	110	110	110
In, Pounds/hr					
Fuel	19	163	1,010	32	44
Sorbent	0	0	32	21	5
Oxygen	0	0	1,702	0	0
Purge Air	545	0	166	0	0
Nitrogen	5,019	0	0	0	0
Steam	0	293	2,346	0	0
Total	5,583	457	5,256	53	48
Out, pounds/hr					
Synthesis Gas	5,941	532	5,701	0	0
PCD Solids	1	1	15	36	66
Reactor	0	0	2	4	11
Total	5,942	534	5,718	41	77
(In-Out)/In, %	-6.4%	-16.8%	-8.8%	23.1%	-58.7%
(In-Out), pounds per hour	-359	-77	-462	12	-28

Table 3.4-7 Sulfur Balances

Operating Period	Average Relative Hours	Feeds (In) Coal lb/hr	Products (Out) Syngas[1] lb/hr	PCD Solids lb/hr	SP Solids lb/hr	Total lb/hr	In - Out lb/hr	(In- Out)/In %	Sulfur Removal Gas %	Products %	Solids %	Sulfur Emissions lb SO_2/MMBtu
TC13-1	7	13.5	8.3	0.4	0.0	8.7	4.8	35.6	38	4	3	0.90
TC13-2	18	16.3	7.4	0.7	0.0	8.1	8.2	50.2	55	9	4	0.54
TC13-3	29	14.7	6.3	0.8	0.0	7.1	7.6	51.8	57	11	5	0.46
TC13-4	41	13.2	6.4	0.7	0.0	7.1	6.1	46.1	52	10	5	0.46
TC13-5	53	10.9	5.4	0.7	0.0	6.1	4.8	43.7	50	11	6	0.38
TC13-6	61	9.0	5.5	0.7	0.0	6.2	2.8	31.2	39	11	8	0.40
TC13-7	73	8.8	6.3	0.8	0.0	7.0	1.7	19.8	28	11	9	0.42
TC13-8	95	8.7	6.8	1.0	0.0	7.8	0.9	10.5	22	13	11	0.45
TC13-9	104	10.4	7.7	1.0	0.0	8.8	1.6	15.6	26	12	10	0.44
TC13-10a	143	41.5	29.6	8.7	0.2	38.5	3.0	7.3	-12	23	21	2.65
TC13-10b	151	42.1	31.2	10.0	0.3	41.5	0.6	1.5	26	24	24	2.71
TC13-11	165	42.2	35.2	12.6	0.1	47.9	-5.7	-13.4	17	26	30	3.01
TC13-12	178	70.9	54.0	19.0	0.4	73.4	-2.5	-3.5	0	26	27	2.72
TC13-13	199	58.9	51.0	17.8	0.0	68.8	-9.8	-16.7	13	26	30	2.88
TC13-14	215	57.1	47.6	9.0	0.0	56.6	0.5	0.8	17	16	16	2.94
TC13-15	226	41.5	33.8	4.8	0.0	38.6	2.9	6.9	19	12	12	2.39
TC13-16	249	35.6	26.3	3.0	0.2	29.5	6.1	17.2	26	10	8	2.33
TC13-17	268	24.1	-	6.5	0.1	-	-	-	-	-	27	-
TC13-18a	281	24.4	26.5	5.7	0.1	32.2	-7.8	-32.1	-9	18	23	2.33
TC13-18b	289	24.3	25.8	6.1	0.0	31.9	-7.6	-31.3	-6	19	25	2.25
TC13-19	300	21.9	18.4	3.8	0.0	22.2	-0.4	-1.6	16	17	17	1.61
TC13-20	318	17.8	19.1	2.8	0.0	21.9	-4.1	-23.1	-7	13	16	2.53
TC13-21	337	19.0	19.3	3.0	0.0	22.3	-3.4	-17.8	-2	13	16	2.57
TC13-22a	380	18.9	16.5	4.0	0.0	20.4	-1.5	-8.2	13	19	21	2.11
TC13-22b	391	17.5	16.0	5.4	0.0	21.4	-3.9	-22.5	8	25	31	2.01
TC13-23	413	26.1	22.6	5.0	0.0	27.7	-1.6	-6.1	13	18	19	1.93
TC13-24	442	31.4	28.5	3.4	0.1	32.0	-0.7	-2.1	9	11	11	2.20
TC13-25	456	37.1	27.4	4.5	0.2	32.1	4.9	13.3	26	14	12	1.98
TC13-26	463	44.3	30.5	5.2	0.2	35.9	8.4	19.0	31	14	12	1.96
TC13-27	471	39.0	30.5	5.1	0.2	35.7	3.3	8.5	22	14	13	1.93
TC13-28	483	28.5	28.5	4.8	0.2	33.5	-5.0	-17.4	0	15	17	1.88
TC13-29	503	24.1	26.3	5.1	0.1	31.5	-7.4	-30.6	-9	16	21	1.78

Notes:

1. Syngas sulfur emissions determined from Syngas Combustor SO_2 analyzer.
2. Sorbent feed to the Transport Gasifier occurred during TC13-10a through TC13-21.
3. TC13-1 to TC13-12 and TC13-17 to TC13-29 were air blown; TC13-13 to TC13-16 were oxygen blown.
4. TC13-1 to TC13-9 were Powder River Basin, TC13-10a to TC13-14 were low sodium Freedom Mine lignite, TC13-15 was a mixture of high and low sodium lignite, and TC13-16 to TC13-29 was high sodium Freedom Mine lignite.
5. Syngas Combustor SO_2 analyzer was out of service for TC13-17, so sulfur emissions could not be determined.

Table 3.4-8 Energy Balances

Operating Period	Average Relative Hours	Feeds (In)				Products (Out)						In - Out	(In- Out)/In	Efficiency[4]		
														Raw		Projected[3]
		Coal	Air	Steam	Total	Latent Syngas	Sensible Syngas	PCD Solids	Reactor Solids	Heat Loss	Total			Cold	Hot	Cold
		10^6 Btu/hr	10^6 Btu/hr	10^6 Btu/hr	10^6 Btu/hr	10^6 Btu/hr	10^6 Btu/hr	10^6 Btu/hr	10^6 Btu/hr	10^6 Btu/hr	10^6 Btu/hr	10^6 Btu/hr	%	%	%	%
TC13-1	7	17.9	0.5	1.0	19.4	8.1	6.8	0.5	0.00	3.5	18.9	0.5	2.5	42.6	78.8	69.6
TC13-2	18	26.7	0.6	1.0	28.4	15.0	9.2	0.2	0.00	3.5	27.9	0.4	1.5	53.5	86.6	74.0
TC13-3	29	27.1	0.6	1.2	28.9	14.2	9.4	0.3	0.00	3.5	27.4	1.5	5.3	51.8	86.0	71.8
TC13-4	41	27.9	0.7	1.4	29.9	14.8	9.7	0.4	0.00	3.5	28.4	1.5	5.0	52.1	86.2	71.6
TC13-5	53	27.8	0.6	1.5	29.9	14.6	9.4	0.7	0.00	3.5	28.2	1.7	5.7	51.7	85.0	70.9
TC13-6	61	26.6	0.6	1.4	28.6	13.9	9.4	0.8	0.00	3.5	27.6	1.0	3.6	50.5	84.4	69.7
TC13-7	73	28.7	0.7	1.4	30.8	15.1	9.5	1.2	0.00	3.5	29.4	1.4	4.7	51.6	84.0	69.5
TC13-8	95	29.0	0.7	1.4	31.2	17.1	10.5	1.3	0.00	3.5	32.5	-1.3	-4.1	52.8	85.3	69.6
TC13-9	104	33.7	0.7	1.5	35.9	18.5	10.5	1.4	0.00	3.5	33.9	2.0	5.6	54.6	85.5	70.5
TC13-10a	143	21.3	0.6	1.4	23.3	9.3	7.9	0.8	0.02	3.5	21.4	1.9	8.0	43.5	80.1	65.0
TC13-10b	151	22.0	0.6	1.4	24.0	9.6	8.0	0.6	0.02	3.5	21.7	2.3	9.7	44.1	80.8	65.6
TC13-11	165	22.3	0.6	1.3	24.2	10.4	7.8	1.3	0.00	3.5	23.0	1.2	5.1	45.4	79.1	65.5
TC13-12	178	38.0	0.9	1.7	40.6	21.3	11.7	2.9	0.02	3.5	39.4	1.2	2.9	54.1	83.7	66.2
TC13-13	199	33.9	0.2	4.5	38.6	19.4	9.1	4.5	0.00	3.5	36.5	2.1	5.4	53.2	78.2	67.3
TC13-14	215	30.4	0.1	5.4	35.9	16.4	8.3	1.8	0.00	3.5	29.9	6.0	16.7	54.8	82.4	73.5
TC13-15	226	26.6	0.1	3.8	30.5	16.8	7.9	0.9	0.00	3.5	29.1	1.4	4.5	57.8	84.9	77.4
TC13-16	249	20.8	0.0	3.5	24.4	11.8	6.9	0.5	0.01	3.5	22.8	1.6	6.7	52.0	82.3	76.6
TC13-17	268	21.6	0.6	1.4	23.6	10.5	9.0	0.4	0.02	3.5	23.5	0.1	0.5	44.9	83.1	67.7
TC13-18a	281	21.5	0.6	1.7	23.7	10.9	8.4	2.2	0.02	3.5	25.1	-1.3	-5.6	43.5	77.2	62.8
TC13-18b	289	21.7	0.5	1.7	23.9	10.8	7.9	2.3	0.00	3.5	24.4	-0.5	-2.0	44.1	76.3	63.2
TC13-19	300	21.7	0.5	1.7	23.9	10.9	7.9	0.3	0.00	3.5	22.7	1.3	5.4	48.1	83.1	70.6
TC13-20	318	14.5	0.4	1.6	16.5	6.2	6.0	0.6	0.01	3.5	16.2	0.2	1.4	37.9	74.7	66.1
TC13-21	337	14.5	0.4	1.5	16.5	6.4	6.1	0.6	0.01	3.5	16.6	-0.1	-0.7	38.8	75.4	66.5
TC13-22a	380	15.4	0.4	1.3	17.1	4.8	4.9	2.3	0.00	3.5	15.5	1.6	9.3	30.9	62.6	55.7
TC13-22b	391	16.0	0.4	1.4	17.7	4.6	4.9	3.2	0.00	3.5	16.3	1.4	8.0	28.4	58.7	49.9
TC13-23	413	23.2	0.5	2.4	26.0	8.3	6.7	5.0	0.01	3.5	23.5	2.5	9.8	35.3	63.9	51.3
TC13-24	442	25.6	0.5	2.7	28.8	9.0	7.6	4.3	0.01	3.5	24.5	4.3	14.9	37.0	68.0	52.6
TC13-25	456	27.2	0.5	2.6	30.2	9.7	7.2	4.5	0.02	3.5	25.0	5.3	17.5	38.9	67.8	54.0
TC13-26	463	30.3	0.6	2.5	33.3	11.5	7.7	4.6	0.02	3.5	27.4	6.0	17.9	42.1	70.3	56.6
TC13-27	471	29.8	0.5	2.6	33.0	10.9	7.8	4.6	0.02	3.5	26.9	6.1	18.4	40.6	69.8	55.4
TC13-28	483	29.2	0.6	2.6	32.3	10.8	7.6	4.6	0.01	3.5	26.5	5.8	17.9	40.7	69.3	55.3
TC13-29	503	28.1	0.5	1.8	30.5	11.6	7.3	4.7	0.01	3.5	27.1	3.4	11.2	42.8	69.7	57.9

Notes:

1. Nitrogen and sorbent assumed to enter the system at ambient temperature and therefore have zero enthalpy.
2. Reference conditions are 80 ^{o}F and 14.7 psia.
3. Commercially projected efficiencies assume that only air nitrogen is in the synthesis gas and that the reactor is adiabatic.
4. Efficiencies based on the products method.

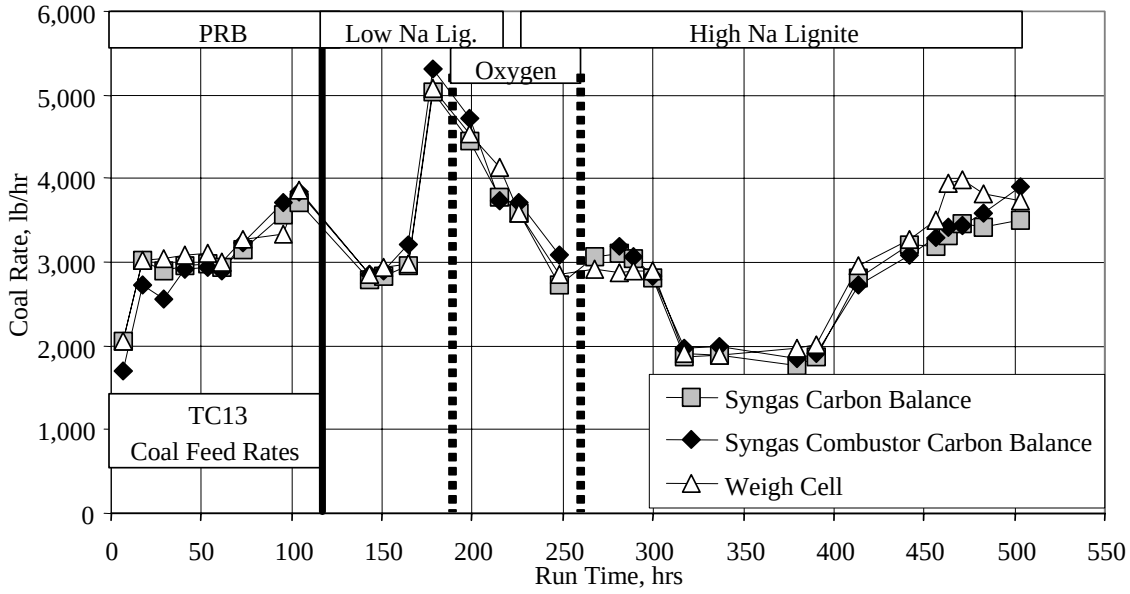

Figure 3.4-1 Coal Rates

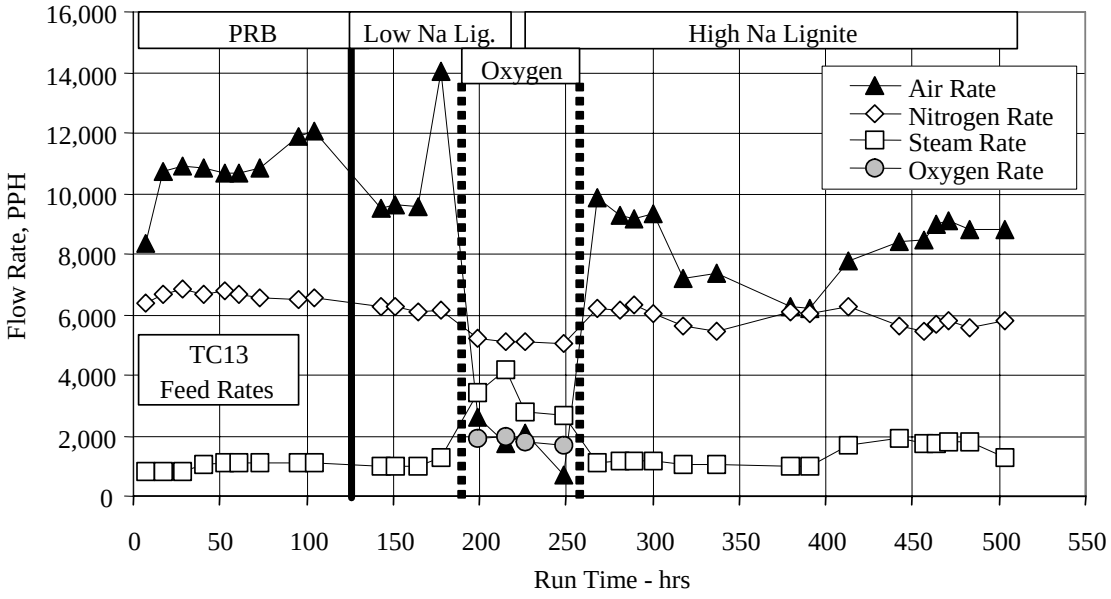

Figure 3.4-2 Air, Nitrogen, Oxygen, and Steam Rates

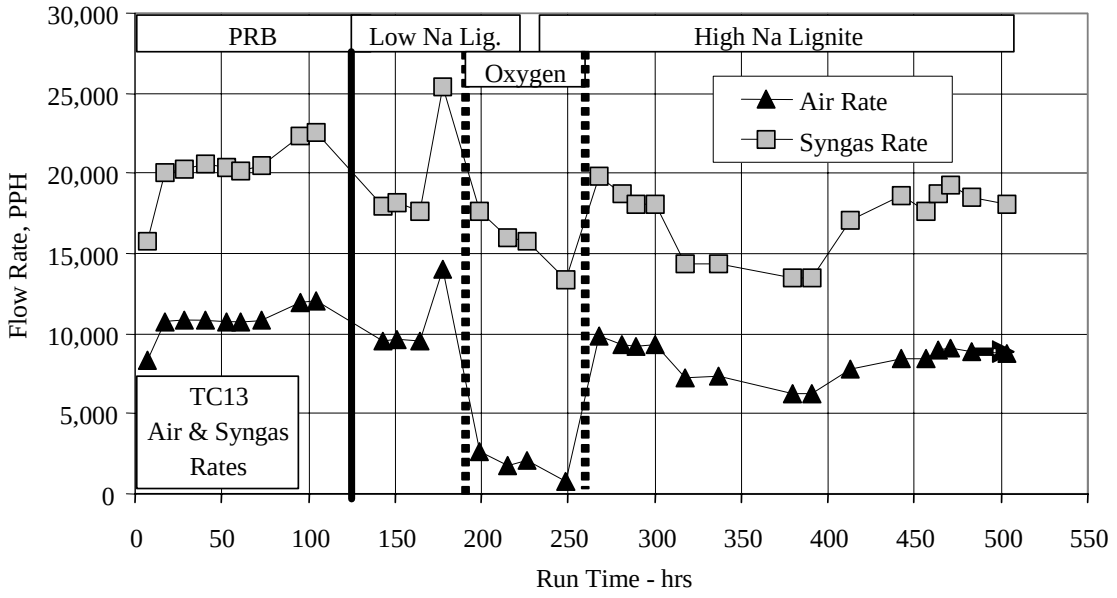

Figure 3.4-3 Air and Syngas Rates

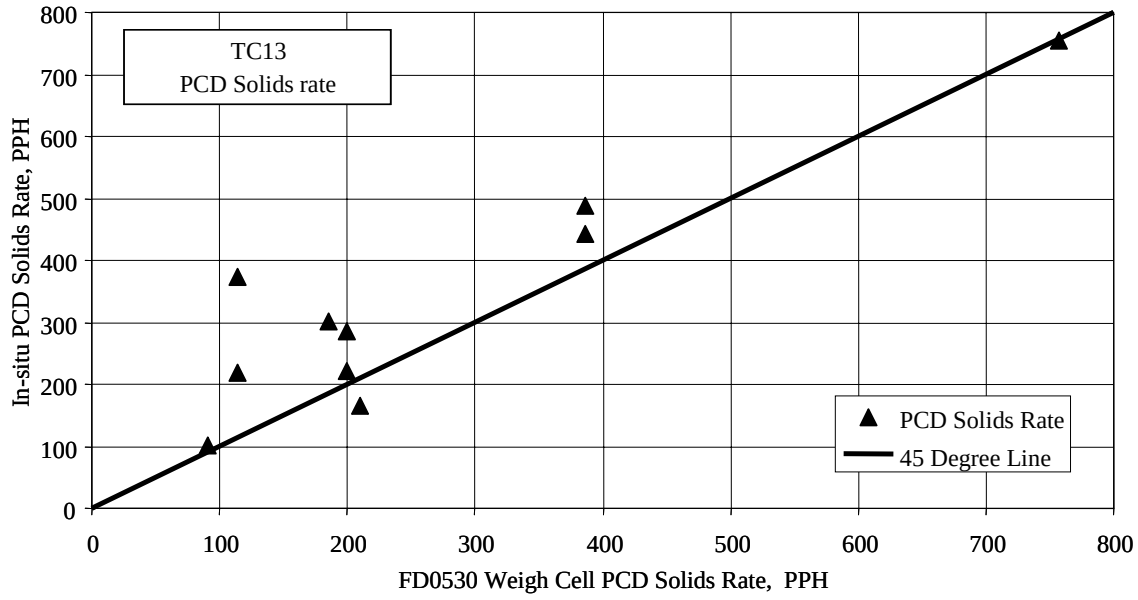

Figure 3.4-4 PCD Solid Rates

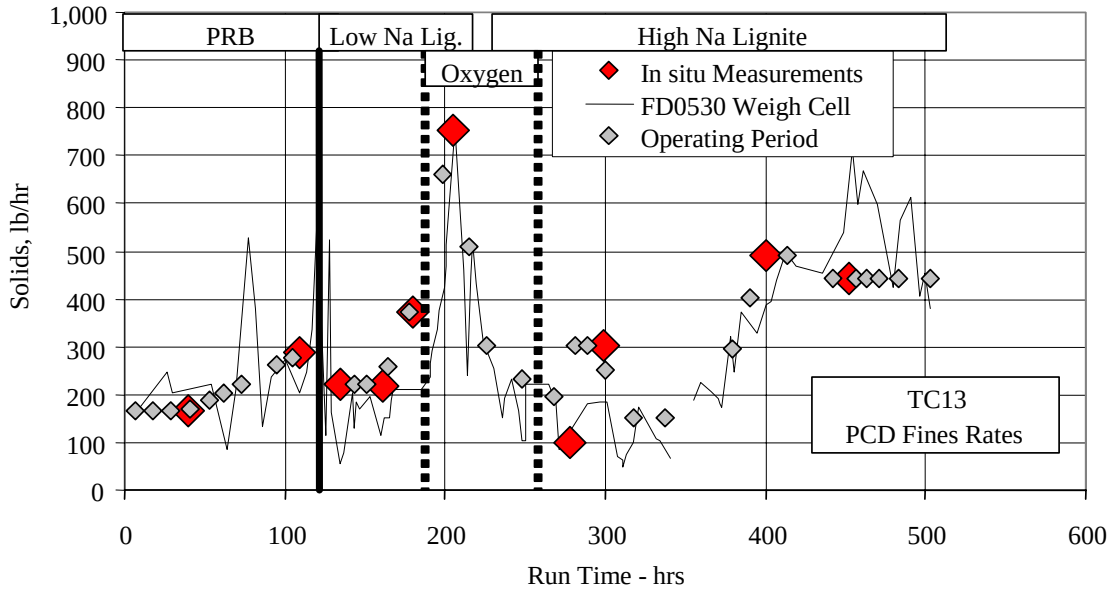

Figure 3.4-5 PCD Fines Rates

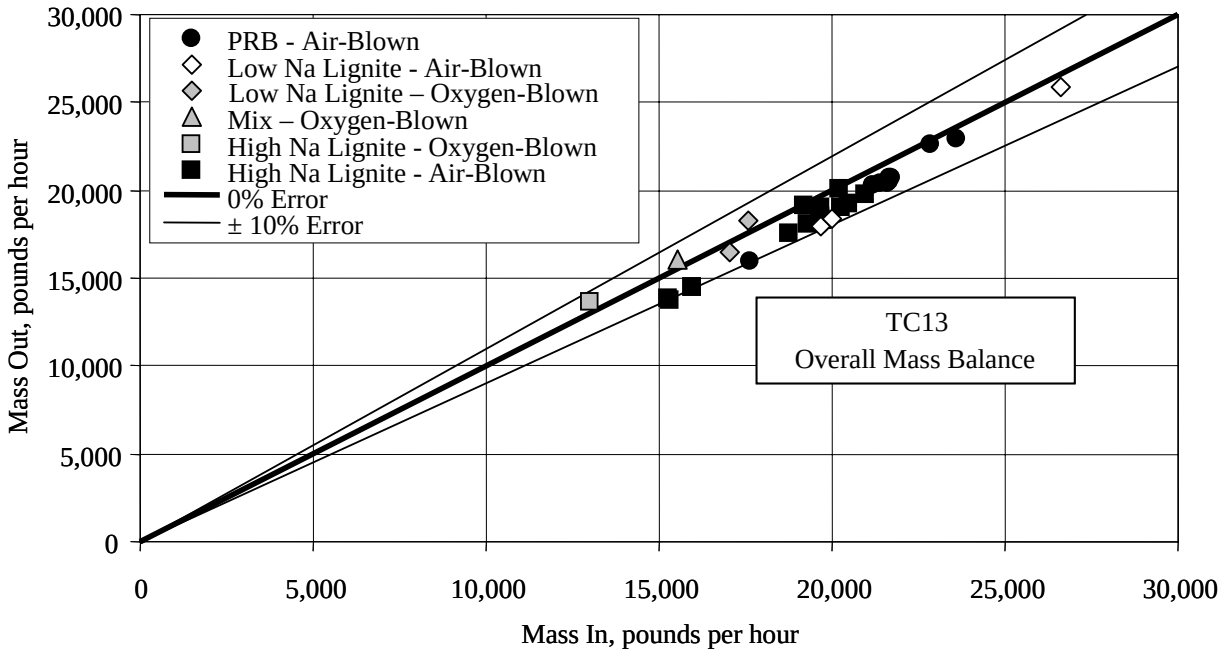

Figure 3.4-6 Mass Balance

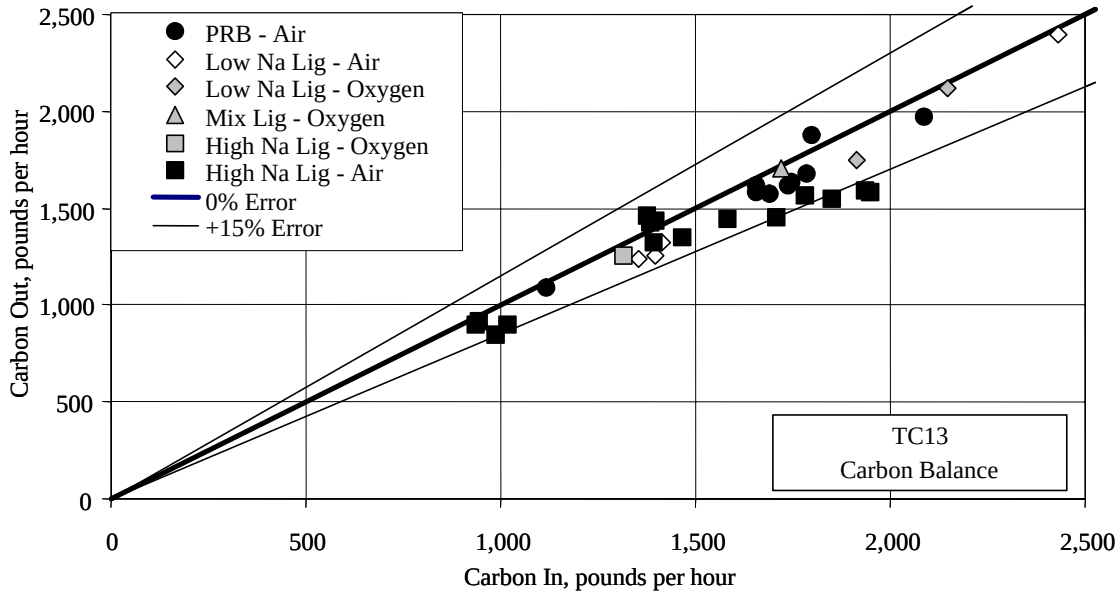

Figure 3.4-7 Carbon Balance

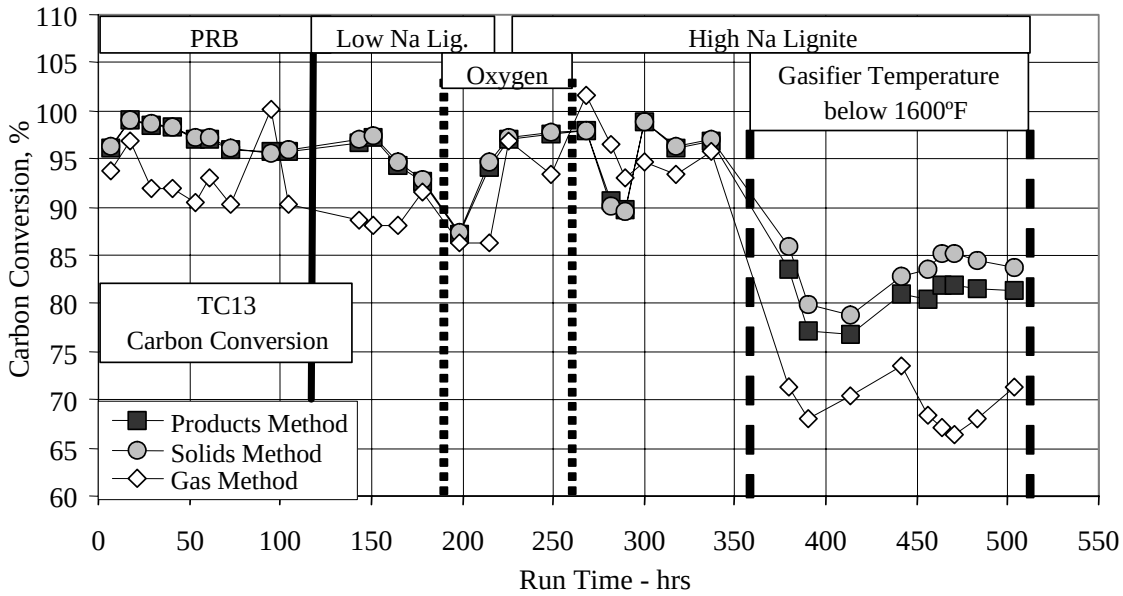

Figure 3.4-8 Carbon Conversion

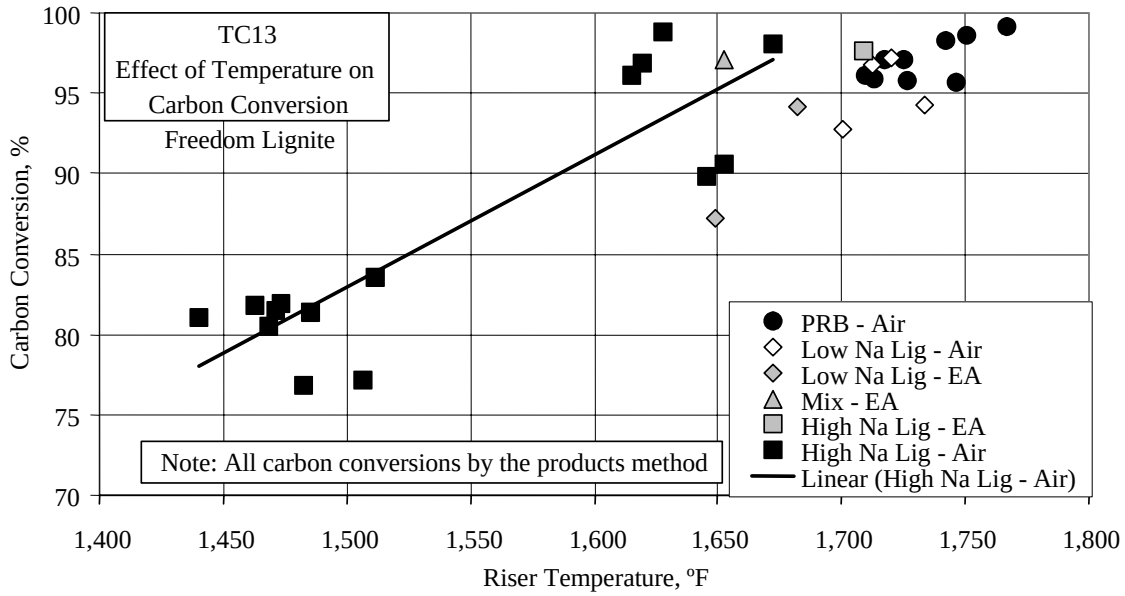

Figure 3.4-9 Carbon Conversion and Riser Temperature

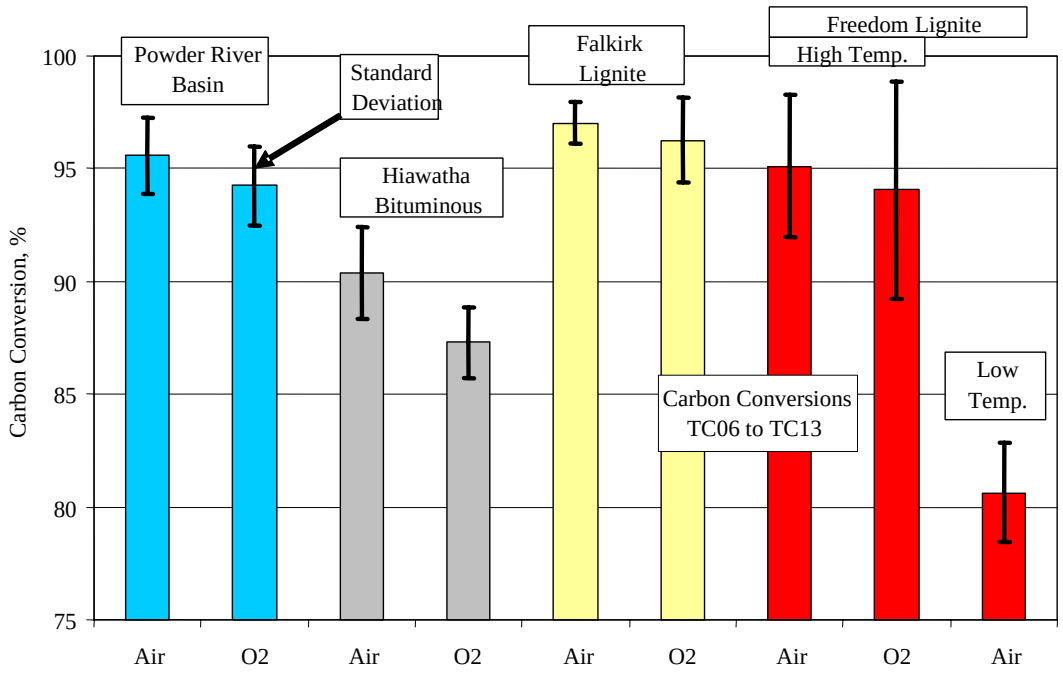

Figure 3.4-10 Carbon Conversion of Four Coals

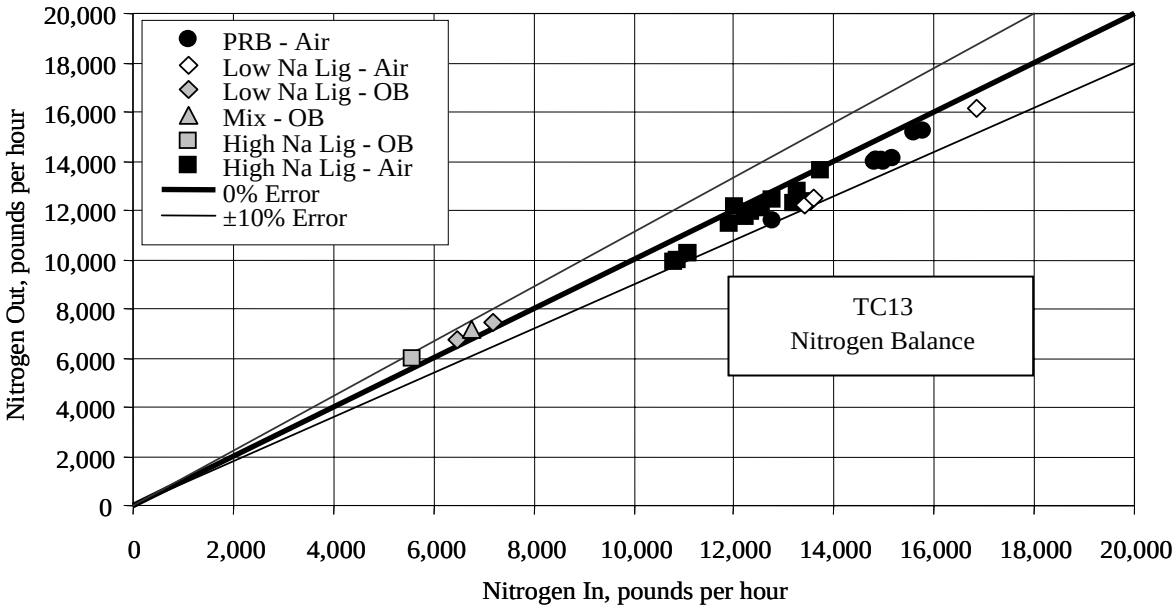

Figure 3.4-11 Nitrogen Balance

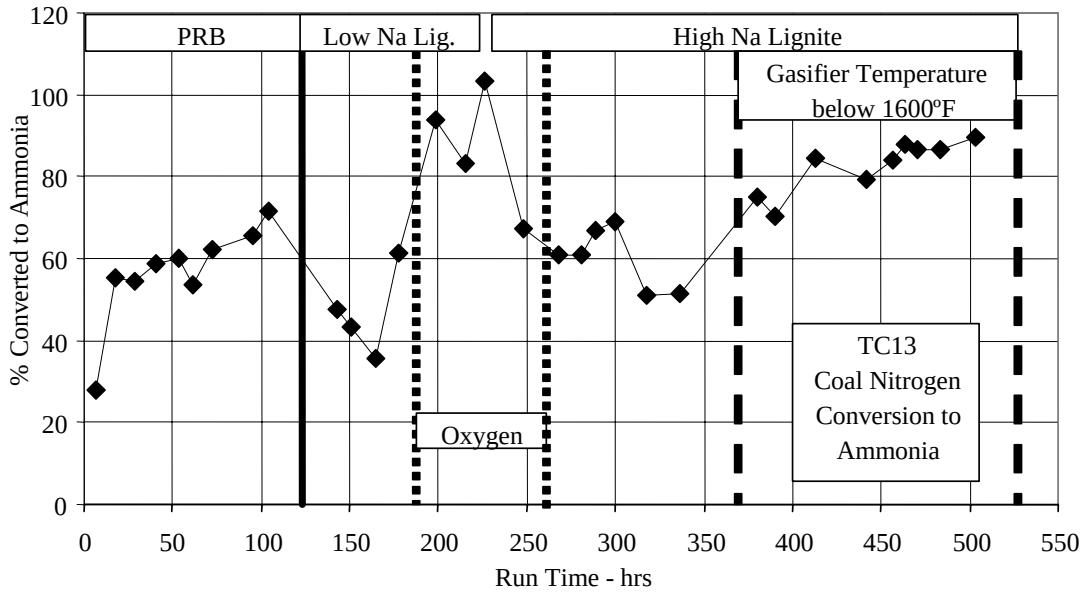

Figure 3.4-12 Coal Nitrogen Conversion to Ammonia

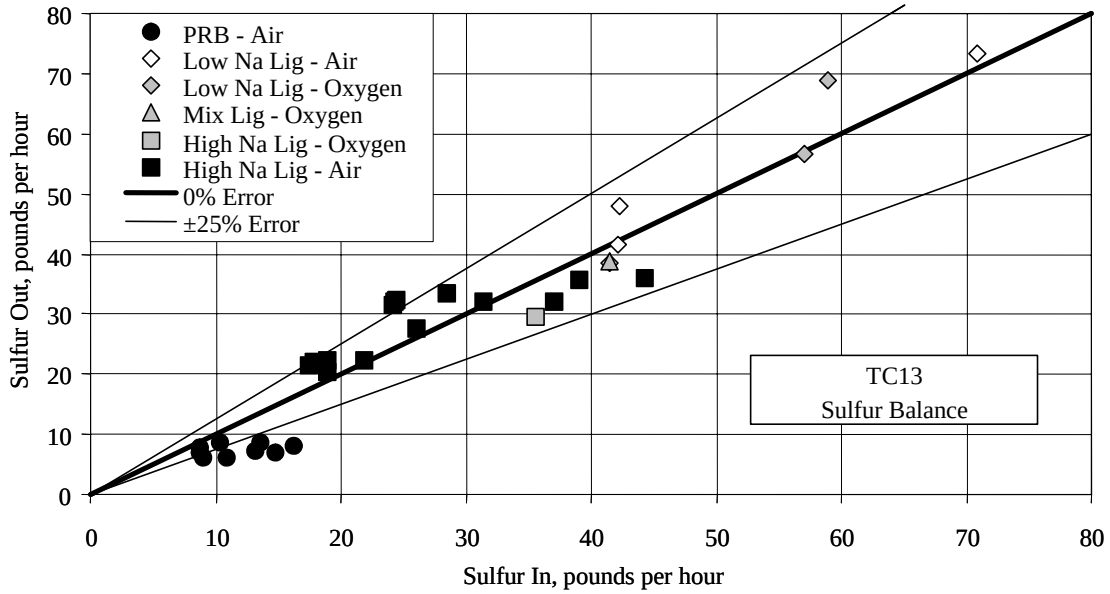

Figure 3.4-13 Coal Nitrogen Conversion to Ammonia and Percent Overall O_2

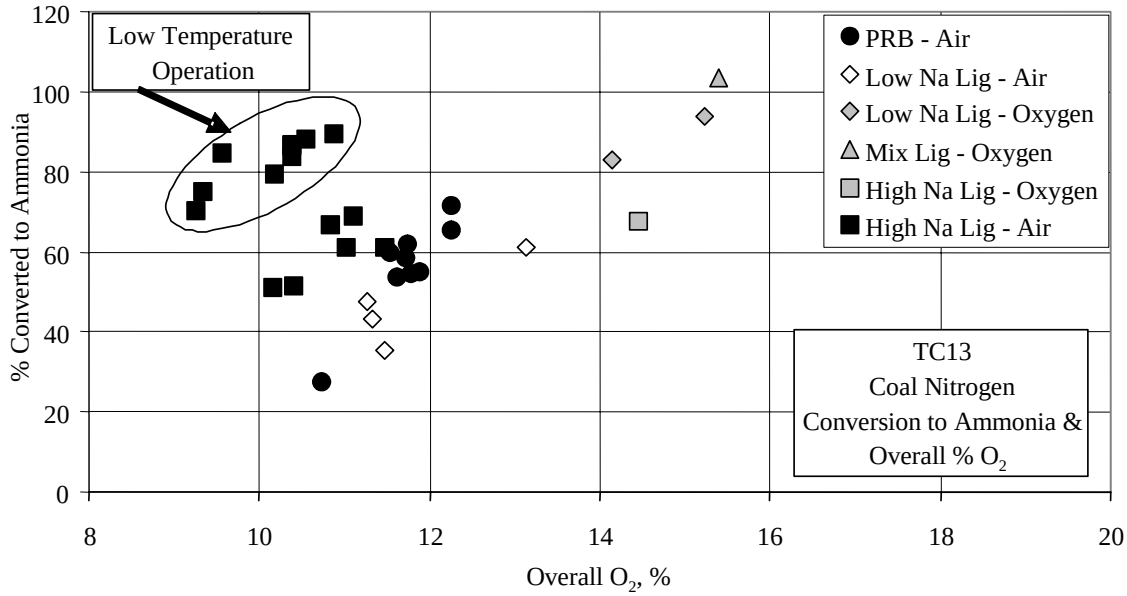

Figure 3.4-14 Sulfur Balance

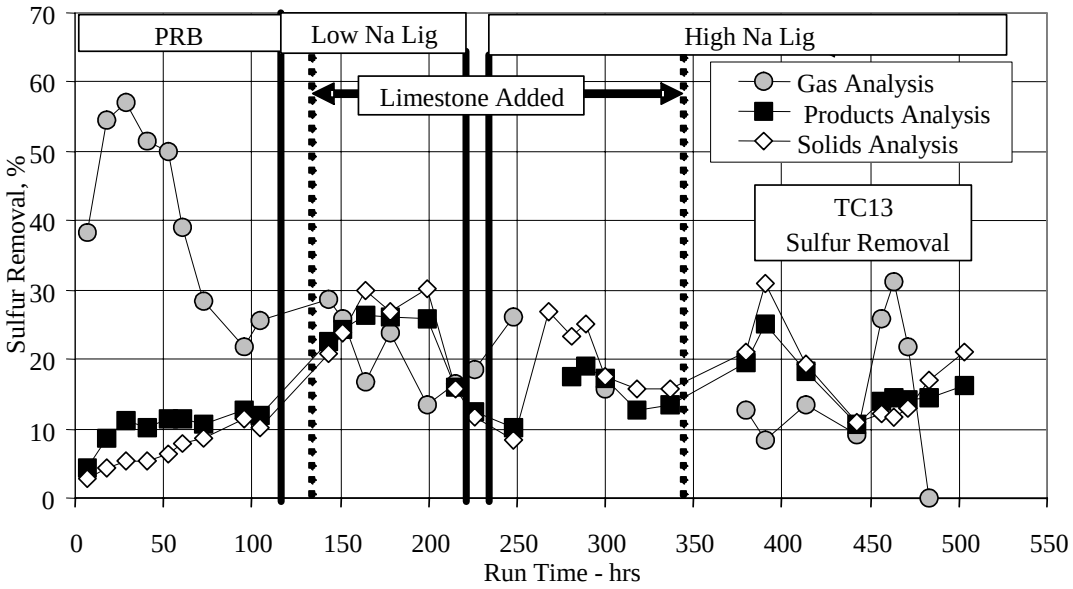

Figure 3.4-15 Sulfur Removal

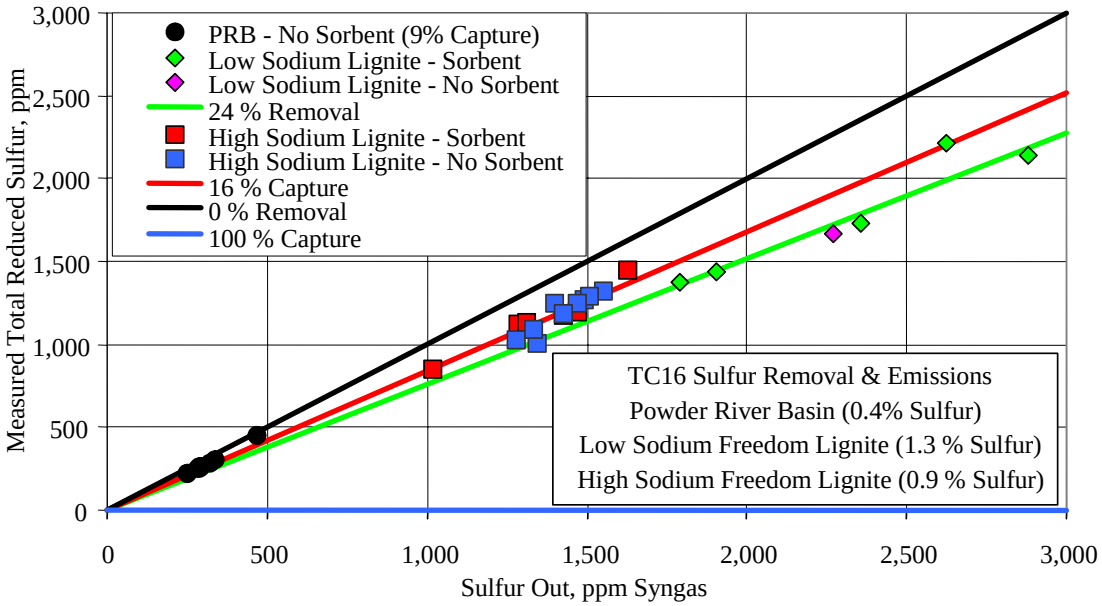

Figure 3.4-16 Sulfur Emissions

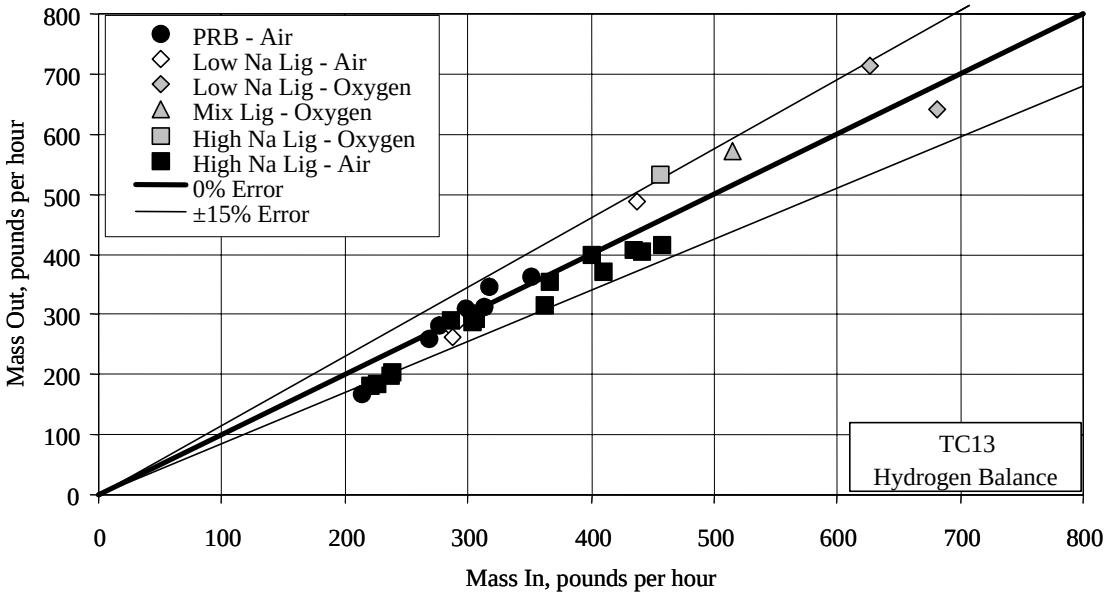

Figure 3.4-17 Hydrogen Balance

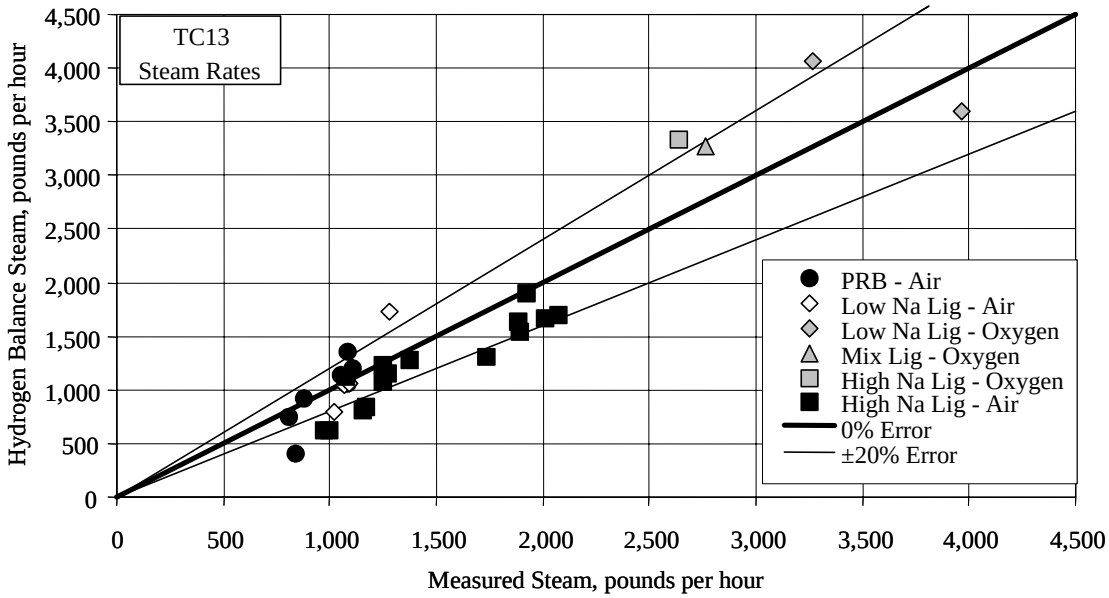

Figure 3.4-18 Steam Rates

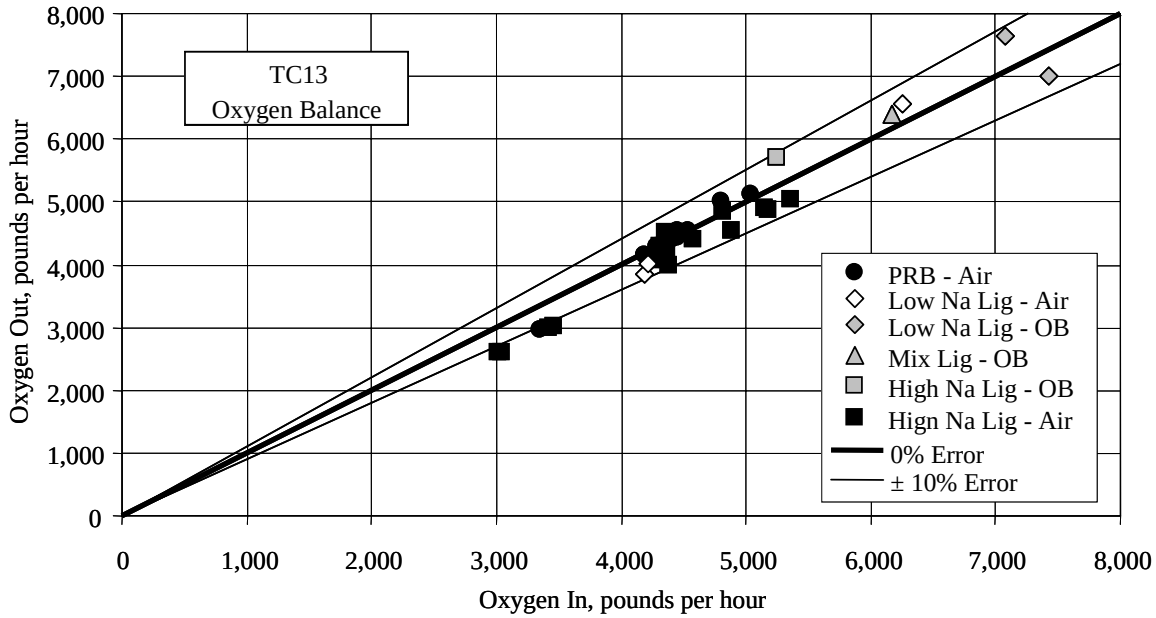

Figure 3.4-19 Oxygen Balance

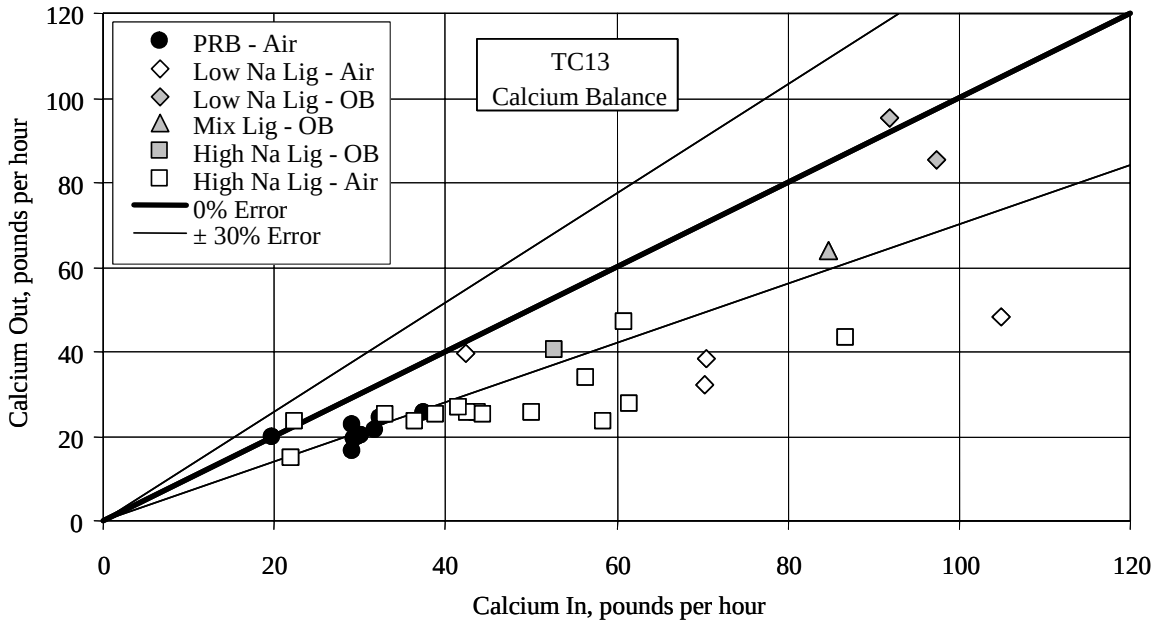

Figure 3.4-20 Calcium Balance

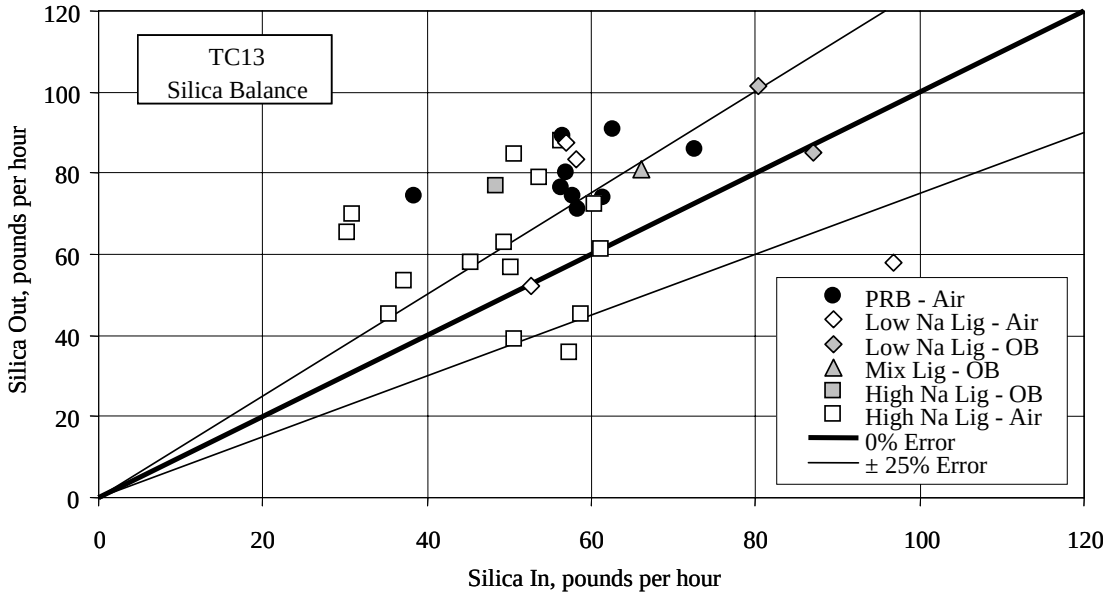

Figure 3.4-21 Silica Balance

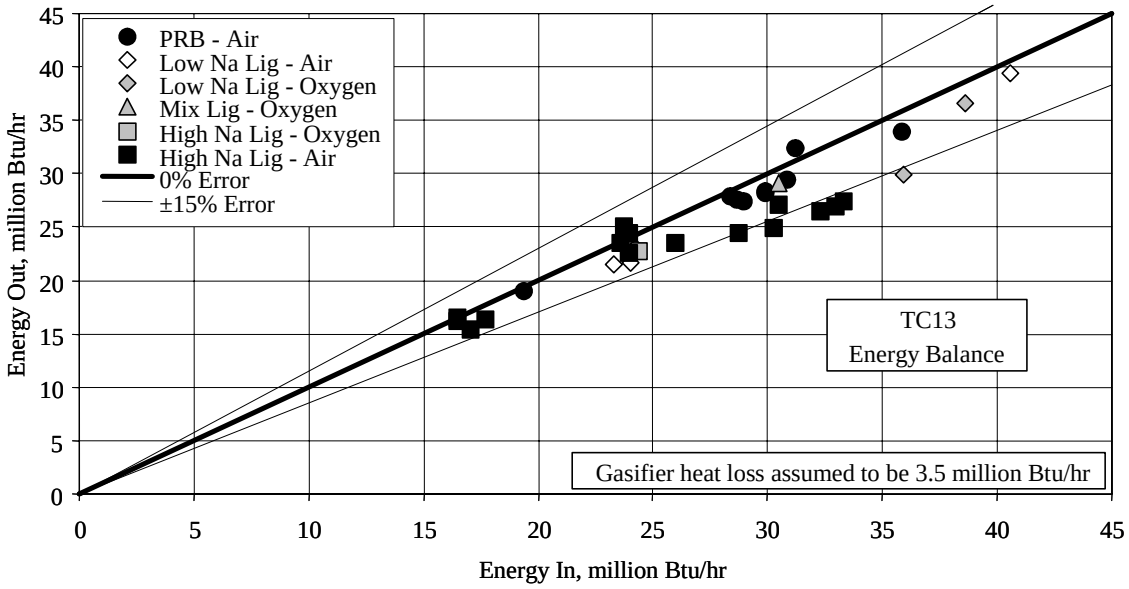

Figure 3.4-22 Energy Balance

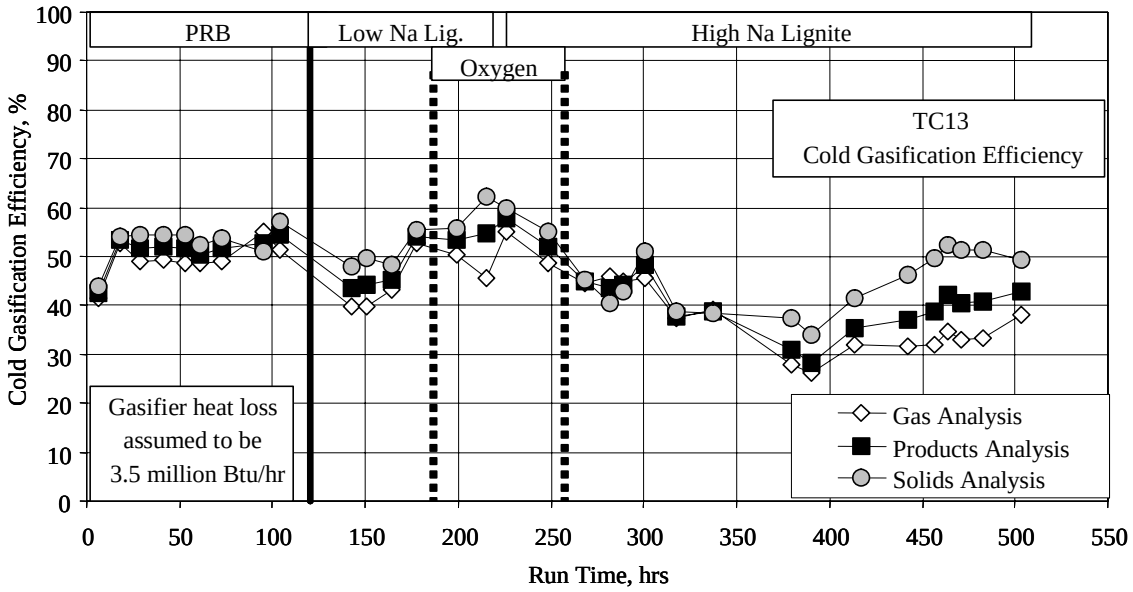

Figure 3.4-23 Cold Gasification Efficiency

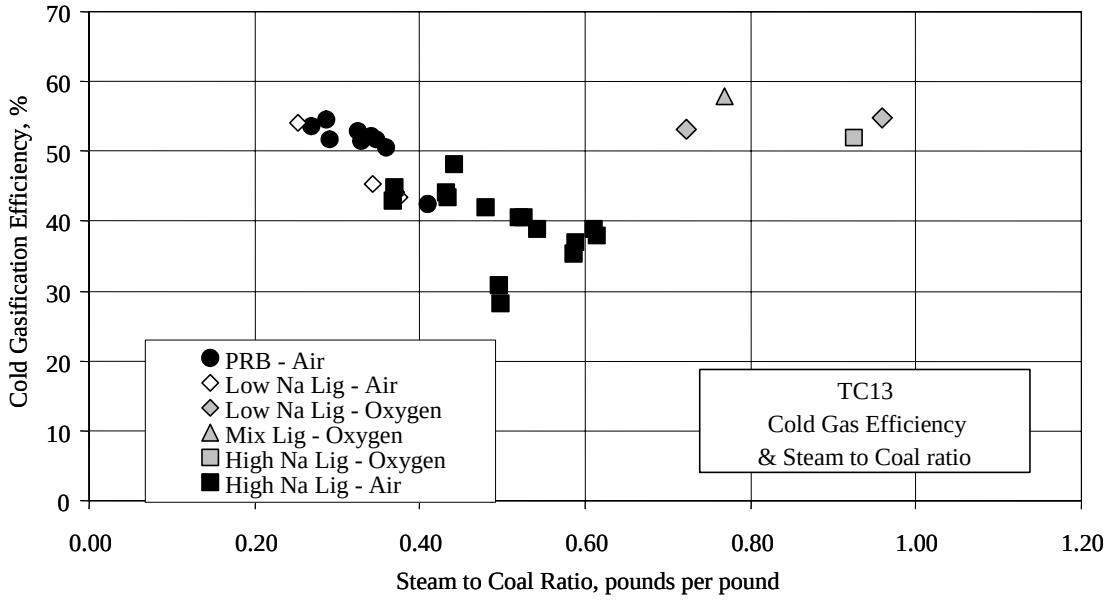

Figure 3.4-24 Cold Gasification Efficiency and Steam-to-Coal Ratio

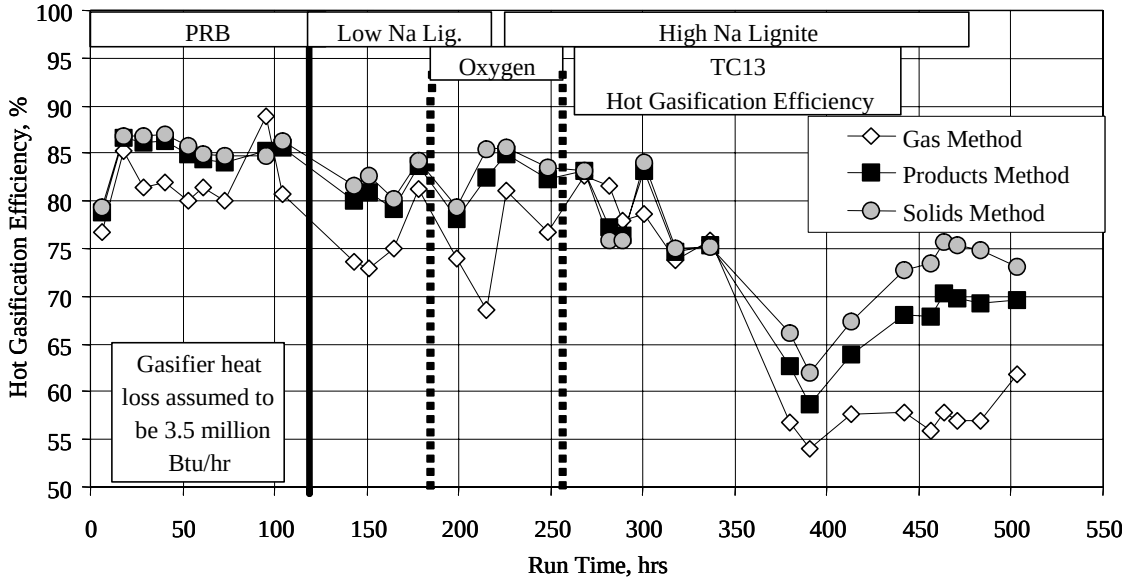

Figure 3.4-25 Hot Gasification Efficiency

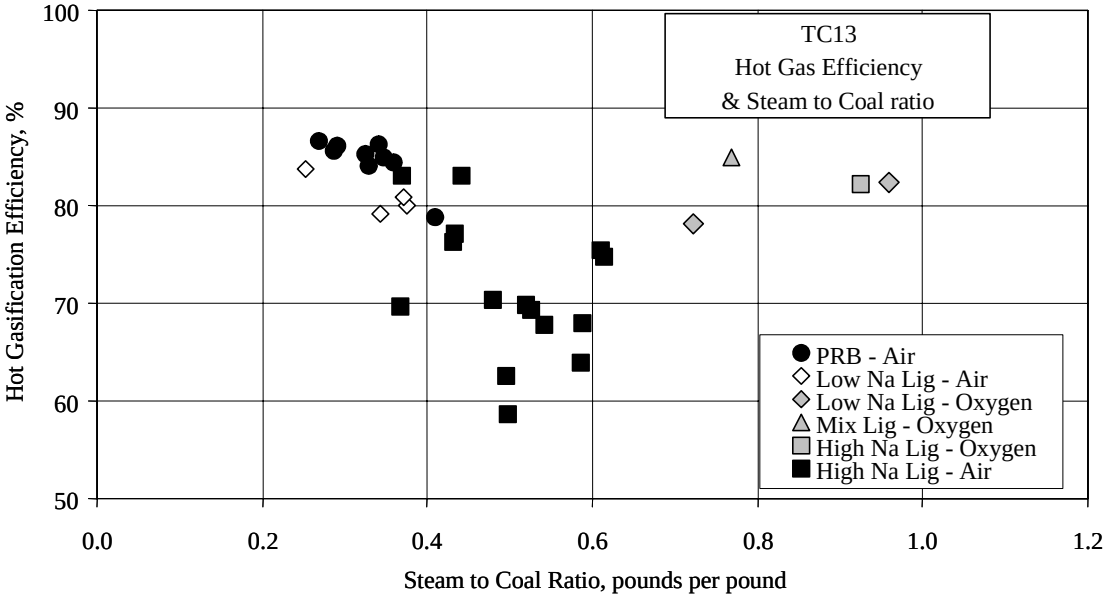

Figure 3.4-26 Hot Gasification Efficiency and Steam-to-Coal Ratio

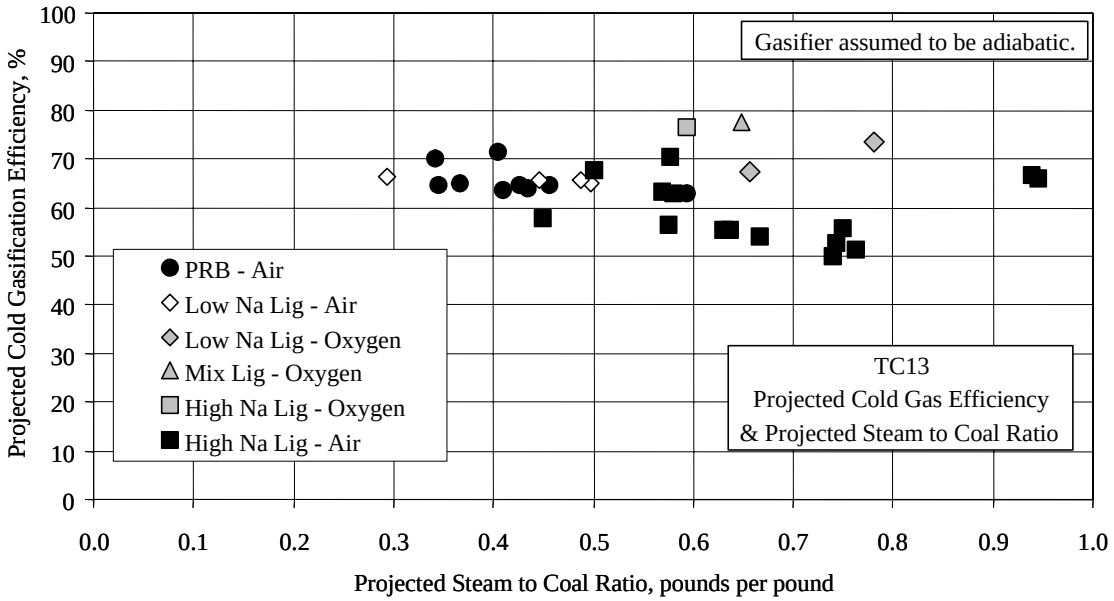

Figure 3.4-27 Commercially Projected Cold Gasification Efficiency

3.5 Atmospheric Fluidized-Bed Combustor Operations (AFBC)

Prior to the start of TC13, a new, replacement feeder was installed on the bottom of the gasification ash (g-ash) feed vessel. The original feeder was damaged near the end of TC10. During TC11 and TC12, g-ash was fed directly to the ash silo because previous operation with PRB had shown that the gasifier did not produce a g-ash with levels of reactive sulfides above 500 mg/kg when operating with PRB.

The AFBC system was started on September 29 with the startup of the AFBC air compressor and the lighting of the AFBC start-up heater. The system transitioned to normal operations on October 2. The system operated until October 12 when the gasifier entered a brief outage. The start-up burner was used to keep the AFBC warm during the outage. The system operated normally again from October 15 to 19 when the gasifier entered another brief outage. The AFBC again operated normally beginning October 23 until the end of the run on November 3. During the course of TC13, the fuel oil system operated 504 hours and the g-ash feeder operated for 319 hours. The AFBC bed temperature averaged about 1,410°F during TC13 and generally ranged from 1,350 to 1,500°F.

The replacement g-ash feeder operated more reliably during TC13 than the previous feeder had performed. The feed rate was a bit smoother, which can be attributed to less blow-by than in the old, worn feeder. This allowed some work on a control loop for the g-ash feed rate. The feeder was able to deliver g-ash at a minimum rate of about 400 pph up to a maximum rate of about 1,500 pph. Unfortunately, there still is not a good correlation between the feeder speed and either the volumetric or weight-based feed rate.

On October 4, the shift coordinator reported a hotspot of about 700°F on the AFBC. A subsequent thermal inspection revealed three other hotspots on the skin on the AFBC. Air cannons were directed at each of the known hotspots and the bed temperature was lowered slightly. Figure 3.5-1 is of one of the hotspots after the air cannons were started. An inspection of the refractory after the end of the test run showed that the refractory had been cycled enough times to have reached the end of its useful life. The bottom 6 feet of the refractory was replaced in the outage following TC13.

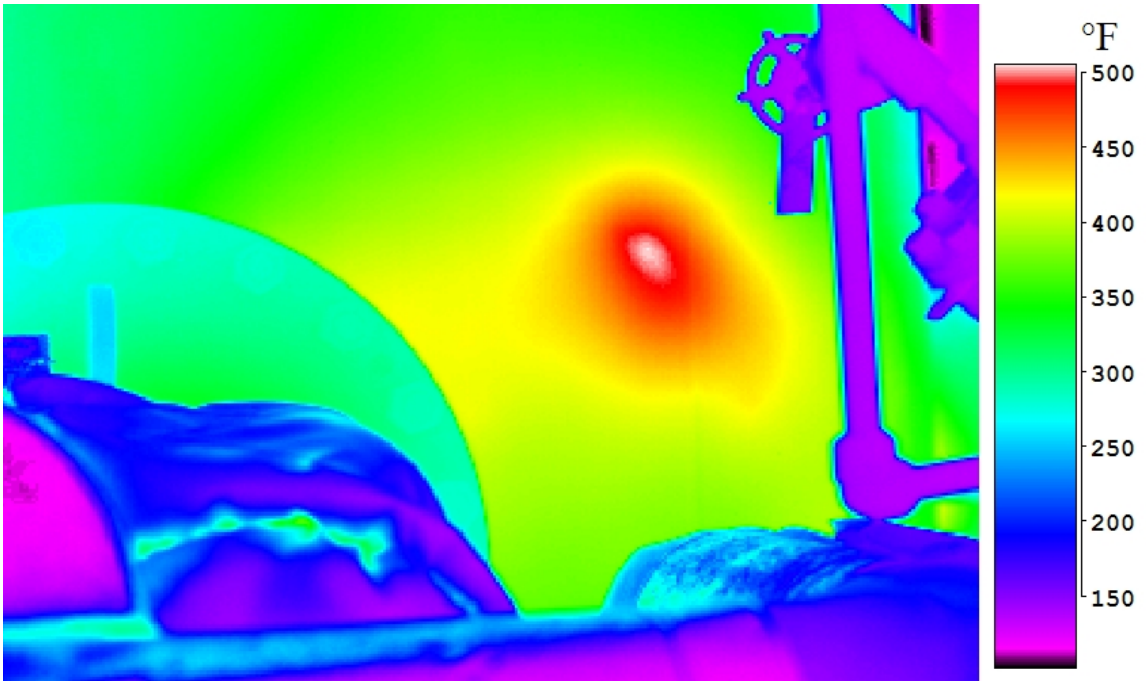

Figure 3.5-1 Sulfator Hotspot

3.6 PROCESS GAS COOLERS

Heat transfer calculations were done on the Primary Gas Cooler, HX0202, and the Secondary Gas Cooler, HX0402, to determine if their performance had deteriorated during TC13 due to tar or other compounds depositing on the tubes.

The Primary Gas Cooler, HX0202, is between the transport reactor cyclone, CY0201, and the Siemens Westinghouse PCD, FL0301. During TC13, HX0202 was not bypassed, and took the full gas flow from the transport reactor. The Primary Gas Cooler is a single pass heat exchanger with hot gas from the transport reactor flowing through the tubes and the shell side operating with the plant steam system. The pertinent equations are:

$$Q = UA\Delta T_{LM} \tag{1}$$

$$Q = c_p M(T_1 - T_2) \tag{2}$$

$$\Delta T_{LM} = \frac{(T_1 - t_2) - (T_2 - t_1)}{\ln \frac{(T_1 - t_2)}{(T_2 - t_1)}} \tag{3}$$

Q = Heat transferred, Btu/hour
U = Heat transfer coefficient, Btu/hr/ft^2/°F
A = Heat exchanger area, ft^2
ΔT_{LM} = Log mean temperature difference, °F
c_p = Gas heat capacity, Btu/lb/°F
M = Mass flow of gas through heat exchanger, lb/hr
T_1 = Gas inlet temperature, °F
T_2 = Gas outlet temperature, °F
$t_1 = t_2$ = Steam temperature, °F

Using Equations (1) through (3) and the process data, the product of the heat transfer coefficient and the heat exchanger area (UA) can be calculated. The TC13 HX0202 UA is shown on Figure 3.6-1 as 2-hour averages, along with the design UA of 5,200 Btu/hr/°F and the pressure drop across HX0202. If HX0202 is plugging, the UA should decrease and the pressure drop should increase. The UA deterioration is a better indication of heat exchanger plugging because the pressure drop is affected by changes in flow, pressure, and temperature.

The UA was above the design UA of 5,200 Btu/hr/°F for almost all of TC13, though the values varied wildly. The cause of the variation is due to the wide range of gasifier operating conditions during the run. The early air-blown operations saw steadily increasing gas flows accompanying steadily increasing values of UA. Initially the UA was about 5,500 Btu/hr/°F.

By the end of the early air-blown operations the UA had increased to 8,000 Btu/hr/°F. Upon transitioning to oxygen-blown operation, the UA dropped and was maintained between 5,500 and 6,500 Btu/hr/°F. After a short outage, the UA was 6,900 Btu/hr/°F after a return to air-blown operations. Over the next 125 hours, the UA steadily dropped to a value of 4,700 Btu/hr/°F during a period of cautious operations. The UA then climbed to a value of 6,500 Btu/hr/°F by the end of the test run. These values compare favorably to the UA of 5,100 Btu/hr/°F that was normal during TC12.

The pressure drop values for HX0202 in TC13 were not available for the first period of air-blown operation and for the oxygen-blown period because of an incorrectly purged or partially plugged pressure tap. During the second half of the run, the pressure drop was both steady and low, averaging about 0.6 psi., which is lower than the 0.5 to 1.2 psi in TC12.

The Secondary Gas Cooler, HX0402, is a single-pass heat exchanger with hot gas from the PCD flowing through the tubes and the shell side operating with plant steam system. Some heat transfer and pressure drop calculations were performed using HX0402 operating data to determine if there was any plugging or heat exchanger performance deterioration during TC13.

Using Equations (1) through (3) and the process data, the product of the heat transfer coefficient and the heat exchanger area (UA) can be calculated. The UA for TC13 testing is shown on Figure 3.6-2 as 2-hour averages, along with the design UA of 13,100 Btu/hr/°F. If HX0402 is plugging, the UA should decrease and the pressure drop should increase.

For most of TC13, the UA of HX0402 was slightly below the design of 13,100 Btu/hr/°F. As with HX0202, there was quite a bit of variability in the data for HX0402 due to the changing operating conditions during TC13. During the initial air-blown testing, the values ranged from 12,500 to 13,800 Btu/hr/°F with a general increase in UA as the total gas flow rate increased. After transitioning to oxygen-blown testing, the UA dropped to 11,100 to 12,200 Btu/hr/°F. When air mode operation resumed, the value ranged generally from 12,000 to 13,000 Btu/hr/°F. The TC13 data compares well with the data from TC12. The TC13 average during air-blown operation was slightly lower than the average of 13,500 Btu/hr/°F in TC12 and slightly higher than the average of 10,500 Btu/hr/°F in TC12 in oxygen-blown operation.

The HX0402 pressure drop changed significantly during TC13 as the gas flow rate changed with operations. There were no signs of plugging and the pressure drop ranged from 1.5 to 2.6 psi.

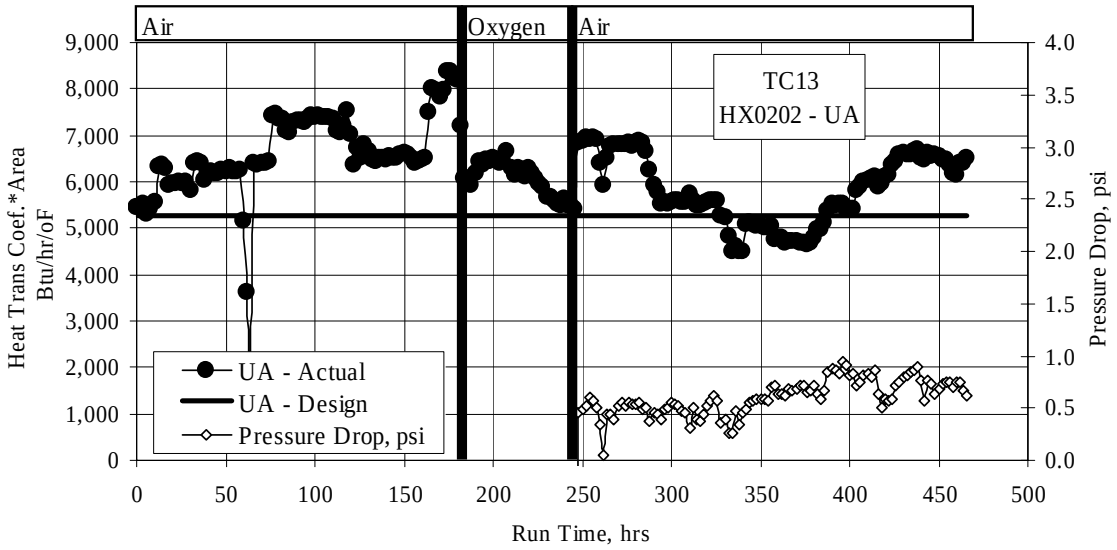

Figure 3.6-1 HX0202 Heat Transfer Coefficient and Pressure Drop

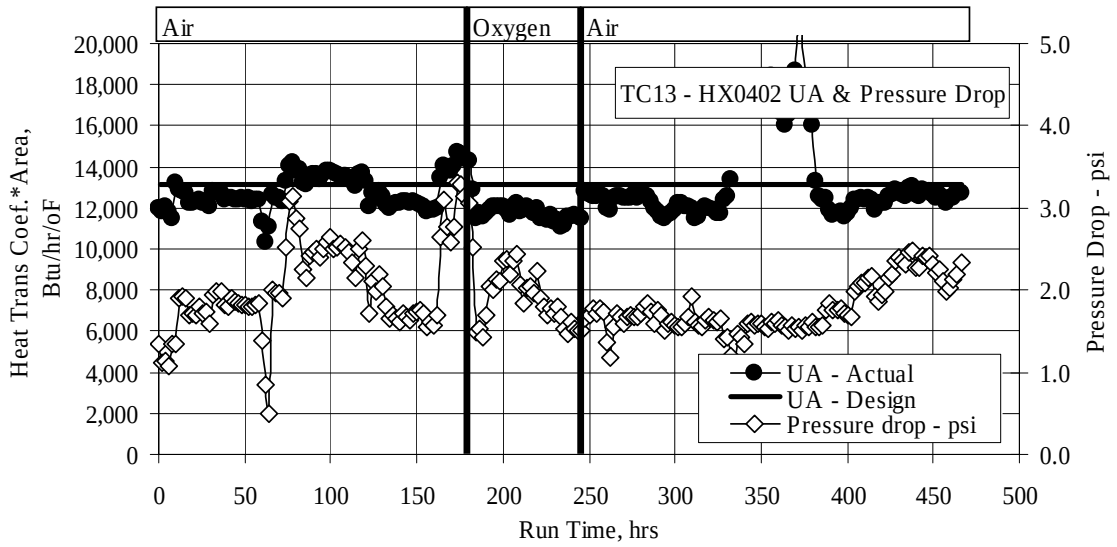

Figure 3.6-2 HX0402 Heat Transfer Coefficient and Pressure Drop

4.0 PARTICLE FILTER SYSTEM

4.1 RUN OVERVIEW

TC13 was an opportunity to evaluate the effects of two types of lignite coals on PCD performance and operation. Both high- and low-sodium versions of Freedom North Dakota lignite were gasified after initial startup on PRB coal. Prior to the test, there were concerns about the high-sodium lignite causing problems in the PCD because of sticky dustcakes, but this was not realized. In general, TC13 was characterized by stable PCD operation with low pressure drop. However, laboratory measurements indicated that there were differences in the flow resistance characteristics of the gasification ashes produced by the three coals.

PCD particle emissions were generally low although slightly elevated emissions were measured on two occasions. Emissions measured right after startup appeared to be mostly made up of trash particles from debris in the duct, while on the sixth day of the run an apparent small leak developed that resolved itself over a two day period.

Because of the lack of dust bridging problems in the PCD in recent test programs, tests were conducted duing TC13 to evaluate the effects of reduced back-pulse pressures and longer back-pulse cycle times on the PCD. Back-pulse cycle times as long as 20 minutes and pressures as low as 320 psid were used without obvious adverse impact on the PCD.

As discussed in the previous sections, there were three shutdowns during TC13, two due to gasifier circulation problems, and one due to a blown seal on the FD0502 screw cooler. Despite these and other disturbances in system conditions, no adverse effects were noted on the PCD. In total, 501 hours of on-coal operation were accumulated on the installed filters and failsafes.

Subsequent inspection of the PCD after the end of the test campaign indicated that there were no problems with dust bridging, and residual dustcakes were typically thin. As discussed in more detail later, the source of the small apparent leak on day six could not be identified.

The remainder of this section on PCD performance contains the following subsections:

- PCD Operations, Section 4.2 - This section describes the hardware configuration of the PCD, as well as the main events and operating parameters affecting PCD operation. Operation of the fines removal system is also included in this section.
- PCD Hardware Inspection and Analysis, Section 4.3 - The complete inspection performed following TC13 is discussed in this section including details of the post-run conditions of various PCD components and of the fines removal system. Flow resistance and strength measurements of filter elements are presented here.
- Gasification Ash (G-Ash) Characteristics and PCD Performance, Section 4.4 - This section includes a detailed discussion of measured PCD performance and particle emission rates. This section also includes g-ash physical and chemical properties, as well as an analysis of the effects of these characteristics on PCD performance.

4.2 PCD OPERATION

This section will describe the filter and failsafe layouts for TC13, the effects of coal-feed rate and coal type on PCD ΔP, results of back-pulse optimization testing, as well as problems with the PCD solids removal system.

4.2.1 Filter Elements and Failsafe Devices

The filter element layout for TC13 is shown in Figure 4.2-1. The installation included 36 Pall 1.5-m FEAL filter elements with fuses and 49 Pall 1.5-m FEAL filter elements without fuses. Seven of the filters were installed in Siemens Westinghouse inverted filter holders. Only Pall FEAL filter elements were installed during TC13. This was done because it was discovered in testing in the cold flow PCD model that the Pall Hastelloy X and HR160 filter elements had excessive levels of particle penetration during back-pulsing. Only Pall FEAL filter elements will be tested in the PCD until these issues with solids penetration through the filter media are resolved.

A semicircle of blanks were also installed in the lower plenum to evaluate the use of spacing changes to avoid bridging. This feature of the filter layout has been used since TC08, but dust bridging has not occurred since then so the effectiveness of this technique has not been validated yet.

The following table outlines the exposure hours of the Pall FEAL filter elements that were installed for TC13.

Exposure Hours after TC13	Number of FEAL Filters Exposed
4,223	4
3,753	2
2,810	23
2,150	1
1,842	10
1,426	44
1,234	1

Commercial viability will require filter elements that can operate for at least 1 year. As shown in the table, a few of these elements are now at approximately half that level with no failures during on-coal operation. Flow test and strength test results for selected filters will be discussed in the subsequent section covering the post-run activities.

Figure 4.2-2 shows the layout of the failsafe devices installed for testing during TC13. The failsafes that actually were in use as safety devices were:

- 47 PSDF failsafes.
- 35 Pall FEAL fuses.
- 3 Siemens Westinghouse ceramic failsafes with CeraMem media.

The PSDF designed failsafe utilizes different alloys as its filter media. The following table outlines the different alloys that were tested during TC13 with its corresponding total gasification exposure time:

PSDF Failsafe Filter Media Alloy	Total Gasification Exposure, Hours	Number Tested During TC13
Haynes 230	3,981	1
Fechralloy Hoskins 875	2,808	1
Haynes HR-160	2,808	1
Haynes HR-160	2,820	1
Haynes HR-160	2,513	2
Haynes HR-160	2,149	1
Haynes HR-160	1,841	27
Haynes HR-160	1,233	3
Haynes 188	2,149	4
Haynes 214	2,149	3
Haynes 556	2,149	2
Haynes 556	2,062	1

These different media will be monitored and flow tested after each run to determine if corrosion or plugging/blinding is more prevalent with some types of alloy/designs than with others.

Inspection and flow testing of selected failsafes after the completion of TC13 is discussed in a subsequent section of this report (Section 4.3).

4.2.2 General Operation and PCD Pressure Drop

The PCD setup and operating parameters for TC13 are summarized in Table 4.2-1. Particle collection performance of the PCD was generally good although a small leak developed on day six of the test campaign. This leak gradually cleared up over the next 48 hours until the outlet emissions were below the lower measurement limit. This will be discussed in more detail in subsequent sections.

Figure 4.2-3 shows the normalized baseline and peak pressure drops for the PCD during TC13. The periods of operation with PRB and the low- and high-sodium lignite coals are indicated on the figure. Three forced outages occurred during the run, two of which were associated with plugging of the gasifier loopseal related to the high-sodium lignite coal and were not associated with the PCD. One outage occurred because of a leak in the shaft packing on the FD0502 screw cooler, which is located below the PCD hopper. This is considered to be a piece of PCD-related equipment, and this event will be discussed in the later section on PCD inpections and hardware analysis.

Analysis of the PCD pressure drops in Figure 4.2-3 indicates that the baseline pressure drop generally remained below 80 inWC. Some initial baseline creep was obvious in the first days of the run as a stable residual dustcake was established.

Wide variations are seen in peak ΔP indicating differences in the PCD ΔP rise rate. The majority of these variations are caused either by changes in back-pulse timer settings (discussed in the following section) or by changes in particle loading entering the PCD which can largely be related to coal feed to the gasifier. The effect of coal-feed rate can be clearly observed during the operating period from October 24 through 29 where each of the step changes in PCD ΔP can be related to an increase in coal feed. Baseline ΔP can also be seen to be affected by the increases in coal feed.

Comparison of the periods with the three different coal types does not suggest dramatic differences in PCD operation related to the characteristics of the coal. The flow resistance and physical characteristics of the dusts generated from the three coals will be further evaluated in Section 4.4. That analysis will show that there were differences in these coals that were masked by changes in coal-feed rate, etc.

4.2.3 Back-Pulse Optimization

During recent previous test programs, back-pulse pressures were high and back-pulse time short to prevent a reoccurrance of dust bridging in the PCD. Back-pulse pressures had been kept at 400 psi above duct pressure (psid) for the upper plenum and at 600 psid for the lower plenum. The ratio of these pressures is roughly equivalent to the relative numbers of filter elements in each plenum. However, such frequent and hard pulses were felt to have a number of detrimental effects on the operation of the gasifier and on PCD hardware and cost.

Dust bridging had not been encountered in the PCD since TC09 on bituminous coal and not since TC06 with PRB coal. In addition, changes in gasifier operation had reduced the levels of tar-like substances in the syngas, which were a prime suspect for contributing to bridging problems by making the dust cake sticky. It now seemed clear that bridging could be avoided with very aggressive pulse cleaning and it was determined that efforts would be made in TC13 to define the minimum limits on effective pulse cleaning.

During TC13, the back-pulse pressures were reduced to 320 psid for the upper plenum and 400 psid for the lower plenum. The back-pulse timer was varied from 5 to 20 minutes depending on the dust loading entering the PCD. The variation in timer setting can be seen in Figure 4.2-4, which plots the back-pulse time along with peak and baseline ΔP as a function of time throughout TC13. During startup and outages the timer was set to 30 minutes. During operation on coal, the most prevalent timer setting was 15 minutes. When coal feed was high (running the fluidized-bed feeder, FD0200) and the particle mass entering the PCD was high, the timer generally had to be reduced to 10 minutes to prevent exceeding the maximum tube sheet ΔP of 275 inWC. (The downward spike labelled "High ΔP Trigger" on the graph indicates a period of very high coal feed where the back-pulse was triggered by the high ΔP limit prior to manually changing the timer.) The timer was reduced to 5 minutes on several occasions during gasifier upsets and prior to coal type changes in anticipation of problems.

During one period of very low coal feed the timer was increased to 20 minutes without adverse effects.

Overall, there were no obvious adverse effects from operating with longer back-pulse intervals or with lower back-pulse pressures. Although not quantifiable, the consensus of the gasifier team was that the lower pressure and longer time between back-pulses was good for gasifier operation. Efforts to optimize back-pulse parameters will continue in future test programs.

4.2.4 PCD Solids Removal System Problems

Because of past problems with seal failures on the sphere valve located on the PCD dust discharge system, a rotating disk valve made by the Everlasting Valve Company was installed above the sphere valve. The rotating disk valve was believed to be a more reliable design that did not have resilient seals, which could be a source of leaks. Unfortunately, the Everlasting valve failed to operate on several occasions resulting in the valve being left open and solids flow control was returned to the sphere valve. Apparently, gasifier upsets resulting in heavy bed material carryover, caused solids packing in the Everlasting valve that blocked the movement of the disk. Despite these problems, the dust discharge system was operational throughout the run.

On October 28, 2003, the drive-end seal failed on the FD0502 screw cooler that cools the dust collected in the PCD before it enters the dust discharge system. The seal was last modified before TC07 and had accumulated 2,727 hours of gasification operation before failure. A gasifier outage was required to replace the seal.

Additional discussion of both dust removal system problems and the lessons learned from these failures can be found in the section on hardware inspection and analysis (Section 4.3).

Table 4.2-1

PCD Operating Parameters

Number of Filter Elements	85
Filter Element Layout Number	29 (Figure 4.2-1)
Filtration Surface Area	241.4 ft^2 (22.4 m^2)
Pulse Valve Open Time	0.2 Seconds
Pulse Time Trigger	5 to 20 Minutes
Pulse Pressure, Top Plenum	320 psi Above System Pressure
Pulse Pressure, Bottom Plenum	400 psi Above System Pressure
Maximum ΔP Trigger	275 inWC
Inlet Gas Temperature	~600 to 800°F (135 to 425°C)
Filter Face Velocity	~ 3.0 to 4.5 ft/min (1.5 to 2.2 cm/sec)
Inlet Particle Loading	~5,700 to 41,300 ppmw
Outlet Particle Loading	<0.1 to 2.5 ppmw
Baseline Pressure Drop	~50 to 75 inWC (125 to 190 mbar)

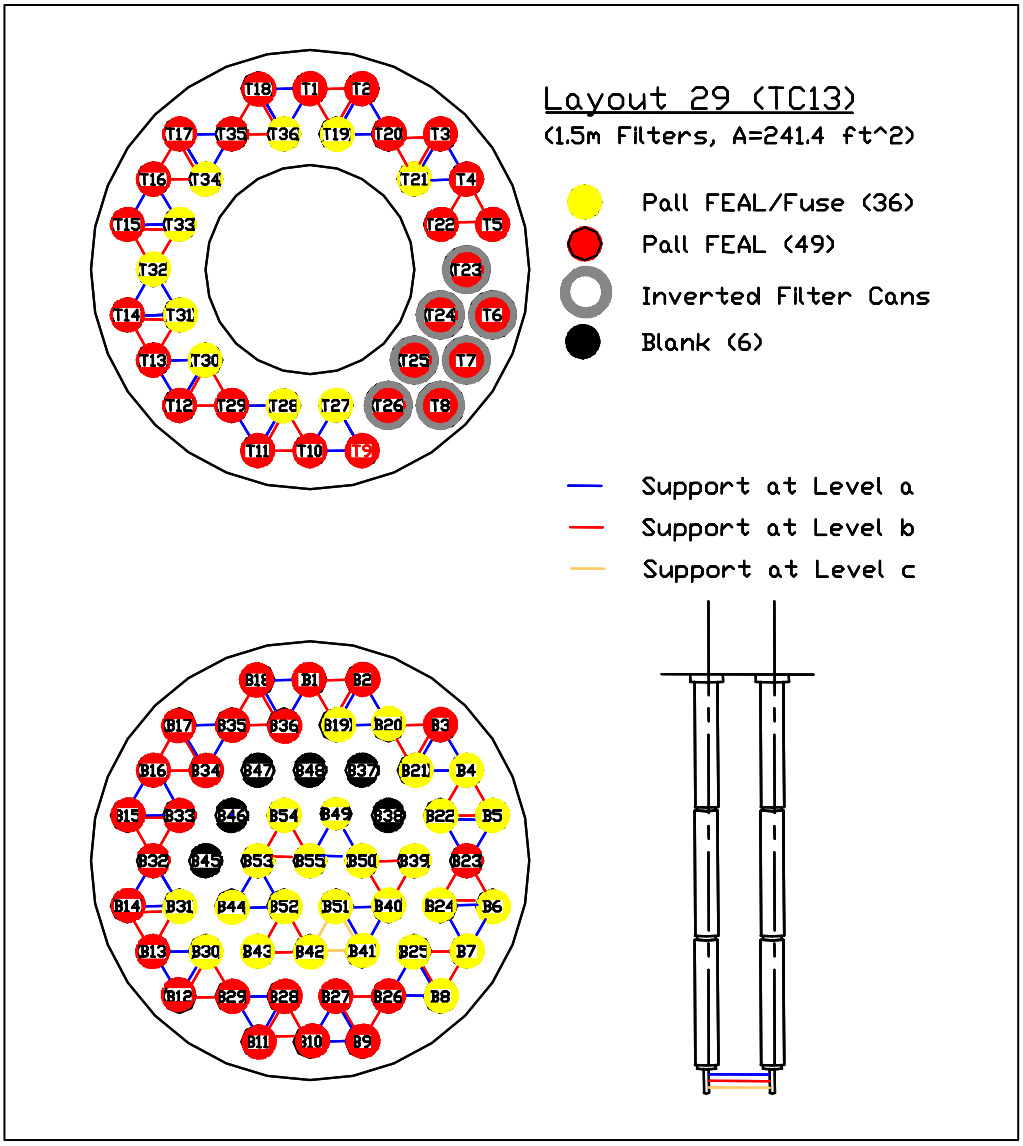

Figure 4.2-1 PCD Filter Element Layout

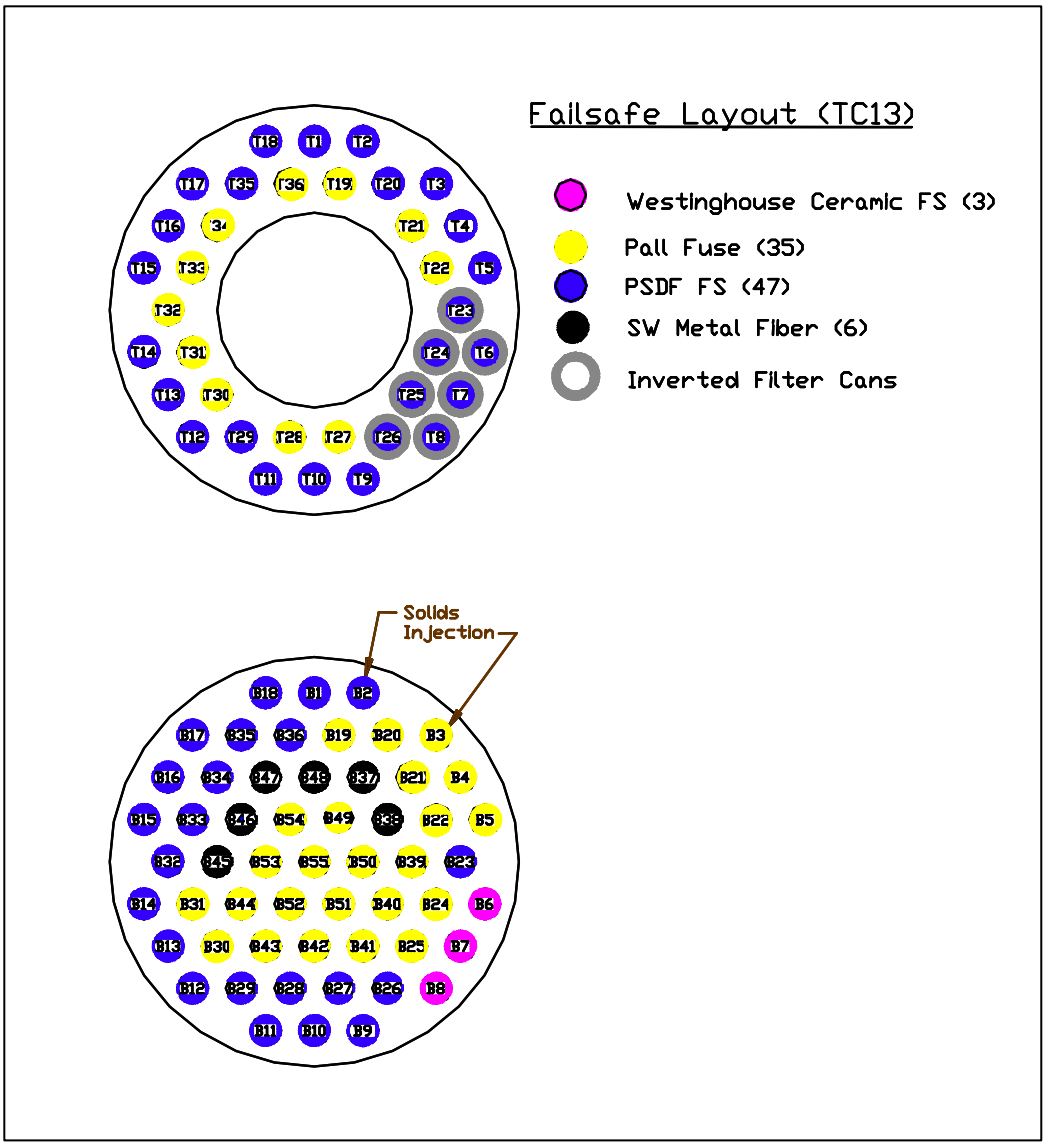

Figure 4.2-2 Westinghouse PCD Failsafe Layout

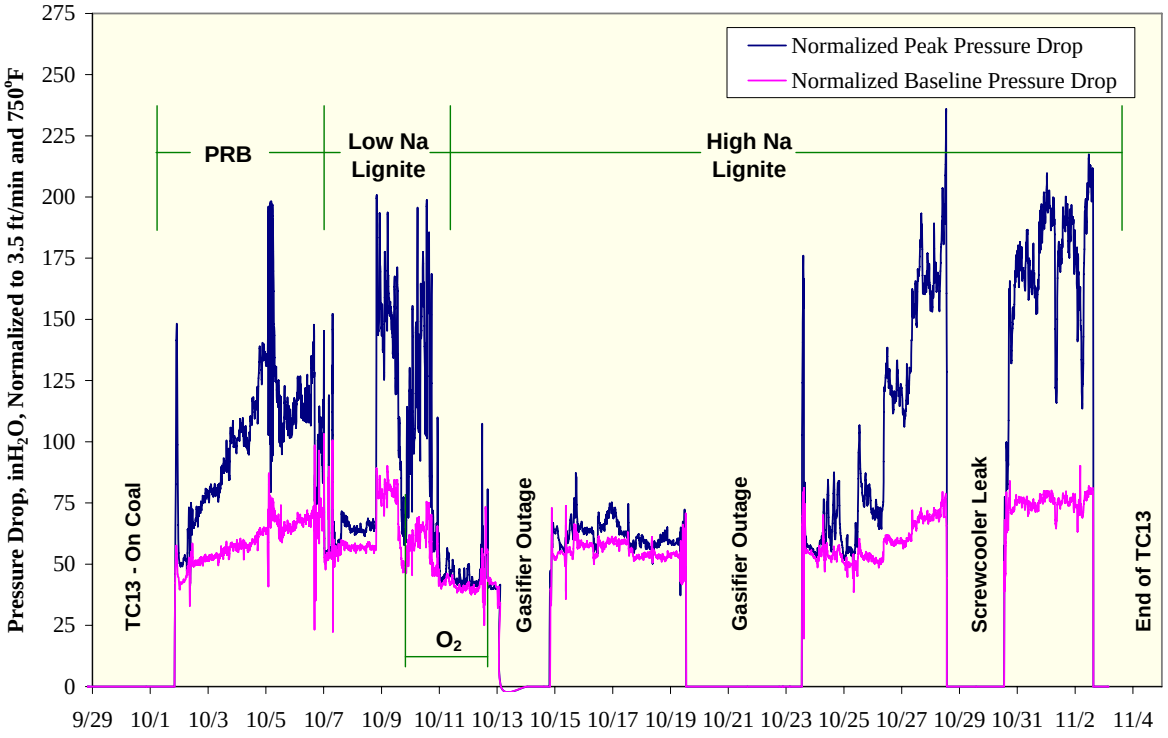

Figure 4.2-3 PCD Normalized Pressure Drops

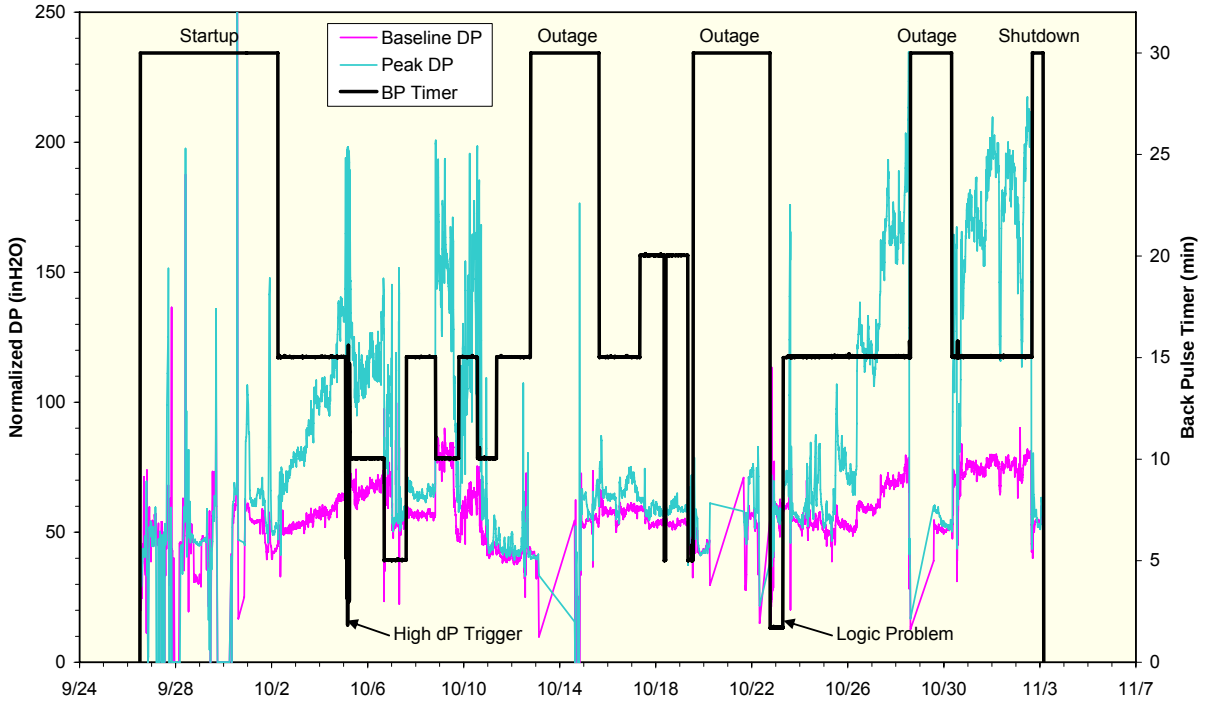

Figure 4.2-4 PCD Pressure Drop and Effect of Back-Pulse Timer

4.3 PCD HARDWARE INSPECTION AND ANALYSIS

During the TC13 outage, the PCD internals were removed from the vessel and inspected. The outage inspection included examinations of the filter elements, their fixtures to the plenums, solids deposition, and auxiliary equipment. Filter elements and failsafe devices were removed and tested for both flow resistance and strength. The subsequent sections will detail the analysis of the hardware components of the PCD system.

4.3.1 Filter Element and Seal Leaks

As mentioned previously, an elevated outlet loading (0.25 ppmw – see Section 4.4) suddenly occurred in the middle of the test program. The outlet loading did return to below the detection limit within a couple of days; therefore, we suspected that there could be a legitimate leak through one of the filter elements or filter gaskets. In order to locate the source of particle penetration, all filter elements and failsafe devices were removed from the PCD for inspection and testing. The intent was to locate a failsafe that had an increased flow resistance, which would indicate a plugged failsafe device. Each filter element was closely inspected visually with no damage noted. The welds were examined without finding any separation from the filter media or cracks.

In this PCD design, leakage through the fiber gaskets used to seal the filter elements to the tube sheet could also cause elevated particle loading. During the inspection, each of the filter gaskets was inspected. Figure 4.3-1 shows these gaskets on the bottom plenum after TC13. The gaskets appeared to be undamaged with no streaks of particulate that would indicate obvious particle penetration. Also, as discussed in the next two sections, neither the Pall filters with internal failsafes nor the stand-alone failsafes had flow resistance values that suggested that any one failsafe was plugged because of a filter element leak. It is possible that there was a leak past one of the gaskets that seals the failsafe to the PCD tube sheet. If solids penetrated through the tube sheet gasket, then they would have bypassed the failsafe device. Inspection of these gaskets is problematic as they are badly disturbed on disassembly. The reason for the elevated particulate loading during TC13 is not resolved at this time.

4.3.2 Filter Element Flow Resistance Evaluation

Forty-two Pall FEAL filter elements removed after TC13 were flow tested. Thirty-six of these filters had an internal fuse while six did not. Hours on these elements ranged from 1,234 to 4,223. All flow tests were conducted using air at ambient temperature. Loose char was blown off the outside surfaces with compressed air before flow testing, but the filter elements were not water-washed or chemically cleaned.

Results for the elements with a fuse are shown in Figure 4.3-2 as a plot of pressure drops versus face velocities. At a face velocity of 3 ft/min, the pressure drops ranged from 19 to 32 inWc except for one element which had a much lower pressure drop of 12 inWc. These elements in virgin condition had pressure drops of 4 to 7 inWc at a face velocity of 3 ft/min. All flow-test results for FEAL elements with a fuse after gasification operation are compared in Figure 4.3-3, which shows the pressure drops measured at a face velocity of 3 ft/min versus hours in operation. Some individual elements have been removed and flow tested after several

gasification runs and the pressure drops measured on these elements are plotted versus hours in operation in Figure 4.3-4. Figure 4.3-4 shows that the residual pressure drop on most elements has increased since the first time they were tested after gasification operation. The changes in pressure drop may result from different operating or shutdown conditions for each run, however, these elements will be tested after each gasification run to determine if the flow resistance is actually increasing with time.

A plot of pressure drops versus face velocities for elements without a fuse is shown in Figure 4.3-5. At a face velocity of 3 ft/min, the pressure drops ranged from 6 to 15 inWc. These elements in virgin condition had pressure drops of 2 to 3 inWc at a face velocity of 3 ft/min. All flow-test results for FEAL elements without a fuse are compared in Figure 4.3-6, which shows the pressure drops measured at a face velocity of 3 ft/min versus hours in operation. The elements tested with the most hours had the highest pressure drops; however, there are far too few tests to determine if the flow resistance is increasing with operation or if the differences seen in this figure are the result of differences in operating and shutdown conditions or simply element-to-element variability.

Low powered photomicrographs of cross sections of both the main body and fuse of Filter Element 39151 are shown in Figures 4.3-7 and 4.3-8. The faces shown in these figures were fracture surfaces obtained by snapping a c-shaped section in two by hand. Very little particulate is seen in the pores of the main body of the element, but there is much more particulate in the pores of the fuse. The higher porosity and larger pore size of the fuse allows particles to pass more deeply into the fuse and then become lodged. This leads to the greater increase in flow resistance in the elements with a fuse. The mechanism for particles getting to the fuse is not known. This element was in operation during some runs with Hastelloy X and HR160 sintered fiber elements suspected of excessive penetration, so the particles could have come from those runs.

4.3.3 G-Ash Deposition

Figure 4.3-9 shows the upper and lower plenums with attached filter elements being removed from the PCD vessel after TC13. There was no dust bridging present nor was there any evidence that bridging had been present prior to shutdown. The shutdown was "clean," which means that the both the top and bottom plenums were back-pulsed after shutdown. The average residual dustcake thickness was ~0.010 inches, which is consistent with other gasification runs. The inspection revealed that the dust buildup on the filter element holders, upper and lower ash shed, and filter element support brackets was not very significant. The thin residual dust cake on the filter elements and the small buildup on the different PCD internals indicate that tar condensation was not a problem during TC13.

Seven prototype inverted filter element assemblies supplied by Siemens Westinghouse have been installed in the PCD since TC08. Figure 4.2-1 shows their position on the top plenum. Inspection after TC13 showed no indication of dust leakage or bridging. Therefore, further testing will continue in TC14.

4.3.4 Failsafe Evaluation

As discussed in a previous section (Section 4.2), six different filter materials were used with the PSDF failsafes. After TC13, all 47 of these devices were removed for evaluation. One of the test objectives for the PSDF-designed failsafe is to determine whether or not the different alloys of the porous material blinds over time. Each failsafe was flow tested and inspected under the microscope. Neither the flow test nor the visual inspection revealed that any of the alloys of PSDF-designed failsafe device are blinding due to some corrosion reaction. Also, this inspection did not reveal any abnormalities that might indicate a filter element or filter gasket leaked during TC13. Therefore, these failsafe devices will be reinstalled for further testing during TC14.

During TC13, three second-generation Siemens Westinghouse ceramic failsafes were exposed to syngas in the PCD. Further testing on these ceramic failsafe devices is important, since interest in high-temperature sorbents for ammonia and tar cracking continues to increase. The projected temperature range for these sorbents is 1,300 to 1,400°F. Therefore, high temperature materials for filter media need to be developed and tested. After TC13, the ceramic failsafes were visually inspected and flow tested. No damage was noted on any of the failsafes during the inspection. The differences between the flow tests before and after TC13 were negligible (See Figures 4.3-10 through 12). To date, these failsafe devices have accumulated approximately 1,431 hours of gasification operation. The ceramic failsafe devices will be reinstalled for further testing in TC14.

4.3.5 Back-Pulse Pipe Inspection

The back-pulse pipes were removed and inspected during this outage. There was no significant damage noted on the back-pulse pipes. The inner liner appeared to be in good condition (See Figure 4.3-13). In the past some pitting has been noted on the back-pulse pipes near the flange. The pitting did not appear to be any worse than after the last outage. There was, however, a thin layer of condensed tar on the pipe, which has been a concern from a corrosion standpoint. It does not appear that these tars are detrimental to the back-pulse pipes. These pipes have been exposed to over 3,500 hours on-coal gasification operation without any significant signs of corrosion.

4.3.6 PCD Screw Cooler Leak

Before TC07 several modifications were made to the drive-end stuffing box to increase reliability. These modifications were documented in the TC07 run report. Since the modifications improved the performance during TC07, similar changes were implemented to the nondrive-end before TC08. FD0502 has performed well since the modifications were applied.

On October 28, 2004, the drive-end seal on FD0502 blew out, which required the process to shut down. The drive-end of FD0502 accumulated 2,727 on-coal hours before it failed. One of the methods that has been used to determine the success of the new stuffing box modifications is tracking the packing follower gap. The follower is used to compress the shaft seal rings to establish a purge pressure seal to prevent process gas from leaking past the shaft. Once there is no more room to compress the follower, it is time to replace the seals. The packing follower gap on the drive-end, before it failed, was 0.5 inches. Therefore, in the future once the gap

approaches 0.5 inches, the packing will be replaced so a seal failure will not interrupt plant operations.

The nondrive-end packing follower gap was approximately 0.8 inches. It was decided to replace the nondrive-end packing, since FD0502 was disassembled during the outage. The nondrive-end packing appeared to be in good condition. The nondrive-end packing had accumulated over 2,500 hours of on-coal operations.

Although the drive-end seal failed during TC13, the seal modifications are seen as a promising improvement to FD0502 operations. Before TC07, the seals on FD0502 were replaced during each outage, because there was no confidence that the seals would maintain their integrity from one run to the next. Therefore, the seal modifications have significantly increased the reliability of FD0502. During the outage, both the drive-end and nondrive-end seals were replaced for TC14.

4.3.7 PCD Solids Depressurization System

The fine solids depressurization system (FD0520) required a lot of attention from operations, maintenance, and process engineering during TC13. The conveying line between FD0520 and FD0530 was found to be eroded on two occasions, requiring the line to be repaired. Also, as mentioned in the PCD operations section, the Everlasting rotating-disk valve failed to cycle on many occasions throughout the run.

Prior to TC11, the conveying line between FD0520 and FD0530 was modified in order to prevent the conveying line from plugging, and improve accessibility to the line. Therefore, the long radius bends were replaced with 45-degree laterals, which had purge ports at each bend for access. However, the line modifications exacerbated the erosion problems within this line. During TC13, one of the 45-degree laterals eroded. During the outage, the wall thickness along the conveying line was inspected. The original pipe wall thickness was 0.5-inches. But the wall thickness around the area where the solids impacted was ~0.3 inches. Therefore, it was decided to replace the 45-degree laterals with 90-degree T-bends.

The rotating-disk valve installed above the PCD dust removal system that was discussed in Section 4.2 did not operate reliably during TC13. The valve was removed during the outage and inspected. There was a large amount of solids within the valve cavity. It is believed that the problem of the valve binding can be alleviated by installing an automatic purge that fluidize the material when the valve actuates. Inspection of the Everlasting valve seat revealed no signs of erosion.

During the outage, the vent valves on FD0520 were removed and inspected. There was no sign of erosion. When periods of high solids carryover to the PCD occur, the FD0520 system can be overwhelmed. The bypass line around the FD520 system that was installed to help alleviate this problem was cycled many times during TC13. Inspection during the outage revealed no sign of erosion in the conveying line or the isolation valves.

4.3.8 Filter Material Test Results

Pall PSS FEAL iron aluminide (Fe_3Al) element 39151 was removed after TC13 with 3,753 hr in gasification operation and tested. This element was first installed for operation in TC06B and remained in operation during all runs through TC13. A material description of the Pall PSS FEAL elements was provided in previous reports and is not repeated here.

The element was tested according to the test matrix shown in Table 4.3-1. Specimens required to conduct the testing were removed from the element as shown on the cutting plan of Figure 4.3-14. Specimen configurations are shown in Figures 4.3-15 and 4.3-16. The same specimen configurations and test methods were used as in previous test programs.

Room temperature and 750°F axial tensile stress-strain responses are shown in Figure 4.3-17, and room temperature hoop tensile stress-strain responses are shown in Figure 4.3-18. All results are summarized in Tables 4.3-2 and 4.3-3. Tensile strength and strain-to-failure are plotted versus hours in operation in Figures 4.3-19 and 4.3-20. Results from all previously tested FEAL elements are also shown in these figures. The axial results indicate no degradation in either the strength or ductility up to 3,753 hrs in gasification operation at a nominal temperature of 700 to 1,000ºF with most operation between 700 and 800ºF. The hoop tensile strength was ~30 percent lower than the average hoop strength of all previously tested elements. There has been some variability in strengths from the FEAL elements and this lower strength may represent variability and not degradation. Another FEAL element with a similar number of gasification hours will be tested soon to verify that the lower hoop tensile strength of this element is a result of element-to-element variability and not degradation.

Table 4.3-1

Test Matrix for Filter Element 39151

Test	Orientation	Replications at	
		Room Temperature (RT)	750°F
Tension	Axial	3	3
Tension	Hoop	3	

Table 4.3-2

Axial Tensile Test Results for Pall PSS FEAL Element 39151

Element	Specimen Number	Hours in Operation	Test Temperature (°F)	0.05% Yield Strength (psi)	Ultimate Strength (psi)	Young's Modulus (msi)	Strain-to-Failure (mils/in.)
39151	Tn-Ax-112	3,753	RT	13.3	14.5	5.21	3.7
39151	Tn-Ax-114	3,753	RT	11.8	14.2	5.18	4.5
39151	Tn-Ax-116	3,753	RT	13.8	15.2	4.24	4.8
	Average			13.0	14.6	4.88	4.3
39151	Tn-Ax-113	3,753	750	9.8	14.6	4.18	9.1
39151	Tn-Ax-115	3,753	750	9.4	14.6	4.73	9.3
39151	Tn-Ax-117	3,753	750	10.1	15.7	4.05	11.6
	Average			9.8	15.0	4.32	10.0

All operation at SCS-PSDF in gasification mode. Nominal operating temperature was 700 to 1000°F.

Table 4.3-3

Room Temperature Hoop Tensile Test Results for Pall PSS FEAL Element 39151

Element	Specimen Number	Hours in Operation	Maximum Hydrostatic Pressure (psig)	Ultimate Strength (psi)	Young's Modulus (msi)	Maximum Strain at O.D. (mils/in.)	Remarks
39151	Tn-Hoop-435	3,753	830	12,210	5.05	2.67	
39151	Tn-Hoop-436	3,753	670	10,250	5.13	1.97	
39151	Tn-Hoop-437	3,753	510	7,850	5.34	1.39	
39151	Tn-Hoop-438	3,753	670	10,880	5.06	2.17	
39151	Tn-Hoop-439	3,753	700	11,650	4.56	2.65	
39151	Tn-Hoop-440	3,753	760	11,860	4.98	2.67	
Average			690	10,783	5.02	2.25	
Standard Deviation			98	1,463	0.23	0.47	
Coefficient of Variation (COV)			14%	14%	5%	21%	

All operation at SCS-PSDF in gasification mode.
Nominal operating temperature was 700 to 1000°F.

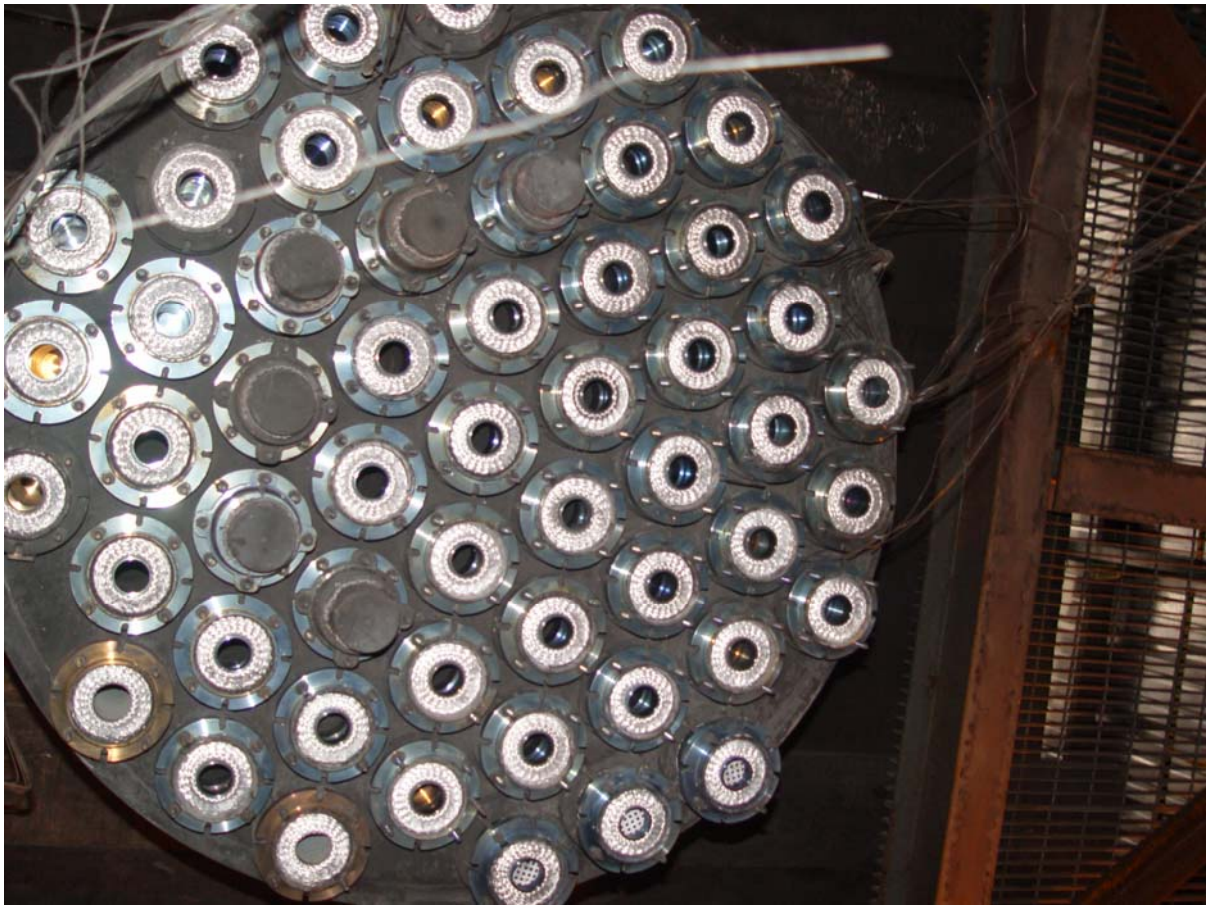

Figure 4.3-1 Primary Filter Gaskets on the Lower Plenum After TC13

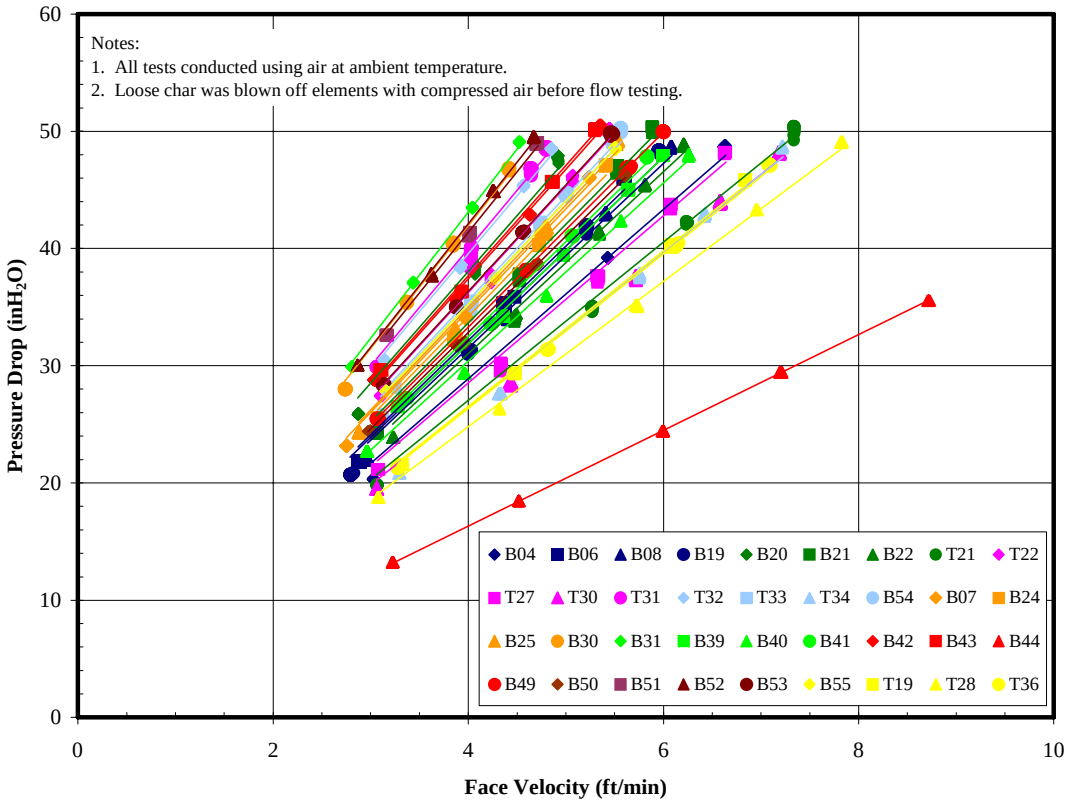

Figure 4.3-2 Pressure Drop Versus Face Velocity for Pall FEAL Elements With a Fuse After TC13

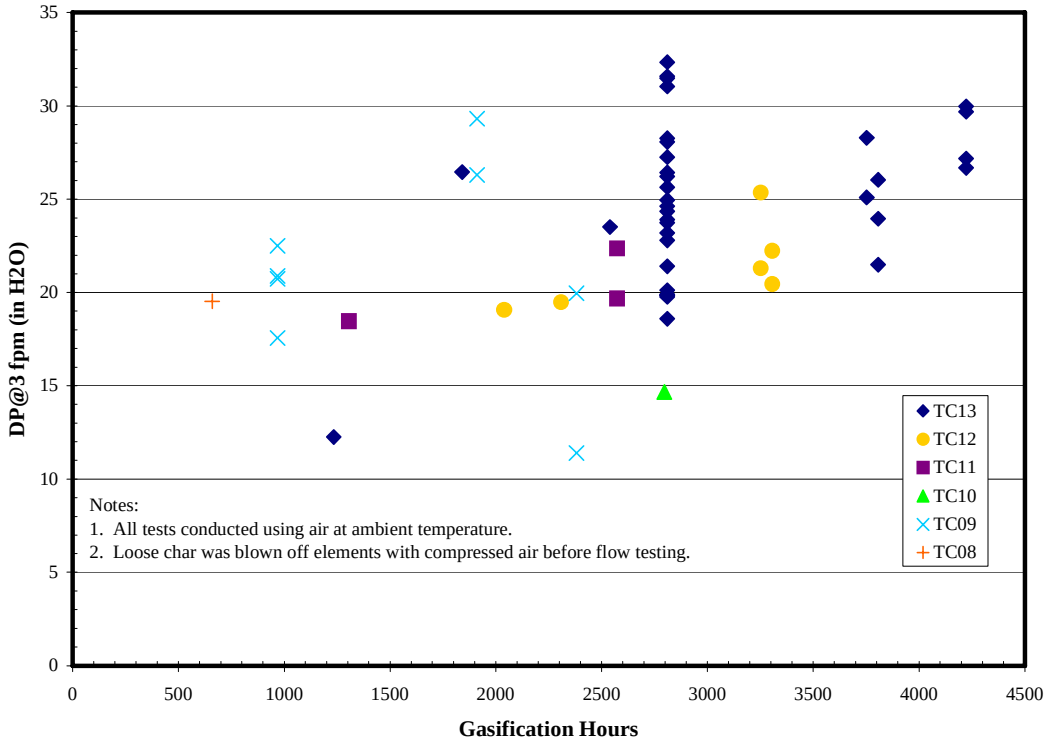

Figure 4.3-3 Pressure Drop at 3 ft/min Face Velocity for Pall FEAL Elements With a Fuse

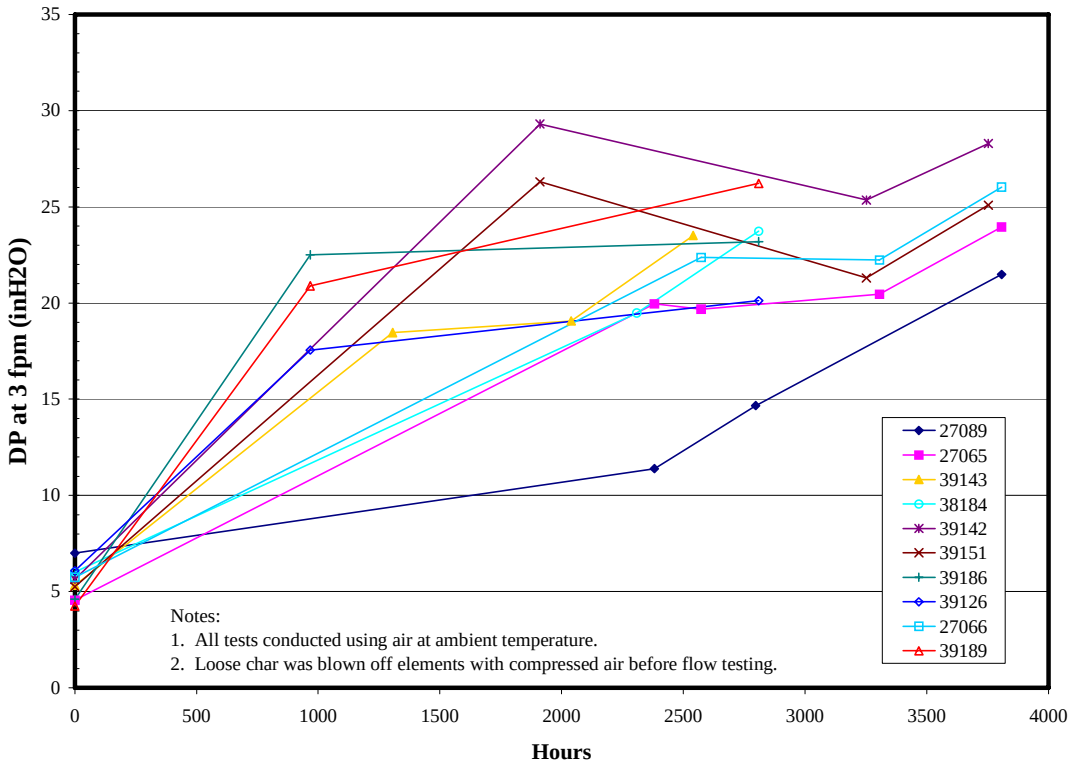

Figure 4.3-4 Pressure Drop at 3 ft/min Face Velocity for Pall FEAL Elements With a Fuse

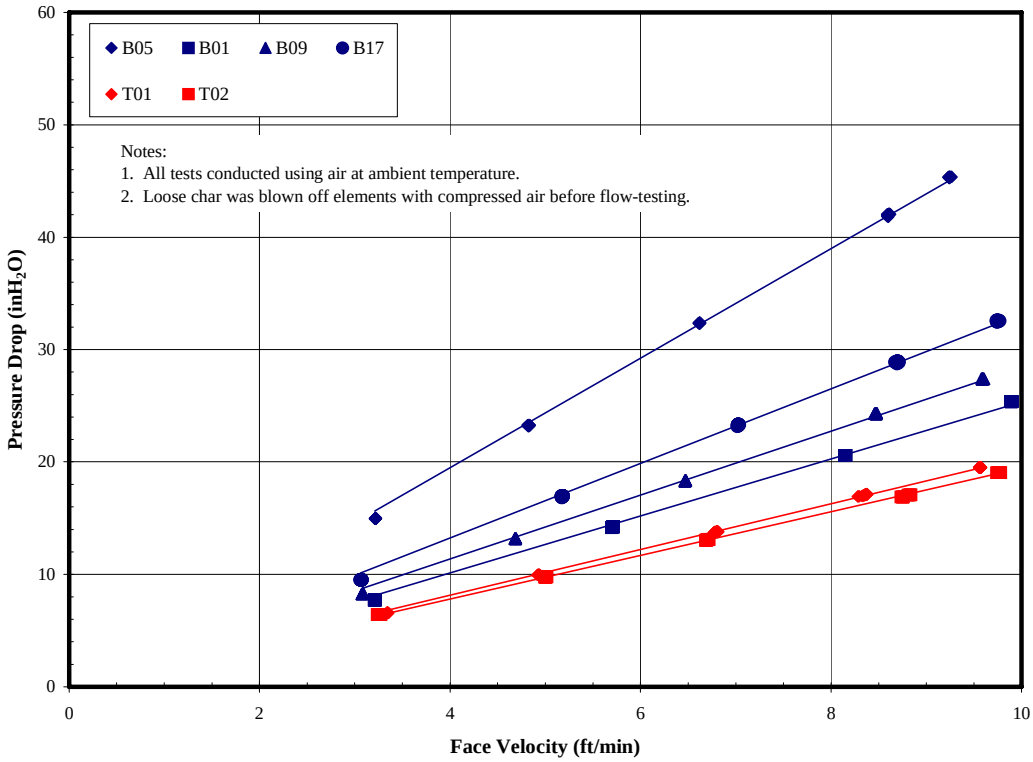

Figure 4.3-5 Pressure Drop Versus Face Velocity for Pall FEAL Elements With No Fuse After TC13

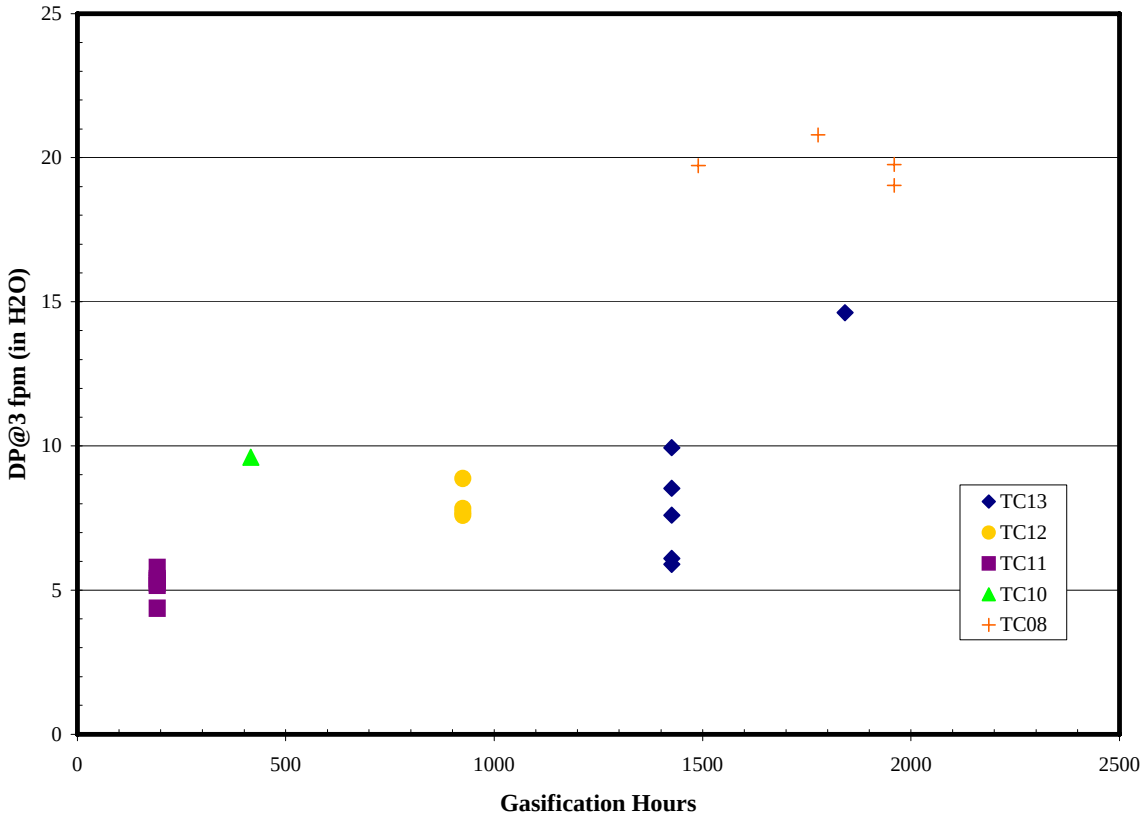

Figure 4.3-6 Pressure Drop at 3 fpm Face Velocity for Pall FEAL Elements Without a Fuse

Figure 4.3-7 Cross-Section of the Main Body of Element 39151 After TC13

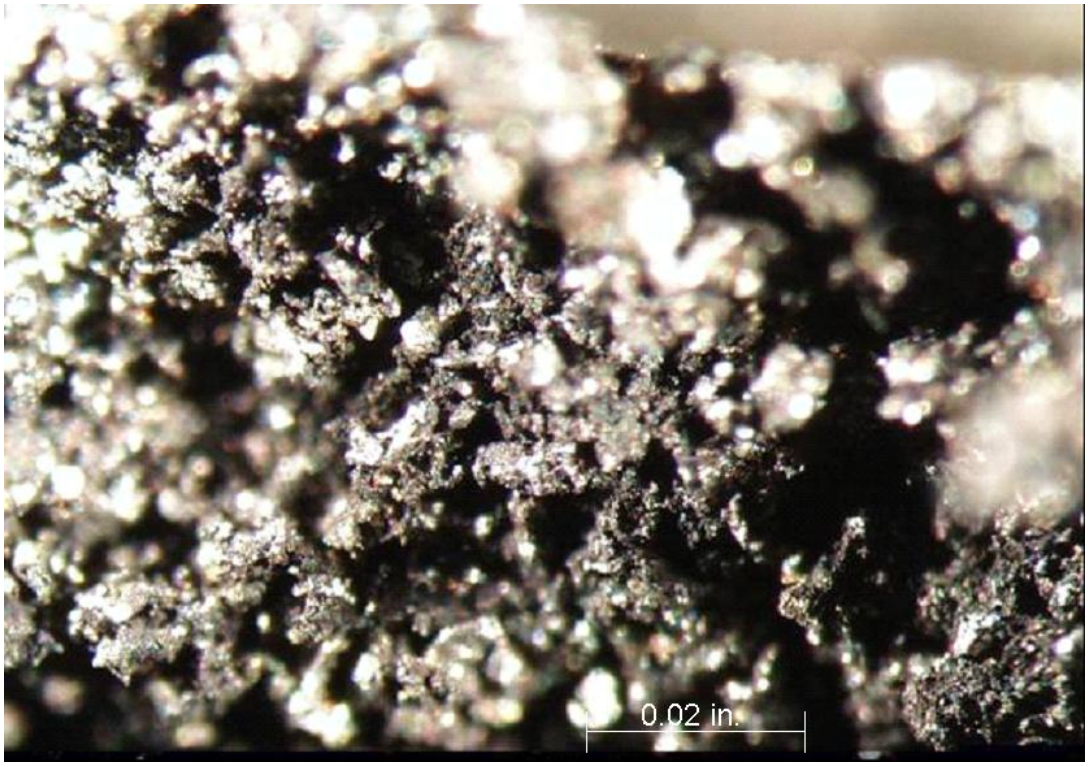

Figure 4.3-8 Cross-Section of the Fuse of Element 39151 After TC13

Figure 4.3-9 Filter Internals After TC13

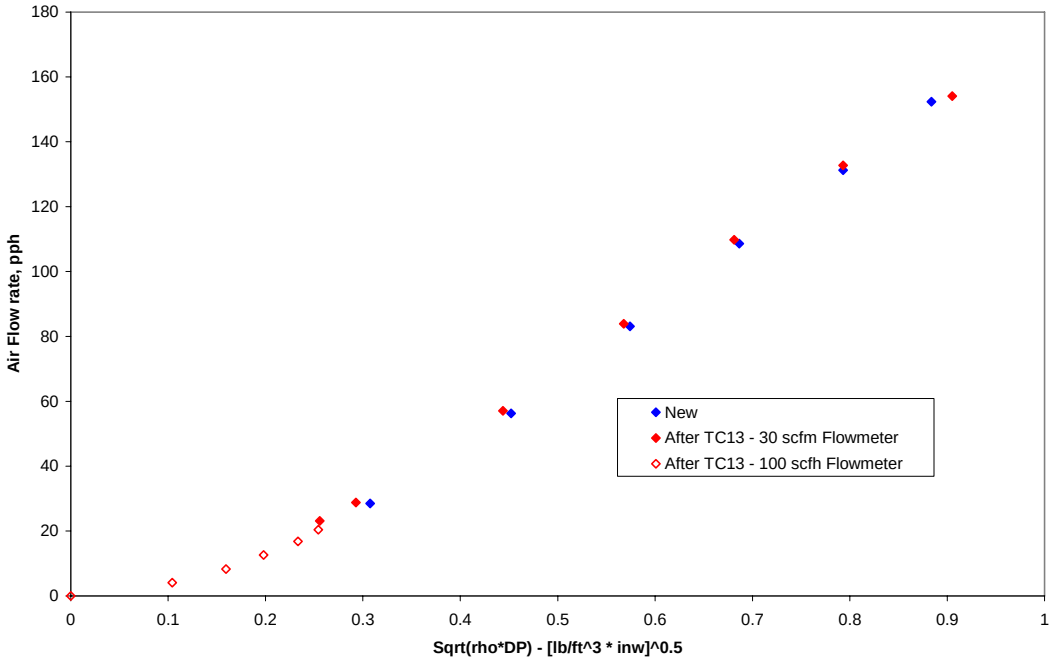

Figure 4.3-10 Ceramic Failsafe 4Ba Flow Test Results Before and After TC13

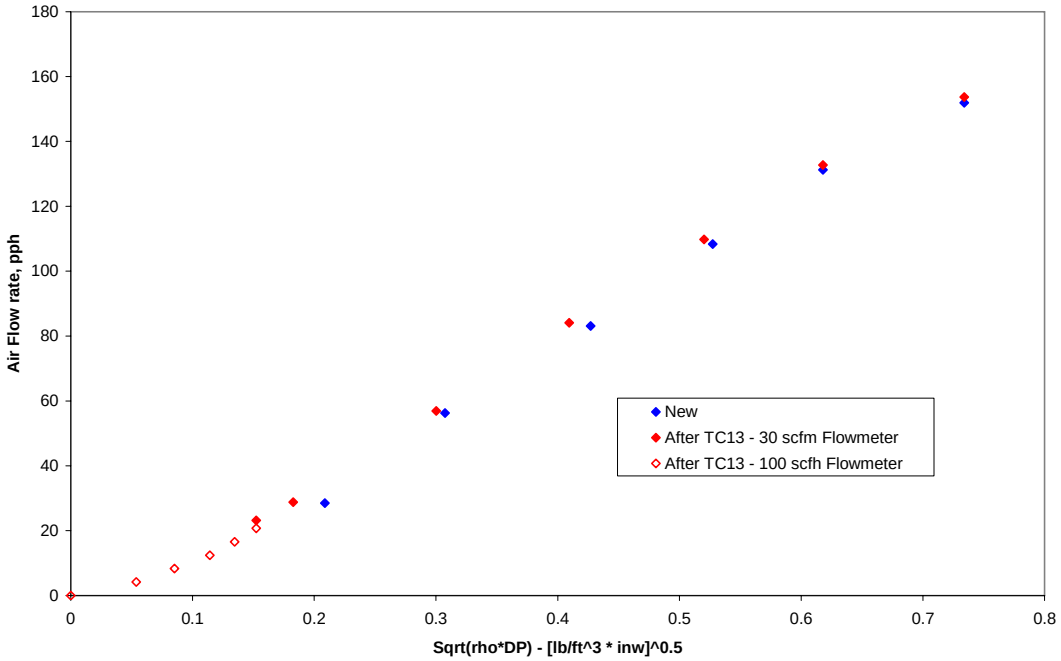

Figure 4.3-11 Ceramic Failsafe 5C Flow Test Results Before and After TC13

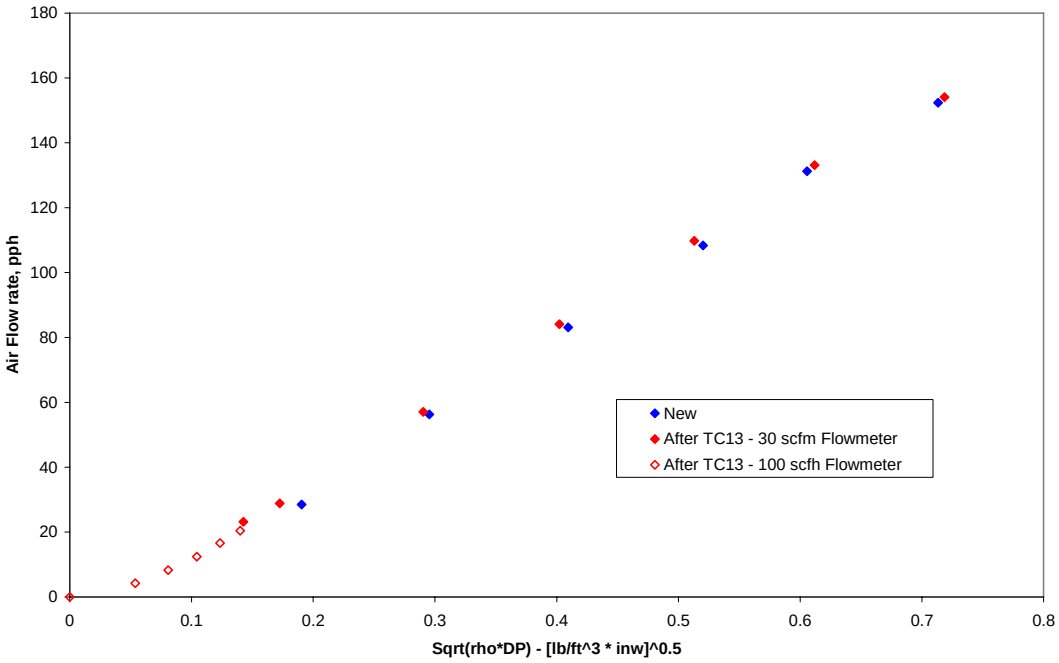

Figure 4.3-12 Ceramic Failsafe 5e Flow Test Results Before and After TC13

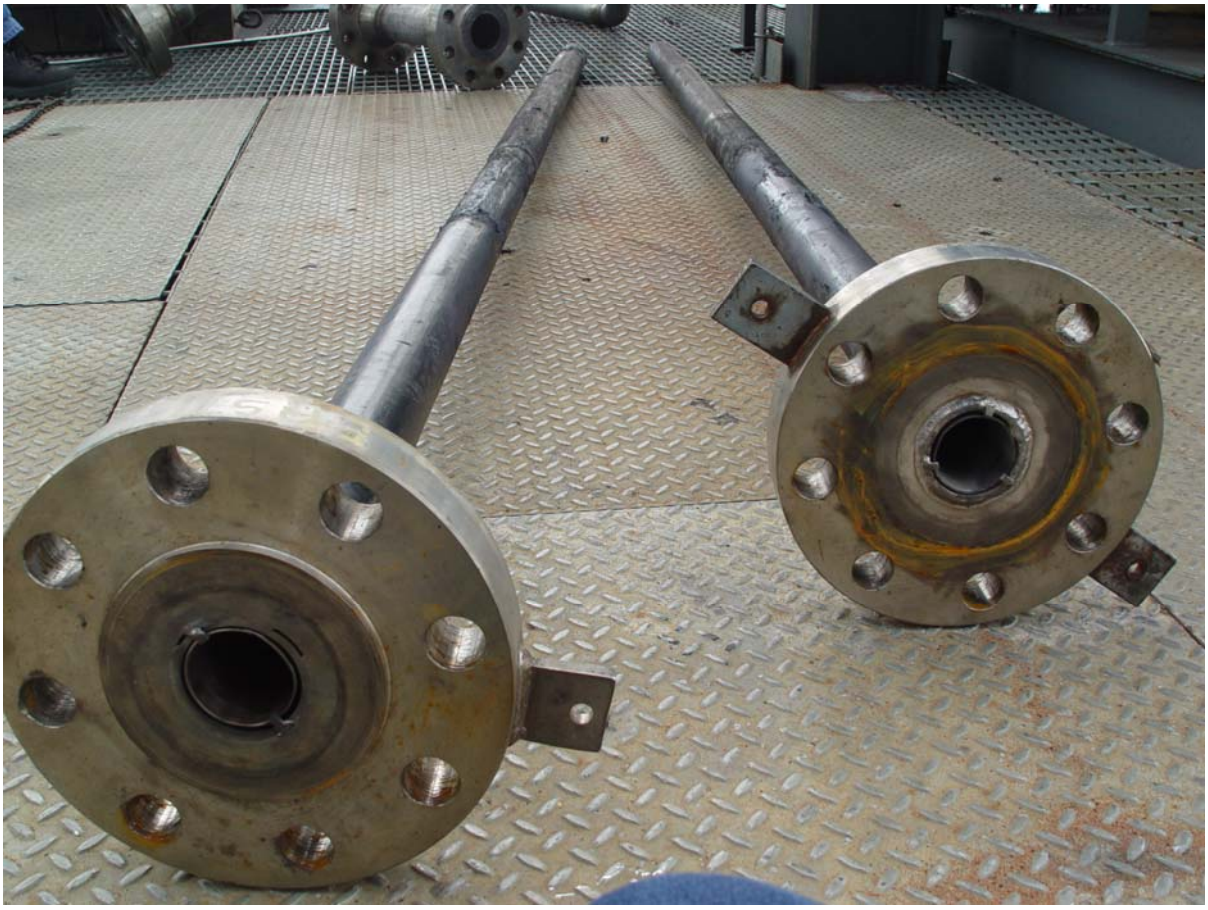

Figure 4.3-13 Back-Pulse Pipes After TC13

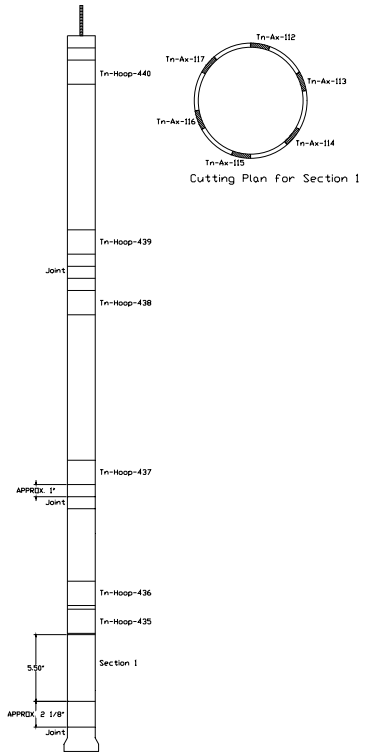

Figure 4.3-14 Cutting Plan for Pall PSS FEAL Filter Element 39151

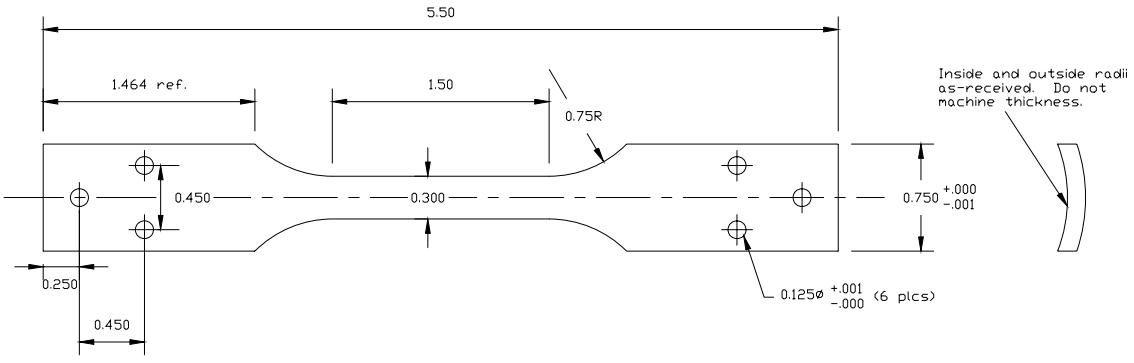

Notes:
1. All dimensions are in inches.
2. Tolerances unless noted:
   x.xxx +/−0.001
   x.xx +/−0.010

Figure 4.3-15 Axial Tensile Specimen Configuration for Pall PSS FEAL

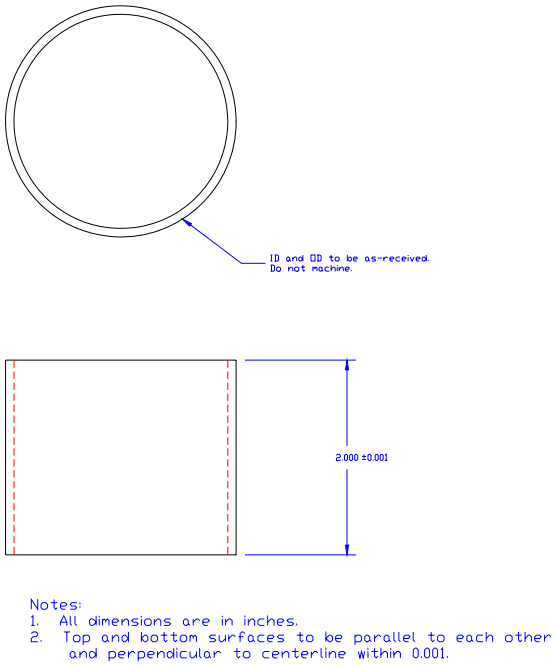

Figure 4.3-16 Hoop Tensile Specimen Configuration for Pall PSS FEAL

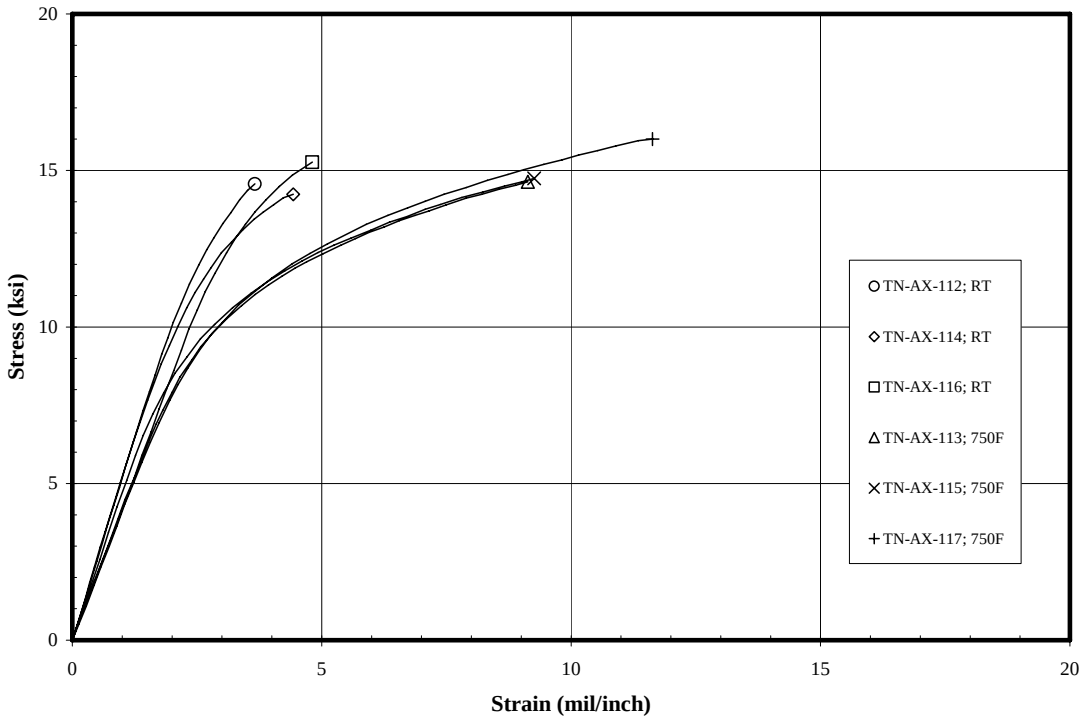

Figure 4.3-17 Axial Tensile Stress-Strain Responses Temperature for Pall PSS FEAL

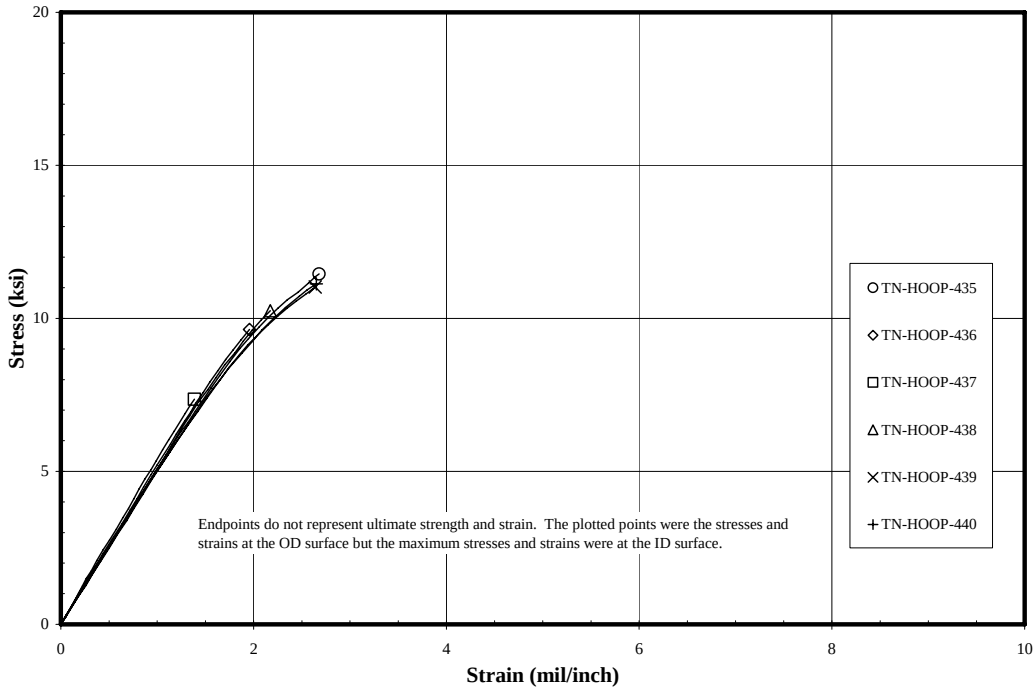

Figure 4.3-18 Hoop Tensile Stress-Strain Responses at RT for Pall PSS FEAL

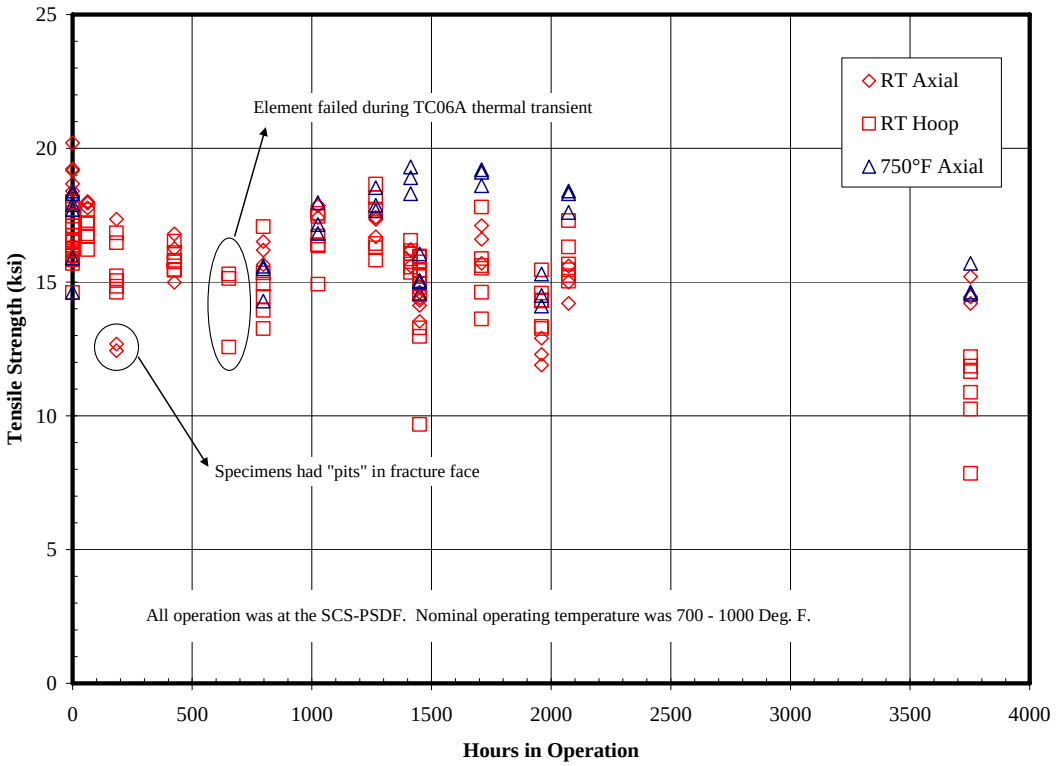

Figure 4.3-19 Tensile Strength Versus Hours of Gasification Operation for Pall PSS FEAL

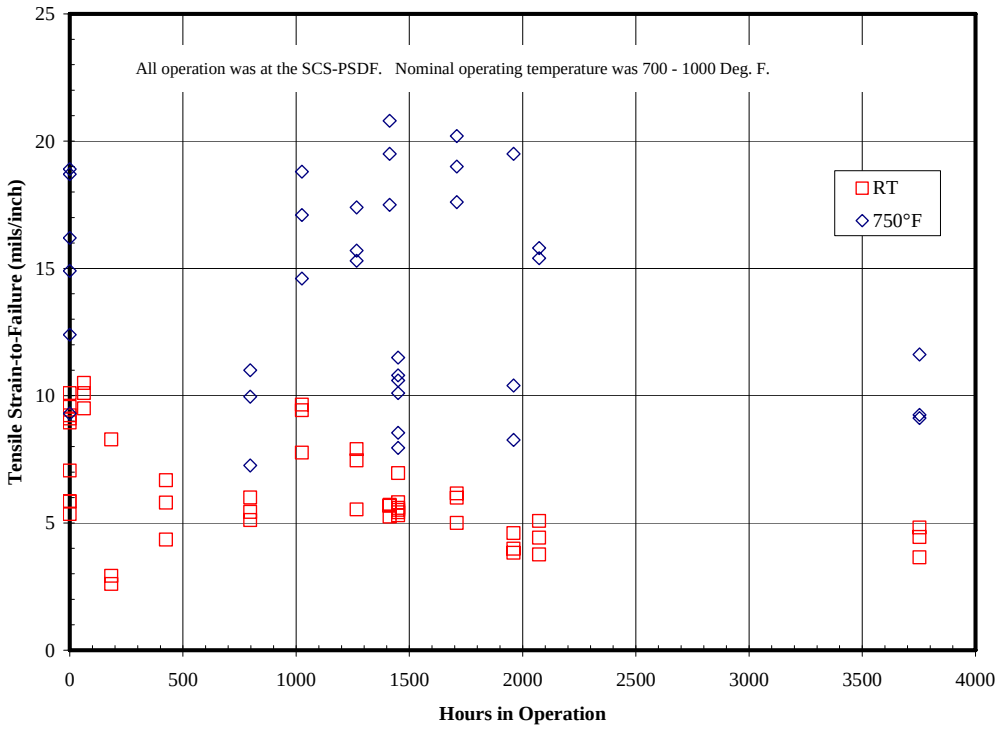

Figure 4.3-20 Tensile Strain-to-Failure Versus Hours of Gasification Operation for Pall PSS FEAL

4.4 GASIFICATION ASH CHARACTERISTICS AND PCD PERFORMANCE

TC13 was the first opportunity to study the characteristics of gasification ash (g-ash) produced from the Freedom North Dakota lignite and to investigate the effects of this fuel on PCD performance. Both a low-sodium and a high-sodium form of the Freedom lignite were tested, allowing an evaluation of the effects of sodium content on the g-ash characteristics and PCD performance. All of the low-sodium lignite tests were conducted with limestone addition, while the high-sodium lignite was tested both with and without limestone addition. This allowed us to compare the characteristics of the high-sodium g-ash produced with and without limestone addition to better understand the effects of the limestone on g-ash properties and chemistry. We were also able to compare the g-ash produced from the low-sodium lignite with limestone addition and the high-sodium lignite with limestone addition to better understand the effects of sodium content on the g-ash characteristics. The properties of the TC13 g-ash were also compared to those of other g-ash from previous runs to provide a better understanding of how the Freedom lignite compares with other types of coal in terms of PCD performance.

In the TC11 and TC12 reports, we examined the effects of carbon content on particulate properties and drag. We noted that both drag and specific-surface area were strongly correlated with the carbon content of the g-ash. In view of these correlations, the effects of carbon content received attention again in the analysis of the TC13 data. As discussed below, this investigation showed that the PCD transient drag increased as the carbon content of the g-ash increased. Laboratory drag measurements showed the same trend in samples collected from the PCD hopper. As in TC11 and TC12, it was also noted that the specific-surface area of the g-ash increased with increasing carbon content. This trend was true for both the in situ samples and the PCD hopper samples used for the laboratory drag measurements.

In addition to the effect of carbon content, drag measurements were made to examine the differences between the low- and high-sodium lignites. The plots of transient drag versus carbon showed good correlations for both the low- and high-sodium lignites, but the data for the two types of lignite fell on two distinct trend lines. This result suggested that there was a real difference in drag between the low- and high-sodium lignites.

The remainder of this section details the differences between the various Freedom lignite samples (high-sodium/low-sodium, high carbon/low carbon, with limestone/without limestone) and examines the effects on physical properties, chemistry, drag, and PCD performance.

4.4.1 In situ Sampling

As in previous test programs, in situ particulate sampling was performed at the inlet and outlet of the PCD to quantify the particulate collection efficiency and to relate PCD performance to the characteristics of the dust entering the control device. The measurements were made using the SRI in situ batch sampling system described in previous reports. Measurements were made for each of the major operating conditions of TC13: Air-blown operation with PRB, low- and high-sodium lignite and oxygen-blown operation with low-sodium lignite. The results of the PCD inlet and outlet sampling are discussed in the next two sections, respectively (Sections 4.4.1.1 and 4.4.1.2).

4.4.1.1 PCD Inlet Particle Mass Concentrations

Particle mass concentrations and mass rates measured at the PCD inlet are given in the left half of Table 4.4-1. An unusual degree of variation is observed in the inlet particle loadings with mass rates varying from 101 to 755 lb/hr. This cannot be completely attributed to differences in coal characteristics since all of the coals used in TC13 were similar in ash content. Likewise, the chemical analyses of the in situ samples do not indicate that high sorbent or sand addition rates are responsible for the wide range of values.

The particulate mass rate is plotted as a function of coal-feed rate in Figure 4.4-1. The solid line on the graph is the average relationship between coal feed and mass rate from TC12. The PRB and low-sodium lignite, air-blown data agree well with the TC12 trend. A linear regression to the PRB and air-blown, low-sodium lignite data is indicated by the dash-dot line. However, starting about half way through the test campaign the mass rate from the reactor increased by a factor of 2.5 relative to the coal-feed rate. This increase began during the transition to oxygen-blown operation with low-sodium lignite coal and continuing through the high-sodium lignite test. In the past, the mass rate data for a given coal have fallen on the same trend regardless of the oxidant used, and there was no significant difference in coal properties that should have caused this increase. It will be shown in a future report that this trend of high mass output from the transport reactor continued through TC14 as well. After TC14, the refractory in the recycle cyclone was found to be damaged in a way that could reduce its collection efficiency. The data presented here appear to indicate that the damage actually occurred in the middle of TC13. Data collected in TC15 indicate that the repair of the refractory restored the collection characteristics of the cyclone.

Limestone was added to the Transport Reactor for inlet runs 3 through 8. Although limestone addition has been shown to affect mass concentration to the PCD in some previous tests, this effect could not be observed in TC13. As discussed in a subsequent section on dust chemistry, the amount of limestone added was relatively small and unlikely to be resolved by these measurements.

4.4.1.2 PCD Outlet Particle Mass Concentrations

Particle concentrations measured at the PCD outlet are included in Table 4.4-1 and compared to other test programs in Figure 4.4-2. Generally, the outlet particle concentration was below the lower measurement resolution limit of 0.1 ppmw. A slightly elevated concentration was measured on the first day of the test campaign and subsequent microscopic examination suggested that this material was mostly made of large trash particles and was not indicative of a PCD leak.

After 6 days of operation, there was an emission event that is not so easy to explain. On October 8, 20003, the PCD outlet concentration was measured to be 0.25 ppmw. Operation had been relatively stable and unremarkable since the previous measurement on October 7, 2003, indicated a particle concentration well below the lower measurement limit. The following day the concentration was reduced but still measurable. Microscopic examination indicated fine particles on the sample filters consistent with a small PCD leak. By the next day, the concentration had decreased below the measurement limit.

Based on the PCD outlet data, which included the initial leak-tight performance, sudden increase, followed by gradual tapering off of emissions, it was anticipated that a filter element had developed a small crack or other small leak that had been stopped by a plugged failsafe. Unfortunately, at the conclusion of TC13, the entire PCD was disassembled and every failsafe was flow tested without finding any evidence of a plugged or even dirty failsafe. The source of the particle emissions has not been identified. While the magnitude of the leak was not great and the measured concentration is not likely to damage most downstream equipment, our inability to identify the cause of this event is troubling. In future test programs we will continue to monitor and to identify the sources of elevated particle concentrations. A more sensitive real-time monitor (discussed below) would improve our ability to analyze these events.

4.4.1.3 Syngas Moisture Content

Also included in Table 4.4-1 are the syngas moisture measurements made in conjunction with the particulate sampling runs at the PCD outlet. The measurements yielded moisture values in the range of 8.1 to 19.6 percent by volume during air-blown operation and 32.6 percent by volume during oxygen-blown operation. The syngas moisture content is normally higher during oxygen-blown operation, because higher rates of steam addition are required to cool the lower mixing zone.

4.4.1.4 Real-Time Particle Monitoring

The PCME DustAlert-90 particulate monitor was operational and apparently functioning throughout TC13. Figure 4.4-3 shows the output of the PCME for the 3 day period just before and during the time that the elevated particle concentration was observed. Both the instantaneous and averaged output are shown. Interestingly, the monitor was outputting a higher value on October 7, 2003, when no emissions could be detected by the in situ samplers than it was on the two subsequent days of elevated loadings. This is consistent with previous results indicating that the PCME is not capable of measuring concentrations below approximately 1 ppmw. The output of the instrument during this period appears to be dominated by noise and is not generating a meaningful signal.

A new particle monitoring system consisting of a sample extraction system provided by the Gas Technology Institute (GTI) and coupled with an optical, single-particle counter supplied by Process Metrix is planned for evaluation in the fall of 2004. This monitoring system has the potential of detecting particle concentrations that are an order of magnitude lower than the PCME can measure. If this system can meet its measurement potential and demonstrate acceptable reliability it could provide much needed real-time monitoring capability at low concentration that would make analysis of particle emissions much easier and more precise.

4.4.2 Particle-Size Analysis of In situ Particulate Samples and PCD Hopper Samples

As in previous tests, a Microtrac X-100 particle-size analyzer was used to measure the particle-size distributions of the in situ particulate samples collected at the PCD inlet and the PCD hopper samples used for the laboratory drag measurements. The results for these two types of samples are discussed separately in Sections 4.4.2.1 and 4.4.2.2.

4.4.2.1 Particle Size of In situ Particulate Samples

Figure 4.4-4 shows differential mass particle-size distributions measured on the PCD inlet in situ samples. The four data sets previously described are compared on the graph. Shown on this absolute mass basis, the data track the particle mass data discussed above. However when compared on a differential percentage basis in Figure 4.4-5 many of the differences are removed. The lignite coals all have fewer fine particles and somewhat more large particles than the PRB coal, but the differences are not very significant. We would not expect dramatic effects on PCD performance to result from these differences in size distribution although some reduction in normalized dust cake drag might be expected with the slightly coarser lignite size distribution.

4.4.2.2 Particle Size of PCD Hopper Samples

Figure 4.4-6 compares the range of in situ size distributions from the previous graph with the four hopper composite samples used for the laboratory drag measurements (RAPTOR). Although there are some real differences in the very largest portion of several of the distributions, these particles generally do not end up in the RAPTOR sample and thus do not affect the results. At the fine end of the distribution, all of the hopper samples lie at the very upper end of the in situ samples. If the hopper samples contain more fine particles than the dust collected in the PCD then the lab measurements may give higher drag than that observed for the actual PCD. We will revisit this issue in the subsequent section on drag comparisons (Section 4.4.6).

4.4.3 Measurement and Sampling of PCD Dustcakes

At the conclusion of TC13, the PCD was shut down clean. Coal feed was terminated at about 15:00 on November 2, 2003, and PCD back-pulsing was continued for about 13 hours until approximately 04:00 on November 3, 2003. The PCD was back-pulsed a total of 28 times after the termination of coal feed: four times at an interval of 15 minutes and then 24 times at an interval of 30 minutes. Based on past experience, this extensive back-pulsing should have removed all of the transient dustcake, leaving only the residual cake on the filter elements.

Table 4.4-2 summarizes the thickness and areal loading measurements made on the remaining residual cake and compares the measurements to those made on residual cakes from previous runs. As noted in the TC12 Run Report, all of the average thickness measurements made since TC06 have been about 0.010 in. The consistency of the average residual cake thickness from the various runs suggests that the residual cake thickness is independent of coal type. From the consistency of measurements made on residual cakes from clean shutdowns and residual cakes from semidirty shutdowns, it may also be inferred that extensive back-pulsing after shutdown does not alter the residual cake thickness.

After TC10, it was noted that the residual cake was thicker on HR-160 and Hastelloy-X elements than it was on FEAL elements. It was speculated that the differences in cake thickness might be related to differences in the effectiveness of the back-pulse cleaning caused by the higher flow resistance of the dirty HR-160 and Hastelloy-X elements. In TC13, all of the elements were FEAL, but there were still noticeable differences in the cake thickness as shown in the table. These differences in cake thickness may be related to differences in the flow resistance of the failsafes, which could also cause variations in the effectiveness of the back-pulse cleaning. Flow

tests of the dirty failsafes that were removed after TC13 showed that the flow resistance varied as follows:

B-11 (PSDF/HR-160) > B-14 (PSDF/H-556) > B-7 (Pall Fuse + Ceramem) > B-8 (Pall Fuse + Ceramem)

With the exception of the B-11 measurement, the cake thicknesses follow the same trend as the flow resistance. We suspect that the B-11 measurement is in error, because the calculated cake porosity is unusually low (80.9 percent versus 88.6 to 92.6 percent for the other three measurements).

Taken together with the previous thickness measurements, the TC13 data suggest that the residual cake thickness on an individual filter element may vary with the type of filter element and with the type of failsafe used. Nevertheless, the average thickness has been consistently about 0.010 in. after every run since TC06. Therefore, the average thickness does not appear to be a strong function of the filter element type, failsafe type, or coal type.

4.4.4 Characteristics of In situ Samples, Hopper Samples, and Residual Dustcake

This section describes the physical properties of the in situ samples collected at the PCD inlet, the PCD hopper samples used for the laboratory drag measurements, and the dustcake samples collected after the run.

4.4.4.1 Characteristics of In situ Particulate Samples

Tables 4.4-3 and 4.4-4 give the physical properties and chemical compositions of the in situ samples collected at the PCD inlet and the PCD hopper samples that were used for the laboratory drag measurements. As indicated in the tables, the first two in situ samples were collected during gasification of PRB coal, the next four in situ samples were collected during gasification of low-sodium Freedom lignite, and the last four in situ samples were collected during gasification of high-sodium Freedom lignite. Limestone was added during all but four of the runs as indicated in the table. No distinction is made between samples collected under air- and oxygen-blown conditions, since previous tests have shown that the choice of oxidant has no significant effect on particulate characteristics.

Since the low-sodium lignite was high in sulfur, limestone was added during the collection of all of the in situ samples and hopper samples from the low-sodium lignite. As noted in the tables, two of the high-sodium lignite in situ samples and one of the high-sodium hopper samples were collected during limestone addition. The summary table below compares the in situ particulate characteristics and composition obtained with the low-sodium lignite with limestone addition and the high-sodium lignite with and without limestone addition.

Lignite	Low-Sodium	High-Sodium	
Limestone Added	Yes	Yes	No
Bulk Density, g/cc	0.28 - 0.44	0.27 - 0.66	0.37 - 0.41
Skeletal Particle Density, g/cc	2.40 - 2.96	2.37 - 2.87	1.84 - 1.92
Uncompacted Bulk Porosity, %	84.0 - 88.3	77.0 - 88.6	78.6 - 79.9
Specific Surface Area, m^2/g	65 - 298	49 - 280	71 - 85
Mass-Median Diameter, μm	16.8 - 23.1	21.0 - 22.5	13.5 - 21.7
Noncarbonate Carbon, wt %	13.7 - 46.9	8.8 - 38.1	58.6 - 64.9
$CaCO_3$ + CaS + CaO, wt %	22.7 - 31.7	25.5 - 28.0	10.1 - 11.7
Inerts (Ash/Sand), wt %	30.4 - 62.2	36.4 - 63.2	25.0 - 29.8

There do not appear to be any significant differences between the low- and high-sodium g-ash produced with limestone addition. However, there are some major differences between the high-sodium g-ash produced with and without limestone addition. As expected, the samples with limestone addition have higher particle density, higher lime content, and lower carbon content.

The following table compares the average characteristics of the TC13, TC12, and TC11 in situ samples obtained without limestone addition. The low-sodium Freedom lignite is not included in the table since it was not tested without limestone addition. However, it has already been established that there was little difference between the TC13 low- and high-sodium g-ash.

	TC13	TC12	TC11
Coal	High-Na Freedom Lignite	PRB	Falkirk Lignite
Limestone Added	No	No	No
Bulk Density, g/cc	0.39	0.27	0.52
Skeletal Particle Density, g/cc	1.88	2.34	2.62
Uncompacted Bulk Porosity, %	79.3	88.5	80.4
Specific Surface Area, m^2/g	78	166	57
Mass-Median Diameter, μm	17.6	16.2	17.6
Noncarbonate Carbon, wt %	61.7	34.1	8.9
$CaCO_3$ + CaS + CaO, wt %	10.9	14.2	16.8
Inerts (Ash/Sand), wt %	27.4	50.7	74.3

Compared to PRB g-ash, the Freedom and Falkirk lignite g-ash have higher bulk densities, lower bulk porosities, and lower surface areas. Based on these differences, the lignite g-ash should have less flow resistance, or lower drag, than does the PRB g-ash. The table below compares the characteristics of the TC13 and TC12 in situ samples produced with limestone addition. The TC11 g-ash is omitted from this comparison because there was no addition of limestone during TC11. In this case, however, both the low- and high-sodium Freedom lignites are included, since both types of the lignite were tested with limestone addition.

	TC13	TC13	TC12
Coal	Low-Na Freedom Lignite	High-Na Freedom Lignite	PRB
Limestone Added	Yes	Yes	Yes
Bulk Density, g/cc	0.38	0.47	0.38
Skeletal Particle Density, g/cc	2.65	2.62	2.56
Uncompacted Bulk Porosity, %	85.6	82.1	85.1
Specific Surface Area, m^2/g	176	165	107
Mass-Median Diameter, μm	20.1	21.8	15.9
Noncarbonate Carbon, wt %	28.2	23.4	19.8
$CaCO_3$ + CaS + CaO, wt %	26.0	26.8	39.1
Inerts (Ash/Sand), wt %	45.8	49.8	41.1

This comparison shows that the low- and high-sodium g-ash are very similar. This result is not surprising since the low- and high-sodium lignite come from the same mine, and the only difference is the location within the seam. Compared to the PRB g-ash with limestone addition, both of the lignite g-ash produced with limestone addition have higher surface areas. This is the opposite of what was observed in the g-ash produced without limestone addition, where the lignite g-ash had less surface area than the PRB g-ash.

The addition of limestone seems to significantly increase the average surface area of the lignite g-ash samples (165 to 176 m^2/g with limestone versus 78 m^2/g without limestone); but there is so much variation between individual samples that the difference may not be statistically significant. The limestone addition seems to have the opposite effect with PRB g-ash (107 m^2/g average with limestone versus 166 m^2/g average without addition), and in this case the differences are definitely real from a statistical point of view. These results suggest that the limestone may sometimes develop more surface area when it is used with the lignites than when it is used with PRB coal. This may not necessarily be a direct effect of the coal type, but it could be related to differences in the thermal conditions achieved with the two types of coal, which would potentially produce differences in limestone calcination rate and reaction rate with H_2S. The surface area of calcined limestone has been shown to vary with the rate of calcination and with maximum temperature (Borgwardt, R.H., "Calcination kinetics and surface area of dispersed limestone particles," *AIChE Journal*, Vol. 31, No. 1, pp. 103-111., 1985).

4.4.4.2 Characteristics of PCD Hopper Samples Used for Drag Measurements

In addition to the in situ samples, Tables 4.4-3 and 4.4-4 include data for PCD hopper samples that were used for laboratory drag measurements. The selected hopper samples represented both the low- and high-sodium Freedom lignites, but not the PRB coal, since we already have

extensive data on PRB g-ash. Since the TC12 drag measurements showed an apparent effect of carbon content on drag, we selected three different sets of high-sodium Freedom hopper samples that covered different ranges of carbon content as follows:

- Low-carbon (AB14014, AB14027): 18 to 22 percent carbon
- Medium-carbon (AB14028-AB14031): 35 to 44 percent carbon
- High-carbon (AB14150): 57 percent carbon

With the low-sodium Freedom lignite, only a medium-carbon range (37 to 39-percent carbon) was selected for the laboratory drag measurements, since the effect of carbon was already being investigated with the high-sodium lignite g-ash. Limestone was being added during the collection of all of the hopper samples from the low-sodium lignite. Limestone was also being added during the collection of the high-sodium, high-carbon hopper sample as noted in the tables.

The following table compares the average characteristics of the four composite hopper samples used for the lab drag measurements.

Composite	Low-Sodium	High-Sodium		
Carbon Content Range	Medium	Low	Medium	High
Limestone Added	Yes	No	No	Yes
Bulk Density, g/cc	0.41	1.04	0.58	0.45
Skeletal Particle Density, g/cc	2.30	2.43	2.18	1.93
Uncompacted Bulk Porosity, %	82.4	57.4	73.3	76.7
Specific Surface Area, m^2/g	N.M.	10	55	75
Mass-Median Diameter, μm	17.4	64.5	23.9	19.6
Noncarbonate Carbon, wt %	39.1	19.9	40.0	57.0
$CaCO_3$ + CaS + CaO, wt %	24.1	5.1	8.8	16.7
Inerts (Ash/Sand), wt %	36.7	75.0	51.3	26.3

Comparing the two medium-carbon samples with and without limestone addition, the sample with limestone addition has a slightly higher particle density (2.30 versus 2.18 g/cc) due to the higher density of the lime-related components. The high-carbon sample with limestone addition, however, has a relatively low particle density (1.93 g/cc), because the high concentration of low-density carbon offsets the effect of the lime-related components. The low-carbon sample without limestone addition has the highest density (2.43 g/cc), but it also has an unusually large mass-median diameter and an unusually high concentration of inerts. Based on these characteristics, we suspect that this sample contains a significant amount of bed material.

Fortunately, the presence of the bed material in this sample should not affect the laboratory drag measurements, because those particles are too large to be entrained in the RAPTOR apparatus.

Despite the effects of limestone addition, the surface areas of the composite samples seem to be directly related to their carbon content, as seen in previous tests. The effect of carbon content on drag is discussed in Section 4.4.5.

4.4.4.3 Characteristics of Residual Dustcake Samples

As mentioned previously, TC13 was concluded with a clean shutdown of the PCD followed by extensive back-pulsing of the PCD. Inspection of the PCD revealed that there was only residual cake (no transient cake) left on the filter elements after the run. Comparison of the cake thickness with previous residual cakes suggests that the extensive back-pulsing did not affect the thickness of the cake. However, it is still possible that the particle-size distribution and other properties of the residual cake could have been altered by the extensive back-pulsing.

Tables 4.4-5 and 4.4-6 give the physical properties and chemical composition of the TC13 residual dustcake. The table below compares the residual dustcake characteristics to those of the TC13 in situ particulate samples.

	Residual Cake	PRB In situ	Low-Na In situ	High-Na In situ	High-Na In situ-Sodium
Limestone Added	-----	No	Yes	Yes	No
Bulk Density, g/cc	0.31	0.28	0.38	0.47	0.39
Skeletal Particle Density, g/cc	2.17	2.62	2.65	2.62	1.88
Uncompacted Bulk Porosity, %	85.7	89.5	85.6	82.1	79.3
Specific Surface Area, m^2/g	88	152	176	165	78
Mass-Median Diameter, μm	9.7	16.9	20.1	21.8	17.6
Noncarbonate Carbon, wt %	38.6	24.5	28.2	23.4	61.7
$CaCO_3$ + CaS + CaO, wt %	13.5	18.0	26.0	26.8	10.9
Inerts (Ash/Sand), wt %	47.9	57.5	45.8	49.8	27.4

TC13 was begun with PRB coal without limestone addition, followed by a transition to the low-sodium lignite with limestone addition. The run was then ended with high-sodium lignite, first with limestone addition and then without limestone addition. In terms of chemical composition and most physical properties, the residual cake does not appear to be very similar to any of the in situ samples. Compared to the PRB g-ash, the residual cake has a much lower particle density, much lower surface area, and significantly higher carbon content. Therefore, it is clear that the PRB g-ash that formed the original residual cake has been replaced, at least in part, by the lignite g-ash. In the hot-gas filtration literature, the residual cake is sometimes referred to as the permanent cake, but this results clearly shows that it is not permanent.

The table below compares the average properties of the residual dustcake from TC13 with those from other test campaigns using different types of coal. In cases where multiple coal types were tested during a run, the coal type listed is the last one used in the run. The dustcakes from TC08 and TC07 are not included because the physical properties of the TC08 cake were altered by partial oxidation, and the properties of the TC07 cake were biased by coke feed at the end of the run.

	TC13	TC12	TC11	TC10	TC09	TC06
Coal	High-Na Freedom Lignite	PRB	Falkirk Lignite	PRB	Hiawatha Bituminous	PRB
Limestone Added at End of Run	No	Yes	No	No	No	Yes
Bulk Density, g/cc	0.31	0.29	0.34	0.23	0.24	0.25
Skeletal Particle Density, g/cc	2.17	2.27	2.32	2.06	2.12	2.28
Uncompacted Bulk Porosity, %	85.7	87.2	85.3	88.8	88.7	89.0
Specific Surface Area, m^2/g	88	82	20	92	114	257
Mass-Median Diameter, μm	9.7	9.6	4.5	4.5	12.4	9.3
Noncarbonate Carbon, wt %	38.6	26.8	19.5	49.6	52.3	40.1
$CaCO_3$ + CaS + CaO, wt %	13.5	23.0	14.9	10.0	7.4	25.7
Inerts (Ash/Sand), wt %	47.9	50.2	65.6	40.4	40.3	34.2

The residual cakes produced from the Freedom and Falkirk lignites have relatively high bulk densities and relatively low bulk porosities compared to the residual cakes from PRB coal and from the Hiawatha bituminous coal. Otherwise, they are fairly similar to other recent PRB cakes, except for the TC06 PRB cake, which had an unusually high surface area. The TC06 in situ samples also had very high surface areas, and there was some char bridging at the end of TC06. If the dustcake sample were contaminated with bridged material that was similar to the in situ samples, the bridging contamination could account for the unusually high surface area of the TC06 cake.

The main differences between the Freedom and Falkirk residual cakes are in the surface area and carbon content. The residual cake from the Freedom lignite has about twice the carbon content as does the residual cake from the Falkirk lignite. The cake from the Freedom lignite also has a much higher surface area. The difference in surface area seems reasonable, since previous work has shown that surface area generally increases with increasing carbon content.

4.4.5 Laboratory Measurements of Gasification Ash Drag

The RAPTOR apparatus described in previous reports was used to measure the normalized drag of the g-ash as a function of particle size. The four hopper samples used for these measurements have been described in previous sections and consisted of three samples of high-

sodium lignite with different carbon contents and one low-sodium sample with moderate carbon content. These samples were chosen to represent a range of carbon contents, because data from TC11 with lignite coal indicated that carbon content can play a controlling role in dust cake drag. An effect of carbon content on drag was also observed in TC12 with PRB coal.

The drag results as a function of particle size for the TC13 samples are shown in Figure 4.4-7. Each of the regression lines on the figure is marked with the noncarbonate carbon content of the sample. A general trend of increasing drag with increasing carbon content can be observed in the drag data. This trend is in agreement with the previous TC11 data which are shown in Figure 4.4-8. Overlaying the data sets for the two lignites does not produce perfect agreement, but the medium carbon data sets do match up reasonably well.

These results will be considered further when comparing lab measurements with actual PCD operation in the next section.

4.4.6 Analysis of PCD Pressure Drop

The effect of the lignite g-ash on the pressure drop of the PCD was analyzed by calculating a corresponding value of transient drag using the measured pressure drop, gas flow, and particle concentration values during the PCD inlet mass concentration tests discussed previously (Table 4.4-1). The calculation procedure, which has been described in previous reports, was applied to all of the in situ sampling runs, and the results are summarized in Table 4.4-7. The calculated transient drag at PCD conditions is listed under the column heading "PCD." The corresponding normalized value of transient drag at room temperature is listed under the heading "PCD@RT." This value can be compared directly with the lab-measured drag values, which will be discussed later.

It was observed in the previous section that the lab drag measurements were affected by the carbon content of the dust. The PCD transient drag values (corrected to room temperature) are plotted as a function of noncarbonate carbon content in Figure 4.4-9, where a strong effect of carbon on drag can also be observed. Also, from this graph, it seems obvious that the low and high-sodium versions of the Freedom lignite fall on different trend lines. For the same carbon content, the low-sodium Freedom lignite generated a dust cake that had about twice the drag as the high-sodium version of the lignite. The data collected during TC11 with the Falkirk lignite are also plotted on the figure and appear to agree reasonably well with the low-sodium Freedom data, although the range of carbon contents and drag values was more limited with Falkirk coal. The two PRB data points from TC13 are plotted along with the regression line to all previous PRB gasification data and are in reasonable agreement with the previous trend. The PRB drags are higher than all of the lignite coal data.

Clearly variations in carbon content help explain variations in the drag within an individual coal type. The variation of drag by almost a factor of six during the low-sodium Freedom test appears to be directly related to a factor of four increase in carbon content of the dust cake. However, it is also clear that there are differences between the coal types that are not addressed simply by the carbon content. One difference is particle size, but other factors have yet to be identified.

During previous gasification runs with PRB coal, the RAPTOR data as a function of particle size has been fairly consistent within a single test program. Thus, a simple linear regression between drag and median particle size could be used to compare lab and actual PCD data. With the lignite coals tested in TC13, this is clearly not adequate as the lab-measured drag varied by more than a factor of two at the same particle size. For comparison with TC13 PCD pressure drop data, the particle size, carbon content, and drag data from Figure 4.4-7 were used to calculate a multiple linear regression, with drag as the dependent variable, using the statistics software SigmaStat. This approach accounted for a considerable amount of the variation in the data. The calculated r^2 of the regression was improved from 0.66 for correlation between only drag and size to 0.90 for correlation of drag to both carbon and size. The regression equation for the high-sodium lignite was:

High-Sodium Lignite Drag = 10 ^ (2.586 – 0.917 * Log(MMD) + 0.00771 * NCC)

Where:
MMD is the mass-median particle diameter of the sample in microns.
NCC is the noncarbonate carbon content of the sample in wt percent.

As mentioned above, the effect of carbon content on the low- and high-sodium Freedom dusts are different, with the data for low-sodium Freedom dust agreeing better with the low-sodium Falkirk dust. Since there was only one sample of low-sodium Freedom (only one carbon value cannot be used for regression analysis) a second regression was calculated for the all of the low-sodium lignite samples. The regression equation is shown below and correctly indicates greater effects of both carbon content and size for the low-sodium lignites.

Low-Sodium Lignite Drag = 10 ^ (2.601 – 0.964 * Log(MMD) + 0.0103 * NCC)

The values of NCC and MMD used to calculate the lab drag for each PCD test condition are shown in Table 4.4-7 along with the calculated drag from the multiple regressions in the column labeled "RAPTOR."

Figure 4.4-10 compares the normalized PCD transient drag at room temperature (PCD@RT) to the corresponding individual values of RAPTOR drag calculated from the multiple regression. Although most previous data had some scatter, in general, the data points were scattered around the perfect agreement line. However, for the TC11 and TC13 lignite data, all but one of the data points fall above the line suggesting that the RAPTOR is over-predicting the drag values. That is, the actual PCD pressure drop is lower than the lab measurements predict. The dashed line on the figure is a linear regression to the lignite data which indicates that on average the lab measurements are about 65 percent higher than the PCD pressure drop. This effect could be partially caused by the higher concentration of fine particles in the hopper samples (Figure 4.4-6) or it might be attributed to lower areal loading than that calculated by the total inlet loading (some of the lignite may tend to drop out before reaching the filters). We will continue to investigate this phenomenon in future tests of lignite coal.

4.4.7 Conclusions

During the latter part of TC13, the particle mass entering the PCD was higher than in previous test programs. Data from subsequent test programs indicated that at least part of the increase

was related to the performance of the recycle cyclone. The increased mass loading to the PCD increased the areal loading of the PCD dustcake and increased pressure drop. However, since the normalized drag of the dust was moderate, this did not result in any problems with PCD operation.

PCD outlet emissions were generally below 0.1 ppmw, the lower limit of measurement resolution. The major exception occurred after 6 days of clean operation when the outlet particle concentration suddenly increased to 0.25 ppmw. The emissions gradually decreased over a 2-day period until the concentration was again undetectable. Flow testing did not find any plugged failsafes, and thus this event cannot be related to a known leak. We will continue to investigate this phenomenon if it occurs in future test programs.

Characterization of the TC13 in situ samples showed that there were no significant differences in the physical properties or bulk chemistry of the low- and high-sodium lignite g-ash produced with limestone addition (except of course for the difference in sodium content). However, there were some major differences between the high-sodium g-ash produced with and without limestone addition. As expected, the samples with limestone addition had higher particle density, higher lime content, and lower carbon content. Despite these differences, the limestone addition did not have a significant effect on drag. This result is not too surprising since the components contributed by the limestone and its reaction products only account for about 15-wt percent of the total solids entering the PCD. The chemical analysis and density measurements are sufficiently accurate to resolve the effect of 15-wt percent limestone-related components, but the drag measurements are subject to much more uncertainty.

Compared to PRB g-ash, both the Freedom and Falkirk g-ash have higher bulk densities, lower bulk porosities, and lower surface areas (when comparing the g-ash alone without any limestone addition). The lower surface area could be a contributing factor in the relatively low drag of the lignite g-ash compared to PRB g-ash.

When the PRB and lignite g-ash is compared with limestone addition in both cases, the lignite g-ash has higher surface areas on average, although there is considerable variation between samples. The opposite trend was observed in the average surface areas of the g-ash produced without limestone addition, where the average surface area of the lignite g-ash was below that of the PRB g-ash. This result suggests that the surface area of the limestone may not necessarily be the same when it is used with the lignites as it is when it is used with the PRB coal. This result is not too surprising, since the surface area of calcined limestone has been shown to vary with temperature and rate of calcination.

Examination of the TC13 residual dustcake showed that the average cake thickness was about 0.01 in. For all of the previous gasification test campaigns (TC06 to TC12), the average residual cake thicknesses have consistently been about 0.01 in. The consistency of this result suggests that the residual cake thickness is independent of coal type. Moreover, the residual cake thickness appears to be unaffected by additional back-pulsing after shutdown, since similar average thicknesses have been achieved with both clean and semidirty shutdowns.

While the average residual cake thickness appears to be consistently around 0.01 in., the TC13 measurements showed that individual thickness measurements varied with the flow resistance of the failsafe measured after the test. With the exception of one measurement that we suspect was

in error, the measured cake thickness increased with increasing failsafe flow resistance. This result seems reasonable, since plugging of the failsafe would lead to less effective back-pulse cleaning and buildup of a thicker residual cake. Therefore, it may be inferred that the residual cake thickness is influenced by the back-pulse cleaning effectiveness, even though it is not affected by additional back-pulsing after shutdown.

Compared to the TC11 residual dustcake from the Falkirk lignite, the TC13 residual cake from the Freedom lignite had a much higher surface area, probably because it had about twice as much carbon. Previous work has shown that surface area generally increases with increasing carbon content in in situ samples, but here the effect can also be seen in comparing residual dustcakes. Compared to residual cakes from PRB coal, the residual cakes produced from the Freedom and Falkirk lignites have relatively high bulk densities and relatively low bulk porosities, but otherwise they are quite similar to PRB cakes.

As in TC11 and TC12, carbon content was found to have a strong effect on the surface area and drag of the TC13 g-ash. Strong correlations between transient drag and carbon content were found for both the low- and high-sodium forms of the Freedom lignite g-ash. The same types of correlations were found for the Falkirk lignite g-ash in TC11 and for the PRB g-ash in TC12, suggesting that drag is very sensitive to carbon conversion with both PRB coal and North Dakota lignites. This effect has important implications, because it shows that changes in gasifier operation that affect carbon conversion can also have dramatic effects on PCD performance. Conversely, these results show that the sizing of a new PCD must take into account the expected carbon content of the g-ash. If the carbon content is overestimated, the PCD will be oversized, resulting in an unnecessarily large capital cost. On the other hand, if the carbon content is underestimated, the PCD may be undersized, making it impossible to operate the plant at full capacity. Either way, there are serious cost implications. Therefore, it is important that PCD design be based on an accurate assessment of the expected carbon conversion/carbon content.

As we found in recent test programs, the drag of the Freedom lignite g-ash was affected by the carbon content of the dust cake. The PCD drag was clearly related to carbon content but the low- and high-sodium coals fell on different trends. The low-sodium Freedom agreed better with the low-sodium Falkirk dust from TC11. The lab measurements indicated that the drag was related to both carbon and particle size. Multiple linear regressions of drag to both carbon and particle size produced much better correlation to the lab data than size alone. Comparison of the lab and actual PCD drags using the multiple regression indicated that the lab measurements overpredicted the actual drag measured in the PCD. This disagreement could be related to different particle size distributions or areal loadings between the RAPTOR and actual dustcake samples.

Table 4.4-1 PCD Inlet and Outlet Particulate Measurements for TC13

Test Date	PCD Inlet					PCD Outlet				
	Run No.	Start Time	End Time	Particle Loading, ppmw	Particle Loading, lb/hr	Run No.	Start Time	End Time	H_2O Vapor, vol %	Particle Loading, ppmw
Air Blown - PRB										
10/2/03	--	--	--	--	--	1	11:20	14:20	8.1	0.14[1]
10/3/03	1	12:30	12:45	9000	166	2	9:00	13:00	10.0	< 0.10
10/6/03	2	9:45	10:00	12800	285	3	9:30	13:30	10.8	< 0.10
Air Blown - Low Sodium Lignite										
10/7/03	3	11:00	11:15	11900	222	4	10:30	14:30	13.6	< 0.10
10/8/03	4	13:30	13:45	12500	218	5	10:00	14:00	12.3	0.25
10/9/03	5	9:10	9:25	15100	372	6	8:30	12:30	13.9	0.11
Oxygen Blown - Low Sodium Lignite										
10/10/03	6	10:10	10:25	41300	755	7	9:45	13:45	32.6	< 0.10
Air Blown - High Sodium Lignite										
10/16/03	7	12:45	13:00	5700	101	8	12:30	14:30	13.1	< 0.10
10/17/03	8	10:10	10:40	16700	300	9	9:00	12:42	13.4	< 0.10
10/27/03	9	11:15	11:30	38800	496	10	10:00	12:00	13.7	< 0.10
10/28/03	--	--	--	--	--	11	10:00	12:49	15.8	< 0.10
10/31/03	10	10:15	10:30	26200	444	12	10:00	14:00	19.6	< 0.10

Notes: 1. Majority of mass appears to be duct debris and not a result of PCD leakage.

Table 4.4-2 Residual Cake Measurements From TC13 and Previous Runs

Element No.	Fail-safe Type	Type of Shutdown	Thickness in.	Areal Loading lb/ft^2	Calculated Porosity %
TC13 Measurements					
B-7	Pall Fuse + Ceramem	Clean	0.012	0.016	88.6
B-8	Pall Fuse + Ceramem	Clean	0.008	0.010	88.9
B-11	PSDF/ HR-160	Clean	0.006	0.013	80.9
B-14	PSDF/ H-556	Clean	0.016	0.013	92.6
Average		*Clean*	*0.011*	*0.013*	*87.8*
Averages from Previous Runs for Comparison					
TC12		Semi-Dirty	0.011	N.M.[1]	N.M.[1]
TC11		Clean	0.013	0.023	84.5
TC10		Clean	0.010	N.M.[1]	N.M.[1]
TC09		Semi-Dirty	0.008	0.006	93.3
TC08		Semi-Dirty	0.010	N.M.[1]	N.M.[1]
TC07		Clean	N.M.[1]	N.M.[1]	N.M.[1]
TC06		Semi-Dirty	0.010	0.020	82.5

1. N.M. = Not Measured.

Table 4.4-3 Physical Properties of TC13 In situ Samples and Hopper Samples Used for RAPTOR

Sample ID	Run No.	Sample Date	Limestone Added	Bulk Density g/cc	True Density g/cc	Uncompacted Bulk Porosity %	Specific Surface Area m^2/g	Mass-Median Diameter μm	Loss on Ignition Wt %
In-Situ Samples									
PRB Coal									
AB13897	1	10/03/03	No	0.30	2.71	88.9	124	14.8	20.39
AB13898	2	10/06/03	No	0.25	2.53	90.1	179	19.1	32.87
Average				*0.28*	*2.62*	*89.5*	*152*	*16.9*	*26.63*
Low-Sodium Freedom Lignite									
AB13899	3	10/07/03	Yes	0.42	2.96	85.8	65	20.4	10.57
AB13900	4	10/08/03	Yes	0.44	2.80	84.3	180	23.1	15.06
AB13901	5	10/09/03	Yes	0.28	2.40	88.3	298	20.2	45.19
AB13902	6[1]	10/10/03	Yes	0.39	2.43	84.0	161	16.8	34.88
Average				*0.38*	*2.65*	*85.6*	*176*	*20.1*	*26.43*
High-Sodium Freedom Lignite									
AB14130	7	10/16/03	Yes	0.27	2.37	88.6	280	21.0	43.05
AB14131	8	10/17/03	Yes	0.66	2.87	77.0	49	22.5	8.37
AB14132	9	10/27/03	No	0.41	1.92	78.6	71	13.5	65.24
AB14133	10	10/31/03	No	0.37	1.84	79.9	85	21.7	71.00
Average				*0.43*	*2.25*	*81.0*	*121*	*19.7*	*46.92*
Hopper Samples Used for Lab Drag Measurements									
Low-Sodium, Medium-Carbon[1]									
AB13852	---	10/10/03	Yes	0.40	2.23	82.1	N.M.[2]	17.9	39.80
AB13857	---	10/10/03	Yes	0.41	2.37	82.7	N.M.[2]	16.9	37.40
Average				*0.41*	*2.30*	*82.4*	N.M.[2]	*17.4*	*38.60*
High-Sodium, Low-Carbon									
AB14014	---	10/23/03	No	0.97	2.42	59.9	12	92.2	21.90
AB14027	---	10/25/03	No	1.10	2.44	54.9	8	36.8	23.97
Average				*1.04*	*2.43*	*57.4*	*10*	*64.5*	*22.94*
High-Sodium, Medium-Carbon									
AB14028	---	10/25/03	No	0.56	2.21	74.7	31	17.6	40.04
AB14029	---	10/25/03	No	0.65	2.22	70.7	47	23.1	35.46
AB14030	---	10/26/03	No	0.57	2.19	74.0	71	20.8	35.01
AB14031	---	10/26/03	No	0.55	2.11	73.9	70	34.3	40.47
Average				*0.58*	*2.18*	*73.3*	*55*	*23.9*	*37.75*
High-Sodium, High-Carbon									
AB14150	---	10/27/03	Yes	0.45	1.93	76.7	75	19.6	62.43

1. Oxygen-blown.
2. N.M. = Not Measured.

Table 4.4-4 Chemical Composition of TC13 In situ Samples and Hopper Samples Used for RAPTOR

Sample ID	Run No.	Sample Date	Limestone Added	$CaCO_3$ Wt %	CaS Wt %	CaO Wt %	Non-Carbonate Carbon Wt %	Inerts (Ash/Sand) Wt %	Loss on Ignition Wt %
In-Situ Samples									
PRB Coal									
AB13897	1	10/03/03	No	4.93	0.67	14.61	19.11	60.67	20.39
AB13898	2	10/06/03	No	6.93	0.49	8.39	29.81	54.38	32.87
Average				*5.93*	*0.58*	*11.50*	*24.46*	*57.53*	*26.63*
Low-Sodium Freedom Lignite									
AB13899	3	10/07/03	Yes	7.34	2.44	14.38	13.70	62.15	10.57
AB13900	4	10/08/03	Yes	16.36	4.80	10.52	18.35	49.97	15.06
AB13901	5	10/09/03	Yes	11.89	8.48	2.34	46.86	30.43	45.19
AB13902	6[1]	10/10/03	Yes	11.14	2.77	11.55	33.84	40.70	34.88
Average				*11.68*	*4.62*	*9.70*	*28.19*	*45.81*	*26.43*
High-Sodium Freedom Lignite									
AB14130	7	10/16/03	Yes	15.66	3.33	6.54	38.09	36.38	43.05
AB14131	8	10/17/03	Yes	8.95	0.04	19.02	8.79	63.20	8.37
AB14132	9	10/27/03	No	9.07	3.38	-0.74	58.55	29.75	65.24
AB14133	10	10/31/03	No	7.55	1.55	1.02	64.90	24.97	71.00
Average				*10.31*	*2.08*	*6.46*	*42.58*	*38.57*	*46.92*
Hopper Samples Used for Lab Drag Measurements									
Low-Sodium, Medium-Carbon[1]									
AB13852	---	10/10/03	Yes	11.11	3.72	9.34	39.13	36.70	39.80
AB13857	---	10/10/03	Yes	N.M.[2]	N.M.[2]	N.M.[2]	N.M.[2]	N.M.[2]	37.40
Average				*11.11*	*3.72*	*9.34*	*39.13*	*36.70*	*38.60*
High-Sodium, Low-Carbon									
AB14014	---	10/23/03	No	5.43	1.14	-0.03	17.92	75.54	21.90
AB14027	---	10/25/03	No	2.59	0.70	0.31	21.92	74.48	23.97
Average				*4.01*	*0.92*	*0.14*	*19.92*	*75.01*	*22.94*
High-Sodium, Medium-Carbon									
AB14028	---	10/25/03	No	6.66	1.92	0.99	40.79	49.64	40.04
AB14029	---	10/25/03	No	4.14	1.89	1.19	43.55	49.22	35.46
AB14030	---	10/26/03	No	5.09	2.16	1.62	40.84	50.29	35.01
AB14031	---	10/26/03	No	5.50	2.33	1.47	34.75	55.94	40.47
Average				*5.35*	*2.08*	*1.32*	*39.98*	*51.27*	*37.75*
High-Sodium, High-Carbon									
AB14150	---	10/27/03	Yes	19.52	3.38	-6.25	57.03	26.32	62.43

1. Oxygen-blown.
2. N.M. = Not Measured.

Table 4.4-5 Physical Properties of TC13 Residual Dustcake

Sample ID	Plenum	Sample Date	Limestone Added	Bulk Density g/cc	True Density g/cc	Uncompacted Bulk Porosity %	Specific Surface Area m^2/g	Mass-Median Diameter μm	Loss on Ignition Wt %
AB14138	Bottom	11/06/03	N/A	0.31	2.17	85.7	88	9.7	46.22

Table 4.4-6 Chemical Composition of TC13 Residual Dustcake

Sample ID	Plenum	Sample Date	Limestone Added	$CaCO_3$ Wt %	CaS Wt %	CaO Wt %	Non-Carbonate Carbon Wt %	Inerts (Ash/Sand) Wt %	Loss on Ignition Wt %
AB14138	Bottom	11/06/03	N/A	9.25	3.26	0.98	38.62	47.89	46.22

Table 4.4.7 Transient Drag Determined from PCD ΔP and from RAPTOR

Run No.	D P/D t, inwc/min	D (AL)/ D t, lb/ft ^{2}/min	FV, ft/min	MMD, µm	NCC, %	Drag, inwc/(lb/ft ^{2})/(ft/min)		
						PCD	PCD@RT	RAPTOR
Air-Blown - PRB								
1	1.03	0.011	3.10	14.8	NA	94	56	49
2	1.76	0.019	3.56	19.1	NA	94	56	39
Air-Blown - Low Sodium Lignite								
3 (1)	0.36	0.015	3.08	20.4	13.7	25	15	30
4 (1)	0.28	0.014	2.77	23.1	18.4	19	12	28
5 (1)	2.50	0.024	3.76	20.2	46.9	103	62	48
Oxygen-Blown - Low Sodium Lignite								
6 (1)	3.01	0.049	3.86	16.8	33.8	61	39	48
Air-Blown - High Sodium Lignite								
7 (1)	0.21	0.007	3.14	21.0	38.1	32	20	47
8 (1)	0.07	0.020	2.97	22.5	8.8	4	2	26
9	1.96	0.033	3.51	13.5	58.6	61	39	100
10	1.95	0.029	3.28	21.7	64.9	67	43	73

1. Limestone added to Transport Gasifier.
2. RAPTOR drag data calculated from multiple regression to both MMD and NCC.

Nomenclature:
ΔP/Δt = rate of pressure drop rise during particulate sampling run, inWc/min.
Δ(AL)/Δt = rate of increase in areal loading during sampling run, lb/min/ft^2.
FV = average PCD face velocity during particulate sampling run, ft/min.
MMD = mass-median diameter of in situ particulate sample, µm.
NCC = Non-Carbonate Carbon.
RT = room temperature, 77°F (25°C).
RAPTOR = resuspended ash permeability tester.

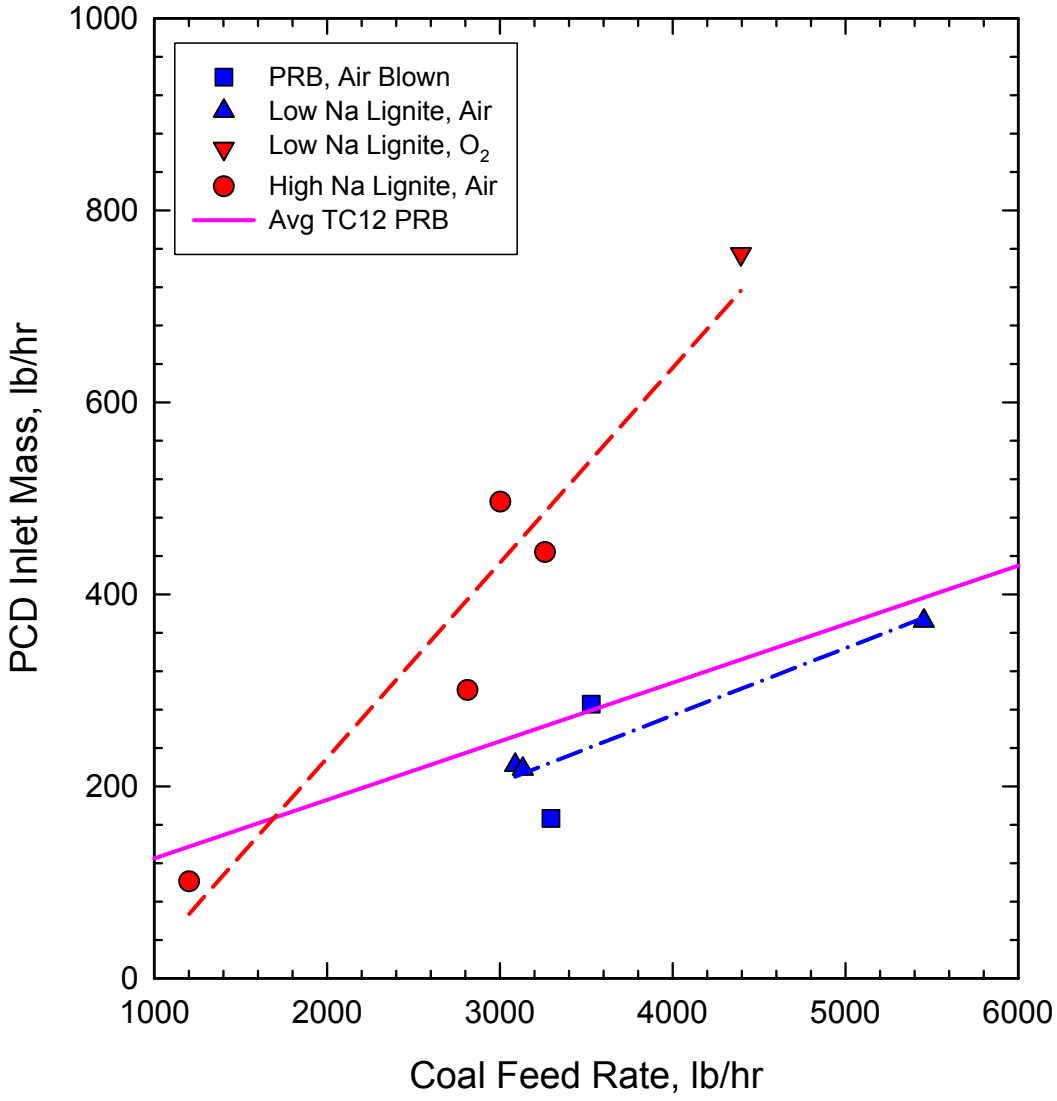

Figure 4.4-1 PCD Inlet Particle Concentration as a Function of Coal-Feed Rate

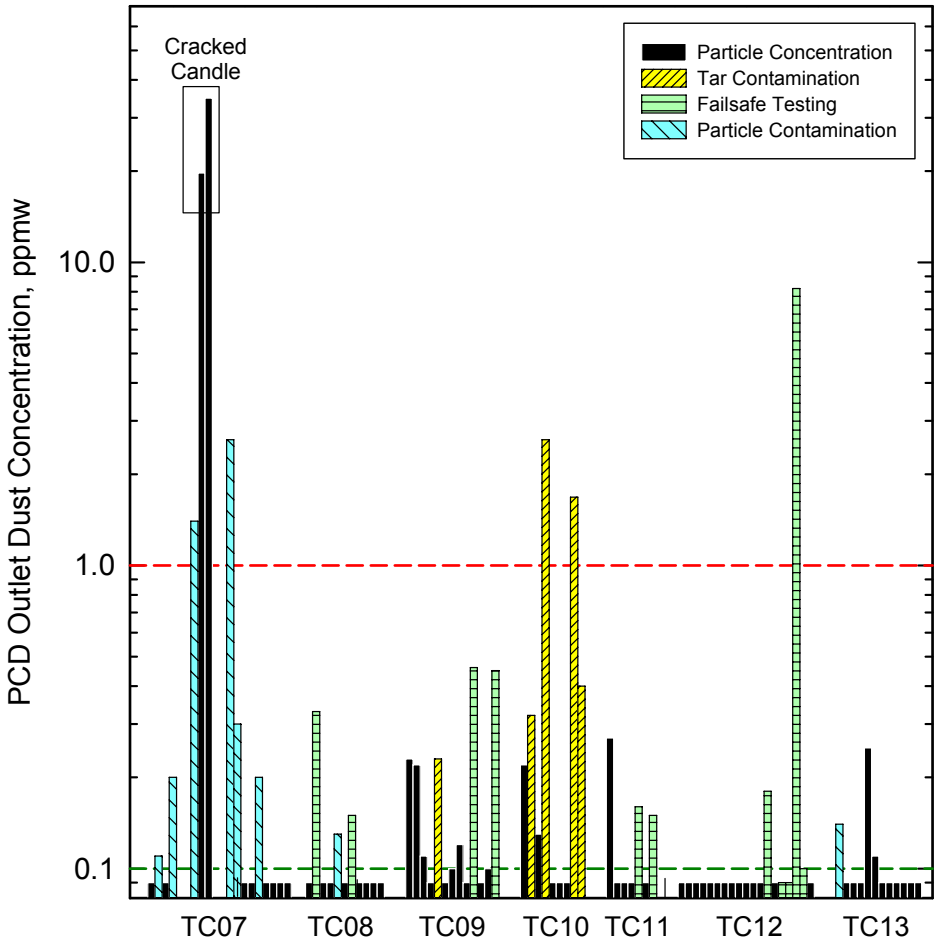

Figure 4.4-2 PCD Outlet Emissions for Recent Gasification Runs

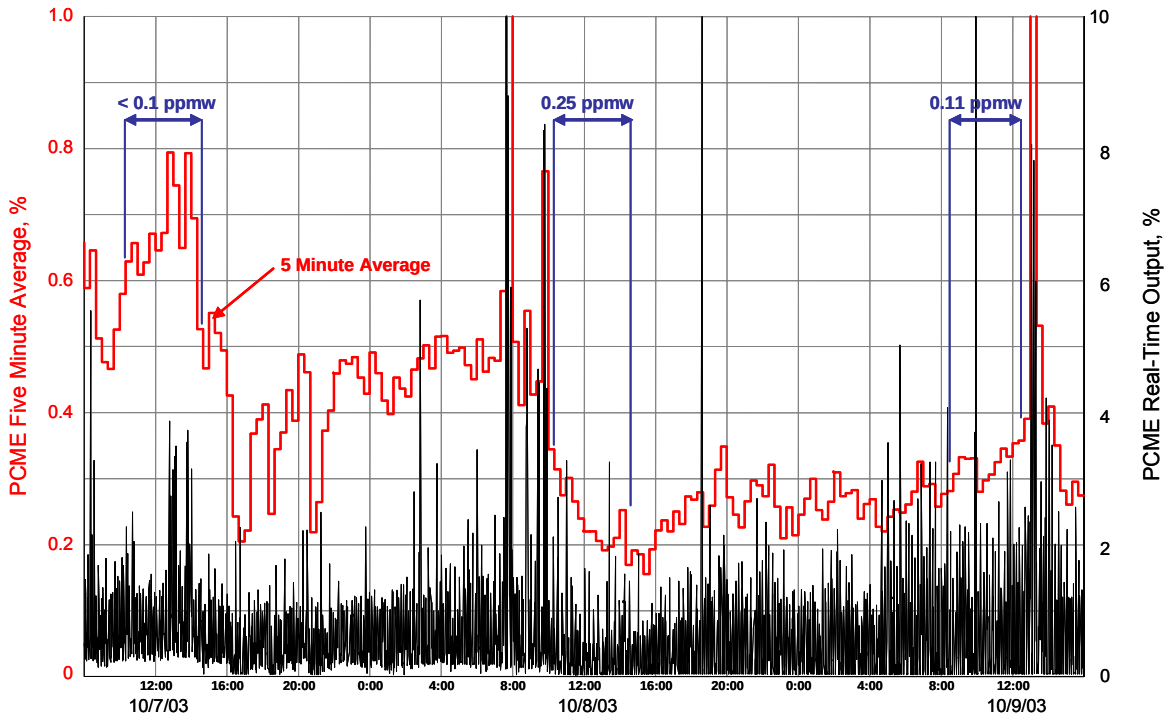

Figure 4.4-3 Relationship Between PCME Output and Actual Particle Concentration

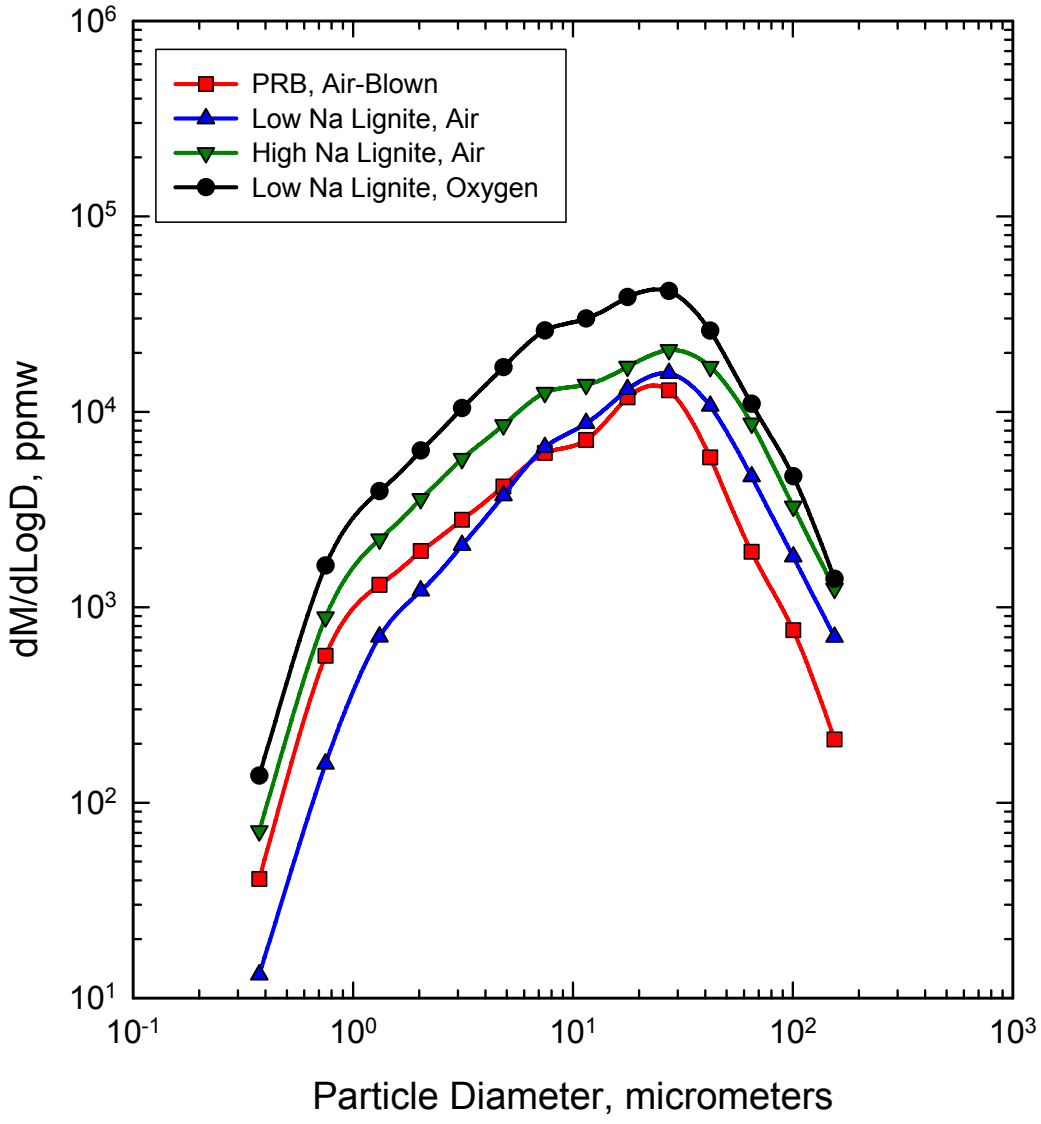

Figure 4.4-4 Comparison of Average PCD Inlet Particle-Size Distributions on Mass Basis

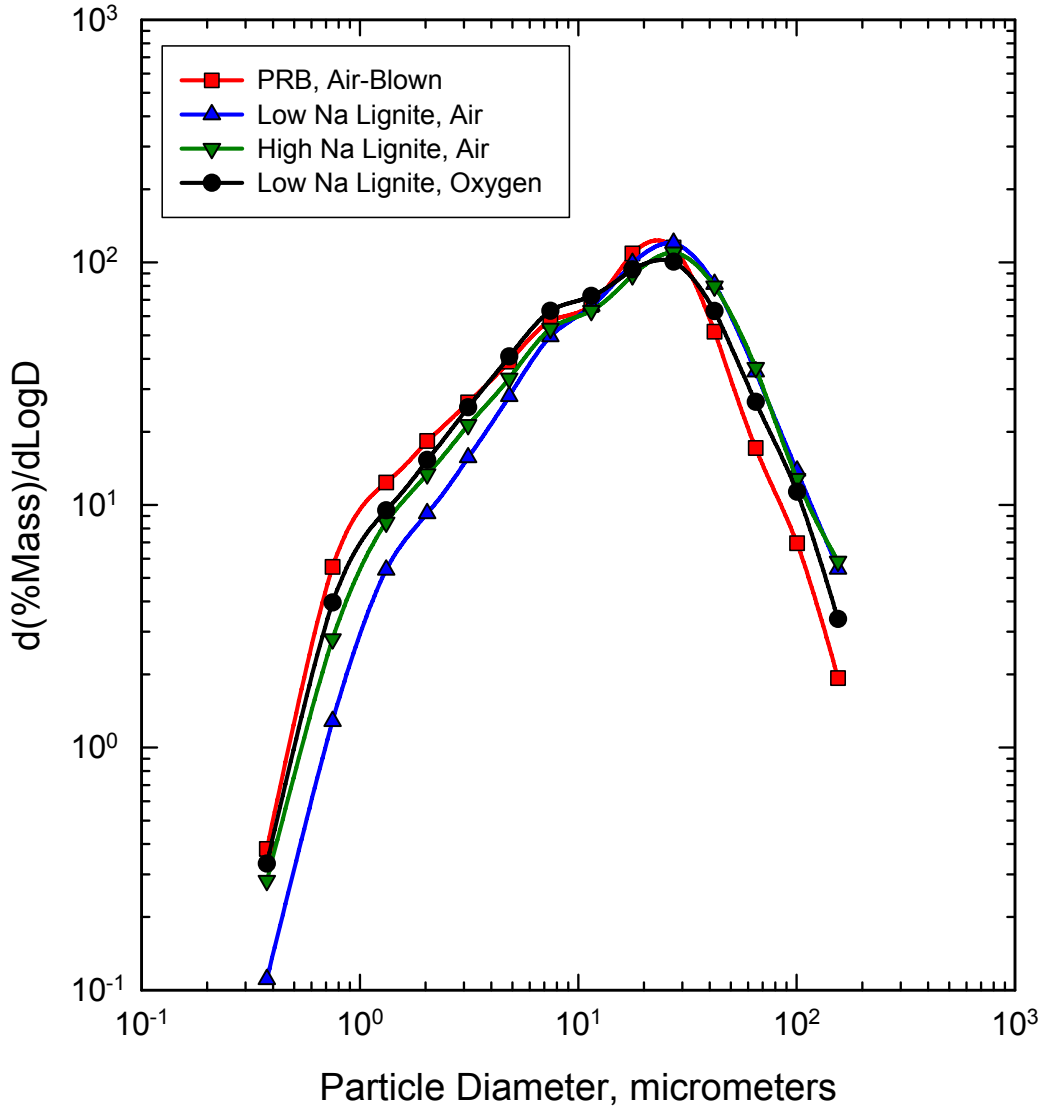

Figure 4.4-5 Comparison of Average PCD Inlet Particle-Size Distributions on Percentage Basis

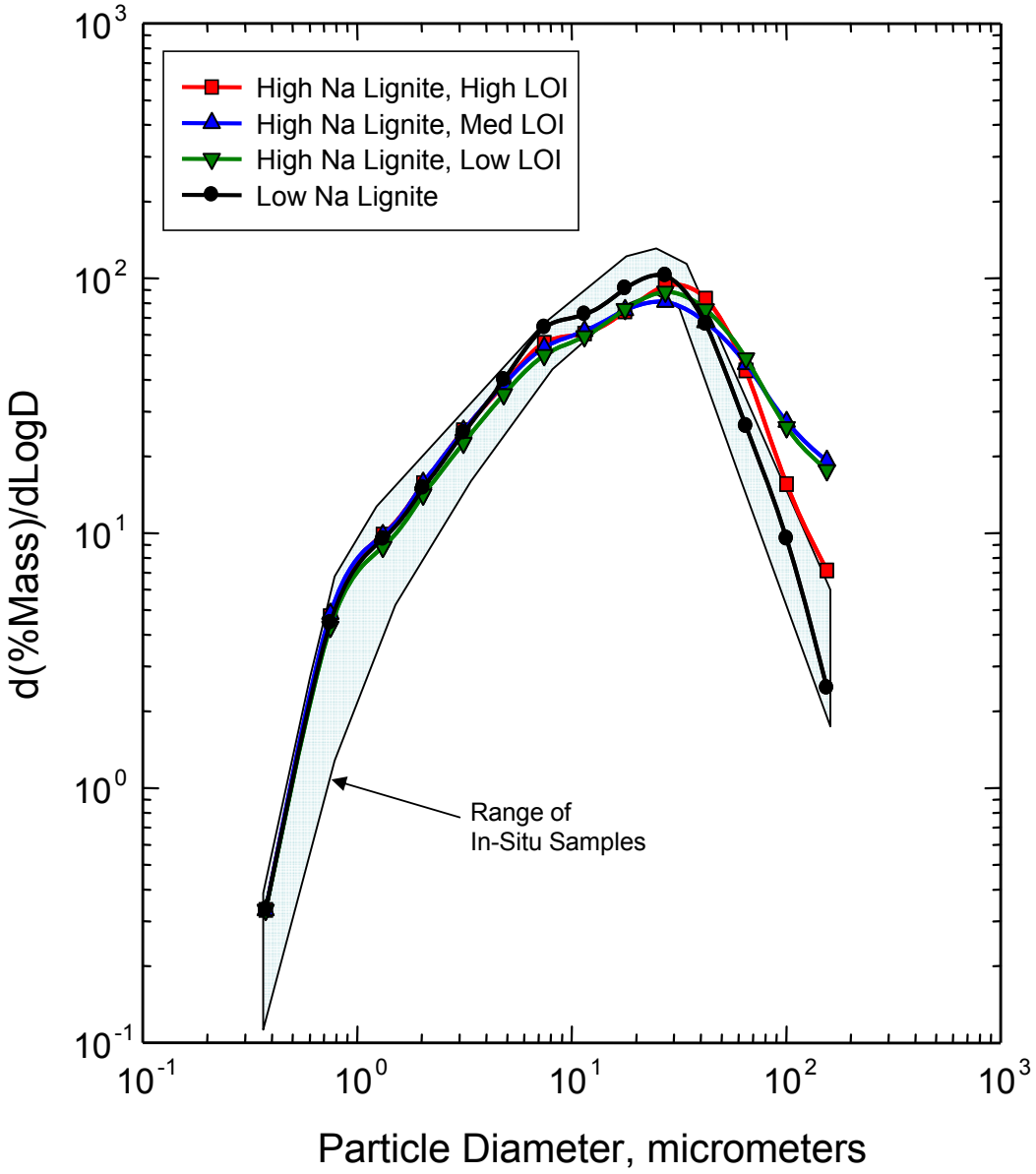

Figure 4.4-6 Comparison of In situ and Hopper Particle-Size Distributions

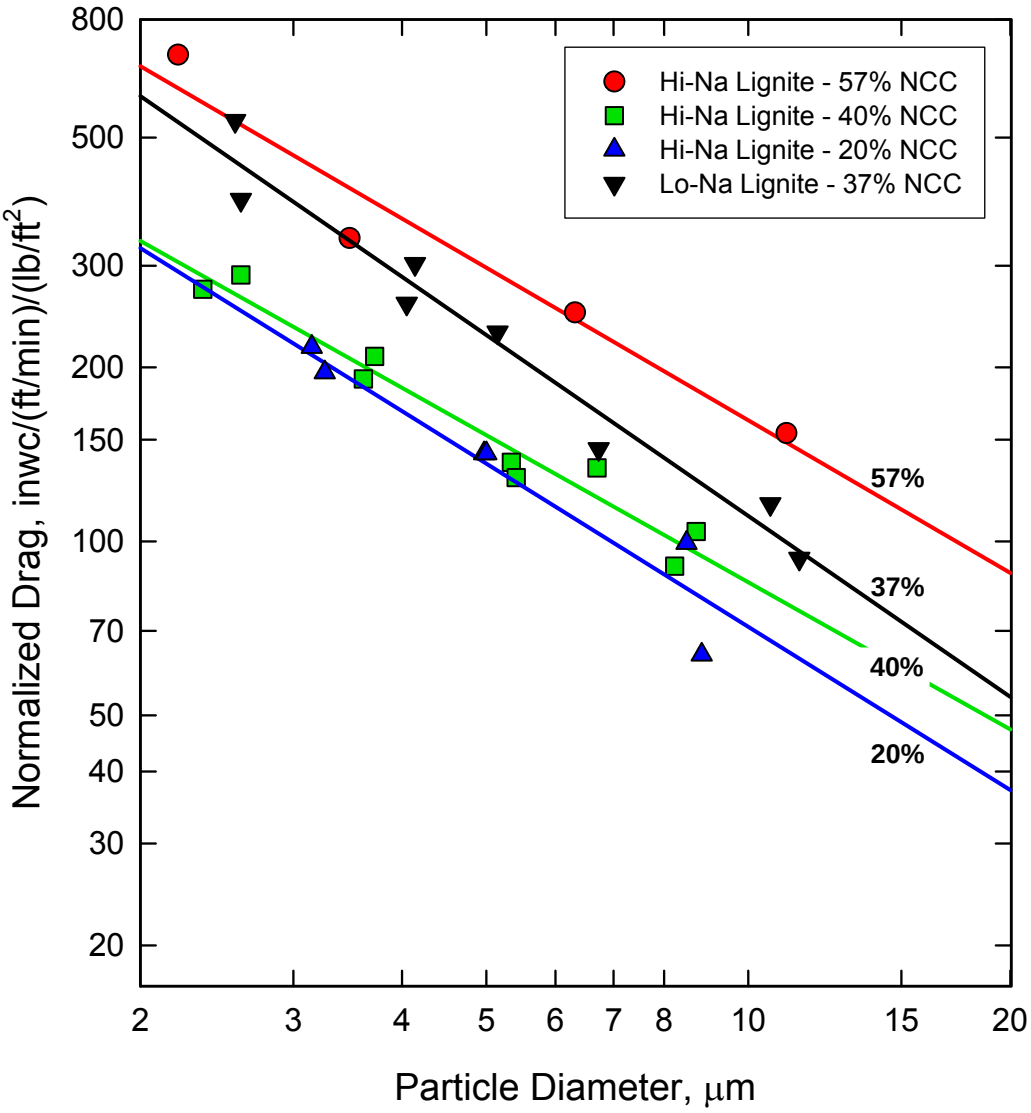

Figure 4.4-7 Laboratory Measurements of TC13 Dustcake Drag Versus Particle Size

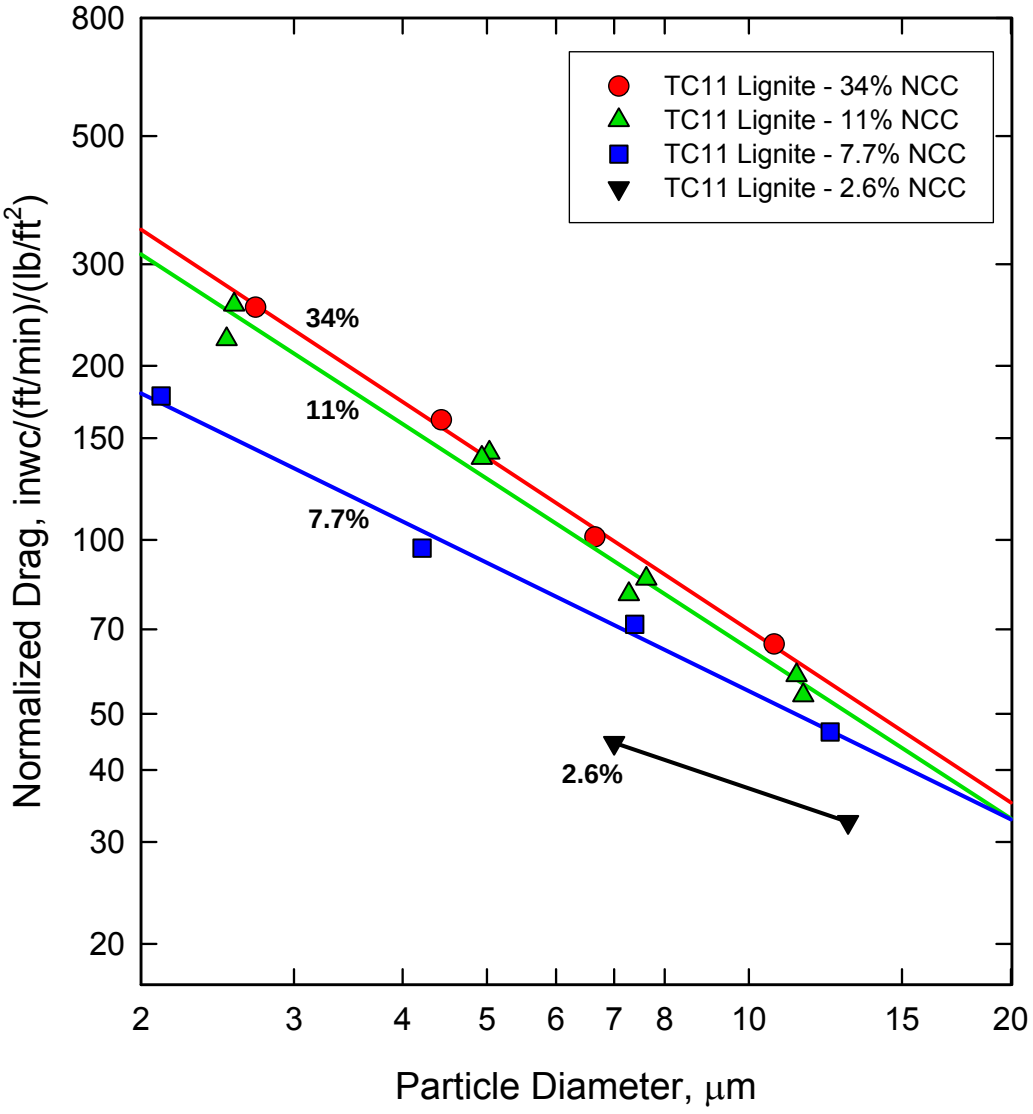

Figure 4.4-8 Laboratory Measurements of TC11 Dustcake Drag Versus Particle Size

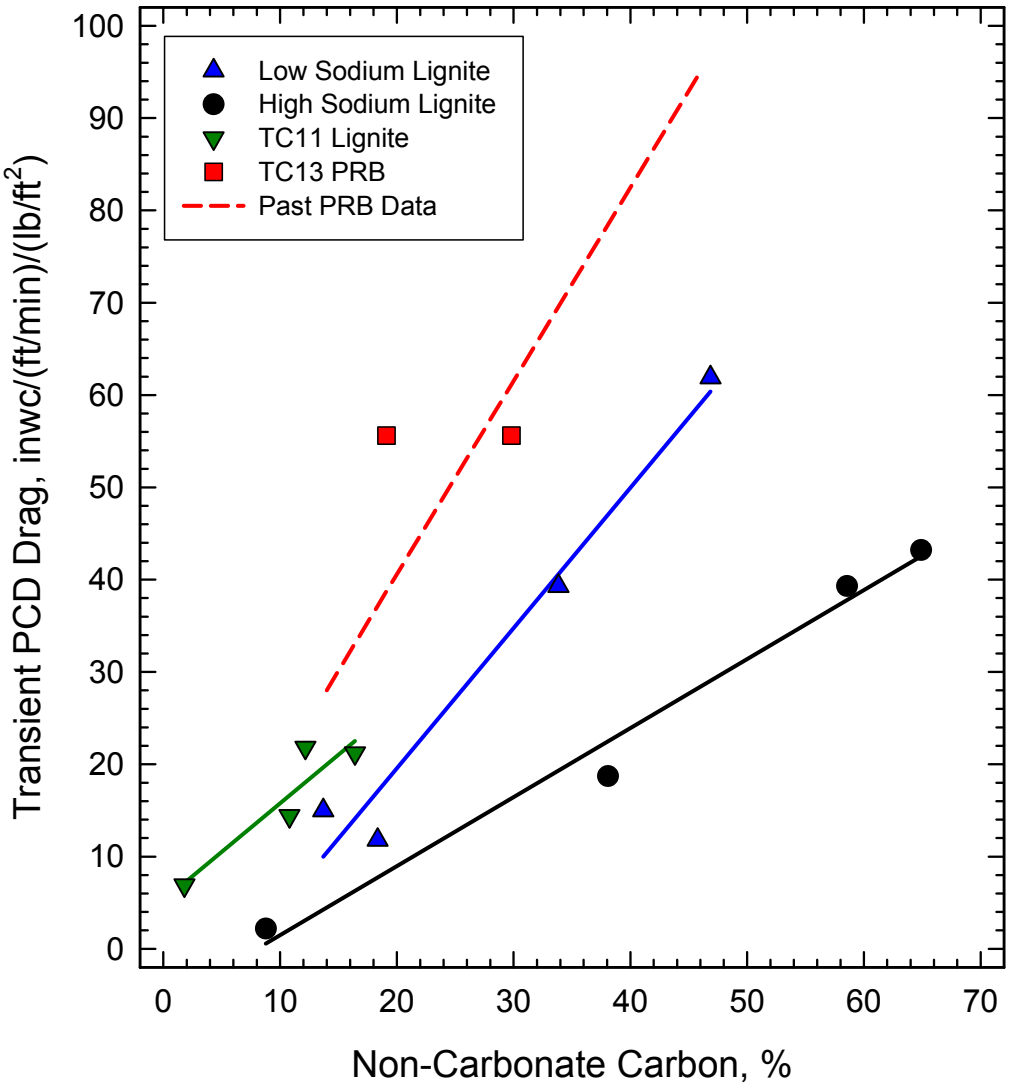

Figure 4.4-9 PCD Transient Drag Versus Carbon Content of G-Ash

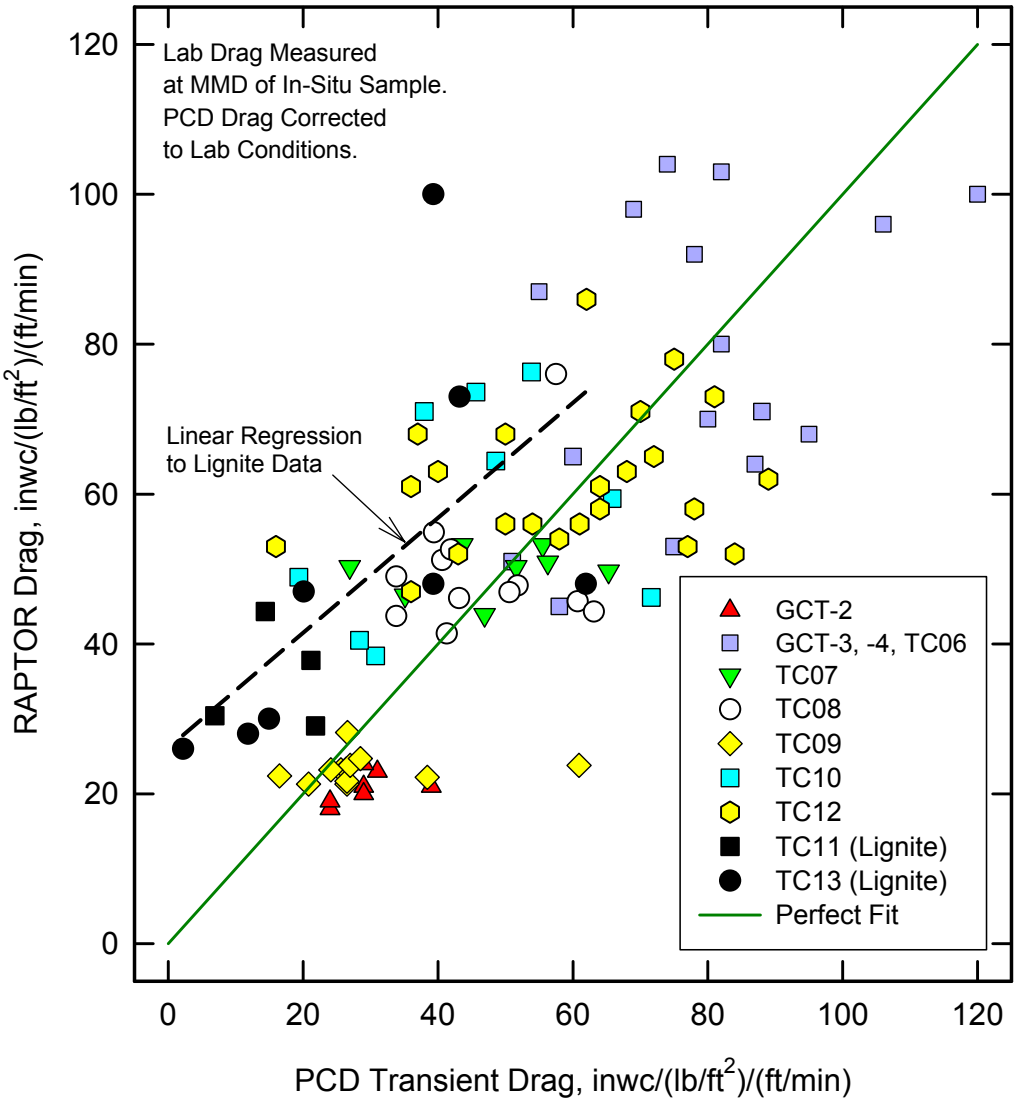

Figure 4.4-10 Comparison of PCD Transient Drag With Laboratory Measurements

TERMS

Listing of Abbreviations

AAS	Automated Analytical Solutions
ADEM	Alabama Department of Environmental Management
AFBC	Atmospheric Fluidized-Bed Combustor
APC	Alabama Power Company
APFBC	Advance Pressurized Fluidized-Bed Combustion
ASME	American Society of Mechanical Engineers
AW	Application Workstation
BET	Brunauer-Emmett-Teller (nitrogen-adsorption specific surface technique)
BFI	Browning-Ferris Industries
BFW	Boiler Feed Water
BMS	Burner Management System
BOC	BOC Gases
BOP	Balance-of-Plant
BPIR	Ball Pass Inner Race, Frequencies
BPOR	Ball Pass Outer Race, Frequencies
BSF	Ball Spin Frequency
CAD	Computer-Aided Design
CAPTOR	Compressed Ash Permeability Tester
CEM	Continuous Emissions Monitor
CFB	Circulating Fluidized Bed
CFR	Code of Federal Regulations
CHE	Combustor Heat Exchanger
COV	Coefficient of Variation (Standard Deviation/Average)
CPC	Combustion Power Company
CPR	Cardiopulmonary Resuscitation
CTE	Coefficient of Thermal Expansion
DC	Direct Current
DCS	Distributed Control System
DHL	DHL Analytical Laboratory, Inc.
DOE	U.S. Department of Energy
DSRP	Direct Sulfur Recovery Process
E&I	Electrical and Instrumentation
EDS or EDX	Energy-Dispersive X-Ray Spectroscopy
EERC	Energy and Environmental Research Center
EPRI	Electric Power Research Institute
ESCA	Electron Spectroscopy for Chemical Analysis
FCC	Fluidized Catalytic Cracker
FCP	Flow-Compacted Porosity
FFG	Flame Front Generator
FI	Flow Indicator
FIC	Flow Indicator Controller
FOAK	First-of-a-Kind
FTF	Fundamental Train Frequency

FW	Foster Wheeler
GBF	Granular Bed Filter
GC	Gas Chromatograph
GEESI	General Electric Environmental Services, Inc.
HHV	Higher Heating Valve
HP	High Pressure
HRSG	Heat Recovery Steam Generator
HTF	Heat Transfer Fluid
HTHP	High-Temperature, High-Pressure
I/O	Inputs/Outputs
ID	Inside Diameter
IF&P	Industrial Filter and Pump
IGV	Inlet Guide Vanes
IR	Infrared
KBR	Kellogg Brown & Root, Inc.
LAN	Local Area Network
LHV	Lower Heating Valve
LIMS	Laboratory Information Management System
LMZ	Lower Mixing Zone
LOC	Limiting Oxygen Concentration
LOI	Loss on Ignition
LPG	Liquefied Propane Gas
LSLL	Level Switch, Low Level
MAC	Main Air Compressor
MCC	Motor Control Center
MMD	Mass Median Diameter
MS	Microsoft Corporation
NDIR	Nondestructive Infrared
NETL	National Energy Technology Laboratory
NFPA	National Fire Protection Association
NO_X	Nitrogen Oxides
NPDES	National Pollutant Discharge Elimination System
NPS	Nominal Pipe Size
OD	Outside Diameter
ORNL	Oak Ridge National Laboratory
OSHA	Occupational Safety and Health Administration
OSI	OSI Software, Inc.
P&IDs	Piping and Instrumentation Diagrams
PC	Pulverized Coal
PCD	Particulate Control Device
PCME	Pollution Control and Measurement (Europe)
PDI	Pressure Differential Indicator
PDT	Pressure Differential Transmitter
PFBC	Pressurized Fluidized-Bed Combustion
PI	Plant Information
PLC	Programmable Logic Controller
PPE	Personal Protection Equipment

PRB	Powder River Basin
PSD	Particle-Size Distribution
PSDF	Power Systems Development Facility
ΔP or DP or dP	Pressure Drop or Differential Pressure
PT	Pressure Transmitter
RAPTOR	Resuspended Ash Permeability Tester
RFQ	Request for Quotation
RO	Restriction Orifice
RPM	Revolutions Per Minute
RSSE	Reactor Solid Separation Efficiency
RT	Room Temperature
RTI	Research Triangle Institute
SCS	Southern Company Services, Inc.
SEM	Scanning Electron Microscopy
SGC	Synthesis Gas Combustor
SGD	Safe Guard Device
SMD	Sauter Mean Diameter
SRI	Southern Research Institute
SUB	Start-up Burner
TCLP	Toxicity Characteristic Leaching Procedure
TR	Transport Reactor
TRDU	Transport Reactor Demonstration Unit
TRS	Total Reduced Sulfur
TSS	Total Suspended Solids
UBP	Uncompacted Bulk Porosity
UMZ	Upper Mixing Zone
UND	University of North Dakota
UPS	Uninterruptible Power Supply
UV	Ultraviolet
VFD	Variable Frequency Drive
VOCs	Volatile Organic Compounds
WGS	Water-Gas Shift
WPC	William's Patent Crusher
XRD	X-Ray Diffraction
XXS	Extra, Extra Strong

Listing of Units

acfm	actual cubic feet per minute
Btu	British thermal units
°C	degrees Celsius or centigrade
°F	degrees Fahrenheit
ft	feet
FPS	feet per second
gpm	gallons per minute
g/cm^3 or g/cc	grams per cubic centimeter
g	grams
GPa	gigapascals
hp	horsepower
hr	hour
in.	inches
inWg (or inWc)	inches, water gauge (inches, water column)
in.-lb	inch pounds
°K	degrees Kelvin
kg	kilograms
kJ	kilojoules
kPa	kilopascals
ksi	thousand pounds per square inch
m	meters
MB	megabytes
min	minute
mm	millimeters
MPa	megapascals
msi	million pounds per square inch
MW	megawatts
m/s	meters per second
MBtu	Million British thermal units
m^2/g	square meters per gram
μ or μm	microns or micrometers
dp_{50}	particle-size distribution at 50 percentile
ppm	parts per million
ppm (v)	parts per million (volume)
ppm (w)	parts per million (weight)
lb	pounds
pph	pounds per hour
psi	pounds per square inch
psia	pounds per square inch absolute
psid	pounds per square inch differential
psig	pounds per square inch gauge
ΔP	pressure drop
rpm	revolutions per minute
s or sec	seconds
scf	standard cubic feet

scfh	standard cubic feet per hour
scfm	standard cubic feet per minute
V	volts
W	watts